

**Pharmaceutical impurity assay method
development using core-shell stationary
phase technology for HPLC and evaluation
of stationary and mobile phases for an
orthogonally selective SFC impurity assay**

by

Orla Gaffney B.Sc.

Thesis submitted for the Degree of Master of Science

Under the supervision of:

Dr Blanaid White (School of Chemical Sciences, DCU)

Dr Damian Connolly (Department of Chemical and Life Sciences, WIT)

Ms Mary O’Gorman (Pfizer Process Development Centre (PDC))

School of Chemical Sciences

Dublin City University

September 2014

Declaration

I hereby certify that this material, which I now submit for assessment on the programme of study leading to the award Master of Science is entirely my own work, that I have exercised reasonable care to ensure that the work is original, and does not to the best of my knowledge breach any law of copyright, and has not been taken from the work of others save and to the extent that such work has been cited and acknowledged within the text of my work.

Signed: _____

ID No.: _____

Date: _____

For Ava, Isabel and Harry

Acknowledgements

I would first of all like to thank the Irish Research Council and Pfizer Process Development (PDC), Cork for giving me the opportunity to do this Masters. To my supervisor in Pfizer PDC, Mary O’Gorman, thank you for all your help and advice throughout the two years. To my DCU supervisor, Dr Blánaid White, I cannot thank you enough for your advice, guidance and unwavering support during my final year and keeping me motivated to finish! Thank you for never giving up and getting me across the finish line. And finally to DCU/WIT supervisor, Dr Damian Connolly, thanks for all your guidance and help throughout the two years.

To the NCSR technical staff, especially Stephen Fuller, thanks for the countless days spent training me on HPLCs and SFCs and countless hours spent repairing and troubleshooting my instruments when things when wrong. To the ISSC lab of Gillian, Nicola Patrick, Amy, Ali, Lily, Sinead and Sara, thanks for all the advice, guidance and friendship throughout the two years and most especially to Disha for all the chats, rants and laughs we had throughout my time in S201 and since!

To the ever extending lunch crew of Nicky, Brian, Sean, Aoife (Dr Boss!), Rachel, Al, Andy, Declan, Hannah, Leeanne, Laura and Sarah for the countless cups of tea, baby scones, lunches, birthday cakes, bbq’s in the sun, games in the grass, advice and chats when I needed them and most importantly our brilliant nights out. They have been some of the funniest and most memorable nights of my college career! You are all some of the best things to come from my time in DCU. To Adelene, Emma, Jade and Laura, thanks for putting up with me and understanding my absenteeism over the past few years , I’ll be more sociable now I promise!

And most importantly, thanks to my parents Michael and Rosemary for your unwavering support throughout my masters and always believing I could do it, even when I didn’t! I couldn’t have got this far without you. To my fantastic sister Michelle, thanks for all the chats, surprise presents when things got tough and hours and hours of laughs and pep talks. To my brothers Paul and Shane, thanks for all your encouragement to keep going and assurance that I would get there eventually! And finally to my gorgeous nieces, Ava and Isabel and nephew Harry to whom this thesis is dedicated to, for always putting a smile on my face.

Table of Contents

Title Page.....	i
Declaration.....	ii
Dedication.....	iii
Acknowledgements.....	iv
Table of contents.....	v
Abbreviations.....	ix
Poster Presentations.....	xi
Abstract.....	xii
1 Chapter 1: Literature Survey.....	1
1.1 Introduction.....	1
1.2 Core shell stationary phases and their place in high performance liquid chromatography (HPLC).	7
1.2.1 Coreshell stationary phases from a historical perspective.	7
1.2.1.1 First generation core-shell particles	7
1.2.1.2 Second generation core-shell particles.....	10
1.2.1.3 Third generation core-shell particles.....	12
1.2.2 Properties of core-shell stationary phases.....	13
1.2.2.1 Shell Thickness	13
1.2.2.2 Particle size distribution.....	15
1.2.3 Comparison of the efficiencies of fully porous stationary phases to core-shell stationary phases	16
1.2.3.1 Van Deemter plots	16
1.2.3.2 Knox plots.....	18
1.2.3.3 Kinetic Plots – Poppe plots	20
1.2.4 Application of core-shell particles	24
1.3 Supercritical Fluid Chromatography (SFC) – A greener alternative to HPLC	27
1.3.1 SFC from an historical perspective.....	28
1.3.2 SFC Hardware.....	29
1.3.3 What are supercritical Fluids?.....	30
1.3.4 SFC - a complementary technique to HPLC?	31
1.3.4.1 Use of modifiers and additives.....	32
1.3.4.1.1 Modifiers.....	32
1.3.4.1.2 Additives.....	35

1.3.4.2	Temperature and pressure of the supercritical fluid.....	39
1.3.5	Applications of SFC.....	40
1.4	Conclusions.....	44
2	Chapter 2: Development of ultrafast pharmaceutical impurity assay using 3rd Generation core-shell stationary phase technologies.....	47
2.1	Introduction.....	47
2.2	Materials and Methods.....	49
2.2.1	Materials	49
2.2.1.1	Chemicals.....	49
2.2.1.1.1	Mobile Phases	49
2.2.1.2	Apparatus	50
2.2.1.2.1	HPLC instrumentation	50
2.2.1.2.2	UPLC instrumentation	50
2.2.2	Methods.....	50
2.2.2.1	Preparation of standards.....	50
2.2.2.2	HPLC Method development	51
2.2.2.3	Calculation of performance parameters.	52
2.3	Results and Discussion	52
2.3.1	Original reversed- phase HPLC method.	52
2.3.2	Transfer of existing impurity analysis method to core-shell Kinetex 2.6 μm reversed phase C_{18} column.	53
2.3.2.1	Isocratic method optimisation.....	54
2.3.2.1.1	Optimising the composition of the organic mobile phase component.....	54
2.3.2.1.2	Optimising the organic component strength of the mobile phase.....	57
2.3.2.1.3	Optimisation of the nature of the aqueous component of the mobile phase.....	64
2.3.2.1.3.1	Changing the concentration of ammonium FB	66
2.3.2.1.3.2	Optimisation of ammonium FB pH	67
2.3.2.1.4	Optimisation of the temperature of the run.....	68
2.3.2.1.5	Increasing the flow rate of the method to obtain a faster separation ...	73
2.3.2.2	Development of a gradient separation.....	74
2.3.2.2.1	Determination of the delay volume of Agilent 1200 series liquid Chromatograph.	75
2.3.2.2.2	Gradient method development.....	77
2.3.2.3	Development of an optimised UPLC method on a core-shell 1.7 μm column.....	86

2.3.2.3.1	Determination of the dwell volume of the Shimadzu Nexera UPLC Liquid Chromatograph.....	86
2.3.2.3.2	Transfer of the 2.6 μm core-shell column RP HPLC method to a 1.7 μm core-shell column.	87
2.4	Conclusions.....	94
3	Chapter 3: The evaluation of stationary phase/mobile phase combinations for the development of an pharmaceutical impurity assay using Supercritical Fluid Chromatography.	96
3.1	Introduction.....	96
3.2	Materials and Methods.....	97
3.2.1	Materials	97
3.2.1.1	Chemicals.....	97
3.2.1.2	Mobile Phases	98
3.2.2	Apparatus	98
3.2.2.1	SFC Instrumentation.	98
3.2.3	Methods.....	99
3.2.3.1	Preparation of Standards	99
3.2.4	SFC Method Development.....	99
3.2.4.1	Stationary Phase Selection	99
3.2.4.1.1	Stationary phase chemistry and mobile phase screening studies.	100
3.3	Results and Discussion	101
3.3.1	Selection of the optimal stationary phase/mobile phase modifier combination for the separation of API Voriconazole and its related impurities, compound X, compound C and compound D.....	101
3.3.1.1	Optimisation of mobile phase for separation of Voriconazole and related impurities compound C and compound D.	102
3.3.1.1.1	Investigation of the effect of a MeOH mobile phase modifier on retention of Voriconazole and related impurities Compound C and Compound D on stationary phases of varying polarities.	102
3.3.1.1.2	Optimal MeOH modified mobile phases	109
3.3.1.1.3	Investigation of the effect of a MeOH mobile phase modifier with 0.1% TFA additive on retention of Voriconazole and related impurities compound C and compound D on stationary phases of varying polarities.	111
3.3.1.1.3.1	Bare silica stationary phase.....	111
3.3.1.1.3.2	Cyano stationary phase	114
3.3.1.1.3.3	Diol stationary phase	116
3.3.1.1.3.4	ethyl-pyridine stationary phase.....	118
3.3.1.1.3.5	Optimal MeOH modified mobile phases with TFA additive.....	119

3.3.1.1.4	Investigation of the effect of MeOH mobile phase modifier with 0.1% TEA on retention of Voriconazole and related impurities compound C and compound D.....	120
3.3.1.1.4.1	Bare silica stationary phase.....	121
3.3.1.1.4.2	cyano stationary phase.....	123
3.3.1.1.4.3	Diol stationary phase.....	125
3.3.1.1.4.4	Ethyl pyridine stationary phase.....	126
3.3.1.1.4.5	Optimal TEA additive mobile phases.....	127
3.3.1.1.5	Investigation of the effect of MeOH modified mobile phase with 20 mM AA additive on retention of Voriconazole and related impurities compound C and compound D.....	127
3.3.1.1.5.1	Silica stationary phase.....	128
3.3.1.1.5.2	Cyano and Diol stationary phases.....	129
3.3.1.1.5.3	Optimal AA additive mobile phases.....	132
3.4	Conclusions.....	134
4	Final conclusions and future work.....	137
5	References.....	140
6	Appendices.....	144
6.1	Chapter 2:.....	145
6.2	Chapter 3.....	152

Abbreviations

2 – EP	2 – ethyl Pyridine
AA	Ammonium Acetate
API	Active Pharmaceutical Ingredient
ACN	Acetonitrile
AMP	Adenylic acid
CO ₂	Carbon dioxide
CSP	Controlled surface porosity
EtOH	Ethanol
FB	Ammonium Formate Buffer
GC	Gas Chromatography
GMP	Guanylic acid
H	Plate height
HETP	Height equivalent of theoretical plates
HPLC	High Performance Liquid Chromatography
IPA	Isopropylamine
IPA	Isopropyl alcohol
LLC	Liquid-Liquid Chromatography
MeOH	Methanol
ODS	Octadecylsilane (C ₁₈)
sCO ₂	Supercritical carbon dioxide
SFC	Supercritical Fluid Chromatography

TEA	Triethylamine
TFA	Trifluoroacetic Acid
UMP	Uridylic acid

Poster Presentations

- 1. O. Gaffney, M. O’Gorman, V. Nelson, D. Connolly, B. White.** *The effect of modifier concentration and the addition of additives to modifiers in Supercritical Fluid Chromatography (SFC)* 64th Irish Universities Chemistry Research Colloquium 2012, June 14-15th 2012, Limerick, Ireland

- 2. O. Gaffney, M. O’Gorman, V. Nelson, D. Connolly, B. White.** *The effect of modifier concentration and the addition of additives to modifiers in Supercritical Fluid Chromatography (SFC)* RSC Analytical Research Forum 2012, July 2-4th 2012, Durham, UK

Abstract

The demand for faster, greener, more cost effective processes is of great importance across all industries including chemical pharmaceutical and petrochemical sectors. As a result the key driver of chromatographic research is addressing these demands. The ultimate goal in liquid chromatography is “The best separation in the shortest time”. While sub 2 μ m fully porous particle stationary phases have addressed this demand for faster more efficiency separations, a research focus which has recently seen a resurgence has been core-shell particle technologies which offer similar performance to sub 2 μ m particles without the added back pressure requirements of sub 2 μ m fully porous particles.

The aim of this study was the development of an ultrafast impurity assay using core-shell stationary phase technology. This involved the transfer of an existing pharmaceutical impurity assay currently using a 5 μ m fully porous stationary phase to core-shell stationary phase technologies of particle sizes 2.6 μ m and 1.7 μ m and subsequent method optimisation. Optimisation of isocratic method parameters such as mobile phase composition, temperature and development of a gradient method led to a reduction in run of 57% for both assays with resolution between critical peak pairs maintained above 2.

Another industrial focus is the development of greener, more environmentally friendly. This has led in recent years to research into alternative techniques to HPLC, one such technique is Supercritical Fluid Chromatography (SFC). The use of non-toxic carbon dioxide as its primary mobile phase means that SFC has the potential to meet this requirement of greener chromatography. SFC lies intermediate of HPLC and GC and possess qualities of both, including gas like viscosity and density whilst maintaining liquid like solvation power. As a result of these increased diffusion and low viscosity of supercritical fluid compared to solvents used in HPLC, much higher flow rates can be utilised allowing for faster separations and higher throughput, thus addressing both the desire for faster and greener chromatographic processes. SFC has also the distinct advantage of providing orthogonal selectivity to HPLC and thus is an attractive complementary technique.

The second aim of this study was the evaluation of stationary phase and mobile phase combinations for the development of ultrafast SFC pharmaceutical impurity method. Four stationary phases were chosen; bare silica, cyano, diol and 2-ethyl pyridine along mobile phase containing a methanol modifier and additives such as TFA, TEA and AA. All four stationary phases were found to provide orthogonal selectivity to the existing reversed phase HPLC method. Run times were in the region of 30% to 75% faster than the original HPLC method up to 50% faster than the newly developed core-shell stationary phase HPLC methods in some cases.

1 Chapter 1: Literature Survey

1.1 Introduction

High performance liquid chromatography (HPLC) is a well-established analytical technique. It has formed the basis of many analytical methods in laboratories around the world for more than 20 years. While it is one of several techniques used in the separation and analysis of chemical mixtures, HPLC for many reasons, has seen its popularity soar above other techniques; reasons include, its wide applicability as a separation technique, its excellent assay precision and the wide variety of equipment and related products which are commercially available[1]. HPLC in the pharmaceutical industry is used in variety of assays including; the determination of chemical substance and purity determination of possible degradation products to determine possible shelf lives of drugs[2]

The goal in chromatography can be loosely defined as the best separation achievable in the shortest amount of time. This has become increasingly important in recent years as fast analysis time is a key driver of chromatographic research.[3] Guillaume *et al.*[4] noted that the increasing demand for high-throughput separations in fields such as toxicology forensics and clinical chemistry as a driving force while Wren and Tchrlitcheff [2] state that in the pharmaceutical industry, while there is a need for reduced run times there is also a need for similar or improved efficiencies to those that are achieved currently being achieved by conventional LC.

One of the best ways of increasing efficiency while also decreasing analysis time is by decreasing particle size of columns used. Van Deemter plate theory states that decreasing particle size leads to a decrease in height equivalent of theoretical plates (H), thus an increase in efficiency[5]. The Van Deemter equation (Eqn. (i)) was one of the earliest applications of rate theory and its relationship to column efficiency.

$$H = A + \frac{B}{u} + Cu \quad \text{Eq. (i)}$$

A = Eddy Diffusion B = Longitudinal Diffusion C = Mass Transfer u = Linear Velocity (mm/sec)

Taking into account, the physical, kinetic and thermodynamic properties of a separation, the van Deemter equation relates variance per unit length H (plate height) to linear mobile phase velocity (u) (measured in mm/sec). The A , B and C terms of the equation are defined as follows; A = eddy diffusion, B = longitudinal mass transfer and C = resistance to mass transfer. Together these terms are the contributing factors of band broadening – a key source of efficiency loss in chromatography [6]. The Van Deemter equation is used to predict the optimum linear velocity of mobile phase at which the lowest plate height (H) can be achieved[5]. Van Deemter theory suggests that smaller particle sizes leads to increased efficiencies and thus smaller plate heights due to a reduced C term as a result of better mass transfer properties, due to shorter diffusion path lengths of smaller particles and also a reduction in the A term. This is shown below in Fig. 1.1.1 where the Van Deemter curves of particle sizes ranging from 10 μm down to 1.7 μm are compared. The plots show that as particle size (d_p) decreases, the H 's are significantly reduced. According to van Deemter theory, the A term of the Van Deemter equation (Eq.(i)), often referred to as the “packing term”, is a function of particle size so as particle size decreases so does the overall plate height. Also shown in this plot, at smaller particle sizes, increasing the linear mobile phase velocities do not have not have the significant negative impact on efficiency that plagues larger particle sizes like 5 and 10 μm , demonstrated by the much flatter Van Deemter curves of decreasing particle size. The “flatness” of the Van Deemter curve is a function of the C term (the resistance to mass transfer)

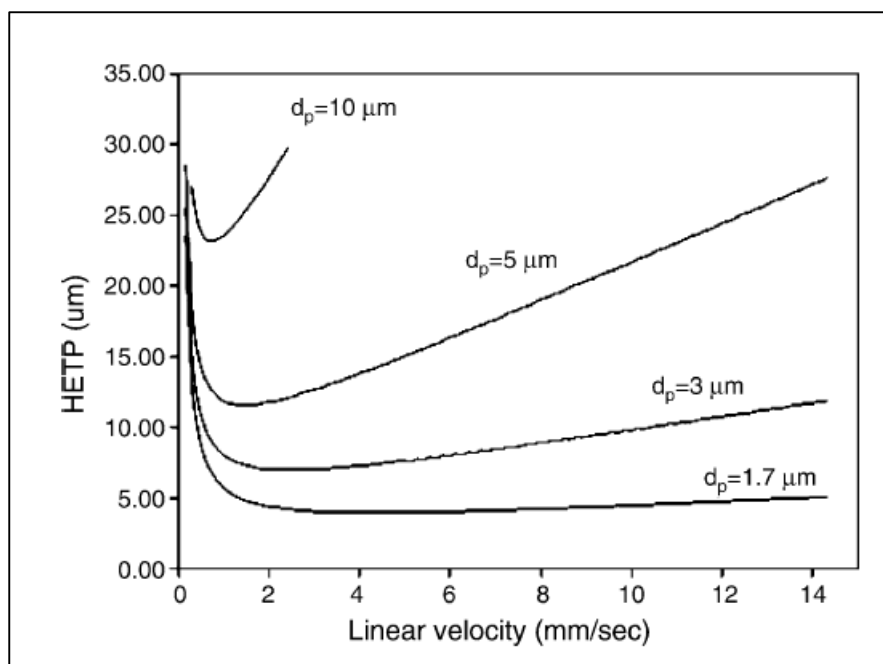


Fig. 1.1.1: Van Deemter curves for different particles sizes (10, 5, 3, 1.7 μm) illustrating reduction in HETP with decreasing particle size. Reproduced from Ref [7]

As smaller particles mean faster and more efficient separations, a key focus point of chromatographic research has been developing increasingly smaller particles to fulfil the need for faster, more efficient separations. A bi-annual survey carried out by Ronald E. Mayors for the chromatography magazine LC-GC examined the trends in liquid chromatography (LC) usage by their readers, but more specifically the current trends in the LC column usage, which documents the trend in reducing particle sizes[8]. 324 readers were surveyed for this study. The data collected included particle sizes used at the time of each survey, and showed a clear trend of decreasing particles size usage over the past 20 years for which surveys have been carried out. The statistics are given in Table 1.1.1.

Table 1.1.1: Results of survey carried out to determine column particle size usage across LC-GC readers. Sample size: 324. Table reproduced from Ref [8]

Analytical HPLC particle size trend 1985 – 2011*.						
	Percentage of respondents using these particle sizes					
Year	<2 µm	2- 2.9 µm	3-4 µm	5-7 µm	10 µm	> 10 µm
1985	nq**	nq	6.1	53	38	2.7
1989	nq	nq	6.3	54	36	3.9
1994	nq	nq	20	56	21	3.7
1997	nq	nq	18	59	20	2.7
2007	7.1	nq	38	48	6	0.7
2009	14	nq	39	42	4.3	0
2011	12	25	24	38	1.7	0

* normalised data

** “nq”: not queried

During the late eighties particle sizes in categories “10 µm” and “5-7 µm” were the most popular, while in the nineties 5-7 µm still remained the most popular, however popularity of 10 µm columns has seen a significant decrease with a surge in the popularity of the smaller 3-4 µm particles. This preference of decreasing particle size continued into the 2000s where particles of 4 µm in diameter or less held the majority share of columns used. Majors[8] attributes the persistence with 5-7 µm particles to users having validated methods which were developed on 5 µm columns who did not want to have to re-validate a method for smaller particles unless it was absolutely necessary.

While smaller particles produce higher efficiencies than larger particles, there is a trade-off in that the back pressure associated with these columns significantly increases. A consequence of this increased back pressure is friction heating across the column leading to the formation of temperature gradients. According to Gritti *et al.*[9] the amount of heat produced is the combined result of the pressure gradient and the linear velocity and while this is not significant for columns packed with larger particles with column length of 15-20 cm whose operational pressure is in the region of 200-400 bar, it becomes increasingly significant for particle sizes of sub 3µm which are run at a pressure of 400 – 1000 bar. Temperature gradients across the column were shown to affect the efficiency of the column. Gritti *et al.* [9] report a 6 fold increase in the C term of the Van Deemter equation of a 1.7 µm column, run at

above 400 bar determined experimentally when compared to predicted values due to transcolumn thermal heterogeneity. As well as affecting the efficiency of a column, increased back pressure and frictional heating also affect retention factors. In an effort to estimate the effect of frictional heating, Nováková *et al.* [10] carried out two concurrent experiments on an Acquity BEH C₁₈ column (50 x 2.1 mm, 1.7 μm) whereby for experiment 1, a low flow rate was applied and temperature was systematically increased from 30 to 60°C in approximately 4°C increments, and for the second experiment a constant temperature of 30°C was applied while the flow rate was increased to induce pressures of 100, 300, 600 and 1000 bar on temperature in the column. The retention factors of a range of compounds were compared for both experiments. The authors found that when chromatograms run at 300, 600 and 1000 bar and a constant temperature of 30°C, were compared to the those run at 100 bar and varying temperatures, perfect overlays of chromatograms were achieved when those carried out at 300 bar were compared to those carried out at 100 bar and 34°C. Chromatogram overlays are given in Fig. 1.1.2. This was also true for the 600 and 1000 bar chromatograms were separations equates to temperatures of 38 and 46°C respectively, indicating that the increased pressure has a significant effect on the temperature with in the column due to frictional heating. This reduction in retention factor due to frictional heating is also noted by de Villiers *et al.* [11] where a 10% decrease in retention factor is noted when pressure is increased from 212 to 718 bar. It is clear that this significant increase in back pressure and associated frictional heating has a major effect on the chromatography obtained.

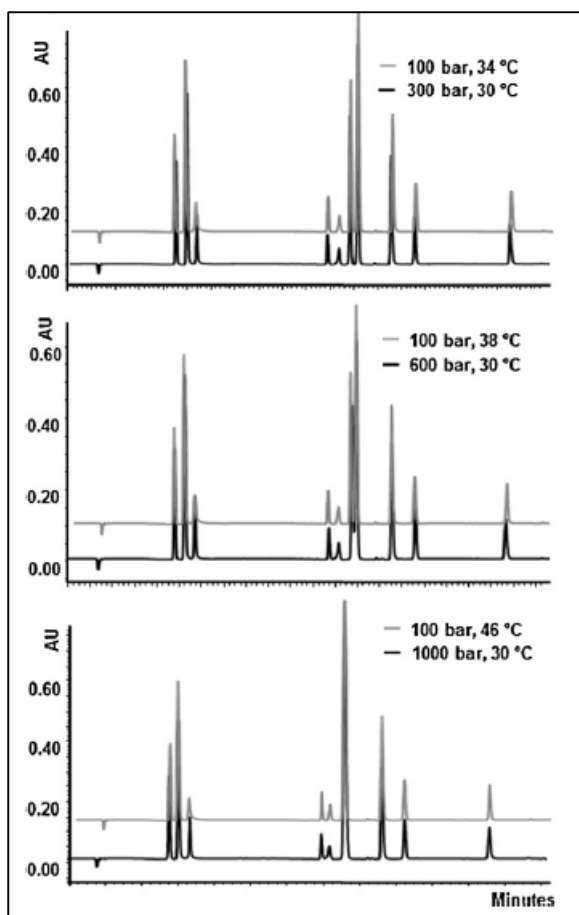


Fig 1.1.2. Estimation of frictional heating using overlay chromatograms obtained at 300, 600 and 1000 bar and its corresponding temperatures. Data obtained on an Aquity BEH C₁₈ column (50 x 2.1 mm, 1.7 μm) at 34, 38 and 46°C. Reproduced from Ref. [10]

Additionally, this increase in back pressure means that conventional HPLC instruments with a pressure maximum of 400 bar can no longer be used. Therefore it is necessary to use specialised ultra-high pressure instruments which are capable of reaching 1000 bar. The need for specialised instruments make moving to smaller particle sizes unattractive due to the cost associated with replacing existing conventional LC instruments.

An alternative to sub 2 μm stationary phases which have been re-developed in recent years is core-shell stationary phases. Core shell particles offer sub 2 μm column performances without the added back pressure constraints and have become a very attractive alternative. These stationary phase technologies will be discussed in more detail below.

1.2 Core shell stationary phases and their place in high performance liquid chromatography (HPLC)

A huge area of interest in the last 7 years in chromatographic research has been the use of core-shell particles as stationary phase materials. “Core shell” or “superficially porous” particles, as their names suggests, are particles which involve a solid silica core around which there is a porous shell. For the purposes of this review, these particles shall be referred to as core-shell particles throughout, unless otherwise stated.

Core shell particles are by no means a new stationary phase technology. These particles have been in existence for nearly 50 years since the early days of modern LC [12]. However, despite their inception in the 1960's, core-shell stationary phases were slow to evolve [13-15]. It has only been in recent years that the focus of chromatographic research has reverted back to these particles types, primarily since they became commercially available in 2006 [16].

1.2.1 Coreshell stationary phases from a historical perspective.

1.2.1.1 First generation core-shell particles

The primary driver for the development of early core-shell particles was to increase efficiency, as diffusion through a thin porous shell, rather than through a fully porous particle, (which at the time were in the region of 80 μm) would be faster and thus more efficient[17]. Kirkland first mentioned the use of modified glass bead supports modified with a porous thin layer for use in gas liquid chromatography in 1965[13]. These glass particles ranging in size from 60-80 μm and were modified in one of two ways; 1) coating with a 0.1- 1 μm layer of diatomaceous earth or 2) coated with a silica sol of the same dimensions. These particles were packed into columns and coated with a liquid phase and used as stationary phases for gas chromatography (GC). Kirkland[13] reported that beads modified with thin porous films significantly improved the performance of glass beads as a support for GC. He also reported reduced HETPs for modified beads when compared to unmodified beads at higher linear velocities both for the diatomaceous earth coated beads and those coated with

silica sol as shown in Fig. 1.2.1 below illustrates HETP plots for naphthalene both on unmodified silica supports and those modified with silica sol or a layer of diatomaceous earth. When compared with unmodified glass beads at higher linear velocities, those modified with a silica sol or diatomaceous earth layer have significantly shallower Van Deemter curves, indicating greater efficiency at higher linear velocities.

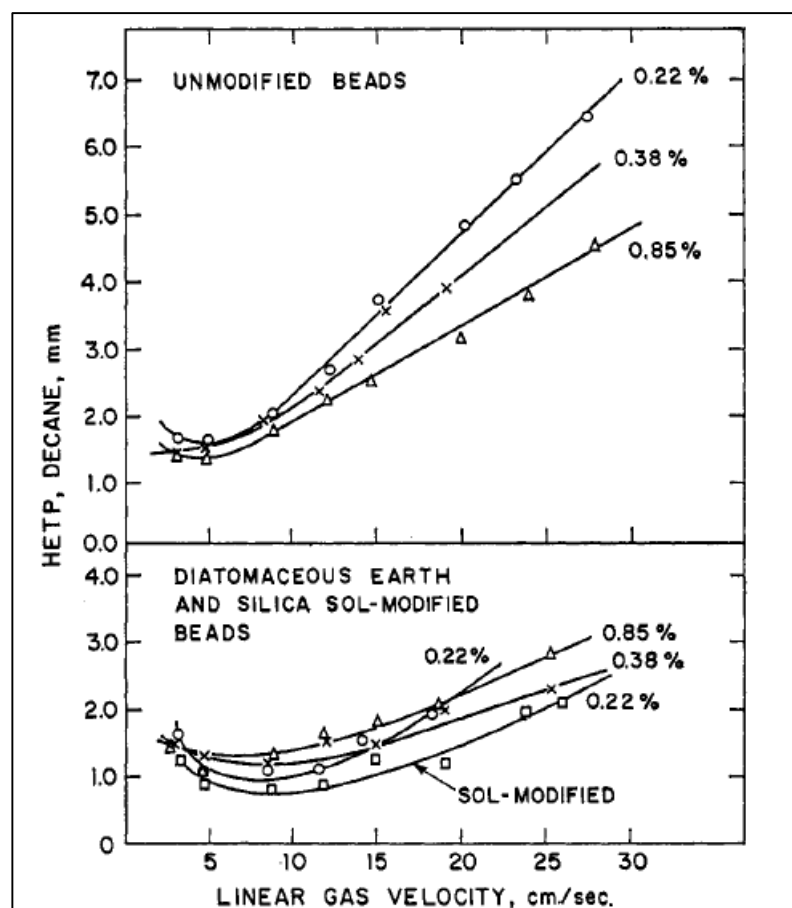


Fig. 1.2.1: HETP vs. flow rate plots for Naphthalene. Columns are modified and unmodified glass spheres of 60-80 μm in diameter for gas chromatography. Reproduced from ref [13]

Around this time Horvath and Lipsky[15] also suggested the use of pellicular particles instead of fully porous particles as stationary phases. These particles consisted of a “thin skin” coating on the surface of a glass support. The authors coated an ion – exchange resin on the surface of glass spheres and used these for the rapid separation of nucleoside phosphoric acids. These pellicular particles were produced by coating 50 μm glass spheres with a solution of styrene, divinylbenzene and benzyl peroxide in ether. The solvent was then evaporated and the resulting

coating polymerised and cross-linked at 90°C and further converted into an anion exchange resin with benzyl – dimethylammonium. They were then packed into a 19 cm, 1 mm i.d. column and used for the separation of a variety of nucleotides including adenylic acid (AMP), urydylic acid (UMP) and guanylic acid (GMP). The results showed a significant decrease in analysis time (of ~ 90 mins) compared to more commonly used column chromatography using a strong anion exchange resin which required more than 20 hours to separate the same components[15].

Again in 1969 Kirkland[14] reported the use of “controlled surface porosity” (CSP) supports for LC and GC, similar to what he reported previously. However the core of these materials was silica based rather than glass based. These CSP supports differed from Horvath’s pellicular particle as they had a thicker layer or “shell” of a controlled thickness and pore size. Kirkland reported better performance of these new CSP’s when compared to both GC and LC. In GC, the occurrence of pools of liquid at contact points in glass beads in traditional stationary phases was eliminated with CSP’s which lead to increased efficiency. It was also found that an increase in linear velocity could be achieved, without a significant decrease in efficiency. At a linear velocity of 0.4 cm/sec, plate height of 0.4 mm were achieved, for benzyl alcohol, while at a higher velocity 4 times that at 1.6cm/sec, plate heights of ~0.6 mm were achievable. This is in comparison to plate height for the same compound using a diatomaceous support of 1.0 mm at 0.4 cm/sec, increasing to 2.0 mm at 1.2 cm/sec, at which point no further data is recorded, this is illustrated below in Fig. 1.2.2. In liquid – liquid chromatography (LLC), when compared with columns packed with diatomaceous earth, there was a significant decrease in HETP. This decrease was attributed to the contributions to resistance to mass transfer of the two particle types with CSP’s being significantly better. Their mechanical strength and spherical shape resulted in higher column stability and better column reproducibility and were designed to be suitable for use with LLC[17]

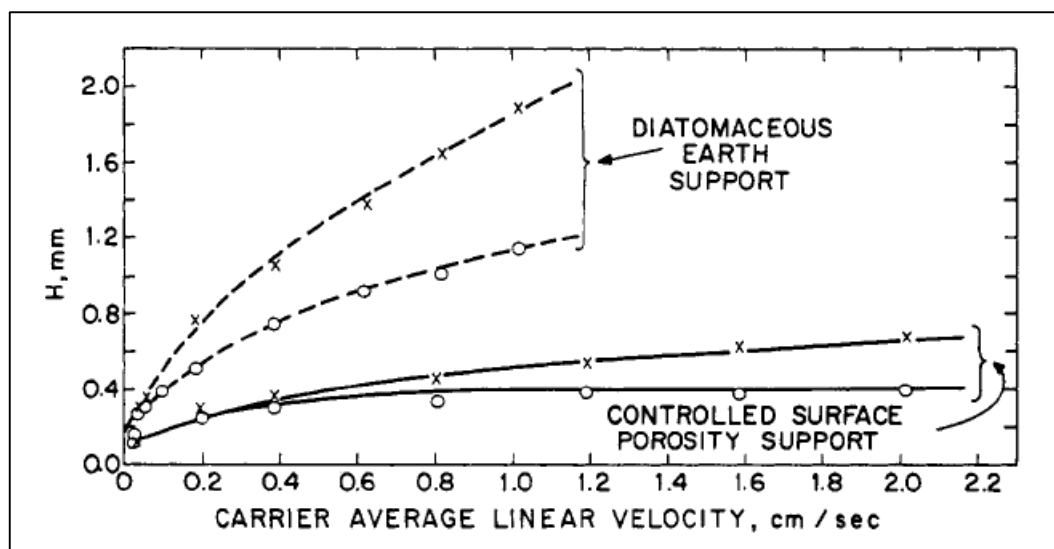


Fig. 1.2.2: Comparison of diatomaceous earth vs. controlled porosity for LC showing reduction in H for controlled porosity particles. Reproduced from ref [14]

While these particles showed potential and some particles were eventually commercialised under the trade name Zipax amongst others, for these types of separations they quickly fell out of favour due to their inherent irreproducibilities.[17] Guiochon and Gritti [17] also attributed Van Deemter plate theory[5], which approximated that column efficiency was inversely proportional to the particle size, for the demise of pellicular and core-shell particles during this time as much work was being carried out on reducing the particle size of fully porous particles in order to increase efficiencies[5]. Comparing the scales used for the HETP vs. linear velocity plots shown in Fig. 1.2.2 with those which will be shown later in Fig. 1.2.6, there is a 3-order of magnitude decrease in both the scale used for linear velocity (going from cm/sec to mm/sec) and HETP (mm to μm) in modern day Van Deemter plots. It is clear that these pellicular and CSP particles were vastly inferior to what was to come later, as illustrated in sections 1.2.1.2 to 1.2.1.3.

1.2.1.2 Second generation core-shell particles

While smaller fully porous particles were preferred over larger core-shell particles due to their much smaller diffusion path lengths and higher sample load capacity, Kirkland[18] observed that core-shell particles still had an advantage over fully porous particles for some applications, for example, the separation of macromolecules favoured core-shell columns due to their size and poor diffusional properties. This then led to the development in the early 90's of a second

generation of core-shell particles which were especially designed for the separation of macromolecules[18]. The particles developed were 5 μm core-shell with a $\sim 1 \mu\text{m}$ porous shell, resulting in $\sim 7 \mu\text{m}$ particles, significantly smaller than the $\sim 50 \mu\text{m}$ particles which were reported in the past [13-15]. These particles were produced by co-spray drying an aqueous silica sol mixture and dense silica beads in order to produce a uniform porous shell around the solid core and subsequently sintering them to induce strength. The particles were then rehydroxylated for subsequent modification. These particles were used for size exclusion chromatography without further modification, while particles were modified with C_8 groups for reversed phase chromatography. The particles were compared with fully porous particles of approximately 8.7 μm in diameter. The authors found that for reversed phase chromatography, macromolecules could be separated in a fast time using flow rates higher than is possible for fully porous particles. Fig. 1.2.3 below shows the separation of 5 macromolecules in less than 90 sec with a flow rate of 5 ml/min and a back pressure of 150 bar. The flow rate used in this study for the fully porous particles in this study was 2.0 mL/min.

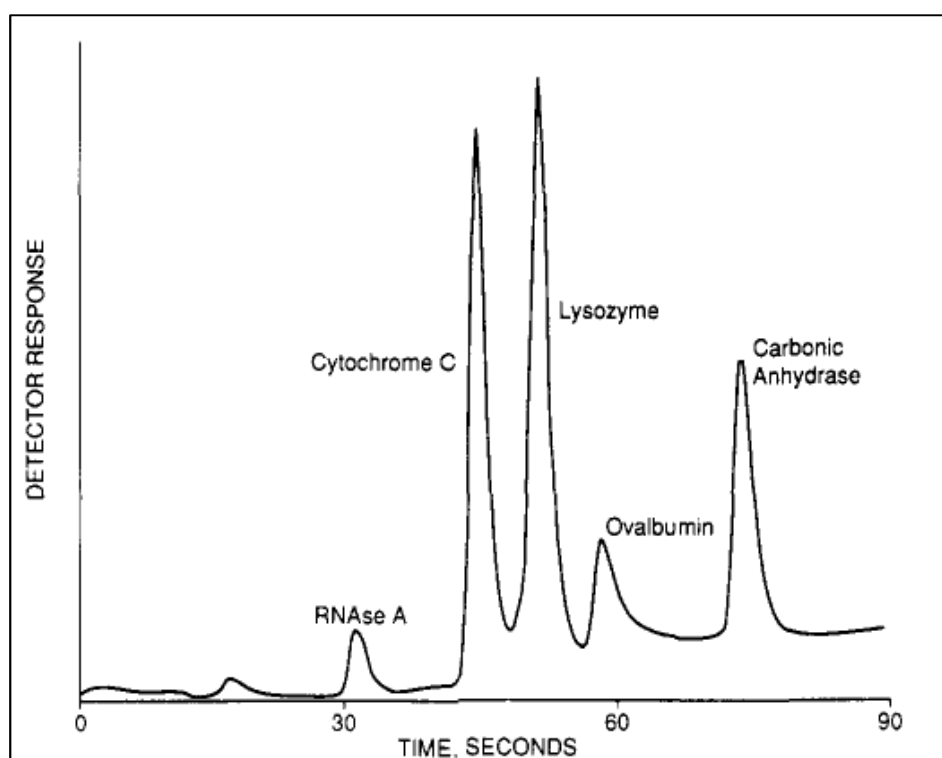


Fig. 1.2.3: Separation of proteins using “poroshell” column, 15x0.46cm, Conditions: Gradient mobile phase 25% ACN/0.1% TFA to 75% ACN/0.1% TFA in 4 mins, flow rate 5.0 mL/min, column temp: 80°C. Reproduced from reference [18]

Kirkland suggested that these superficially porous particles were better suited to the separation of macromolecules rather than small molecules as diffusion of large molecules in and out of pores was significantly slower than small molecules, resulting in enhanced kinetic properties of thin porous shell which proved more useful for large molecules rather than small [18]. Around the year 2000, this stationary phase was marketed commercially as “Poroshell” by Agilent[19] for the separation of macromolecules and while they proved superior for the separation of proteins and peptides[20, 21] with authors quoting an increase of 50% in peak capacity obtained compared to their fully porous counterparts [21], they met with limited success, most likely due to their niche market applicability.

1.2.1.3 Third generation core-shell particles

The drive towards ever decreasing particle sizes resulted in the development of particles with diameters less than 2 μm . While these columns delivered increased efficiencies, the resultant back pressures meant they were no longer compatible with conventional standard HPLC systems. This led to a renewed interest in core-shell particles with the launch of the 2.7 μm Halo core-shell particle from Advanced Material Technologies in the mid 2000’s. This product then re-ignited the interest in core-shell technologies and a number of other companies followed suit such as Phenomenex with the launch of its Kinetex 2.6 μm column[22] and more recently its 1.7 μm column. The 2.7 μm Halo core-shell particle consisted of a 1.7 μm non porous silica core with a 0.5 μm thick shell[23]. These particles produced efficiencies which rivalled and even surpassed the efficiencies which could be obtained on sub 2 μm fully porous columns at the time. Typical reduced plate height which would be obtained on a fully porous particle was approximately 2 mm; however Halo core-shell particles were capable of obtaining reduced plate height of as small as 1.5mm for small molecules. Such efficiencies had never been seen before[23]. Additionally these particles demonstrated significantly lower back pressure than comparable sub 2 μm columns. Fig. 1.2.4 below shows a plot of back pressures obtained on Halo 2.7 μm columns versus, their fully porous 1.7, 1.8 and 1.9 μm counterparts. The plots showed a 3-4 fold decrease in the back pressures generated for Halo columns at 0.5 ml/min when compared to a 1.7 μm fully porous

column. Also noteworthy is that even at twice the speed (1.1 mL/min) the Halo column was still capable of producing a 35% decrease in back pressure when compared to the 1.7 μm fully porous particle. The comparable efficiencies paired with the drop in back pressure meant that core-shell particles became quite favourable.

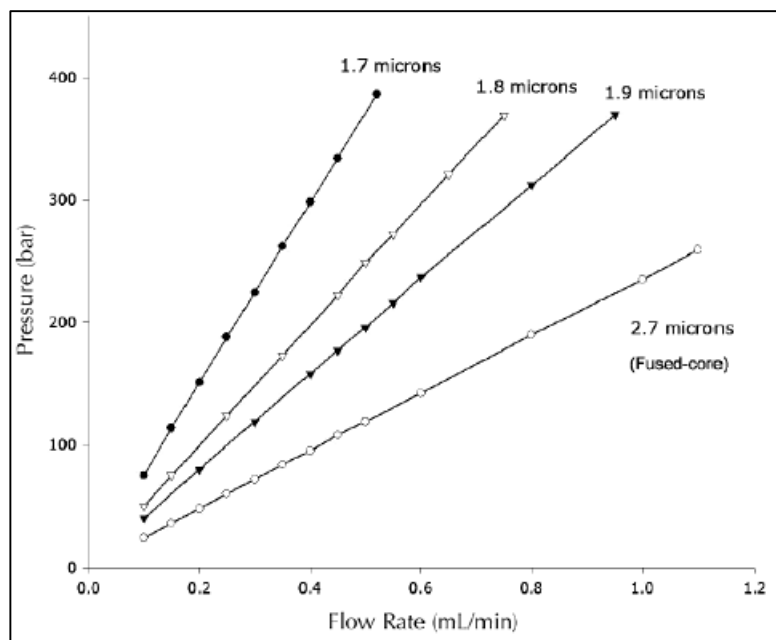


Fig 1.2.4: Column pressure plots for columns of sub 2 μm fully porous and core-shell particles and 2.7 μm core-shell particles illustrating lower back pressures for core-shell particles. Reproduced from Ref [23]

1.2.2 Properties of core-shell stationary phases

Core shell stationary phases are widely quoted as being of superior performance when compared to their fully porous counter parts. Intensive studies have been carried out to investigate the causes. Coreshell thickness and particle size distribution are hypothesised to influence performance most; these are discussed below.

1.2.2.1 Shell Thickness

Studies by Omamogho and Glennon [24], Gritti *et al.* [25, 26] and Kirkland [27] have found shell thickness is an important parameter in controlling the performance of columns packed with shell particles. A study by Omamogho and Glennon of an 1.7 μm core-shell column (EiS-150-C₁₈) which was packed in house, with a shell

radius of 0.15 μm versus a commercially available 1.7 μm core-shell column (Phenomenex Kinetex) with a shell size of 0.23 μm and two commercially available fully porous columns (Agilent Zorbax XDB 1.8 and Water Acquity BEH 1.7 μm) showed a significant decrease in the HETP obtained for Eis-150- C_{18} of 24% when compared to both the fully porous Zorbax column and the other 1.7 μm core-shell columns. Kirkland *et al.* [28] (see Fig. 1.2.5 below) found that at lower linear velocities, differences in the shell thickness do not show any significant difference in the reduced plate heights which are observed. However, at higher mobile phase velocity a thinner shell offers reduced plate height when a 4 μm fused core column with a 0.2 μm shell was compared to the same size particle with a 0.6 μm shell. This trend is in line with the expected improved mass transfer for the thinner shell, this is especially apparent for the higher molecular weight analyte verapamil.

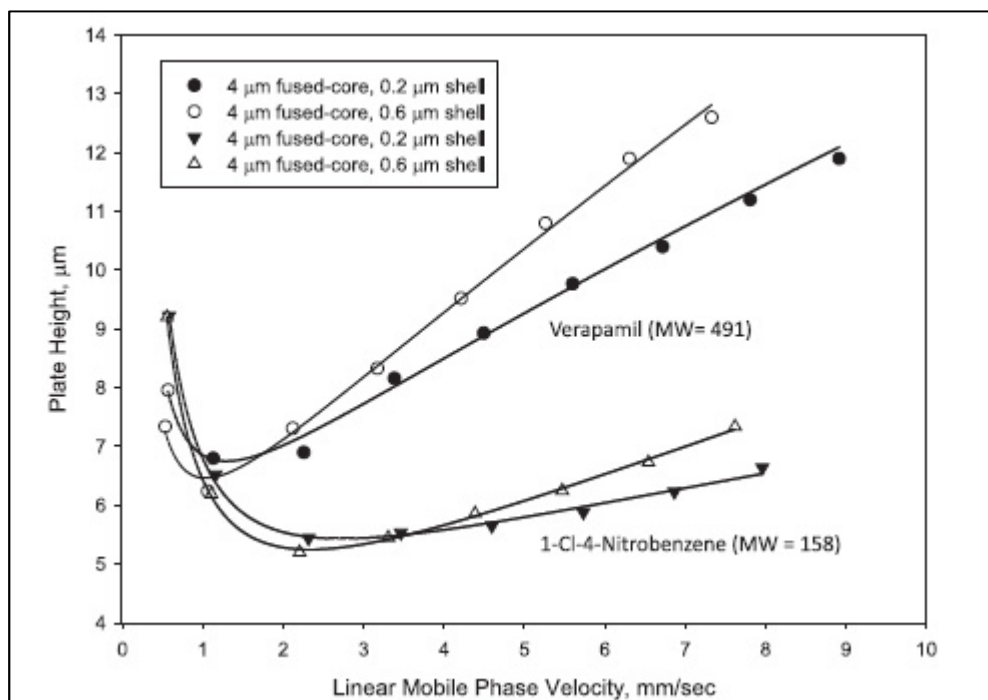


Fig. 1.2.5: Effect of porous shell thickness and solute molecular weight on column efficiency. Columns 4 μm fused core with 0.2 μm /0.6 μm shell. Mobile phase: Analytes 1-Cl-4-nitrobenzene and Verapamil Mobile Phase. 30% acetonitrile/70% 0.1% aqueous trifluoroacetic acid, Temperature: 40°C Reproduced from ref[28]

Omamogho *et al.* [29] also reported better efficiencies with thinner shell sizes. For three 1.7 μm EiroshellTM C_{18} (EiS- C_{18}) with shell sizes of 150, 250 and 350 nm resulted in, reduced plate heights (h_{min}) of 1.9, 2.2 and 2.5 respectively. The contributions of the B-term to h_{min} were 0.43, 0.66 and 0.79 for the three respective shell size. This decrease with decreasing shell size was attributed to a number of

factors including: 1) reduced porosity with decreasing shell size – porosity is governed by shell size so solutes spend less time in the column and band broadening is reduced and 2) the ratio of solid core to shell size – a larger shell size and smaller core provide more column area for solute to interact with.

A concern with core-shell particles is their volume fraction will be substantially lower due to their partially porous nature and thus their loading capacity will be much lower than that of fully porous particles. For some core-shell particles this has proved somewhat unfounded with studies showing that core-shell particles such as Halo 2.7 μm core-shell particles, with a shell diameter of 0.5 μm , retained a volume fraction of 80%, however other similar sized core-shell particles, such as Kinetex 2.6 μm core-shell particles only maintained a volume fraction of 58% when compared to their fully porous counterparts [30]. This is the only study which has been carried out and there is a lack of other substantial evidence to validate or nullify these concerns. Therefore no definitive conclusion can be drawn on whether core-shell particles can maintain the same sample loading capacity as their fully porous counterparts without significantly more research.

1.2.2.2 Particle size distribution

A parameter which sets core-shell particles apart from their fully porous counterparts is their particle size distribution. A narrow particle size distribution is important as it leads to greater packing efficiency and in turn leads to a reduced A term in the Van Deemter equation – a major source of band broadening and loss in efficiency. Because core-shell particles consist of a solid core, the size of this core is better predicted leading to a narrower size distribution of particle sizes[31]. Gritti *et al.*[32] report a standard deviation of 5% in particle size distribution for Halo 2.7 μm core-shell particles while a much larger standard deviation of 13% is seen for a column packed with porous 3 μm type B silica. Type B silica is a newer generation silica which is synthesised from an organic sol starting material, as opposed to inorganic sol (type A)[33]. The primary advantage of this type of silica is its trace levels of metal impurities compared to type A silica resulting in the lack of need to base deactivate the silica support for analysis of more basic compounds required when higher levels of metal impurities are present. The difference in particle size

distribution between porous particles and their fully porous counterparts is also shown by DeStefano *et al.* [23] who report a standard deviation of 5-6% for core-shell particles and 19% for fully porous particles. Omamagho and Glennon[24] report a massive 33% and 27% standard deviation for zorbax XDB 1.8 μm and Acquity – BEH 1.7 μm fully porous particles respectively. This is compared to a standard deviation of just 6.1% and 5.2% in the case of Kinetex 1.7 μm and Eiroshell Eis-150 core-shell particles respectively. As previously noted, a narrow particle size distribution leads to a reduction in the packing term (A) of the Van Deemter equation leading to higher efficiencies. For this reason, core-shell particles packed columns are a very attractive alternative to fully porous particle packed columns.

1.2.3 Comparison of the efficiencies of fully porous stationary phases to core-shell stationary phases

1.2.3.1 Van Deemter plots

As mentioned previously, the Van Deemter equation (Eqn (i)) [5] was one of the first applications of rate theory and its relationship to column efficiency. This equation is used to predict the optimum linear velocity (u) at which the lowest plate height (h) can be achieved, taking into account the physical, kinetic and thermodynamic properties of separation.

$$H = A + \frac{B}{u} + Cu \quad \text{Eqn (i)}$$

Van Deemter theory[5] suggests that smaller particle sizes leads to increased efficiencies and thus smaller plate heights due to a reduced C term as a result of better mass transfer properties, due to shorter diffusion path lengths of smaller particles and also a reduction in the A term. This theory can also be applied to core-shell particles where a key advantage of core-shell columns is their lower H value when compared with fully porous columns of the same particle size and dimensions. DeStefano *et al.*[28] showed that when a 5 μm core-shell column was compared with a 5 μm fully porous column, core-shell plate heights (HETP) were significantly reduced both for small molecules and larger molecule. Fig 1.2.6. below shows a representative Van Deemter plot, where for the larger verapamil solute, a minimum HETP of ~6.1 mm for the core-shell particle column and ~10.8 mm fully porous

particle column respectively were obtained and a minimum HETP of ~5.4 mm and ~10.7 mm for the core-shell and fully porous particle columns respectively were obtained for the smaller 1-Cl-4-nitrobenzene solute.

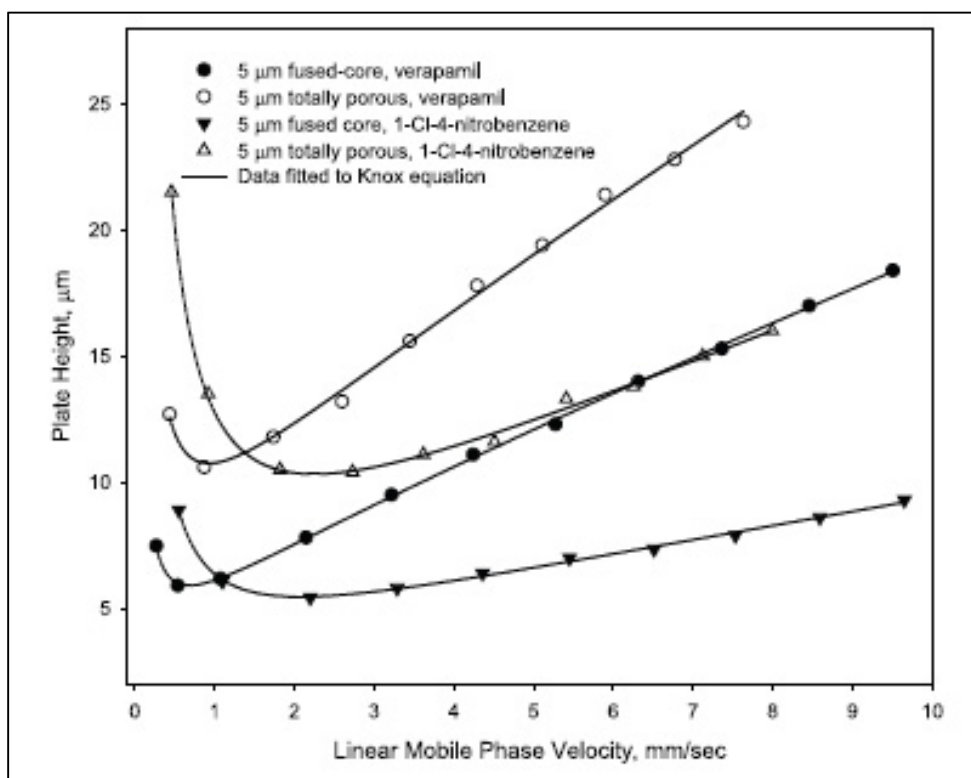


Fig 1.2.6: Comparison of Fused-Core and totally porous particles. Columns: 4.6 mm×150 mm; 5 μm Halo fused core with 0.6 μm shell and 5 μm totally porous particles. Analytes 1-Cl-4-nitrobenzene and Verapamil – Mobile phase: 35% acetonitrile/65% aqueous 0.1% trifluoroacetic acid; temperature 40°C. Reproduced from Ref [28]

As seen, core-shell columns are capable of producing higher efficiencies when compared to fully porous columns packed with particles of the same size, as a consequence it can be theorised that larger core-shell particles are capable of producing efficiencies as good if not better than comparable smaller fully porous particles. This theory was proven in the work of Oláh et al.[34], where a 2.6 μm Kinetex core-shell column showed similar and often improved minimum plate heights when compared its smaller fully porous counterparts. The 1.7 μm Acquity and 1.9 μm Hypersil Gold fully porous particles were shown to have a minimum plate height of 4.6 μm and 5.4 μm respectively while the Kinetex 2.6 μm core-shell particle had a minimum plate height of 5.0 μm when estradiol was analysed. As can be seen from the analysis of Van Deemter plots, core-shell particles show increased efficiencies when compared to their fully porous counterparts, which further

supports the argument that core-shell particles can out-perform their fully porous counterparts.

1.2.3.2 Knox plots

However, while the Van Deemter equation is widely used, it still has its limitations, with one of the main limitations being that the Van Deemter plot is dependent on particle size and is also system specific [35]. This has led to the equation being modified to become the Knox equation [36]. The advantage of the Knox equation for comparing core-shell columns is that particle size is independent, as will be discussed below, and also takes into account the porosity of the column. The Knox equation (Eq.(ii)) is given below.

$$h = Av^{0.33} + \frac{B}{v} + Cv \quad \text{Eq. (ii)}$$

Similar to the Van Deemter equation A, B and C are constants which define a set of constants pertaining to diffusion and mass transfer of the mobile phase. A is eddy diffusion combined with mobile phase mass transfer, B is longitudinal mass transfer, C is stationary phase mass transfer, h is reduced plate height and v is reduced velocity. While the Van Deemter equation treats all contributions to band broadening as individual contributions, the Knox equation differs here, as mass transfer is split into two types, mobile phase mass transfer and stationary phase mass transfer. Stationary phase mass transfer becomes term C while eddy diffusion and mobile phase transfer become term A[36]. The reason given by Snyder et al.[37] for this is due to the fact that where two interparticle flow streams recombine, there is a loss in velocity due to remixing, therefore it is necessary to treat these two processes as a single band broadening event. Knox [35] also stated that this combined A term is by far the most important contribution to dispersion and band broadening.

It is also necessary to note that the Knox equation is a dimensionless equation[38]. This equation is particle size independent, both the HETP (H in Van Deemter equation) and mobile phase velocity (u in Van Deemter equation) are calculated to be independent of particle size giving rise to reduced plate height (h) and reduced velocity (v). “h”, the reduced plate height is calculated as plate height divisible by

the mean particle diameter (d_p) (Eq. (iii)) while “ v ” the reduced velocity is a function of particle size, “ u ”, the linear velocity and also the diffusion coefficient of the analyte in the mobile phase (D_M). (Eq. (iv)). Knox stated that the advantage of using reduced parameter such as “ h ” and “ v ” was that columns of different particle size and the use of different eluents could be directly compared as well as comparisons between two different chromatographic system such as GC and LC[39].

$$h = H/d_p \quad \text{Eq. (iii)}$$

$$v = ud_p / D_M \quad \text{Eq. (iv)}$$

Cunliffe and Maloney used a Knox plot to compare the performance of sub 2 μm fully porous particle columns to core-shell columns independent of their particle size[16]. Columns chosen for this study included, Supelco Ascentis Express C_{18} 2.7 μm , Advanced Material Technology Halo C_{18} 2.7 μm along with a range of sub 2 μm fully porous particles. This study found that the core-shell columns had a reduced plate height of approximately 2 in the case of the Ascentis C_{18} and of less than 2 for the Halo C_{18} column. This is compared to reduced plate heights of ~ 3 for Zorbax and Acquity fully porous columns and ~ 4 in the case of the Thermo columns tested. Fig 1.2.7 below illustrates representative Knox plot obtained. This study showed that despite the larger particle size, core-shell columns were still capable of producing efficiencies which were as good if not surpassing that of fully porous columns with smaller particle sizes. Another point to note here is that the core-shell columns continue to maintain low reduced plate height at higher reduced linear velocities when compared to the fully porous columns. As both the Van Deemter and Knox plots have demonstrated, efficiency is superior on core-shell columns when compared to their fully porous counterparts. The advantage of Knox plots versus Van Deemter plots is the fact that Knox is dimensionless. While Van Deemter plots are capable of comparing columns of different particle sizes, Knox plots provide direct comparison of column efficiencies or plate height, as particle size and linear velocity are independent.

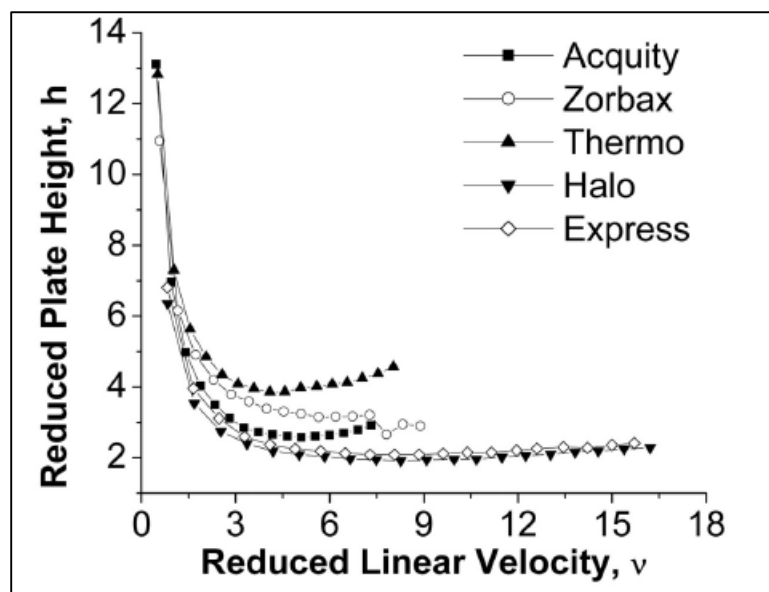


Fig. 1.2.7: Knox plots for Naphthalene for the five columns analysed. Column dimensions 2.1 x 100 mm. Particle sizes: Acquity: 1.7 μm , Zorbax: 1.8 μm , Thermo: 1.9 μm , (all fully porous particles) Halo: 2.7 μm , Express: 2.7 μm (both core-shell particles) Mobile Phase: 50:50 ACN:Water. Reproduced from Ref. [16]

1.2.3.3 Kinetic Plots – Poppe plots

In recent years kinetic plots such as Poppe plots, have been developed as another tool by which LC columns of different particle types and sizes can be compared against each other[40]. Unlike Knox and Van Deemter plots, Poppe plots take into account the permeability of columns as well as maximum operating pressure in their calculations. They are used to help visualise the compromise between speed and efficiency in isocratic mode, or peak capacity in gradient mode [41]. Poppe plots allow optimal conditions such as flow rate and column length to be determined under a given set of separation conditions such as a fixed run time and utilising the maximum pressure attainable on a column, as a result it is possible to compare different column types and length under ideal conditions rather than arbitrary conditions[42]. Poppe plots consist of N (number of theoretical plate) plotted against plate time (t_0/N) which is a measure of void time (t_0), divided by plate number in the case of isocratic separations[43]. This was further expanded by Wang *et al* [44] to include gradient separations where plate time is replaced with gradient time (t_g) and theoretical plates by peak capacity (n). Poppe plots can either be constructed using Van Deemter or Knox values for plate height(H) and linear velocity(u). Using a

range of void volumes (t_0) together with linear velocity of an unretained solute(u) interstitial linear velocity (u_e) and total and interstitial porosity (ϵ_{tot} , ϵ_o) column lengths (L) are determined by Eq. (v), this in turn is used to calculate the pressure drop (ΔP) which is calculated by Eq. (vi) where Φ is the flow resistance, η is mobile phase viscosity and d_p is particle size[42]. The optimal plate count (N) and plate count production (N/t_0) can then be calculated and a Poppe plot constructed as shown in Fig. 1.2.8

$$L = ut_0 = \left(\frac{\epsilon_o}{\epsilon_{tot}} \right) u_e t_0 \quad \text{Eq. (v)}$$

$$\Delta P = \Phi \eta \frac{u_e L}{d_p^2} \quad \text{Eq. (vi)}$$

Zhang *et al* [42] used these Poppe plots to compare the performance of 2.7 μm superficially porous particles with a pressure limit of 600 bar with sub 2 μm fully porous particles with a pressure capacity of 1000 bar. A theoretical Poppe plot comparing both stationary phases is shown below in Fig. 1.2.8. The plot shows that on the left side which equates, both curves converge which indicates that both columns produce similar efficiencies when the analysis is very fast ($t_0 < 10\text{s}$) while on the right hand side of the graph, the curves begin to diverge and the 2.7 μm core-shell column (B) (backpressure 570 bar) outperformed the 1.7 μm fully porous column (A) (back pressure 950 bar) at longer analysis times, with a 2 fold increase in plate counts even at $t_0 > 1000$ sec. This plot also shows that for a theoretical column packed with 2.7 μm fully porous particles (C) run at the same pressure of the core-shell column (570 bar), the core-shell column would theoretically still outperform its fully porous counterpart both on the left at very fast conditions and on the right where the dead time is greater than 1000 sec.

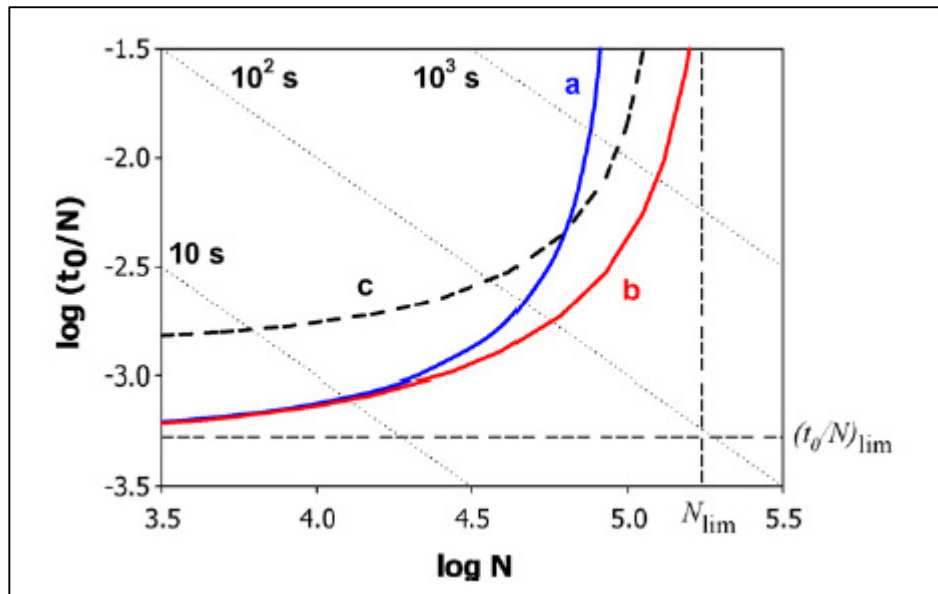


Fig. 1.2.8: Theoretical isocratic Poppe plots for packed bed columns. Each dotted line represents a constant column dead time. Case a: 1.7 μ m BEH C18 at $\Delta P_{max} = 950$ bar. Case b: 2.7 μ m Halo C18 at $\Delta P_{max} = 570$ bar. Case c (hypothetical): 2.7 μ m BEH C18 at $\Delta P = 570$ bar. Reproduced from Ref [42]

This theoretical model was proved to be quite accurate under experimental conditions where slightly higher plate counts were observed for the fully porous column for very fast separations whereas the total analysis time was 40% shorter for the superficially porous column for a 5cm column while at longer column lengths of 45 cm, the core-shell column was seen to outperform the fully porous column with both higher plate counts and shorter analysis times. Table 1.2.1 below shows a comparison of the calculated and experimental data for dead time, plate count and back pressure for both the fully porous and core-shell columns. There are no significant differences between the experimental and calculated values which indicates that the theory is quite accurate and gives a good indication of column performance at maximum pressures.

Table 1.2.1: Comparison of the calculated and experimental column dead time, plate count and backpressure on Halo C18 phase and BEH C18 phase at various column lengths. Reproduced from Ref [42]

BEH C18 L (cm)	Calculated F (ml/min)	Calculated			Experimental			T_{inlet} (°C)	T_{outlet} (°C)
		t_0 (s)	N_{max}	ΔP (bar)	t_0 (s)	N	ΔP (bar)		
5	1.07	5.2	7400	950	5.2	6200	917	22.3	31.3
10	0.53	20.9	20900	950	21.7	18900	823	22.0	27.2
15	0.36	47.0	33400	950	46.0	28600	914	21.4	25.5
30	0.18	188.2	56500	950	188.3	55400	986	21.3	22.0
45	0.12	423.4	67200	950	433.3	64700	976	21.0	21.7
Halo C18 L (cm)	Calculated F (ml/min)	Calculated			Experimental			T_{inlet} (°C)	T_{outlet} (°C)
		t_0 (s)	N_{max}	ΔP (bar)	t_0 (s)	N	ΔP (bar)		
5	1.55 (1.50 ^a)	3.1	4800	570	3.2 ^a	5900 ^a	595 ^a	22.6	28.3
10	0.78	12.5	15100	570	12.5	16000	573	22.2	26.5
15	0.52	28.2	27100	570	29.5	26000	551	22.3	25.3
30	0.26	112.9	60300	570	117.4	55800	565	21.9	23.6
45	0.17	254.0	84700	570	270.8	76800	563	21.1	22.0

^a Experiment on the 5 cm Halo C18 column was conducted at 1.50 ml/min due to its higher pressure.

Wang *et al.* [45] also report similar findings to Zhang[42] shown in Table 1.2.2, stating that 2.7 μm core-shell columns gave better performance over their smaller 1.8 μm fully porous counterparts and indeed 1.7 μm core-shell stationary phases at longer run times when the dead time is in excess of 30 sec. When similar particle sizes were compared (2.7 μm core-shell particle and 3.0 μm fully porous) there was a 36% increase in efficiency for core-shell particles with efficiency rising from 140,000 to 191,000. Also while larger particles are more efficient at longer run times, it was also shown in this analysis that the smaller 1.7 μm core-shell column outperformed the fully porous particle at shorter dead times of >10 sec with an increased plate count of approximately 8% from 20,200 to 21,800. This increase was not as significant as seen for larger particles, however showed that 1.7 μm core-shell particles are capable of equalling and slightly out performing their fully porous counterparts.

Table 1.2.2: Comparison of optimum conditions from the analysis of Poppe plots obtained for fully porous 1.8 μm and 3.0 μm particles and 1.7 μm and 2.7 μm superficially porous particles. Reproduced from Ref [45]

Optimization results	2.7 μm SPPs (600 bar)	1.7 μm SPPs (1000 bar)	1.8 μm totally porous (1000 bar)	3.0 μm totally porous (600 bar)
$t_0 = 10\text{ s}$ ($t_R = 1\text{ min}$)				
Optimum L (cm)	10.5	8.5	8.4	10.9
Optimum u_e (cm/s)	1.36	1.11	1.25	1.63
N_{max}	17,300	21,800	20,200	11,900
$t_0 = 100\text{ s}$ ($t_R = 10\text{ min}$)				
Optimum L (cm)	33	27	27	34
Optimum u_e (cm/s)	0.43	0.35	0.40	0.51
N_{max}	81,600	68,900	62,400	56,700
$t_0 = 1000\text{ s}$ ($t_R = 100\text{ min}$)				
Optimum L (cm)	105	85	84	109
Optimum u_e (cm/s)	0.14	0.11	0.13	0.16
N_{max}	191,600	132,700	108,900	140,000

^a Calculation conditions: 40 °C, 30/70 acetonitrile/water, D_m is 1.0×10^{-5} cm²/s.

Wang also points out the ability of the 2.7 μ m core-shell column to be run on a conventional HPLC system with pressure capabilities of 600 bar when extra band broadening is minimised. Thus for slightly lower efficiencies, it is possible to carry out ultrafast separations without the need to purchase expensive high pressure instruments. Another hypothesis which both Wang[45] and Zhang [42] share is that should the back pressure capabilities of the 2.7 μ m core-shell column extend to 1000 bar, efficiency could be further improved.

In conclusion, like Van Deemter and Knox plots, Poppe plots have been shown to be another useful tool in critically comparing column types. Poppe plots provide a more sophisticated method of comparing columns than either Van Deemter or Knox plots. Poppe plots allow optimised conditions e.g. linear velocity (μ) and column length (L) to be determined whilst keeping separation conditions constant, i.e. maximum back pressure and a fixed run time instead of arbitrary values used in Van Deemter and Knox plots.[42] Poppe plots have shown core-shell particles are capable of providing better efficiencies than their smaller fully porous counterparts. Theoretical Poppe plots have also demonstrated that when back pressure capabilities are increased to 1000 bar, 2.7 μ m core-shell columns, have the potential to provide even greater improvement in efficiencies.

1.2.4 Application of core-shell particles

Much of the work carried out on the new generation of core-shell stationary phases has been related to investigation of effect of particle size distribution on efficiency of core-shell particles[23, 24, 32], determination of an optimum shell thickness and their associated mass transfer kinetics [24-26, 29, 32]. Considerable work has also been carried out on column efficiencies in terms of Van Deemter plots [28, 34], Knox plots [16] and kinetic plots such as Poppe plots[42, 45]. However, there has been little work carried out on the evaluation of the core-shell column under real chromatographic conditions. Some of the work which has been carried out has focused on the area of protein separation and is shown below.

The analysis of proteins was carried out by Fekete *et al.* [46] using Phenomenex Aeris™ WIDEPORE column with a 3.6 μ m particle size with a 0.3 μ m diameter. Filgrastin related proteins were separated using the Aeris column as well as other

fully porous and core-shell columns. The peak capacity (n_c) obtained for fully porous columns ranged from 50 to 87 for the most part. An Acquity BEH300 fully porous particle column performed better with a peak capacity of 103, this was comparable to the $n_c = 114$ achieved by the Aeris core-shell column, however this was still a 10% decrease in peak capacity. Fig. 1.2.9 below shows chromatograms of filgrastim related proteins obtained on both the Aeris WIDEPOR and Acquity BEH300 columns. A comparison of the chromatograms not only shows an increase in peak capacity but also a reduction in retention time of ~ 1 minute of the last eluting peak from ~ 5.2 min to ~ 4.0 minutes when the Aeris WIDEPOR column is used.

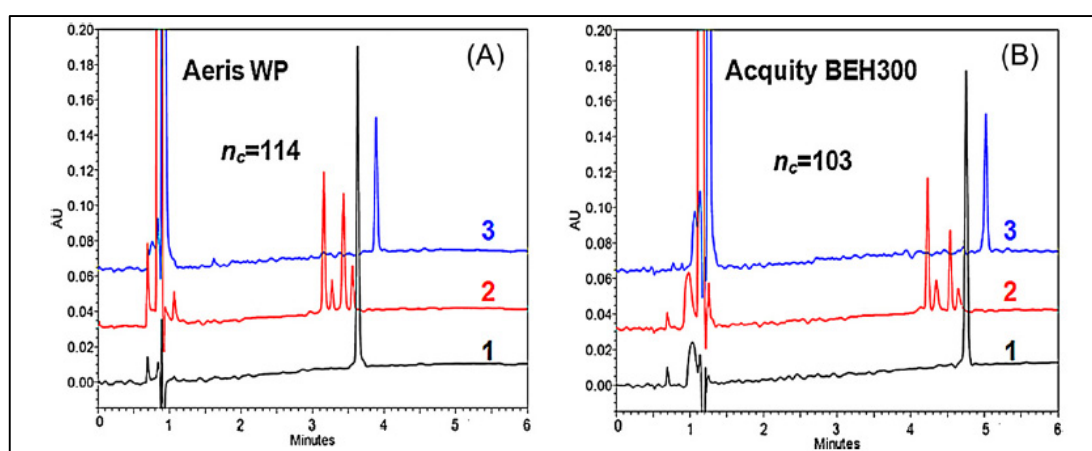


Fig. 1.2.9: Comparative chromatograms of filgrastim related proteins obtained with Aeris WIDEPOR (A) and Acquity BEH 300 (B) 150 x 2.1 mm columns. Chromatogram 1: native filgrastim, chromatogram 2: oxidised forms, chromatogram 3: reduced form. Conditions: Mobile Phase A: 0.1% TFA in water, mobile phase B: 0.1% TFA in acetonitrile, flow rate 300 μ L/min, linear gradient 45-65% in 6.5mins, temp 80°C, detection at 210 nm. Reproduced from ref[46]

Schuster *et al.* [47] carried a similar study where core-shell particle columns were used for a proteomic applications. Here, Advanced Material Technology Inc. Halo Peptide ES-C₁₈ of particle size 2.7 μ m with a shell diameter of 0.5 μ m was compared to fully porous Waters BEH C₁₈ column of 1.7 μ m for proteomic applications. Fig. 1.2.10 shows chromatograms of the separation of range of peptides on 3 different columns used in a peak capacity study, with two columns being core-shell (the only difference being the length of the column used) and one being a fully porous particle column. When comparing the core-shell particle column and fully porous column of the same dimensions, it is shown that the last peptide to elute on the Halo Peptide column, which was known to be Hel 11-7 does not elute in the gradient time on the

BEH column. It was also found that despite peak capacities being approximately 15% higher on the BEH column than the HALO peptide column, the back pressure is almost double that of the HALO Peptide column. The advantage of the core-shell column is shown to be the low back pressure which is associated with it. This is demonstrated by increasing the length of the column by 50% which increases the peak capacity by 9% from 278 to 303 when compared to the fully porous column, while still having a reduction in back pressure of 57% when compared with the shorter fully porous columns run at the same conditions.

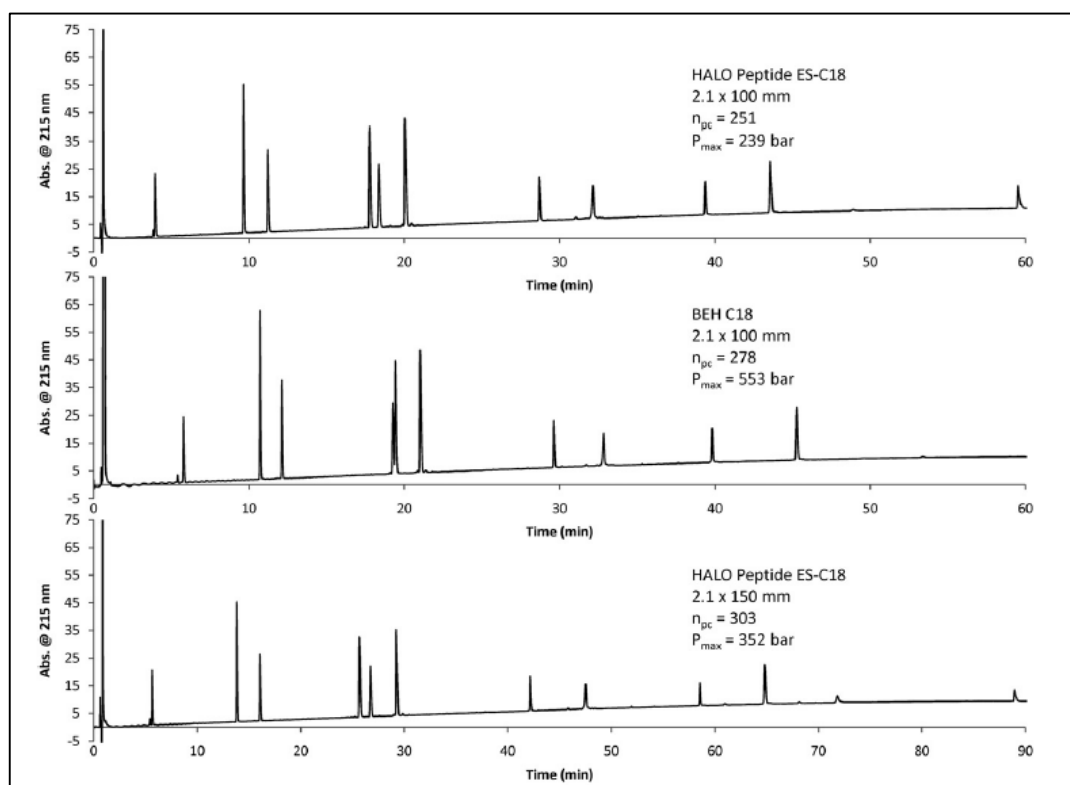


Fig 1.2.10: Representative chromatograms for peak capacity studies. Columns: 2.1 x100 mm HALO Peptide ES-C₁₈, 2.1 x 110 mm BEH C₁₈, 2.1 x150 mm HALO Peptide ES-C₁₈. Flow rate 0.5mL/min, Temperature 45°C; gradient 5-70% in 60 or 90 minutes, A; water/0.1% trifluoroacetic acid; B: 80/20 acetonitrile/water/0.1% trifluoroacetic acid; sample 15 μ L of 11 synthetic peptides (50 ng each). Reproduced from ref[46]

As can be seen core-shell particles have been shown to both match and often rival fully porous particles both of similar sizes and also smaller sizes in terms of efficiency. As seen in section 1.2.3.1, Kinetex 2.6 μ m core-shell particles provide similar and sometimes decreased plate heights (H) when compared to 1.7 μ m and 1.8 μ m core-shell particles. Shell size have been found to be an important parameter in

controlling efficiency with thinner shells providing better efficiency compared to thicker shells as discussed in section 1.2.2.1. Van Deemter, Knox and Poppe plots have provided further evidence of the capabilities of core-shell particles to provide efficiencies that rival their fully porous counterparts.

Much of the applications of core-shell particles have focussed primarily on the separation of proteins and peptides as shown above. The lack of publication of a significant amount of practical applications of core-shell particles could be linked to the trend Majors[8] found during his survey of HPLC column usage across the LC-GC community. Results of the survey found that at the time over 60% of HPLC users still use columns which are between 3 and 7 μm in size. The likely reason for this as hypothesised by Majors was the reluctance to replace larger particle columns with smaller particle columns due to the need for revalidation of method, unless it was absolutely necessary, therefore, industry and LC users in general are slow to adopt this new technology across a wider range of applications.

1.3 Supercritical Fluid Chromatography (SFC) – A greener alternative to HPLC

As mentioned in the introduction a primary driver in chromatographic research at present is the desire for faster, more efficient separations. For this reason, much of the research in HPLC has focussed on the development of new types of stationary phases capable of fulfilling this need. One such way which was discussed in detail in section 1.2 is the development of core-shell stationary phases as alternatives to fully porous sub 2 μm stationary phases. Another factor which is driving chromatographic research today is reduced solvent consumption and the strive for more environmentally friendly practices. While core-shell particles and reduction in stationary phase particles sizes are currently addressing both of these research drivers, there becomes a point at which, decreasing particle size and synthesis of novel core-shell stationary phases which continue to improve efficiency reaches its limit and further reductions in particle sizes will lead to increasing problems such as frictional heating. As a result other chromatographic techniques are being considered in the strive for continuous improvement in the field of separations, which as well as being equal if not superior to HPLC in terms of efficiency and speed, are also a more

environmentally friendly alternative. One such technique is Supercritical Fluid Chromatography (SFC).

SFC is a chromatographic technique which lies intermediate between LC and GC and possesses some of the characteristics of both[48]. The main mobile phase used in SFC is supercritical fluid instead of liquid. Supercritical fluids are neither gases nor liquids but possess properties which are intermediate of the two.[48] Supercritical fluids have a similar density and solvating power to some liquid solvents whilst maintaining more gaseous like properties such as low viscosity and high diffusivity.[49, 50] As a result of the increased diffusion capabilities and low viscosity of supercritical fluids compared to solvents used in HPLC, SFC is an attractive alternative as much higher linear velocities can be used which in turn leads to faster separations and higher throughputs[51]. According to Berger and Smith, packed column SFC when compared to LC is faster, more efficient, has a wider range of selectivity and produced less toxic waste[48]. One of the main supercritical fluids used in SFC is carbon dioxide (CO₂). CO₂ is an inexpensive, non-toxic gas which is produced as a by-product of natural processes such as fermentation and from the chemical industry. This makes it a greener alternative to traditional solvents used in HPLC such as methanol and hexane.[51] A brief history, principles and applications of SFC will be discussed in more detail in the proceeding sections.

1.3.1 SFC from an historical perspective

The inventors of SFC are considered to be Klesper *et al.* [52] in 1962. They describe the separation of porphyrins using supercritical chlorofluoromethanes which they marketed as high pressure gas chromatography. Around this time, Giddings *et al.* [53] carried out similar work, however very little further progress was made on this front at the time, due in part to the exponential growth of HPLC which was occurring around the same time.

It was not until the 1980's that SFC saw a major growth, where much of the work carried out in the 80's was using capillary columns which was likened to GC and used GC style open tubular columns and GC detectors such as Flame Ionisation Detection (FID), electron capture and sulphur chemiluminescence[49]. However, the application of open tubular SFC, according to Taylor, was limited to use in the

petrochemical industry, as the forerunners in the pharmaceutical industry at the time found the technique to be severely lacking due to its poor reproducibility and limited application range, in part due to the low solvating power and polarity of carbon dioxide alone. Another downfall of open tubular SFC was its inability to independently change flow velocity and pressure, the only means of changing pressure was by changing the flow velocity[54]

Around this time, packed column SFC was also being developed. This utilised modified HPLC hardware and is nowadays the most widely used form of SFC. The inclusion of a back pressure regulator allowed the supercritical fluid to be kept at a sufficient pressure to remain under supercritical conditions. The principle advantage of packed column SFC was the ability to directly control the flow rate and outlet pressure of the supercritical fluid independently, something which was not achievable with open tubular SFC.[49] The first commercially available SFC instruments were launched in the late 1990's with several vendors such as Hewlett Packard (now Agilent), JASCO and Gilson now manufacturing instruments. Modern SFC's were in essence the same as HPLC instruments, with the addition of a chilled CO₂ pump, a modifier pump and a back pressure regulator which allowed the pressure to be controlled independently of flow rate.[54]

1.3.2 SFC Hardware

Typical SFC instruments today are based primarily on HPLC instrumentation with adjustments made to accommodate the need for the supercritical fluid solvent – mainly CO₂, to be kept under appropriate conditions. In general, an SFC system consists of a HPLC and an external CO₂ conditioning module[55]. This module is used to transform gaseous CO₂ into its supercritical state. Without the need for LC pump compression requirements, this module cools the CO₂ prior to the pump and contains a back pressure regulator which controls the pressure of the system.

SFC systems are generally binary systems with a CO₂ pump and a second pump for liquid co solvent[51]. There are a number of types of injection including loop injection, in-line injection and in-column injection which allows samples to be directly injected onto the column without dilution. As a generally rule, any HPLC stationary phase can be used for SFC whether typically used for normal or reversed

phase. SFC is compatible with both HPLC detectors such as UV-Vis, diode array and chiral detectors as well as GC detectors such as FID[51]. At all times the instrument is a closed system, ensuring that CO₂ remains in its supercritical state.

1.3.3 What are supercritical Fluids?

A supercritical fluid is defined as a compound, mixture or element above its critical pressure and temperature[56]. Above a critical temperature and pressure, known as its critical point, a gas cannot be liquefied and exists in a state which is intermittent between a liquid and gas. Carbon dioxide is generally the supercritical fluid of choice for SFC due to its favourable operating conditions, purity, safety, ease of use and low cost[50]. CO₂ has a critical temperature of 31.1°C and a critical pressure of 73.8 bar. It is cheap and readily available, as it is produced as a by-product of chemical industry or natural processes such as fermentation[51]. It is non-toxic and has modest critical parameters, which are mentioned above. As well as this, CO₂ is an attractive alternative to liquid mobile phases like methanol and hexane in terms of waste generated, CO₂ can be de-pressurized post column and CO₂ can be vented or recycled, leaving samples dissolved in a small volume of organic modifier if present, decreasing the total amount of waste generated.[51] Other supercritical fluids such as ammonia have been used, however supercritical ammonia was found to give irreproducible results which may be due to the varying water content of ammonia. Another reason ammonia was seen to be less favourable is due to the fact that it is too aggressive and toxic for use. Ammonia, in the majority of cases, was also found to dissolve silica based materials [57] As the majority of stationary phases are made from silica based materials, this makes it very unsuitable for packed column SFC. Other supercritical fluids used included nitrous oxide which was argued to be a stronger solvent than supercritical Carbon dioxide sCO₂ [58]. However it was found to be entirely unsuitable due to its strong oxidising nature which in the presence of organic co-solvents proved hazardous and was not recommended for use in supercritical fluid chromatography [59].

1.3.4 SFC - a complementary technique to HPLC?

The power of SFC is linked to its primary mobile phase – supercritical fluid and in particular, its liquid like solvating power coupled with reduced diffusivity and viscosity when compared to LC. Diffusion coefficients of supercritical fluids are in the region of $1 \times 10^{-4} - 10^{-5} \text{ cm}^2 \text{ s}^{-1}$ while the diffusion coefficient for liquids and gases are $1 \times 10^{-5} - 10^{-6} \text{ cm}^2 \text{ s}^{-1}$ and $0.1-1.0 \text{ cm}^2 \text{ s}^{-1}$ [48], so while not nearly as diffusive as a gas, supercritical fluids are in the region of 10 to 100 more diffusive than liquids. Table 1.3.1 shows the viscosity of sCO_2 at a range of temperature compared with water and acetonitrile at the same temperature[60], sCO_2 at the same temperature, has at the very least viscosity approximately 1/5 to that of water and in some cases is as much as 20 times less viscous than water. This reduced viscosity and increased diffusivity allow higher flow rates to be used, all whilst keeping back pressure significantly lower than LC, with SFC having a 2/3 fold decrease in back pressure which in turn leads to the potential for longer columns to be used to improve efficiencies. [48, 60]

Table 1.3.1: Viscosity of sCO_2 (100, 200 and 400 bar), H_2O and Acetonitrile (CH_3CN) at different temperatures (20, 40 and 60 °C)

Temperature °C	CO_2 ¹⁴			H_2O ¹⁶	CH_3CN ¹⁶
	Pressure, bar				
20	100	200	400	100.2	35.3
40	8.3	10.3	13.0	54.7	29.2
60	4.9	8.0	10.8	46.7	24.5
	2.4	6.1	9.1		

The solvation power of CO_2 or any supercritical fluid is linked to its density – above a pressure of 32 bar and a temperature of approximately 74°C, sCO_2 behaves like a liquid. CO_2 is very non polar and has a similar polarity to pentane[61] making SFC a similar technique to normal phase HPLC. Another reason why SFC is considered analogous to normal phase is due to the absorption of CO_2 onto the surface of the stationary phase, similar to mobile phase absorption in normal phase LC[62]. Selectivity can be altered in SFC by the addition of an organic modifier [51] which alter the polarity of the mobile phase and also to an extent the polarity of the stationary phase through mobile phase absorption[62]. Selectivity can also be changed by altering the temperature and pressure of the mobile phase, however this method is not as powerful as the addition of an organic modifier. As mentioned

previously, SFC is generally considered analogous to normal phase for this reason it gives orthogonal selectivity to reversed phase HPLC[63, 64]. This orthogonal selectivity makes SFC a very attractive complementary technique which can be used in conjunction with RP HPLC or as an alternative standalone method. The role of modifiers as well as effects of temperature and pressure in separations will be discussed in the following sections.

1.3.4.1 Use of modifiers and additives

1.3.4.1.1 Modifiers

CO₂ is similar in nature to pentane and for this reason is more suited to the separation of moderately polar to non-polar solutes. In order to increase the solvation capacity of CO₂ for the separation of more polar solutes, more polar modifiers are added to CO₂. Some of the modifiers used in SFC are methanol[65-69] and ethanol[70-72] for the separation of more polar compounds. and a mixture of modifier solvents such as methanol and acetonitrile are also used[73, 74]. The addition of modifiers change the density of the mobile phase which has an effect on the elution strength[60], affects the polarity of the mobile phase, changes mobile phase/ solute and stationary phase/solute interactions decreasing retention and improves efficiency and peak shape [60, 69, 75]. Hoffman *et al.*[69] found that the addition of a methanol modifier was more advantageous than acetonitrile in the separation of ethoxylated and propoxylated surfactants on a C₁₈ stationary phase. Methanol as a modifier produced better peak shape with peak asymmetry values of 1.09, 1.10 and 1.14 recorded for methanol modified CO₂ and values of 1.15, 1.21 and 1.44 recorded for an acetonitrile modifier. The improved peak asymmetry values for a methanol modifier were likely due to the greater hydrogen bonding capacity of the methanol compared to acetonitrile and coverage of excess silanols on the surface of the stationary phase by methanol. West *et al.* [76] investigated the effect of a range of alcoholic modifier as well as concentration of modifier on the separation of enantiomeric amino acid derivatives on polysaccharide based chiral stationary phases. The authors found that there was a slight increase in retention when methanol was changed to ethanol and then subsequently to isopropanol as shown in Fig. 1.3.1.

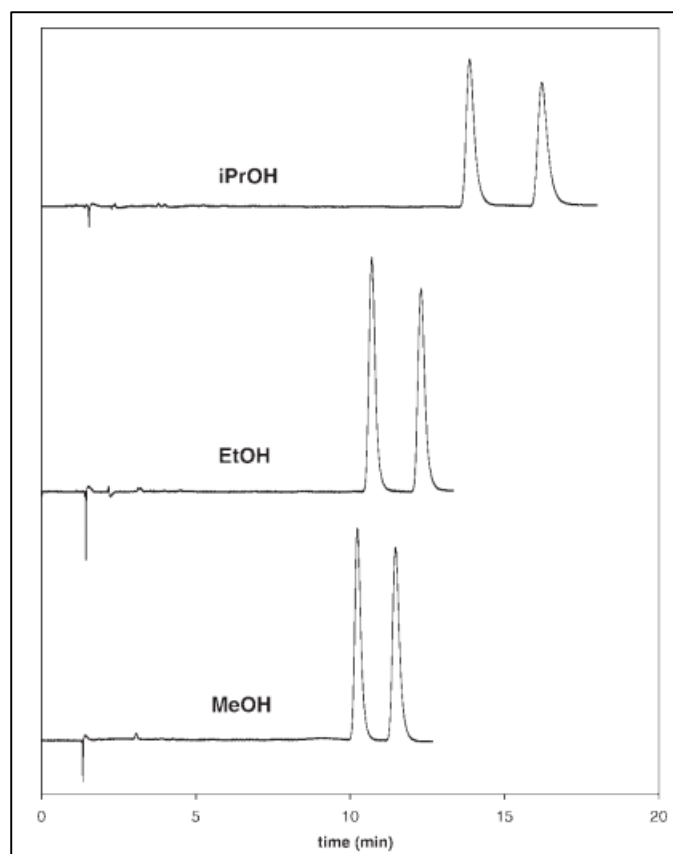


Fig. 1.3.1: Effect of the nature of alcohol modifier in a CO₂ mobile phase on the separation of amino acid derivative PP on a Lux chiral column. Conditions: Modifier percentage: 3%, back pressure 150 bar. flow rate: 3mL/min. Reproduced from Ref. [76]

The increase in the retention between the 3 similar alcoholic modifiers is due to their decreasing polarity, methanol being the most polar and isopropanol, the least. The authors choose ethanol as the modifier of choice for further analysis, as despite having a longer analysis time than methanol, ethanol is a more environmentally friendly and non-toxic option. Isopropanol provided a higher resolution between the enantiomers than either methanol or ethanol however this increase in resolution was offset by the increase in run time of the analysis. A study of effect of modifier concentration on separation, showed as expected retention is decreased with increasing modifier concentration; results showed that a modifier concentration of just 5% was capable of providing adequate resolution between peaks with a reasonable run time. In the majority of cases however, methanol is the modifier of choice for most applications as it produces very efficient separations while also having the advantage of low viscosity, high polarity and a low boiling point [77]. Wenda *et al.*[68] tested the effect of modifier concentration as well as changing density on resolution and selectivity of flurbiprofen enantiomers. Analysis of

flurbiprofen was carried out on an amylose derived, Chiralpak AD-H chiral column, using different concentrations of methanol from 13% to 23% while incrementally changing the back pressure – this change in back pressure changed the density of the mobile phase. Decreased resolution between the enantiomers is shown in Fig. 1.3.2 with increasing density. There is also an overall trend of decreased resolution with increasing methanol concentration. A decrease in retention factor resolution was also noted by Li *et al.*[78] with increasing modifier concentration and also with increasing density.

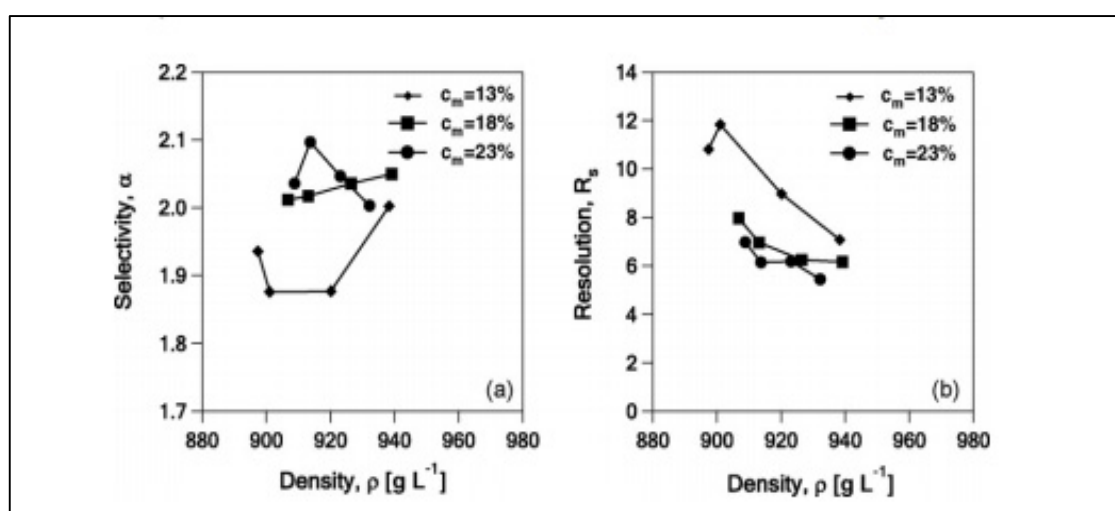


Fig. 1.3.2: Dependence on resolution (right) and selectivity (left) on modifier (methanol) concentration and density of the mobile phase. Analyte: Flurbiprofen enantiomers. Column: Chiralpak AD-H Reproduced from Ref. [68]

Also shown in Fig. 1.3.2 is the effect of methanol concentration on the selectivity of the mobile phase, and thus density was found to have a moderate effect on overall selectivity, while at 18% and 23% methanol concentration and density do not appear to have an effect on the selectivity. More profound effects on selectivity are noted when a lower methanol concentration is used. Wang *et al.*[79] found that for a range of 48 enantiomers, a change in density had little or no effect on selectivity, however the author noted that the effect of density on selectivity is quite a controversial topic with varying opinions on the topic, it is clear that is an area that further research is required.

1.3.4.1.2 Additives

Additives in SFC play a similar role to those used in HPLC such as coverage of stationary phase active sites and suppression of ionisation or ion pairing by solutes[62]. Additives to modifiers are also capable of extending solute polarity and changing the polarity of the mobile phase as well as the stationary phase [62]. Some additives which have been used include water [80] [81] salts such as ammonium acetate [82], basic additives like ammonia [83] and isopropylamine (IPA) [84] and strong acids like trifluoroacetic acid (TFA) [84]. De Klerck *et al.*[84] found that for the separation of a range of enantiomers of basic, neutral and acidic nature, on polysaccharide based stationary phases there was a decrease in retention when applied to the separation of enantiomers with increasing methanol concentration. In this study IPA and TFA were used as additives. The authors found that with the addition of the both additives simultaneously, there was decrease in retention factor of the first peak (k_1) and greater number analytes fully eluted within 30 minutes. TFA and IPA were found to have different effects on the separation; TFA was believed to deactivate free silanol groups by forming hydrogen bonds, as well as lowering the pH of the mobile phase, partially protonating and charging basic functional groups and reducing retention time. IPA was believed to suppress non stereospecific interactions between analytes and the silica matrix of the stationary phase, enhancing enantioselectivity and reducing retention. Patel *et al.*[85] found that for the separation of peptides a methanol:sCO₂ mobile phase gradient containing 0.2% TFA achieved the best separation on an amino column. It was theorised that TFA would fully protonate the peptides in the mobile phase forming a dication while trifluoroacetates present due to the nature of the peptide analytes (which were salts of trifluoroacetate) would be act as a dianion, which lead to ion pairing.

The advantage of using volatile salts like ammonium acetate (AA) as an additive over acid or bases is due to their better compatibility with mass spectrometric detection, as unlike acid and base additives, volatile salts do not cause ion suppression[82]. Gassiot *et al.* [82] demonstrated that the addition of ammonium acetate in increasing concentrations to a methanol mobile phase, both decreased retention and improved peak shape of sulphonamide compounds analysed on a 2-ethylpyridine (2-EP) stationary phase as shown in Fig 1.3.3.

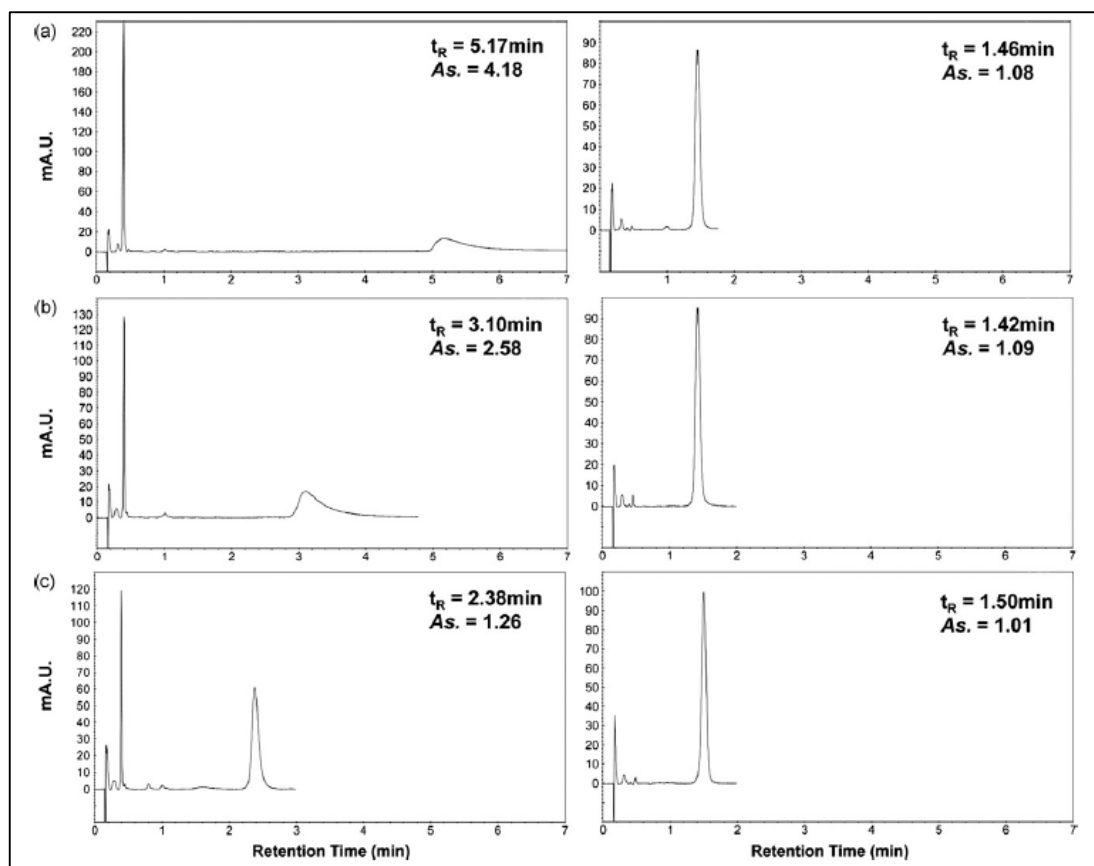


Fig. 1.3.3: Evolution of peak retention time and peak shape with increasing amounts of AA in the modifier. Column: 2-EP, mobile phase 10% methanol in CO₂, 100bar, 35°C, 4 mL/min. Compound on left: sulphonamide 3, right: naproxen. (a) 0.3 mM AA in MeOH (b) 5 mM AA in MeOH (c) 30 mM AA in MeOH. Reproduced from Ref. [82]

Asymmetry of compound 3 (shown on the left side of Fig. 1.3.3) showed a reduction from 4.18 when 0.3 mM AA was added to the methanol modifier to 1.26 when 30 mM AA was added to the methanol modifier, this is coupled with a reduction in the run time for compound 3 of approximately 50%. Also shown in Fig 1.3.3. is the effect of increasing AA concentration on naproxen, whose retention behaviour was not affected by the addition of AA to the mobile phase. The addition of AA was hypothesised to interact with free silanols in the stationary phase and thus decrease retention and improving peak shape of the basic sulphonamide compounds. The non-effect of AA concentration on naproxen is thought to be due to its acidic nature, which in an acidic mobile phase like methanol/CO₂ is uncharged. The retention mechanism for this compound is thought to be predominately due to π - π interactions with the ethylpyridine stationary phase. Zheng *et al.* [86] report similar findings to Gassiot[82] for the separation of sodium sulphonates on silica and cyanopropyl columns. Retention decreased with increasing concentration of AA on a cyanopropyl

column, this was hypothesised to be due to the interaction with available silanol groups at lower concentrations of AA while as AA concentration increases, after all available silanol groups have been masked by ammonium salts, the dominant interaction becomes ion pairing between the ammonium and sulphonate groups, which at increasing concentration, also increase, thus reducing retention. The same group[87] also report similar behaviour with various other ammonium salts such as tetrabutylammonium acetate and ammonium chloride. Examples of salt additives in the literature appear to be confined to the use of ammonium salts and do not extend to other salts which are commonly used in HPLC such as phosphate and formate buffers. This is most likely due to issues with solubility in the CO₂ and organic modifier mobile phases.

In the early years of SFC development, water was used as a modifier – water was added to CO₂ by means of saturation however this proved to be unreliable as the amount of water which was dissolved in the CO₂ varied and so was difficult to control[88]. Water as an additive has proved more successful in recent years with Liu *et al.*[81] reporting a dramatic improvement in peak shape when 5% water was added to methanol modifier when compared to a methanol only modifier when hydrophilic compounds were analysed as shown in Fig. 1.3.4.

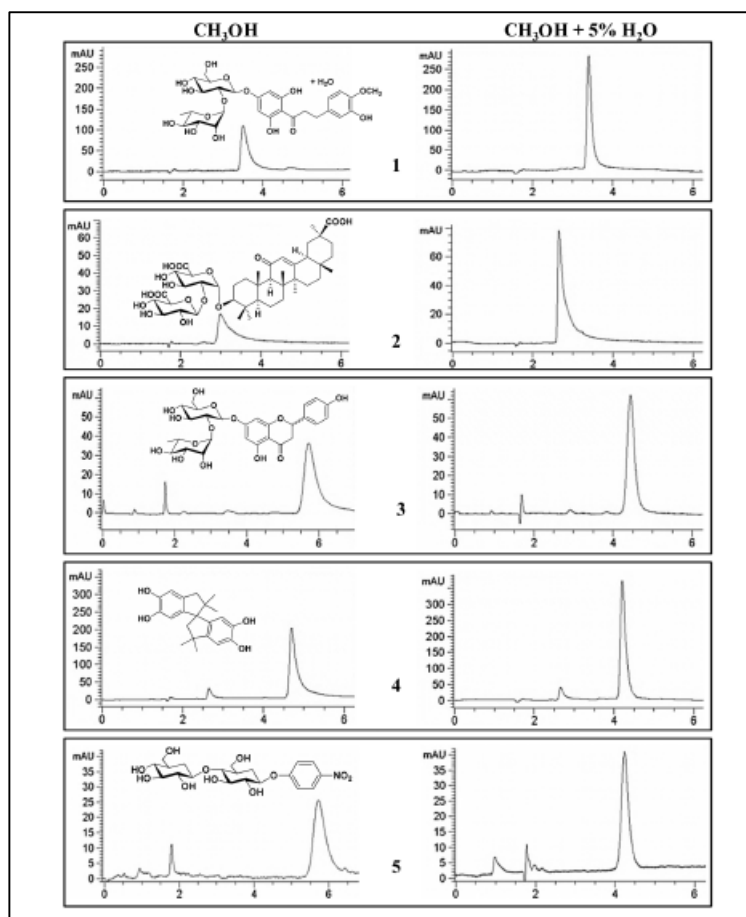


Fig. 1.3.4: Comparison of peak shape of five hydrophilic compounds using methanol (CH_3OH) and methanol + water ($\text{CH}_3\text{OH} + \text{H}_2\text{O}$) modifiers. All columns: $4.6 \times 250 \text{ mm}$ and $5 \mu\text{m}$. CO_2 back pressure and temperature were 100 bar and $40 \text{ }^\circ\text{C}$. Detection: UV 210 or 254 nm. Sample: 1 mg mL^{-1} concentration and $15 \mu\text{L}$ injection volume. Flow rate: 2.1 mL min^{-1} . 1: neohesperidin dihydrochalcone hydrate; column: CN; 30% modifier, 210 nm. 2: glycyrrhizin; column: Synergi; 30% modifier, 254 nm. 3: naringin; column: DEAP; 60% modifier, 210 nm. 4: compound 4; column: Diol; 30% modifier, 210 nm. 5: 4-nitrophenyl β -D-cellobioside; column: BASIC; 60% modifier, 210 nm. Reproduced from Ref. [81]

The improvement in peak shape was thought to be due to the increased polarity of the mobile phase due to the addition of a water additive. This increase in polarity in turn increased the solubility for hydrophilic compounds resulting in the suppression of peak tailing for all 5 highly hydrophilic compounds. It is clear that the use of additives in the mobile phase in SFC are of huge importance and can be used, similar to HPLC to change retention, and perhaps more importantly to improve peak shape of compounds with poor peak shape with a CO_2 /modifier only mobile phase by interaction with surface silanols which reduces peak tailing.

1.3.4.2 Temperature and pressure of the supercritical fluid

Another way to control retention and solvation in SFC is by adjusting the temperature and pressure of the supercritical fluid. While the effects are not as profound as adding a modifier or additive, it is none the less an important method of affecting retention.[60, 62]. The density of the mobile phase is responsible for its solvation capability. In an investigation into the influence of temperature on retention of a range of enantiomeric pairs, West *et al.*[76] showed that by increasing temperature increments from 10 to 40°C, there was an increase in retention due to increased density of the mobile phase which causes a decrease in elution strength. Of the 6 enantiomeric pairs, 5% ethanol in CO₂ was capable of separating all but 1 enantiomer pair on a Lux cellulose 1 column. Lou *et al.*[89] found that while the effect of pressure (at constant temperature) on retention in SFC is quite straight forward with a steady increase in solubility and decrease in retention factor recorded with higher pressures. However the influence of temperature (at constant pressure) is more complicated with a number of factors influencing the retention. The authors found that temperature affects the vapour pressure and density of the supercritical fluid, changing its retentive properties as a result of solute affinity for the stationary phase, for example, as shown in Table 1.3.2, with increasing temperature, anthracene and chrysene's affinity for the C₁₈ (ODS) stationary phase was considerable increased, thus increasing retention.

Table 1.3.2: Relative affinities of anthracene and chrysene for an ODS stationary phase at different temperatures. Reproduced from Ref. [89]

P (bar)	T (°C)		
	50	70	100
<i>Anthracene</i>			
150	1.31	2.25	4.62
250	1.30	2.25	4.63
350	1.31	2.25	4.62
<i>Chrysene</i>			
200	1.30	2.32	5.12
300	1.30	2.33	5.15
350	1.31	2.32	5.11

^a Values relative to the affinities at 40°C.

As well as affecting the solute affinity for the stationary phase, increasing temperature at constant pressure also affects the solubility of the solute. However this is not as straight forward as was the case for increasing pressure at constant temperature. The authors found at a constant pressure of 100 bar, there was first a decrease in solubility, then a subsequent increase in solubility by increasing temperature from 40 to 150 °C incrementally, however at constant pressure of 200 bar a steady increase in the solubility was recorded across the range of temperatures. Toribio *et al.*[90] found that with the separation of range of enantiomers, temperature had varying effects on their retention behaviour citing increasing, decreasing and no effect on retention when temperature was changed. This phenomenon was also noted by Berger *et al.* [91] who also cites varying effects on retention behaviour when temperature is varied and describes the effect of temperature as unpredictable. It is clear that the effect of temperature is not well understood and needs to be investigated further to determine its precise effects on parameters such as retention, solubility and selectivity.

1.3.5 Applications of SFC

As SFC is considered to be analogous to normal phase HPLC it is perhaps unsurprising that SFC has found much of its applicability in the area of preparative chromatography and more specifically in area of chiral chromatography [76, 77, 84, 92-97]. In a recent review Miller[98] cites many advantages of preparative SFC over preparative HPLC which included; more rapid preparative separations, increased throughputs and decreased solvent consumption. Another reason why SFC is preferred over HPLC on a preparative scale was as a result of decreased solvent consumption, less waste was generated making it a greener technique. However, possibly the most important advantage of lower solvent consumption is the higher product concentration which can be obtained as a result of evaporation of the sCO₂ mobile phase, leaving pure product in higher concentrations in less organic solvent[98, 99]. Wang *et al.*[96] report the enantioseparation of 14 different thiazide, flavonone and amino acid derivatives on a novel β-cyclodextrin phenylcarbamate derivative column which were cationic in nature. In the case of the separation of flavonone racemates it was found that position of the phenolic group

on the flavonone was important and that when the phenolic group was in the 4' – position, the cationic stationary phases shows a heightened enantioselectivity. This study also found that the addition of a 1% acetic acid additive had a significant effect on the enantioselectivity of the column in the case of strong acidic analytes where retention time was shortened, however there was little or no effect for weak acidic or basic compounds. The influence of the acidic additive preferentially on the retention of strongly acidic analytes was hypothesised to be due to the masking of the cationic moiety on the chiral selector by the acidic additive which weakened the strong electrostatic interactions between the strongly acidic analyte and the stationary phase normally present thus reducing retention. Interactions between the cationic stationary phase and the weakly acidic and basic analytes were already low so less of an effect was observed. Xiang *et al.*[100] reported the separation of 9 amide enantiomers on various polysaccharide based chiral stationary phases with a variety of mobile phases containing acetonitrile, methanol and isopropanol as modifiers. As is commonly the case, methanol proved to be the most successful mobile modifier with eight of the nine enantiomers efficiently separated on a Chiralpak IC column, while acetonitrile and isopropanol were capable of separating six and one of the 9 enantiomers respectively on the same IC column. Fig. 1.3.5 shows the separation of amide 7 using all 3 modifiers using a Chiralpak IC column. As can be seen, enantiomers are well resolved using all 3 mobile phases. It was noted by the authors that amide 7 was only separated by an IPA/CO₂ mobile phase. IPA was thought to change the 3 dimensional structure of the stationary phase by adsorption leading to steric hindrance for chiral interaction. As amide 7 was the least sterically hindered, it was least affected by the 3 dimensional structural change. The increase in retention noted for an acetonitrile mobile phase(c) when compared to a methanol mobile phase (a) was most likely due to acetonitriles lesser capability for hydrogen bonding with the analytes, leading to higher retention.

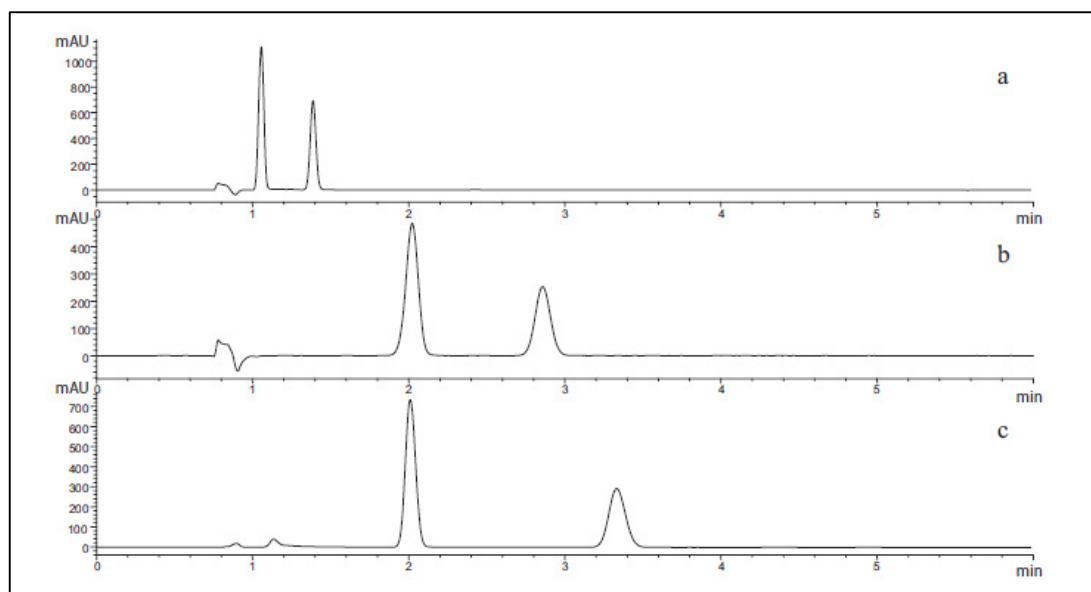


Fig. 1.3.5: The effect of organic modifiers on the separation of amide 7. Conditions: Chirapak IC column, 40 °C, 4 mL/min, back pressure of 150 bar and 10% organic modifier of (a) methanol; (b) isopropanol; and (c) acetonitrile. Reproduced from Ref. [100]

As mentioned previously additives are added to modifiers in order to improve or aid a separation whether it be increasing the polarity of the mobile phase or improving peak shape. In chiral SFC, an additive is often added in order to improve enantioselectivity or peak shape. De Klerck *et al.*[97] report the effect of combining both an acid additive and a base additive and their effect on enantioselectivity of four different polysaccharide stationary phases. While generally, depending on the nature of the compound, either an acid or base is added to a mobile phase, De Klerck showed that combining an acid and base can have unexpected positive effect. Both 0.5% TFA and IPA was added to methanol modified mobile phase and the combination of these two additives provided a wider enantioselectivity than if the two additives were to be used separately. As mentioned previously relating to a similar study carried out by De Klerck and co-workers[84] the role of TFA was most likely to deactivate free silanol groups by forming hydrogen bonds, as well as lowering the pH of the mobile phase, partially protonating and charging basic functional groups, thus reducing retention times. The role of IPA was to suppress non stereospecific interactions between analytes and the silica matrix of the stationary phase, enhancing enantioselectivity and reducing retention.

As shown, SFC is a technique which is typically analogous to normal phase LC due to the polarity of its primary mobile phase, which in most cases is sCO₂. Advantages

of SFC include reduced viscosity and higher diffusivity of the mobile phase, which leads to ability to use faster flow rates than obtainable in HPLC under the same conditions. Lower operating pressures mean longer columns can be used without pressure maximums being reached; this in turn leads to more efficient separations. With the addition of organic modifiers, the selectivity range of SFC can be significantly increased to include more polar solutes. The most widely used modifier in SFC is methanol, due to its high polarity, low viscosity and low boiling point. Similar to HPLC, the use of additives also has a significant effect on chromatography, the addition of additives such as TFA has been found to reduce tailing due to masking silanol interactions of the stationary phase surface. Adjusting the temperature and pressure of supercritical fluid is also another important method of adjusting retention, however the effect of temperature is complex is not fully understood. SFC has found significant applicability in the area of chiral chromatography[90, 94, 101] and has proven to be a very effective method of separating enantiomers without the need for significant quantities of toxic solvent which is normally associated with chiral chromatography on normal phase HPLC. Because the main mobile phase in SFC is CO₂, which is non-toxic, safe to use and easy to dispose of as sCO₂ is just converted back to its gaseous state, there is limited waste generated, making SFC a much greener alternative to traditional LC. The literature search however does highlight gaps which include determination of the exact effect of temperature on selectivity in SFC and also the lack of applications in achiral chromatography.

1.4 Conclusions

There has been significant developments in the area of LC over the last 30 years in terms both hardware and understanding the fundamental principles of HPLC. Over the years the main focus of research in the area has been on achieving the ultimate goal in HPLC – the most efficient separation achievable in the shortest amount of time. From a theoretical point of view, the key to increasing efficiency while also decreasing analysis time lay in reducing the particle size of columns, and this is the approach which many researcher have explored[102, 103]. This is evident in the ever decreasing particle sizes used in chromatography going from $>10\ \mu\text{m}$ columns in the early days to the present sub $2\ \mu\text{m}$ columns on the market today. Another approach taken to addressing the need for efficient separations in the shortest possible time was the development of core-shell particles, which has been discussed here.

Earlier generations of core-shell particles encountered many obstacles, including the sustained drive to develop smaller fully porous particle sizes, which lead to their ultimate demise as the newly developed fully porous particles provide faster and more efficient separation with greater applicability. However development of the new or so-called 3rd generation of core-shell particles, have been proven to provide increased efficiencies when compared to fully porous particles of an equal and indeed smaller particle size due to their narrow particle size distribution which resulted in a reduced A term and also improved mass transfer kinetics. This increase in efficiency meant that larger particle sizes could be used negating the requirement for higher back pressure. Lower back pressure and high efficiency make core-shell particles a very attractive alternative to fully porous sub $2\ \mu\text{m}$ particles.

The majority of the research which has been carried out on core-shell particles relates to their fundamental properties and how these compare to their fully porous counter parts, however, there are limited examples in the literature of core-shell particles columns being used in a real chromatographic environment. This is highlighted by a survey carried out by Mayors for the magazine LC-GC, which found that over 50% of chromatographers still use particle sizes which are greater than $3\ \mu\text{m}$ in size. The review of the literature has highlighted two areas where major gaps appear. The first is in area of the sample capacity of these stationary phases while the other is in the area of the applications which these stationary phase types

are used. Applications in the literature were mainly focussed on the topic of the separation of proteins and peptides, however like their fully porous counterparts, a wide range of stationary phase selectivities are becoming increasingly available, widening the scope and applicability of these stationary phase types.

HPLC as a technique is reaching maturity in terms of instrumentation and also reaching the point at which reducing particle size will no longer continue to have a positive effect on efficiency and speed. While the new generation core-shell stationary phases are being developed to address this issue, other complementary techniques such as SFC have also seen a renaissance. SFC has the advantage of having liquid like solvation properties which the viscosity and diffusive properties are more in line with GC. Supercritical fluids such as CO₂ are cheap, non-toxic, with modest critical parameters making it an ideal solvent for SFC. As well as this, there is very little waste generated with SFC as the supercritical fluid can just be depressurized into its gaseous state and either vented or recycled. Supercritical CO₂ is very non polar and has similar polarity to heptane and for this reason SFC is considered analogous to normal phase LC. With normal phase LC selectivity, SFC has an orthogonal selectivity compared to reversed phase LC. With the addition of organic modifiers to sCO₂, as well as the addition of additives, polarity of the mobile phase can be changed and thus the selectivity of SFC can be altered making it applicable to a wider range of analyte polarities. As well as the addition of modifiers and additives, selectivity and solvation can also be altered using temperature and pressure, which affect the density of CO₂, changing its solubility and selectivity capabilities.

SFC is seen as analogous to a normal phase HPLC and thus for this reason, it finds most applicability in the area of chiral separations. However using a suite of approaches mentioned earlier, SFC holds great potential in the separation of achiral compounds as well due to tuneable selectivity. As well as that, its orthogonal selectivity to reversed phase LC also makes it an attractive complementary technique for a whole host of other applications. This is an area that has yet to be fully explored.

Both of these topics are examined in this thesis. In *Chapter 2*, an existing isocratic impurity assay, method USP 36-NF-31, Voriconazole Monograph; for the separation

of Voriconazole and related impurities Compound X, Voriconazole related compound C (this compound shall be referred to as “compound C”) and Voriconazole related compound D (this compound shall be referred to as compound D), originally carried out on a 4 μm fully porous C_{18} stationary phase was transferred to a 2.6 μm core-shell particle column with further optimisation carried out. Optimisation carried out included, optimisation of the organic mobile phase component composition and concentration, nature of the aqueous component (both concentration and pH) and optimisation of the column temperature. Further gradient optimisation was carried out on this stationary phase also. This method was then further transferred to a 1.7 μm core-shell column with subsequent method optimisation in an effect to further reduce the run time and increase efficiency..

In *Chapter 3*, the evaluation of 16 stationary phase/mobile phase combinations with potential orthogonal selectivity to the methods outlined in chapter 2 was carried out. 4 stationary phases and 4 mobile phases were selected for the study. In all cases the supercritical fluid used was supercritical carbon dioxide (sCO_2) Stationary phases included; silica, cyano, diol and 2-ethylpyridine chemistries. Methanol was selected as the primary modifier in this study. A number of additives to the mobile phase were also investigated, these were; trifluoroacetic acid (TFA), ammonium formate (AA) and triethylamine (TEA). Each stationary phase was analysed using all four mobile phases. A cyano stationary phase with a 20% methanol mobile phase was found to be the most suitable stationary and mobile phase combination for the separation of the separation of Voriconazole and related impurities compound C and D.

2 Chapter 2: Development of ultrafast pharmaceutical impurity assay using 3rd Generation core-shell stationary phase technologies.

2.1 Introduction

The goal in chromatography can be defined as “the best separation achievable in the shortest amount of time”. Some of the most widely used chromatographic techniques include HPLC and GC. HPLC is a very popular and widely used analytical technique and forms the basis of many analytical laboratories around the world. It is used in a variety of settings including research laboratories, academic laboratories and a wide variety of industrial settings including the pharmaceutical and petrochemical industry. [2]

The demand for the best separation in the shortest time has been a key driver in chromatographic research[3]. One approach to this is the reduction of particle size of the columns used, as smaller particles produce fast run times and greater efficiency[5]. Whilst in the past, columns with particle sizes in the region of 5-10 μm were common, recently the trend has been towards smaller particle sizes in the region of sub 2 μm [8]. While these particle sizes produce a fast and more efficient separation, an increase in back pressure is associated with such columns. A typical sub 2 μm column produces far in excess of what a typical HPLC instrument with a 400 bar pressure limit is capable of handling. For this reason, new instruments have been developed capable of coping with such pressures. Another downfall of smaller particle sizes is the frictional heating associated with operating these column types which leads to a decrease in efficiency[11]

An alternative to sub 2 μm columns which have seen a renaissance in recent years have been core – shell particle columns [23, 104]. Core shell particles in the region of 2.7 μm have been found to be capable of producing sub 2 μm particle performance without the associated increase in back pressure [12]. This is an attractive alternative to sub 2 μm particles as standard HPLC hardware can be used. While most research on core-shell particles has primarily focussed on their performance parameters[32, 103], significant research has not been carried out to explore the potentials of these core-shell particles in real chromatographic

applications. Some work has been carried out on the separation of proteins and peptides [46, 105], however there is significant scope to extend the applicability of these particles to a wider ranges of applications such as impurity analysis for pharmaceutical drug products.

Voriconazole (Vfend) is an tri-azole anti-fungal drug used for the treatment of serious fungal infections such aspergillosis and esophageal candidiasis and works by slowing the growth of infection causing fungi[106, 107]. Voriconazole is available in one of three forms; a lyophilised powder used to prepare solution for intravenous injection, film-coated tablets or oral administrations or powder for preparation of oral suspensions.. The current method used for assay and impurity analysis of voriconazole is a reversed phase HPLC assay using a reversed phase C₁₈ column (150 x 0.39 mm, 4 μm) which has a run time of 11 minutes. (USP 36-NF-31, Voriconazole monograph) Voriconazole has 3 known impurities compound C, compound D and compound X (see Fig. 2.1.1).

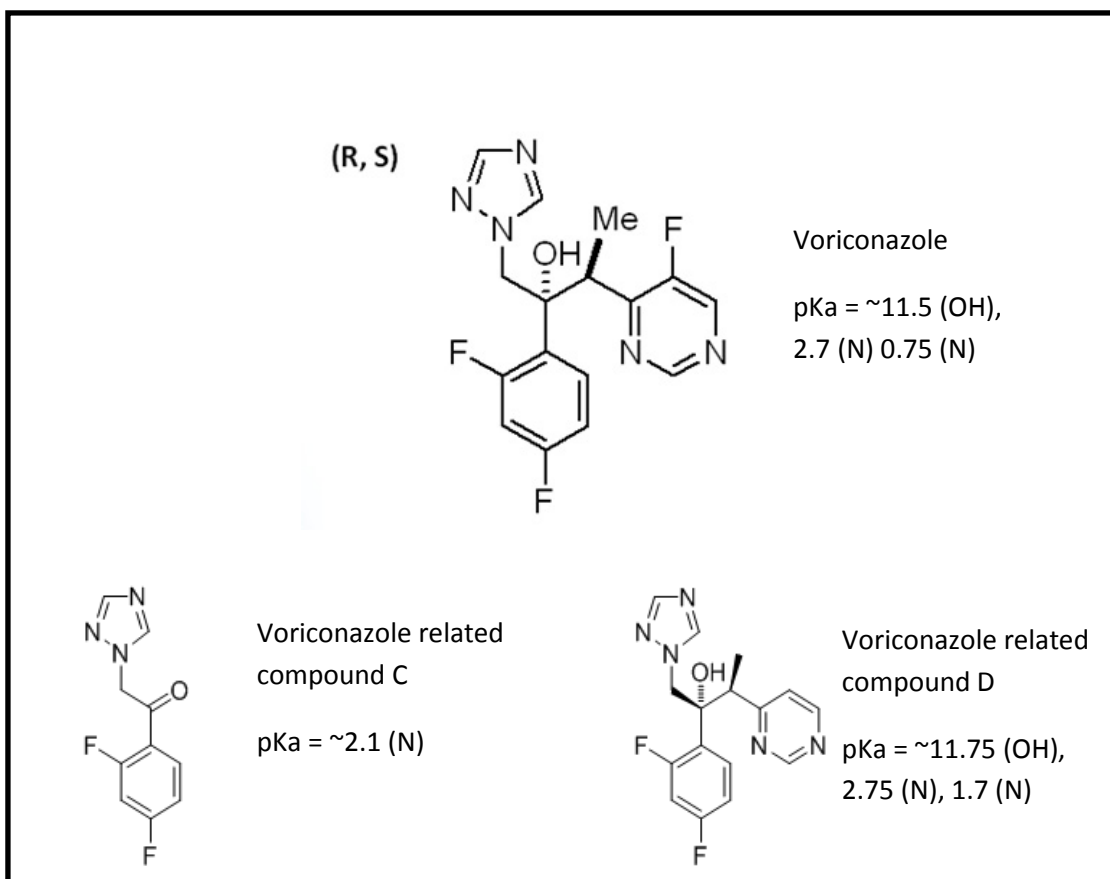


Fig. 2.1.1: Structure of Active Pharmaceutical Ingredient (API) Voriconazole and related impurities compound C, compound D (Structures provided by Pfizer Process Development Centre (PDC), Ringaskiddy, Cork)

The aim of this work was to develop an ultrafast impurity assay to separate, active pharmaceutical ingredient (API) Voriconazole, from its related impurities compound X, compound D and compound C utilising novel core-shell 2.6 and 1.7 μm columns. Optimisation of isocratic method parameters such as mobile phase composition and analysis temperature were carried out initially, ultimately leading to the development of a gradient separation which had a 57% reduction in retention time whilst still maintaining a critical resolution between peak pairs of > 1.7 .

2.2 Materials and Methods

2.2.1 Materials

2.2.1.1 Chemicals

API standard – Voriconazole, impurity standards - compound C, compound D and compound X were obtained from Pfizer Process Development Centre (PDC) (Cork, Ireland). Ammonium formate ≥ 99.995 trace metals basis and formic acid $\geq 96\%$ were obtained from Sigma Aldrich (Dublin, Ireland), HPLC grade Methanol (MeOH) HPLC grade and Acetonitrile (ACN) were purchased from Fisher Scientific (Cheshire, UK). Ultra-pure water was obtained from a Millipore Milli-Q water purification system (Bedford, MA, USA) purified to resistance of $\geq 18.2 \text{ M}\Omega\cdot\text{cm}$

2.2.1.1.1 Mobile Phases

For the Pfizer HPLC method, the mobile phase consisted of 55% v/v 30 mM ammonium formate adjusted to pH 4 with formic acid ($\geq 96\%$ purity), HPLC grade MeOH (30% v/v) and HPLC grade ACN (15% v/v). For method development, the mobile phase consisted of ammonium formate adjusted to the required pH with formic acid ($\geq 96\%$), and HPLC grade ACN. All mobile phases were vacuum filtered using Supelco 0.2 μm nylon 66 membrane filters. (Sigma Aldrich, Dublin, Ireland)

2.2.1.2 Apparatus

2.2.1.2.1 HPLC instrumentation

Chromatographic separations were carried out on an Agilent 1200 series Liquid Chromatograph consisting of a quaternary pump (G1311A), thermostatted autosampler (G1329A), column oven (G1316A) and variable wavelength detector (G1314A). Columns used consisted of a Waters Nova-pak C₁₈ reversed phase column (150 x 3.9 mm, particle size 4 µm) (Waters, Ireland) and Phenomenex Kinetex reversed phase C₁₈ column (100 x 2.1 mm, particle size 2.6 µm), (Phenomenex, Cheshire, England)

2.2.1.2.2 UPLC instrumentation

UPLC chromatographic separations were carried out on a 1.7 µm core-shell Phenomenex Kinetex reverse phase C₁₈ column (100 x 2.1 mm, particle size 1.7 µm), (Phenomenex, Cheshire, England) with a Shimadzu Nexera UPLC (Mason Technology, Dublin Ireland) consisting of 2 x Nexera LC-40AD pumps, Nexera SIL-30AC autosampler, Nexera CTO-30A high temperature column oven, and Prominence SPD-20AV UV-Vis detector.

2.2.2 Methods

2.2.2.1 Preparation of standards

Standards required for running USP 36-NF-31 - Voriconazole monograph were prepared every 7 days in diluent consisting of 55% 30 mM ammonium formate buffer (FB) (pH 4), 30% MeOH and 15% ACN. A stock solution of the Voriconazole including its three known impurities, compound C, compound D and compound X was prepared to a concentration of 250 µg/mL. 12.5 mg of each standard was weighed out and dissolved in 50 mL diluent. This was diluted 10 fold in 50 mL diluent and further diluted 10 fold in 50 mL diluent to a concentration of 2.5 µg/mL. Injection volume for analysis was 20 µL. This sample was known as S3. For HPLC method development using the Phenomenex Kinetex C₁₈ 2.6 µm reversed

phase core-shell column, a stock solution of 250 µg/mL was used with a 0.2 µL injection volume. After initial method development, new diluent was used which consisted of 25% ACN in 30 mM FB (pH 4). Subsequently all standards were prepared in this diluent. The optimisation parameters selected for method development is the shortest run time possible, while maintaining a critical resolution of above 1.7 between peak pairs.

2.2.2.2 HPLC Method development

All method development carried out on the Phenomenex Kinetex core-shell 2.6 µm column was based on an existing USP 36-NF-31 - Voriconazole monograph used for the determination of impurities in Voriconazole. This isocratic method used a C₁₈ - reversed phase column (Waters Nova-pak, C₁₈, 150 x 3.9 mm, 4 µm particle size). Mobile phase consisted of 55% 30 mM FB, 30% HPLC grade MeOH and 15% HPLC grade ACN. As previously mentioned a 20 µL, 2.5 µg/mL sample (S3) was injected onto the column. The flow rate used was 1 mL/min, detector wavelength was 256 nm and a temperature was set to 35°C. When optimising the method for the core-shell column, the isocratic conditions were first optimised. Parameters optimised included; optimisation of the nature of the organic component of the mobile phase, the percentage organic strength of the mobile phase, the nature of the aqueous portion of the mobile phase and finally the temperature of the separation.

The injection volume chosen for method development was 0.2 µL as recommended by Phenomenex. To compensate for the use of a smaller volume of sample being injected on the column, the concentration of the standard injected was increased by the same factor – thus a 250 µg/mL standard (S3a) was injected on to the column. Temperature throughout the study remained at 35°C (unless otherwise stated), detector wavelength of 256 nm and flow rate of 0.3 mL/min also remained constant. A flow rate of 0.3 mL/min was chosen to compensate for the smaller particle sizes of the column, smaller internal diameter and also to maintain a modest back pressure of approximately 230 bar during method development.

2.2.2.3 Calculation of performance parameters.

For all chromatograms obtained, retention factors, resolutions and peak symmetry values were calculated according to the following formulae using Agilent Chemstation and Waters Empower software:

$$\text{Retention factor: } k = \frac{t_r - t_0}{t_0}$$

$$\text{Peak symmetry: } \frac{a_1 + a_2}{a_3 + a_4}$$

$$\text{Resolution: } R_s = \frac{(2.35/2)(T_{R(B)} - T_{R(A)})}{W_{50(b)} + W_{50(a)}}$$

2.3 Results and Discussion

2.3.1 Original reversed- phase HPLC method.

A separation of Voriconazole and its 3 related impurities; compound C, compound D and compound X (S3) was carried out on a Waters NovaPak C₁₈ reversed phase column (150 x 3.9 mm, particle size 4 µm) using the following conditions; flow rate 1 mL/min, temperature 35°C, mobile phase 55:30:15 FB:MeOH:ACN, injection volume 20 µL, detector wavelength 256 nm. The resulting separation is given below in Table 2.3.1 with the chromatogram shown in Fig. 2.3.1.

Table 2.3.1: Analysis of separation of Voriconazole (peak 4) from its related impurities; compound C, compound D and compound X (S3).

Peak	Retention time (mins)	Retention Factor	Symmetry	Peak Width @ half height (mins)	Efficiency (plates per metre)	Resolution
Void	1.069					
Compound X	2.143	1.005	0.8	0.0788	28060	
Compound C	2.491	1.330	0.85	0.07744	41327	2.68
Compound D	5.46	4.108	0.87	0.1657	40080	14.53
Voriconazole	9.221	7.626	0.99	0.2422	53133	10.81

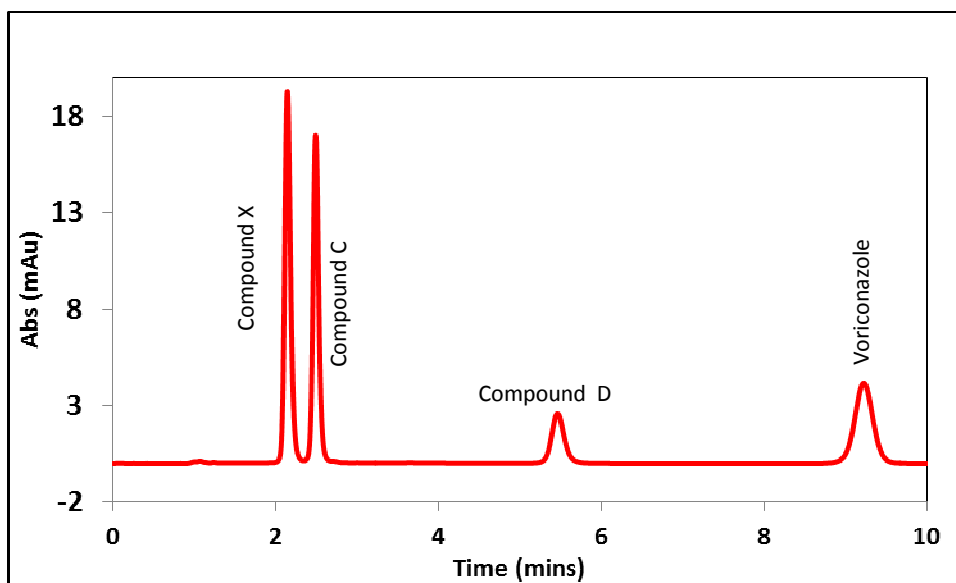


Fig. 2.3.1: Chromatogram illustrating separation of Voriconazole from its related impurities; compound C, compound D and compound X using the original Pfizer Assay and Impurity method for Voriconazole. The conditions were as follows; flow rate 1 mL/min, temperature 35°C, mobile phase 55:30:15 FB:MeOH:ACN, injection volume 20 μ L, detector wavelength 256 nm.

As shown in Table 2.3.1 elution order of the above separation (Fig. 2.3.1) was as follows; compound X, compound C, compound D and Voriconazole. The run time of the impurity assay was 10 min with the last peak (Voriconazole) eluting at 9.221 min. Resolution between the critical peak pair (Impurities; compound X, compound C) was 2.68. Efficiency of the API peak was 53133 plates/metre.

2.3.2 Transfer of existing impurity analysis method to core-shell Kinetex 2.6 μ m reversed phase C₁₈ column.

The aim of this study was to reduce the run time of the existing Pfizer impurity assay in Section 2.3.1 which had a 10 minute. duration. Along with reducing the run time of the assay, it was necessary to maintain adequate resolution between the critical peak pairs of at least 1.7.

2.3.2.1 Isocratic method optimisation

Initially, the separation of S3a was carried out on a 2.6 μm column using the method parameters for the existing USP 36-NF-31 - Voriconazole monograph (Section 2.3.1) with the following adjustments; injection volume chosen was 0.2 μL as recommended by Phenomenex; the flow rate chosen was 0.3 mL/min in order to compensate for the increased pressure observed due to the decrease in particle size and internal diameter of the column compared to the column used for the Pfizer method. To compensate for the 100 fold decrease in injection volume, the concentration of the samples injected onto the column was increased by the same factor; therefore, 250 $\mu\text{g/mL}$ mixed standard samples (S3a) were injected onto the column.

2.3.2.1.1 Optimising the composition of the organic mobile phase component.

The mobile phase used in the initial method for impurity determination was 55% (v/v) 30 mM FB, 30% (v/v) MeOH and 15% (v/v) ACN. This was used as a starting point for the optimisation of the nature of the organic mobile phase. While keeping the aqueous component of the mobile phase constant at 55%, the MeOH concentration was varied, which in turn varied the ACN concentration. Table 2.3.2 below shows the varying concentrations of both MeOH and ACN which were analysed using sample S3a to obtain chromatograms for comparison.

Table 2.3.2: Composition of eluents examined in Isocratic mobile phase

Eluent No.	FB	MeOH	ACN
1	55%	45%	0%
2	55%	40%	5%
3	55%	35%	10%
4	55%	30%	15%
5	55%	25%	20%
6	55%	20%	25%
7	55%	15%	30%

The results of this study are shown in Fig. 2.3.3 and 2.3.4. (Raw data can also be found in Appendix 6.1, Fig. 6.1.1)

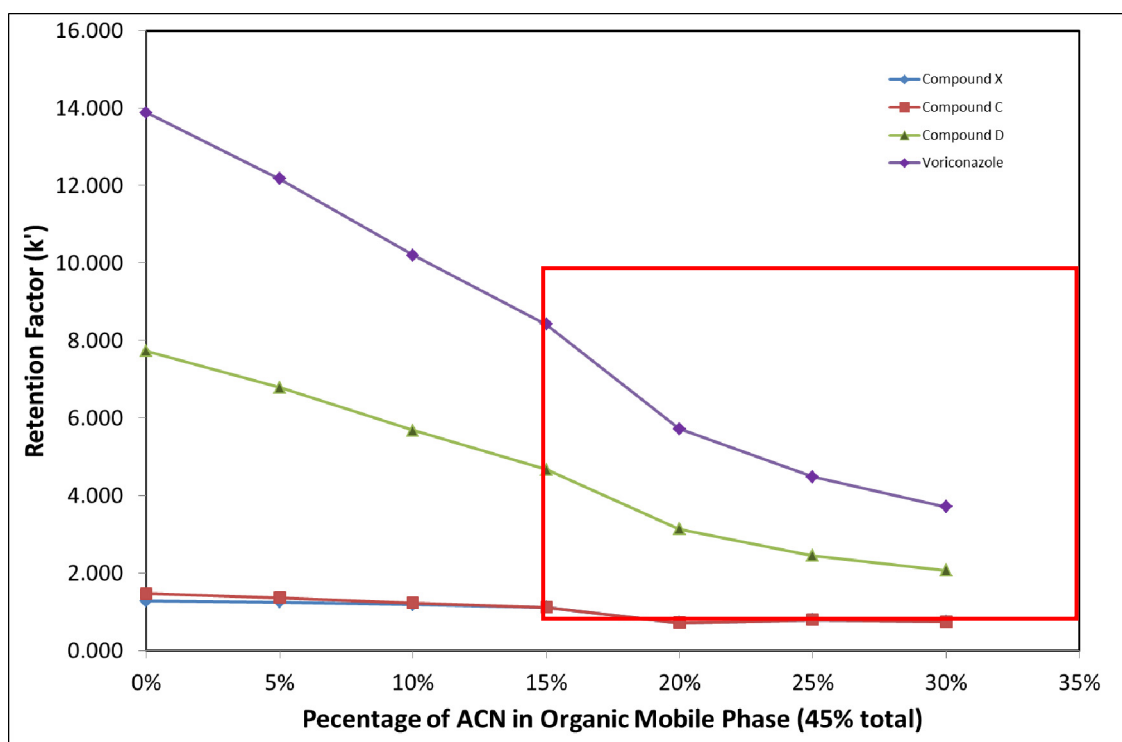


Fig. 2.3.3: Retention factor vs. percentage of ACN present in the mobile phase for Voriconazole (◆), compound X (■), compound C (▲) and compound D (▲). Percentage of FB remains constant at 55% throughout the experiment. Mobile Phase B contained various ratios of methanol and acetonitrile as outline in Table 2.3.2. The red box indicates the data which meet ideal Retention factor criteria of between 1 and 10.

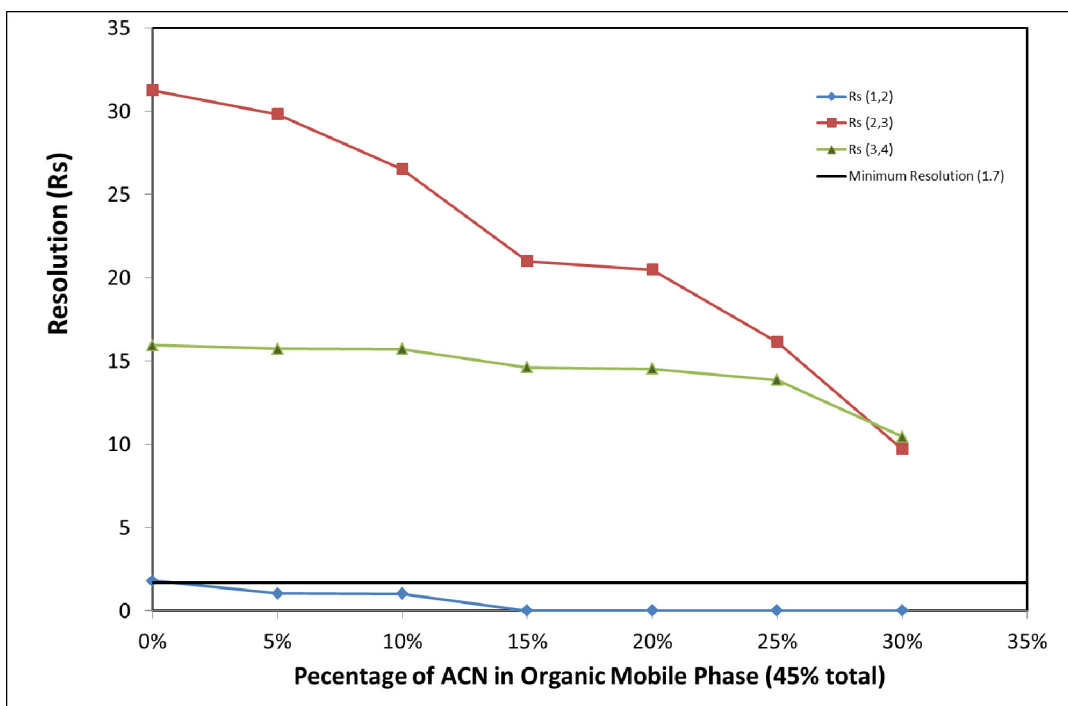


Fig. 2.3.4: Resolution between peak pairs vs. percentage of MeOH/ACN. Peak pairs are as follows (1,2 \blacklozenge): compound X:compound C, (2,3 \blacksquare): compound C:compound D, (3,4 \blacktriangle): (compound D:Voriconazole) Minimum resolution at R_s of 1.7 is indicated by the solid black line.

ACN has a stronger eluting strength than MeOH, so as MeOH was replaced with a greater concentration of ACN and the mobile phase became stronger, retention of analytes was expected to decrease. Retention factors of each of the four compounds show, as expected, that with an increasing % of ACN in the mobile phase, there was decreased retention. As can be seen from Fig. 2.3.4 above and Table 6.1.1 (appendices) impurities compound X and compound C co-eluted with greater than 15% ACN (eluent 4) present in the organic phase. Ideally, retention factors of $1 \leq k \leq 10$ are the most desirable, as retention factors of <1 indicate inadequate interaction of the analyte with the stationary phase, while in the other extreme, retention factors of >10 mean lengthy analysis which do not provide greater resolution as band broadening cause peaks to become shorter and wider. The red box in Fig. 2.3.3 indicated the concentration at which optimal retention factors were achieved i.e. above 15% ACN (eluent 4), however as was previously mentioned, co-elution between compound X and compound C occurred at concentrations above 15% ACN. Therefore mobile phases containing more than 15% ACN in a binary mixture with MeOH (45% total organic) were unsuitable from a retention perspective.

As retention decreased, resolution ultimately decreased for peak pair (2,3) and (3,4) when the percentage of ACN is increased in the mobile phase B. With more than 15% ACN (eluent 4) present in the mobile phase, compound X and compound C co-eluted, as mentioned previously, this in turn meant resolution between this peak pair fell to 0. A resolution of 1.7 for the critical peak pair, in this case - compound X:compound C, was defined as an optimisation parameter at the start of the experiment. The black horizontal line in Fig. 2.3.4 defines the critical resolution limit and as can be seen from Fig. 2.3.4, only at 45% MeOH, 0% ACN (Eluent 1) was this optimisation parameter threshold achieved.

It was therefore evident that a mixed organic composition was not suitable as an organic modifier, as adequate resolution between the peak pair (1,2) was not maintained at any point when ACN and MeOH were combined. For this reason, it was decided to use a single organic modifier for future studies on the effect of the organic component strength on retention of S3a. The organic solvents chosen for all further analyses were 100% ACN and 100% MeOH.

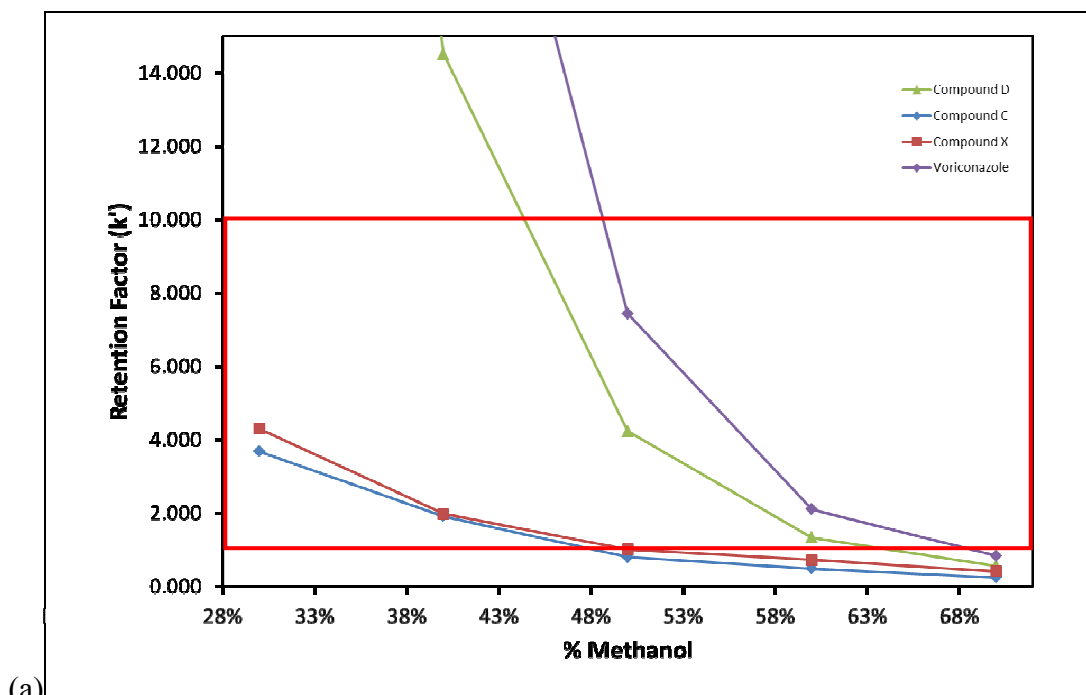
2.3.2.1.2 Optimising the organic component strength of the mobile phase

As mentioned in the previous section (Section 2.3.2.1.1) the use of a mixed organic mobile B component proved unsuitable. As a 45% MeOH (Eluent 1) mobile phase provided good resolution between critical peak pairs (1,81), MeOH was chosen as a potential organic component. From Fig. 2.3.3 however, it was noted that retention factors of analytes at this concentration were outside the ideal retention factor window of $1 \leq k \leq 10$. It was therefore decided to also explore ACN in this study as ACN is a stronger solvent based on the eluotropic series and therefore it was hypothesised that it would be possible to achieve a similar separation using a lower concentration of ACN, thus allowing greater scope for further gradient development if required. Also, MeOH and ACN were expected to have different effects on retention, as MeOH is a protic solvent and participates in hydrogen bonding while ACN has more dispersive effects with analytes. Table 2.3.3 below outlines the different eluents (8-18) which were analysed in this experiment.

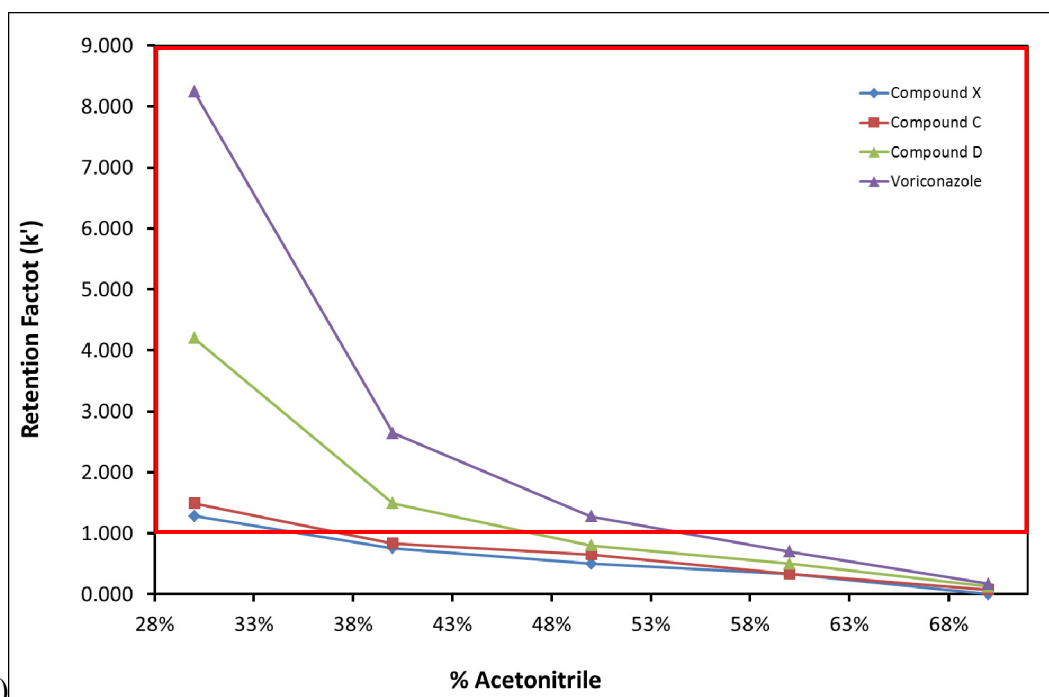
Table 2.3.3: Percentage (%v/v) of ACN/MeOH present in the mobile phase during optimisation of the organic content.

Eluent No.	FB	MeOH	Eluent No.	FB	ACN
			13	75%	25%
8	70%	30%	14	70%	30%
9	60%	40%	15	60%	40%
10	50%	50%	16	50%	50%
11	40%	60%	17	40%	60%
12	30%	70%	18	30%	70%

For comparison purposes a similar concentration range for both MeOH and ACN was chosen as illustrated in Table 2.3.3. The separations achieved using each of the mobile eluents 8 – 18 were evaluated both in terms of retention factor (Fig. 2.3.5) and resolution between peak pairs as shown in Fig. 2.3.6 and 2.3.7. Raw data for this experiment is given in Tables 5.1.2 (MeOH as MPB) and 5.1.3 (ACN as MPB) in appendices.



(a)



(b)

Fig. 2.3.5: Retention factor of Voriconazole (\blacktriangle), compound X (\blacklozenge), compound C (\blacksquare) and compound D (\blacktriangle) vs. increasing (a) MeOH* and (b) ACN concentration. All other conditions remain as per Section 2.3.1 Red box indicated the ideal retention factor window of between 1 and 10,.

* Retention factors for copound D and Voriconazole at 30% and 40% MeOH are off scale, at values of 52.250, 98.746 and 14.505, 26.593 respectively.

From analysis of Table 6.1.2/6.1.3 (appendices) and Fig. 2.3.5, it was noted that the elution order of the first two peaks compound X and compound C switched

depending on whether MeOH or ACN was used as mobile phase B. This change in elution order can be explained by preferential hydrogen bonding interactions between MeOH and the carbonyl functionality of compound C when MeOH was used as a mobile phase B which did not occur when ACN was used. The increased elution strength of ACN compared to MeOH was clearly demonstrated as the total run time with 30% MeOH (eluent 8) was 67 min while with 30% ACN (eluent 14), total run time was just 6 min. This is clearly indicated in Fig. 2.3.5a where the retention factors of both compound D and Voriconazole are both off scale (retention factor cut-off of $k=15$) at 30% and 40% MeOH while at these concentrations of ACN, retention factors are less than 10. The binary nature of ACN/water mixtures and clustering of the ACN molecules around solute molecules with increasing ACN concentration lead to the significant decreases in retention for all four molecules. The red box in Fig. 2.3.5a and 2.3.5b indicates the ideal retention factor window ($1 \leq k \leq 10$) and as can be seen from Fig. 2.3.5b, only 30% ACN (eluent 14) and 50% MeOH (eluent 10) fell within this window as at higher ACN concentrations, retention factors for compound X and compound C fell below 1, indicating insufficient interaction with the stationary phase. This is also the case for higher than 50% MeOH. At lower concentrations of MeOH, retention factors for later eluting peaks compound D and Voriconazole were above the $k = 15$ upper threshold. At greater than 50% ACN or MeOH, solvation properties of the organic solvent becomes more important as the mobile phase is now predominantly organic in nature and so analytes have a greater affinity for the now, less polar mobile phase. Each eluent (8-18) was also analysed with respect to resolution between peak pairs, this data is shown below in Fig. 2.3.6 and 2.3.7.

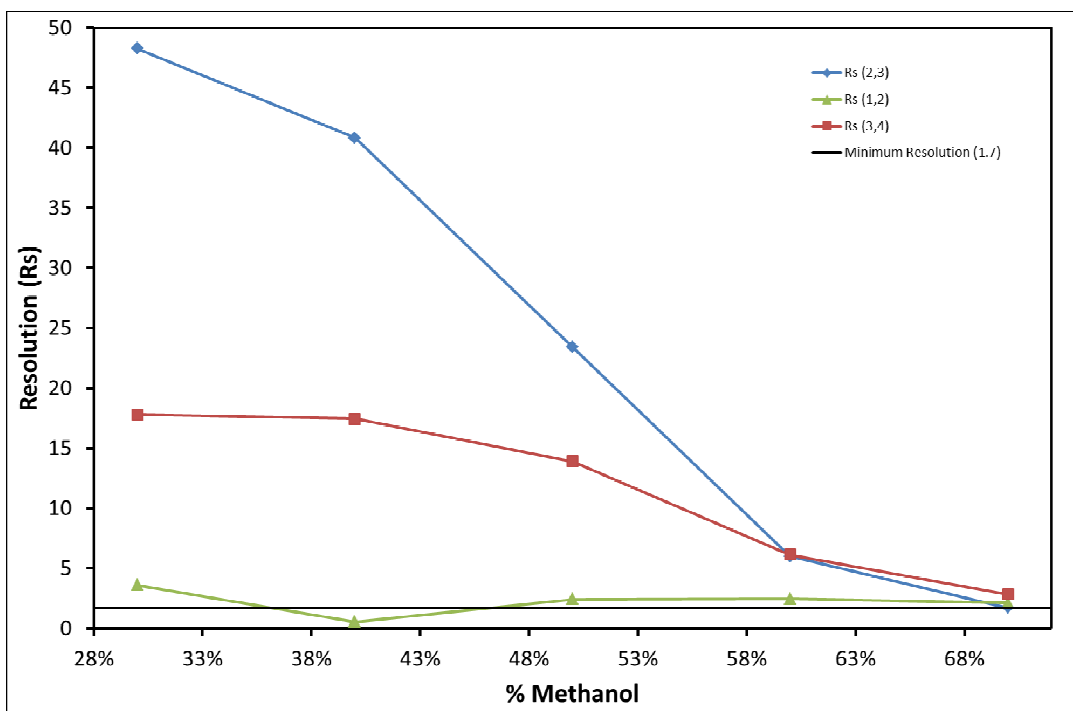


Fig. 2.3.6. Resolution between peak pairs vs. ratio of MeOH concentration. Peak pairs are as follows (1,2)(▲): compound C:compound X (2,3)(◆): compound X:compound D, (3,4) (■): compound D:Voriconazole. All other parameters remain as per Section 2.3.1. Minimum resolution at R_s of 1.7 is indicated by the solid black line.

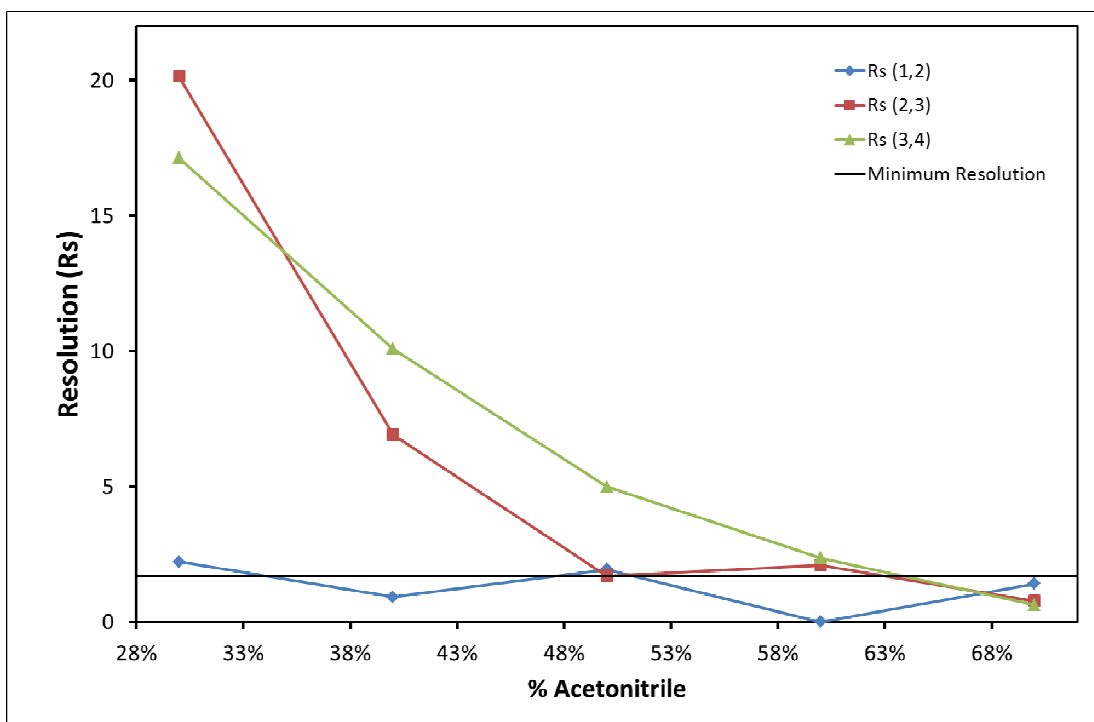


Fig. 2.3.7: Resolution between peak pairs vs. % ACN. Peak pairs are as follows (1,2)(◆): compound X:compound C, (2,3)(■): compound C:compound D, (3,4)(▲): compound D:Voriconazole. All other parameters remains as per Section 2.3.1. Minimum resolution at R_s of 1.7 is indicated by the solid black line.

Resolution is affected by three main parameters: retention, efficiency and selectivity. As a result with decreasing retention and decreased selectivity between peaks, resolution between peak pairs was expected to decrease. This was evident in both experiments where; as the concentration of MeOH or ACN increased, there was decreased retention of analytes and resolution between peak pairs decreased. As analytes began to co-elute at 50% ACN (eluent 10), resolution between peak pair compound X:compound C was lost completely and had a value of 0. Resolution between compound D and Voriconazole decreased from 20.36 with 30% (eluent 14) ACN to just 0.63 when 70% ACN was used (eluent 18). A similar trend was evident for MeOH where resolution between the same peak pair decreased from 13.88 at 50% MeOH (eluent 10) to 2.84 at 70% MeOH (eluent 12). At lower concentrations of MeOH, resolution between peak pair compound D:Voriconazole, resolution remained ~17.5 when both 30% and 40% MeOH were used (eluent 8 and 9). This was due to the large retention factors for Voriconazole of 98.74 and 26.593 at 30% and 40% MeOH respectively. At retention factors of greater than 20, resolution did not increase[6].

From the analysis of the separations using the various eluents (8-18) in terms of retention factor and the obtaining the shortest run time possible only, two possible eluents were highlighted as fit for purpose - eluent 10 (50% MeOH) and eluent 14 (30% ACN), therefore these mobile phase compositions were then investigated in terms of resolution. Critical resolution was defined at the start of the experiment (between peak pair (1,2), which in the case of MeOH was compound C:compound X and compound X:compound C in the case of ACN) was found to pass in both cases with a value of 2.42 recorded in the case of eluent 10 and 2.22 recorded in the case of eluent 14. A summary of both separations are given below in Table 2.3.4.

Table 2.3.4: Best separation achieved using a 50% MeOH (eluent 10) and 30% ACN (eluent 14) and 30 mM FB, pH4 as mobile phase during organic component mobile phase composition study.

Eluent 10: 50% Formate Buffer : 50% Methanol						
	Retention time (mins)	Retention Factor	Symmetry	Peak Width @ half height (mins)	Efficiency (plates per metre)	Resolution
Void	0.728					
Compound C	1.302	0.788	0.670	0.043	62260	
Compound X	1.459	1.004	0.670	0.045	83390	2.420
Compound D	3.803	4.224	0.950	0.083	124970	23.400
Voriconazole	6.140	7.434	1.030	0.122	150780	13.880
Eluent 14: 70% Formate Buffer : 30% Acetonitrile						
Peak	Retention time (mins)	Retention Factor	Symmetry	Peak Width @ half height (mins)	Efficiency (plates per metre)	Resolution
Void	0.683					
Compound X	1.560	1.284	0.770	0.043	99480	
Compound C	1.700	1.489	0.720	0.046	113220	2.220
Compound D	3.552	4.201	0.870	0.074	141140	20.150
Voriconazole	6.315	8.246	0.960	0.121	156270	17.150

With a mobile phase containing 70% 30 mM FB, pH 4 and 30% ACN, the run time of the assay was 6.315 min with a resolution between critical peak pair compound X:compound C of 2.22. A run time of 6.14 min and a resolution between critical peak pair compound C: compound X of 2.42 was achieved using 50% MeOH. Whilst both ACN and MeOH at the above concentrations gave similar results with respect to run times and resolution achieved, a mobile phase containing ACN was deemed to be the most suitable as the retention factor of compound C with a MeOH mobile phase was less than 1. A retention factor of $1 \leq k' \leq 10$ is preferred[37], as retention factors of less than 1 suggests that the analyte has not properly interacted with the stationary phase. ACN also has a lower viscosity and thus a lower associated back pressure than MeOH, allowing for higher flow rates to be used and is also advantageous in gradient method development as changing the concentration of ACN would not produce such a dramatic change in back pressures. This was also a contributing factor in the choice of organic solvent used. Therefore for further method development, the organic solvent and concentration chosen was 30% ACN (eluent 14). When compared to the USP 36-NF-31Voriconazole monograph as shown in Fig. 2.3.1 in Section 2.3.1, there was a decrease in run time of approximately one third, while the resolution between critical peak pair compound

X:compound C (critical peak pair is the same in both cases) decreased from 2.68 to 2.22; however the critical resolution was still maintained above 1.7 so this was deemed acceptable Fig. 2.3.8 below is a representative chromatograph of the separation of S3a and its related impurities. In order to optimise the separation further, the pH and concentration of the aqueous buffer was then investigated, this will be discussed in Section 2.3.2.1.3.

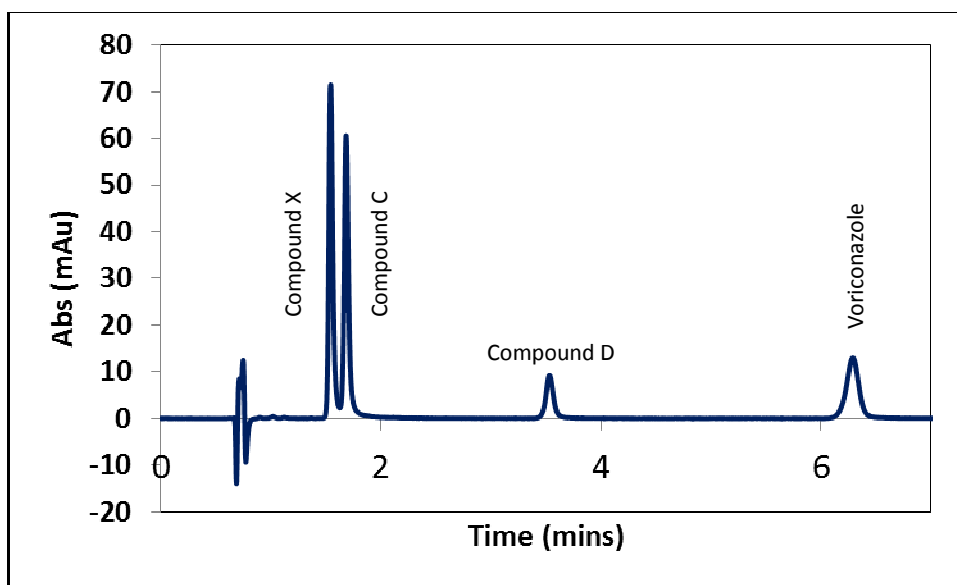


Fig. 2.3.8: Chromatogram of the best separation achieved using 70:30 FB:ACN mobile phase. Conditions were as follows; FB (FB): 30 mM, pH 4, flow rate: 0.3 mL/min, injection volume: 0.2 μ L, column temp: 35°C, detector wavelength: 256 nm.

2.3.2.1.3 Optimisation of the nature of the aqueous component of the mobile phase

Changing the concentration of a buffer affects its buffer capacity – it's ability to maintain a constant pH throughout a separation[108]. The selection of an appropriate buffer concentration and thus its ability to adequately resist small changes to the pH is often of critical importance in HPLC in order to avoid problems such as partial ionisation of an analyte. At 2 pH units less than their pKa, acidic analytes are mainly in their neutral form while basic analytes are protonated, similarly at 2 units above their pKa, the opposite is true, where acids are in their ionic form and bases are neutral. At a pH which is close to their pKa, analytes exist as an equilibrium of both

neutral and ionised forms affecting peak shape and retention due to unwanted strong interactions with surface silanols on the stationary phase. Therefore it is important to select an optimum pH for the analytes to ensure that they are either fully ionised or fully neutral.

In Fig. 2.1.1 the structures and pKa of Voriconazole and related impurities compound C, compound D are shown. Voriconazole and its related impurities are acidic with the highest predicted pKa being 2.75. In order for all analytes to be fully ionised the pH of the mobile phase should be 2 pH units above its pKa. Therefore based on this theory, the optimum pH should be at least 4.75. Therefore, FB was chosen as the buffer for this study as it has a pKa of 3.8 and therefore at pH 4.75 it lies within the appropriate pH range for maximum buffer capacity of ± 1 pH unit.

Using the optimal ACN concentration of 30% (eluent 14) obtained in Section 2.3.2.1.2, the nature of aqueous component of the mobile phase was then analysed. FB was optimised by first changing the concentration and then its pH, as in Table 2.3.5, whilst maintaining the constant FB:ACN ratio of 70:30. All other parameters remained the same as detailed in Section 2.3.1. Table 2.3.5 details the various mobile phase A compositions (eluent 19-27) which were analysed for the separation of S3.

Table 2.3.5: Conditions for experiments carried out when the pH and concentration of FB were systematically changed. Mobile Phase B in all cases was 30% ACN.

Eluent (E)	Ammonium FB	
	pH	Concentration (mM)
19	4.0	10 mM
20	4.0	20 mM
21	4.0	30 mM
22	4.0	40 mM
23	4.0	50 mM
24	3.0	30 mM
25	3.5	30 mM
26	4.5	30 mM
27	5.0	30 mM

2.3.2.1.3.1 Changing the concentration of ammonium FB

Ammonium FB was prepared with concentrations ranging from 10 mM to 50 mM in 10 mM increments (E19-23). This was then adjusted to pH 4 in all cases with formic acid. pH 4 was chosen as a starting point as this was the pH used in the original method outlined in USP 36-NF-31 –Voriconazole monograph. All other method parameters remained the same as detailed in Section 2.3.1. S3a standard was analysed for each mobile phase composition. Results of this experiment are shown below in Table 6.1.4 (appendix) and Fig. 2.3.9 and 2.3.10. Chromatography obtained was analysed in terms of peak symmetry.

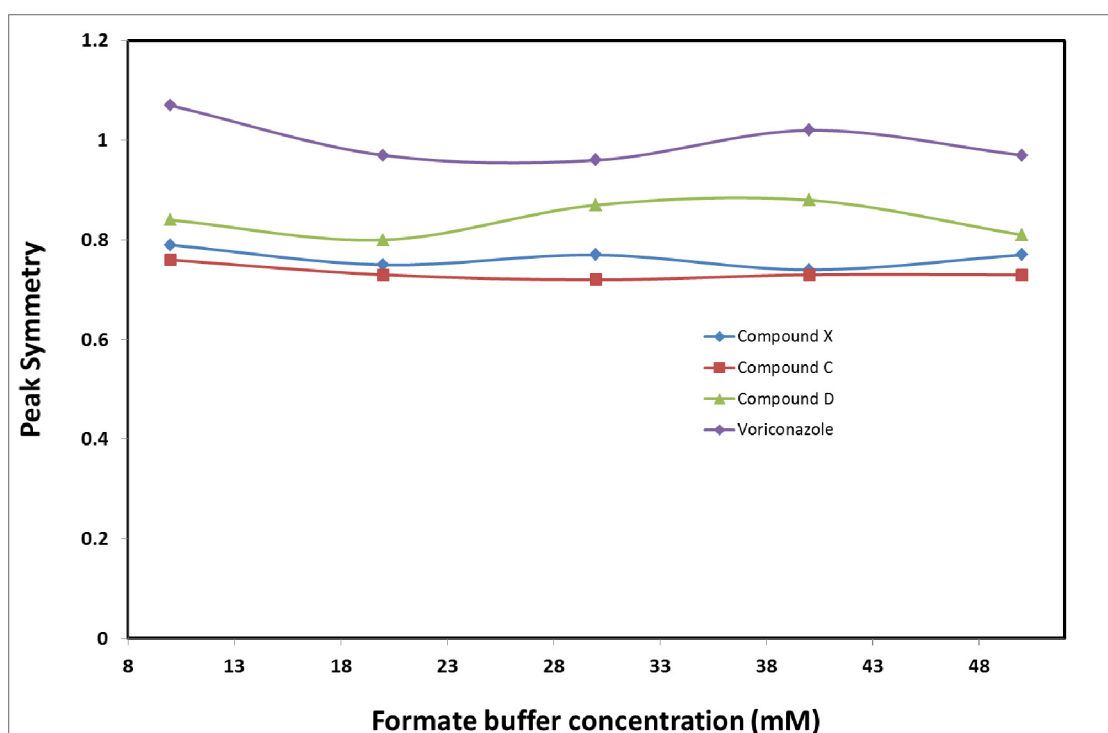


Fig. 2.3.9: Peak symmetry of Voriconazole (◆) and related impurities compound X(◆) compound C(■) and compound D(▲) vs. concentration of FB. Mobile phase: 70:30 FB:ACN. pH: 4.00, column temperature: 35°C, injection vol: 0.2 μL, detector wavelength: 256 nm. *raw data for this study is given in Fig. 6.1.4 (appendices).

Fig. 2.3.9 shows the peak symmetries for all four analytes across the concentration range selected (eluent 19-23). Peak symmetries remained quite constant across the range of FB concentrations investigated. For all analytes a deviation of ± 0.04 units was observed, which indicated that at all buffer concentrations, pH was adequately maintained. A deterioration in peak shape would have indicated insufficient buffer capacity causing partial ionisation of analytes and associated variations in stationary

phase/analyte interactions; however no deterioration was observed. It was concluded therefore that the concentration of ammonium formate should remain at 30 mM based on the data obtained for peak symmetry, as no significant advantages were noted when the concentration was changed. A concentration of 30 mM FB was used for the remainder of the study.

2.3.2.1.3.2 Optimisation of ammonium FB pH

In this investigation, the buffer concentration was maintained at 30 mM while the pH of the mobile phase was changed in 0.5 pH unit increments from 3.0 to 5.0. All other parameters remained as outlined in Section 2.3.1. Again chromatography was analysed terms of peak symmetry. Results of the study are given below in Fig. 2.3.10.

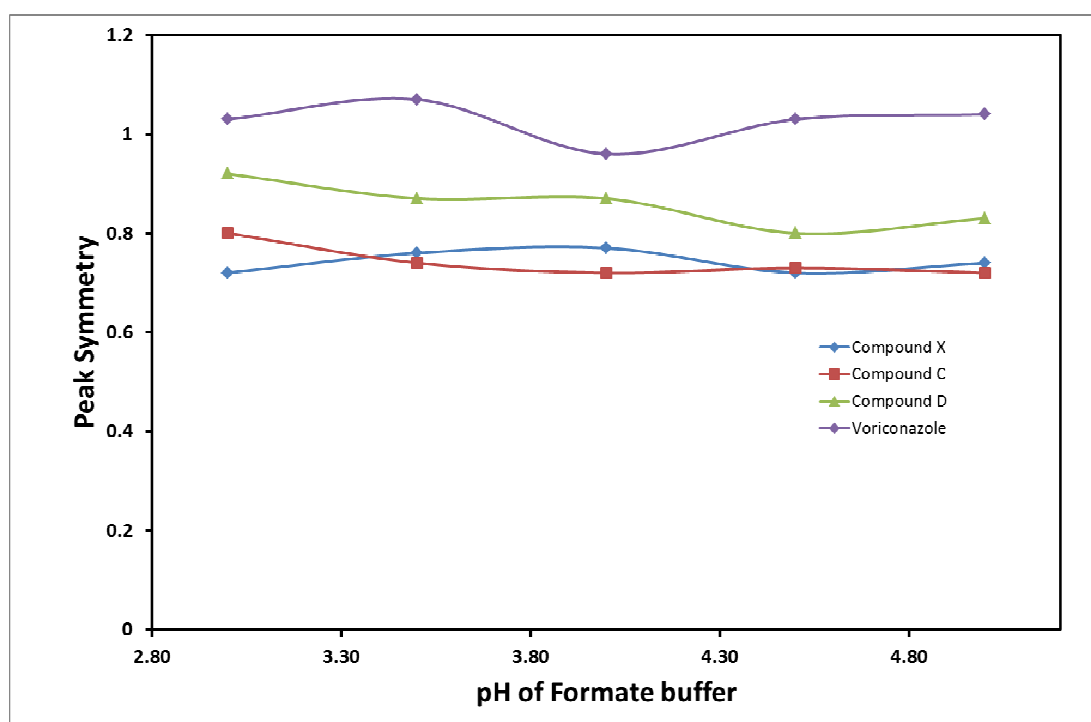


Fig. 2.3.10: Peak symmetry of Voriconazole (◆) and related impurities compound X(◆), compound C(■) and compound D(▲) vs. pH of FB. FB concentration: 30 mM. All other parameters remained as per Fig. 2.3.9. *Raw data is shown in Fig. 6.1.5 (appendices)

At 2 pH units above or below its pKa an analyte is either fully ionised or non-dissociated depending on whether the analyte is an acid or a base. The analyte in this study with the highest predicted pKa was compound D with a pKa of 2.75, therefore,

to ensure that the compound and all other analytes were fully ionised, a pH of 4.75 should have been selected. However during the investigation the maximum pKa was believed to be 2.00 and therefore an optimum pH of 4.00 was chosen. This error was only realised after the investigation was completed. Analysis of Fig. 2.3.10 indicated however that the peak symmetry between pH 4 and pH 5 deviated by <5%. This was not unexpected given that at 1 pH unit above its pKa, 90% of the analyte was in its fully ionised form. A concentration of 30 mM and a pH of 4.00 were used for the remainder of the investigations. The final isocratic parameter which was optimised was temperature.

2.3.2.1.4 Optimisation of the temperature of the run

An increase in temperature was expected to in result in a decrease in retention[37]. Another advantage of higher temperature is a reduction in mobile phase viscosity and thus back pressure so higher flow rates can be used. In this research temperature was varied from 35°C to 55°C in 5°C increments. The mobile phase which was used was 70:30 FB:ACN All other parameters remained the same as outlined in Section 2.3.1.

Results of this study are given in Fig. 2.3.11 and 2.3.12. Similar to the organic component study, the chromatography was analysed in terms of retention factor (k) and resolution between peak pairs.

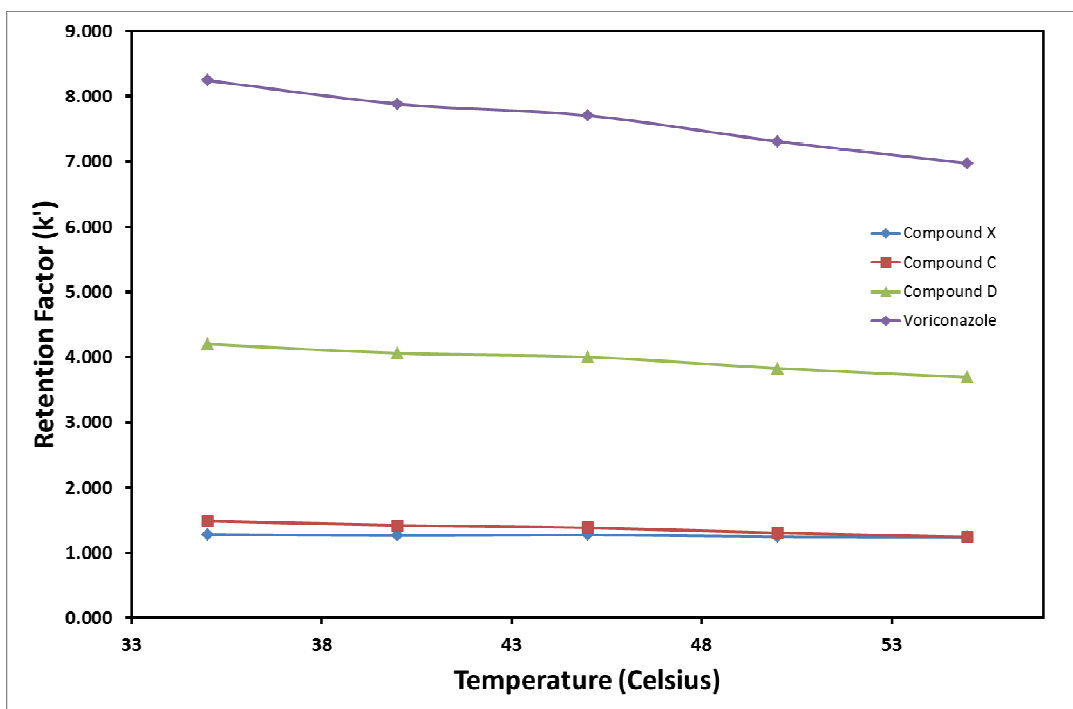


Fig. 2.3.11: Retention factor Voriconazole(◆) and related impurities compound X(◆) compound C(■) and compound D(▲) vs. column temperature. Other chromatographic parameters included: Mobile phase 70:30 30mM FB, pH 4.00:ACN, detector wavelength: 256 nm, injection vol: 0.2 μ L. *Raw data for this experiment is given in Fig. 6.1.6.

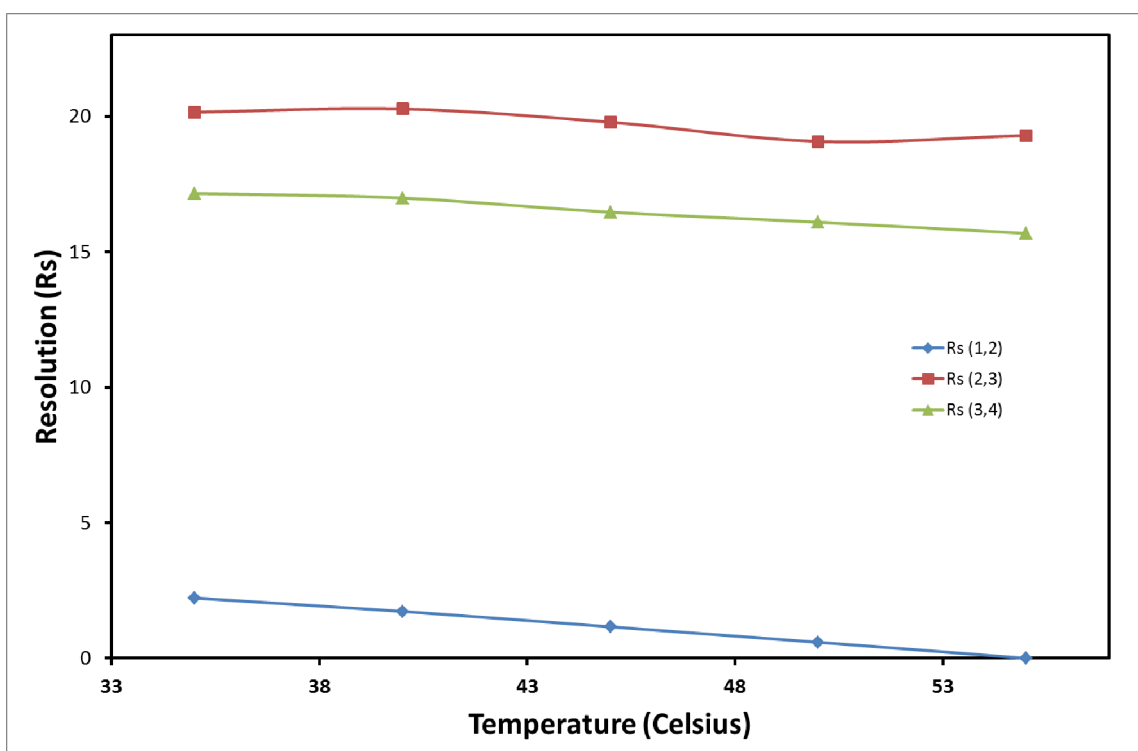


Fig. 2.3.12: Resolution between peak pairs vs. column temperature Peak pairs are as follows (1,2)(◆): compound X:compound C, (2,3)(■): compound C:compound D, (3,4)(▲): (compound D:Voriconazole). Chromatographic parameters as per Fig. 2.3.11.

As expected increasing temperature affected the retention of Voriconazole and its related impurities, with retention of all four components decreasing as column temperature increased as seen from the plots of retention factor vs. column temperature (Fig. 2.3.11). Retention of compound C, compound D and Voriconazole were more significantly affected than the earliest eluting analyte compound X. The decrease in retention of compound C had the greatest impact on the overall separation as with increased temperature, not only did the retention factor continuously decrease across the temperature range 35-55°C from 1.425 to 1.244, the resolution of peak pair compound X and compound C as shown in Fig. 2.3.12 decreased from 2.22 at 35°C, to a resolution of 0 and complete co-elution of the two analytes at 55°C. At 40°C, resolution of this peak pair is just above a critical value of 1.7 at 1.73, however given its closeness to the lower threshold value, this was deemed to be unsuitable.

While increasing temperature was demonstrated a decrease retention when a 70:30 FB:ACN mobile phase was used as shown in Fig. 2.3.12, the loss of resolution between the critical peak pair (compound X:compound C) with increasing temperature meant that this particular mobile phase composition was deemed unsuitable. Table 6.1.3 (appendices) show the raw data from the optimisation of the organic component strength (ACN), illustrating that whilst the total run time of the assay at 25% ACN (eluent 13) (12.882 min) was almost twice that at 30% ACN (eluent 15) 6.315 min), resolution between the critical peak pair also more than doubled, going from 2.22 at 30% ACN to 5.94 at 25%. This increase in resolution was hypothesised to afford a higher temperature to be used, shortening retention times, without bringing the resolution between the critical peak pair (compound X:compound C) close to a critical value of 1.7. Therefore the experiment was repeated with a 25:75 ACN:FB mobile phase (exp 4b). All other parameters remained the same as in Section 2.3.1. The results of this experiment are given in Table 6.1.7 (appendices) and Fig. 2.3.13 and 2.3.14.

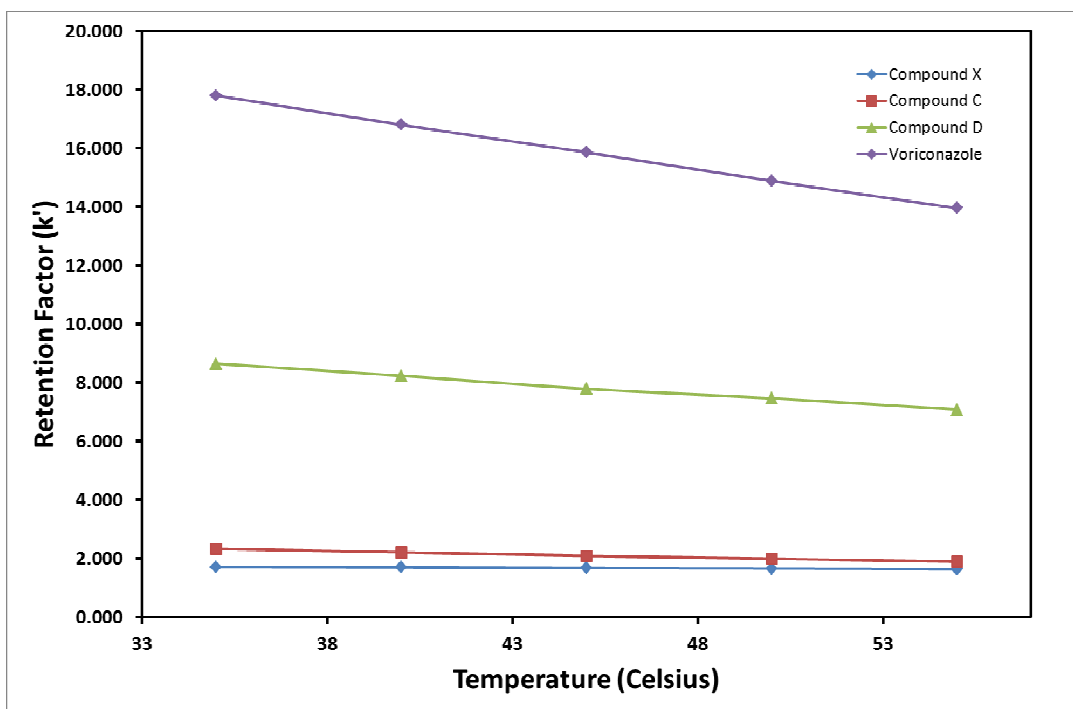


Fig. 2.3.13: Retention factor of Voriconazole(◆) and related impurities compound (◆), compound C (■) and compound D(▲) vs. temperature of column Mobile phase is 25% ACN: 75% ammonium FB. All other parameters remain as per Fig. 2.3.11.

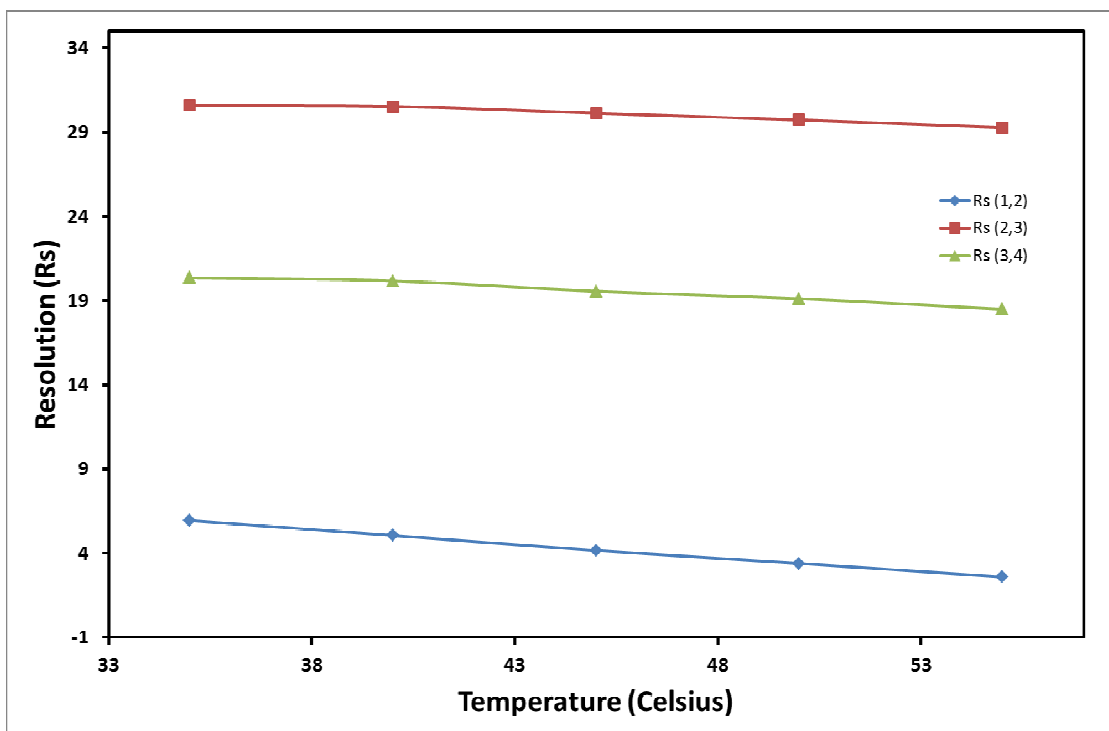


Fig. 2.3.14: Resolution between peak pairs vs. column temperature. Peak pairs are as follows (1,2)(◆): compound X:compound C, (2,3)(■): compound C:compound D, (3,4)(▲): (compound D:Voriconazole). Mobile phase is 25% ACN: 75% ammonium FB. Chromatographic parameters as per Fig. 2.3.11

Similar to the previous temperature study the same trends were observed here, with slightly decreasing retention factors (Fig. 2.3.13) for each of the four components and decreasing resolution between peak pairs (Fig. 2.3.14). However unlike the temperature study using 30% ACN there was still sufficient retention factors of above 1 at all temperatures when 25% MeOH is used. Resolution in all cases is above 2. Despite having adequate resolution between peaks 1 and 2 (compound X:compound C) when a column temperature of 55°C was applied (3.40 @ 50°C, 2.59 @ 55°C) a temperature of 50°C was taken as the optimum temperature using this mobile phase because as well as good resolution, efficiency at this temperature, as seen in Table 6.1.7, was highest here.

Fig. 2.3.15. below shows a representative chromatogram at 50°C. The run time of this impurity assay was now over 1 minute lower than the USP 36-NF-31 Voriconazole monograph, resolution between the critical peak pair compound X:compound C was increased from 2.68 to 2.97. Given that the run time of this assay was now longer than the original method and negating the goal of the development of a faster assay, further method development was necessary.

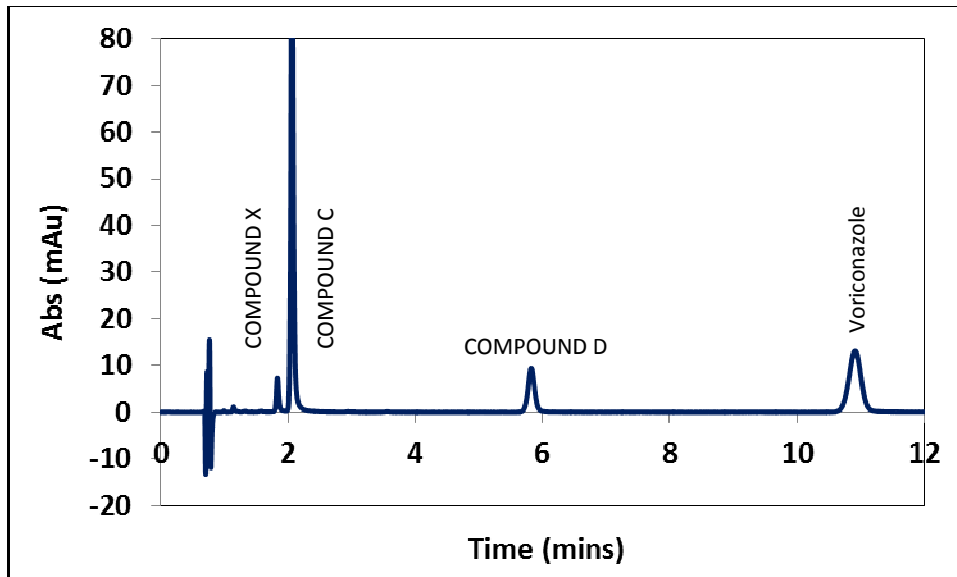


Fig. 2.3.16. Chromatogram of best separation obtained using 75% ammonium FB : 25% ACN with a column temperature of 50°C. All other parameters as described in Section 2.3.1 and 2.3.1.2.

2.3.2.1.5 Increasing the flow rate of the method to obtain a faster separation

Increasing the flow rate of a method decreased analysis time, however also resulted in an increase in the column back pressure. Since the back pressure of the system with the current mobile phase (70:30 FB:ACN) and temperature (55°C) was >200 bar and the instrument and column were capable of reaching pressures of 400 bar, it was hypothesised that while increasing the flow rate by a factor of 2 would increase the back pressure by approximately 2 and theoretically half the run time, back pressure would still remain within the acceptable limit of 400 bar for the instrument.

Details of the method used for this analysis are as follows. Mobile phase: 25% ACN: 75% 30mM ammonium formate (pH 4), flow rate: 0.6 mL/min, column temp: 50°C, detector wavelength 256 nm, injection volume. 0.2 µL. Results of this investigation are tabulated below in Table 2.3.6 and a representative chromatogram is also shown in Fig. 2.3.17.

Table 2.3.6: Results of investigation to increase the flow rate to 0.6 mL/min (600 µL/min)

25% ACN, 75% Formate Buffer, 50° @ 600 µL/min					
Peak	Retention time (mins)	Retention Factor	Symmetry	Efficiency (plates per metre)	Resolution
Void	0.336				
Compound X	0.929	1.765	0.79	117960	
Compound C	1.084	2.226	0.9	129210	4.27
Compound D	3.295	8.807	0.95	151130	20.21
Voriconazole	6.265	17.646	1.14	141960	17.46

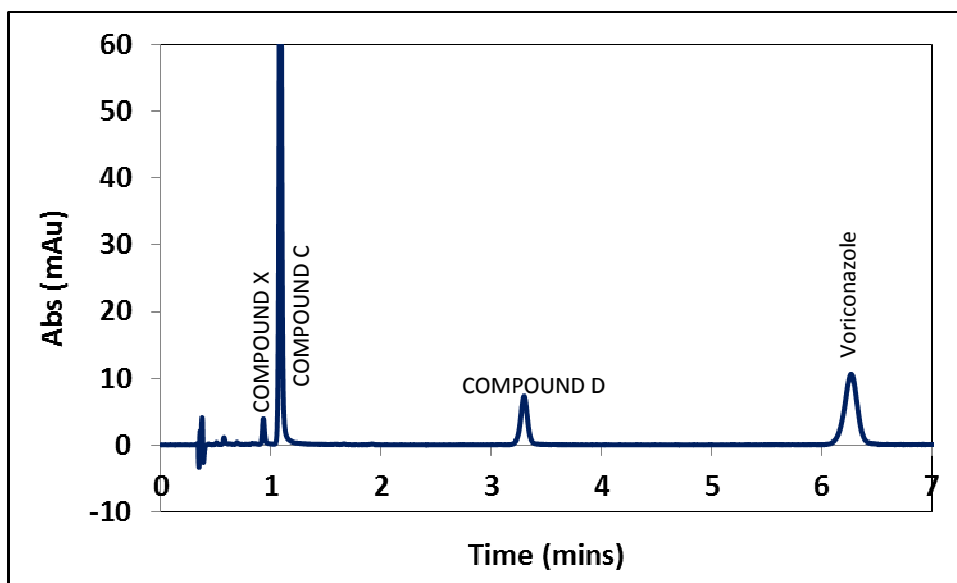


Fig. 2.3.17. Representative chromatogram separation obtained when the flow rate is doubled to 0.6 mL/min. All other parameter remain the same as Fig. 2.3.15

When compared with results from the previous method where 0.3 $\mu\text{L}/\text{min}$ flow rate was used, (Appendices, Table 6.1.3) increasing the flow rate of the run to 0.6 $\mu\text{L}/\text{min}$ led to a 42% decrease in retention time for the API peak from 10.916 min down to 6.265 min. It is noted here, that should an isocratic method have been developed, a Van Deemter study should have been carried out in order to determine the optimum flow rate for maximum efficiency, however as the method development was to ultimately change to a gradient approach, this was deemed unnecessary.

From the optimisation of the nature of the mobile phase and temperature, it was clear that the concentration of organic solvent and the temperature of the column have a greater impact on the chromatography obtained than the nature of the aqueous mobile phase A. While there was a reduction in the run time of the assay of approximately 41% (6.265 min) when compared to the USP method (9.221 min), it was felt that by applying a gradient, run times could be further reduced.

2.3.2.2 Development of a gradient separation

Gradient elution allows the efficient separation of compounds with widely varying polarities and retentions in a reasonable period of time. Development of a gradient separation is often favoured over an isocratic separation due to the fact that at a

single mobile phase B concentration, resolution of early eluting peaks may be low, while strongly retained compounds have excessively long retention times which leads to very broad peaks with small peak heights making them harder to detect [109]. The use of a gradient over an appropriate mobile phase B concentration range in this study was hypothesised to allow the maintenance of adequate resolution between earlier eluting peaks, while the previously more strongly retained compounds are eluted faster with higher B concentrations leading to sharper taller more efficient peaks. Both the gradient length and % ACN at the top end of the gradient were optimised in this experiment. Parameters which were optimised during isocratic optimisation were carried through to gradient development. The optimised parameters for isocratic optimisation were as follows; column temperature 50°C, buffer concentration; 30 mM with a pH of 4, flow rate 0.6 mL/min, detector wavelength: 256 nm.

2.3.2.2.1 Determination of the delay volume of Agilent 1200 series liquid Chromatograph.

The ultimate goal in this HPLC method development was the transfer of the method developed on a 2.6 µm core-shell particle column to a smaller particle size 1.7 µm column. The use of this smaller particle size column required the use of a dedicated instrument capable of handling the high pressure generated by the column. The first step was to calculate the dwell volume of the instrument which was used for the 2.6 µm method development, as dwell volumes vary from instrument to instrument and gradient times must be altered accordingly when methods are transferred between instruments. The delay volume of the Agilent 1200 series liquid chromatograph was determined by injecting a water blank with a mobile phase gradient which involved an isocratic hold for 3 min and a subsequent step from 0% mobile phase B (MP B) to 100% MP B at 3.01 min. MP B was chosen so that at the desired wavelength, the MP would give a detector response. MP B used in this experiment was 1% v/v acetone as acetone has an absorbance at 220 nm. The time taken for a change in baseline absorbance after the step gradient was affected was an indicator of the delay volume of the system. The gradient table used for this experiment is given in Table 2.3.7.

Table 2.3.7: Gradient profile for determination of Agilent 1200 series delay volume.

Gradient for the determination of system dwell volume	
Time (mins)	% Mobile Phase B (1% v/v Acetone)
0.00	0
3.00	0
3.01	100
7.00	100
7.01	0
10.00	0

The time at which 5% of the total absorbance for acetone was observed was recorded. The chromatogram obtained is shown in Fig. 2.3.18. This value was then used to calculate the dwell volume of the system.

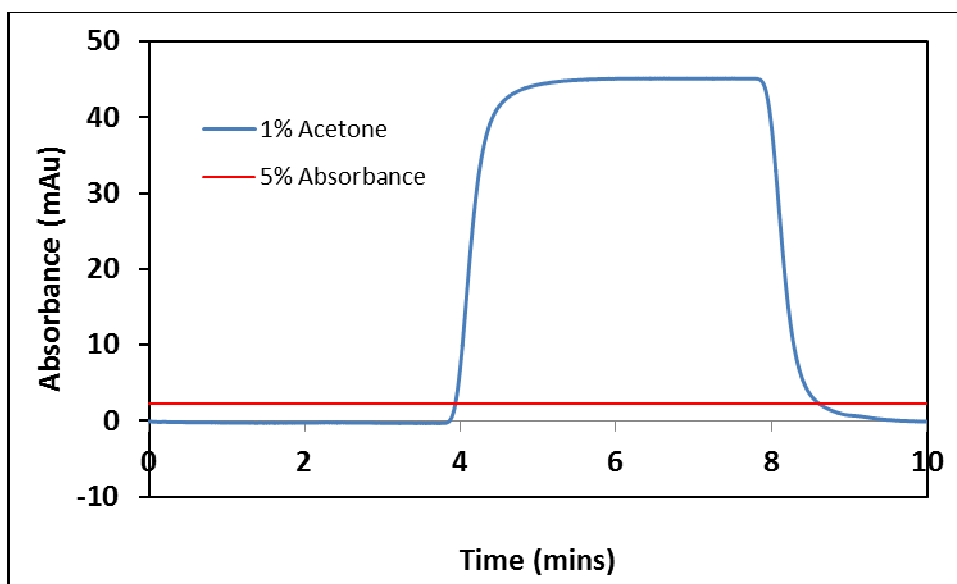


Fig. 2.3.18: Determination of void volume of Agilent 1200 series HPLC. Conditions as outlined in Section 2.3.2.2.1.

5% of the maximum absorbance recorded for a 1% acetone solution was noted at 3.95 min. As the mobile phase composition did not change until 3.01 min, this was subtracted from the total time taken to give a value of 0.94 min. As the flow rate used was 1 mL/min, the dwell volume was calculated to be 0.94 mL. The dwell volume of this system was then later compared to the dwell volume of the Shimadzu

Nexera when transferring the newly developed method and the gradient profiles were adjusted accordingly.

2.3.2.2.2 Gradient method development

As seen in Section 2.3.2.1.5, retention factors of analytes compound D and Voriconazole were 8.807 and 17.646 respectively while resolution between the peak pairs compound C:compound D and compound D:Voriconazole were 20.21 and 17.46 respectively. Retention of both analytes was deemed to be excessive, as too was the resolution between the peak pairs. Development of a gradient method was therefore explored in an effort to reduce retention of these analytes and shorten run times.

To maintain resolution between impurities compound X and compound C obtained during an isocratic run when 25% ACN was used as mobile phase B, a 25% ACN hold was applied for 1.2 min as compound C eluted at 1.084 min. In order to decrease the retention time of well retained compounds, a linear gradient with a final ACN concentration of 80% over 2.8 min was applied. A step from 80% to 25% ACN was then applied with an isocratic hold of 3.0 min in order to re-equilibrate the column. The gradient table and profile are presented in Table 2.3.8. Other separation conditions which were maintained throughout gradient development are as follows; injection volume; 0.2 μ L, flow rate: 0.6 mL/min, column temperature: 50°C, detector wavelength: 256 nm.

Table 2.3.8 Development of an optimum separation using a gradient method on a Phenomenex Kinetex 2.6 μm core-shell stationary phase (2.1 x 100 mm). Gradient profile/conditions of Gradient 1: All other parameters remained constant. Mobile Phase A: 30 mM FB, pH 4.00, Temperature: 50°C, Wavelength: 256 nm, Injection volume 0.2 μL

Gradient 1	
Time (mins)	% ACN
0.00	25%
1.20	25%
4.00	80%
4.01	25%
7.00	25%

The separation obtained was evaluated in terms of run time and resolution between peak pairs. Results of separation are given in Table 2.3.9. When compared to the isocratic run in Section 2.3.2.1.5, overall run time was reduced by approximately 1/3 from 6.265 min to 4.14 min. Critical resolution between impurities compound X and compound C decreased to 3.78, however this was still significantly higher than the resolution threshold of 1.7 which was set previously. Fig. 2.3.19 shows representative chromatograms for this gradient, Gradient 1.

Table 2.3.9: Result of Gradient 1; 1.2 min isocratic hold, 25-80% gradient ramp over 2.8 min, followed by a 3 min 25% ACN isocratic hold.

Gradient 1			
Peak	Retention time (mins)	Retention Factor	Resolution
Void	0.343		
Compound X	0.909	1.650	
Compound C	1.061	2.093	3.860
Compound D	3.244	8.458	28.440
Voriconazole	4.251	11.394	13.180

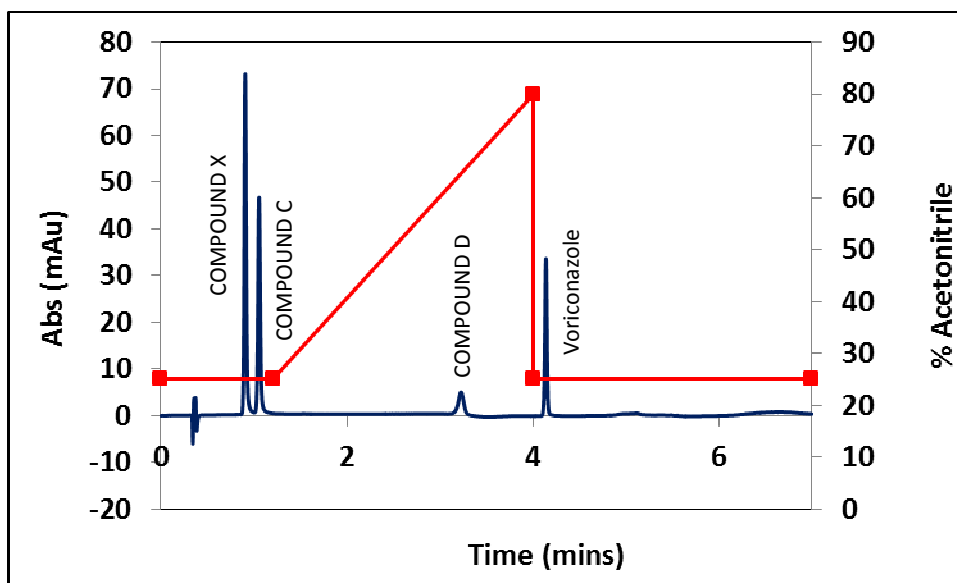


Fig. 2.3.19: Chromatograms of a separation of Voriconazole and its related impurities compound X, compound C and compound D using gradient profiles 1 (shown in red). Conditions for the separation were as follows: Mobile phase FB:ACN. Column temperature: 50°C. Detector wavelength: 256nm. Injection vol: 0.2 μ L

Despite the decrease in overall retention time of the assay and the reduction in the resolution between peak pair compound D and Voriconazole from 17.46 to 13.180, there was no decrease in the retention of compound D which eluted at 3.244 min during the gradient separation – an almost identical retention time as for the isocratic separation shown in Fig.2.3.17. Since a linear gradient did not produce the desired reduction in retention time for this analyte, a step gradient was introduced in order to facilitate a faster transition to higher MP B concentrations and thus reduce retention.

The following step gradient in Table 2.3.10 with a step at 1.2 min and an isocratic hold for 2.8 min. was chosen for analysis. As well as changing to a step gradient rather than a linear gradient, the final concentration of ACN was raised to 90% for this experiment. It was anticipated that this increase in final ACN concentration would further reduce the run time of the assay.

Table 2.3.10 Development of an optimum separation using a gradient method on a Phenomenex Kinetex 2.6 μm core-shell stationary phase (2.1 x 100 mm). Gradient 2 mobile phase conditions. All conditions remained as per Fig. 2.3.19

Gradient 2	
Time (mins)	% ACN
0.00	25%
1.20	25%
1.21	90%
4.00	90%
4.01	25%
7.00	25%

Table 2.3.11: Results of separation of S3 using Gradient 2 profile (Table 2.3.10).

Gradient 2			
Peak	Retention time (mins)	Retention Factor	Resolution
Void	0.343		
Compound X	0.906	1.641	
Compound C	1.055	2.076	3.780
Compound D	3.227	8.408	28.420
Voriconazole	4.140	11.070	12.340

Results of this experiment as given in Table 2.3.11; additionally a chromatogram of the separation is given in Fig. 2.3.20. The results showed that total run time was indeed reduced by almost 1 min. This was due to both an increase in end concentration of ACN and also the switch to a step gradient. It was noted that retention of compound D was still not significantly affected by the step gradient. This was most likely due to the dwell volume of the system, which had not previously been taken into account when developing a gradient profile. The delay volume of the system was 0.94 mL and as a result, with a 0.6 mL/min flow rate, the 90% step did not reach the column until 1.5 min later than originally programmed. As a result, instead of 90% ACN reaching the column at 1.21 min, it instead reached the column at ~ 2.7 min. From the retention times of both Compound C and X, it was noted that both analytes eluted quite rapidly, in ~ 0.4 min when the ACN concentration was raised to 90%.

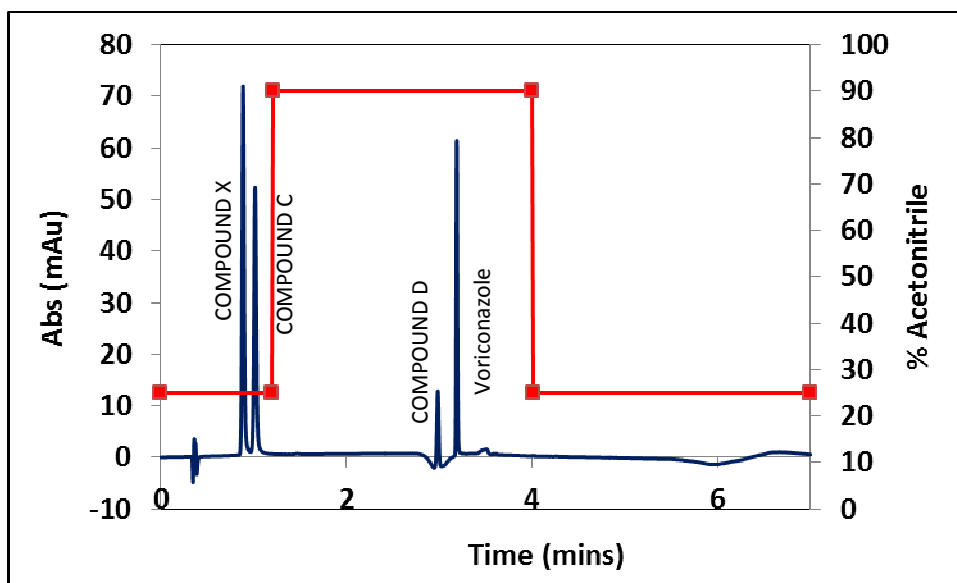


Fig. 2.3.20: Chromatograms of a separation of Voriconazole and its related impurities compound X, compound C and compound D using gradient profile 2 (shown in red). Conditions for the separation as per Fig. 2.3.19.

To counteract the effect of the delay volume, the length of the isocratic hold was shortened systematically in an attempt to reduce the retention of compound X and Voriconazole further. The gradient profiles for this experiment is given in Table 2.3.12. The isocratic hold time was reduced by 0.7 min which was half that of the delay time, the expected result of this was maintenance of the resolution of compound X and compound C, as the gradient step would still not take effect until after both peaks had eluted from the column. Retention of compound D and Voriconazole was expected to be reduced further.

Table 2.3.12: Development of an optimum separation using a gradient method on a Phenomenex Kinetex 2.6 μm core-shell stationary phase (2.1 x 100 mm). Gradient 3 gradient profile conditions. All other parameters remained as per Fig. 2.3.19.

Gradient 3	
Time (mins)	% ACN
0.00	25%
0.50	25%
0.51	90%
4.00	90%
4.01	25%
7.00	25%

Table 2.3.13: Results of separation of S3a using Gradient profile 3 as shown in Table 2.3.12.

Gradient 3			
Peak	Retention time (mins)	Retention Factor	Resolution
Void	0.345		
Compound X	0.878	1.545	
Compound C	0.993	1.878	3.060
Compound D	2.361	5.843	45.020
Voriconazole	2.495	6.232	6.690

As the initial hold time was shortened from 1.20 min to 0.50 min, the anticipated reduction in the retention of both compound D and Voriconazole due to the 90% gradient step reaching the column faster was observed (Table 2.3.13). As was noted with Gradient 2 (table 3.10), compound D and Voriconazole were eluted off the column almost immediately after the 90% step reached the column. Based on previous calculation of a 1.5 min dwell time, 90% ACN was expected to reach the column at 2.20 min. Retention times of compound D and Voriconazole were 2.361 and 2.495 min respectively. Resolution above 3 continued to be maintained for the earlier eluting peak pair, while a resolution of 6.69 was noted for the last eluting peak pair compound D and Voriconazole. Fig. 2.3.21 shows the separation of Voriconazole and its related impurities using mobile phase gradient 3.

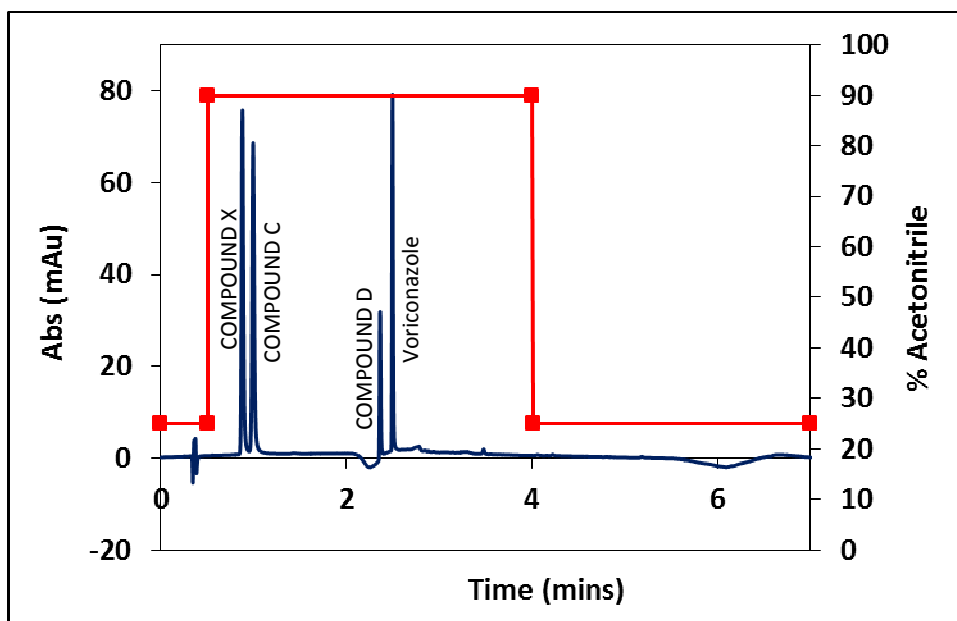


Fig. 2.3.21: Chromatograms of a separation of Voriconazole and its related impurities compound X, compound C and compound D using gradient profiles 3 (shown in red). Conditions for the separation as per Fig. 2.3.19.

As mentioned previously, the expected delay time of the Agilent 1200 series liquid chromatograph at a flow rate of 0.6mL/min was expected to be 1.5 min. While the isocratic hold was reduced to 0.5 min previously, it was hypothesised that this could further be reduced to 0.1 min without significant impact on the resolution of compound X and compound C. As well as this, it was felt that the isocratic hold at 90% could be significantly reduced. The isocratic hold in the previous method was 90% for 3.5 min, however it was felt that an isocratic hold of 0.6 min would be sufficient to elute the last two analytes in an adequate time frame and with sufficient resolution. Adjustment of the gradient in line with the dwell time meant that the gradient would take effect at 1.6 min and be held for 0.6 min, thus eluting compound D and Voriconazole within this time frame. Gradient profiles are given in Fig. 2.3.22.

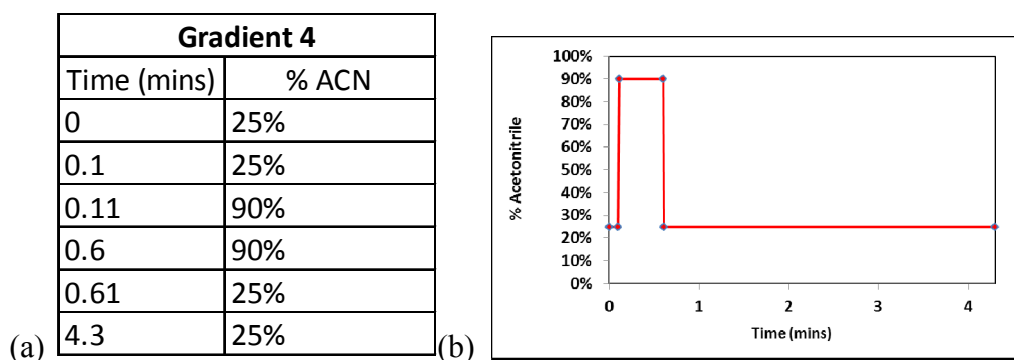


Fig. 2.3.22: Development of an optimum separation using a gradient method on a Phenomenex Kinetex 2.6 μm core-shell stationary phase (2.1 x 100 mm using “Gradient 4” mobile phase conditions (a) and (b) Gradient 4 profile

The result of this final gradient optimisation is given in Table 2.3.14 and Fig. 2.3.23. As hypothesised, resolution was maintained between peak pair compound X and compound C with these analytes eluting at 0.92 and 1.076 min respectively with a resolution of 3.8. The chromatogram in Fig. 2.3.23 shows the separation of voriconazole and its related impurities, as well as the gradient profile and adjusted gradient profile. It can be seen from this chromatogram that when adjusted, the gradient chosen eluted compound X and compound C during the 25% isocratic hold, while analytes compound D and Voriconazole were eluted during the 90% isocratic hold.

Table 2.3.14: Results of separation of S3 using the final optimised gradient, which includes a 0.1 min linear ramp, 0.5 minute hold and a 90% to 25% step.

Gradient 4			
Peak	Retention time (mins)	Retention Factor	Resolution
Void	0.343		
Compound X	0.920	1.682	
Compound C	1.076	2.137	3.800
Compound D	1.926	4.615	25.540
Voriconazole	2.031	4.921	4.500

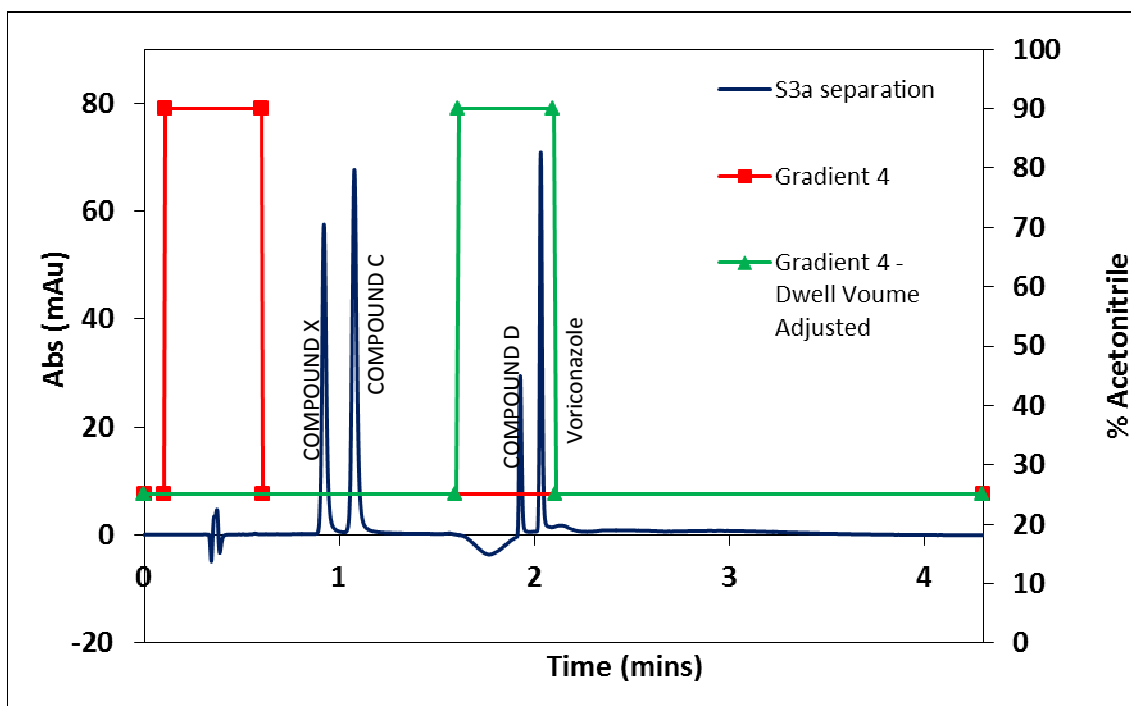


Fig. 2.3.23: Chromatograms of a separation of Voriconazole and its related impurities compound X, compound C and compound D using gradient profiles 4 (shown in red) and gradient 4 adjusted to match dwell volume (shown in green) Conditions for the separation as per Fig. 2.3.18

The final optimised method on the Phenomenex Kinetex core-shell C₁₈ reversed phase column had a run time of 4.3 min, a critical resolution of 3.80 between impurities compound X and compound C and a critical resolution of 4.5 between impurity compound D and Voriconazole. When compared to the original Pfizer impurity assay for Voriconazole, the run time has been shortened by 57% and resolution between the original peak pair (compound X:compound C) has increased from 2.68 to 3.80, while resolution between compound D and Voriconazole has decreased from 10.81 to 4.5. The use of a core-shell stationary phase as well as reduced particle size provided shorter diffusion pathlengths for analytes thus speeding up the separation. Additionally the application of a gradient to this method allowed more strongly retained compounds such as Voriconazole to elute faster and reduced unnecessary resolution between peak pairs. This method was then transferred to a core-shell column with a particle size of 1.7 μm in diameter and further optimised in an effort to reduce run time further.

2.3.2.3 Development of an optimised UPLC method on a core-shell 1.7 μm column

The optimised method from Section 2.3.2.2.2 was then transferred to a smaller 1.7 μm core-shell Phenomenex Kinetex column (100 x 2.1 mm, particle size 1.7 μm) and further optimised to provide the shortest run time possible while maintaining a resolution of at least 1.7 between peak pairs. Again this was carried out by changing the gradient time and the percentage ACN in the mobile phase. Moving to smaller particle size should in theory lead to a faster separation due to shorter interstitial diffusion pathways. Moving to a 1.7 μm particle size column, however, brings the added issue of increased back pressure (>400 bar). For this reason a specialised high pressure instrument is required to cope with the increase in back pressure. The instrument used for this study was a Shimadzu Nexera UPLC Liquid Chromatography capable of withstanding pressures of up to 1000 bar.

2.3.2.3.1 Determination of the dwell volume of the Shimadzu Nexera UPLC Liquid Chromatograph

Determination of the dwell volume of the Shimadzu Nexera liquid chromatograph was carried as per the gradient profile method carried out in to Section 2.3.2.2.1. As mentioned previously (Section 2.3.2.2.1), determination of the dwell volume is required when transferring gradient methods from instrument to instrument as each gradient method is specific to the instrument on which it was developed and adjustments to the gradient timings are necessary to compensate for the differences in dwell volumes between instruments.

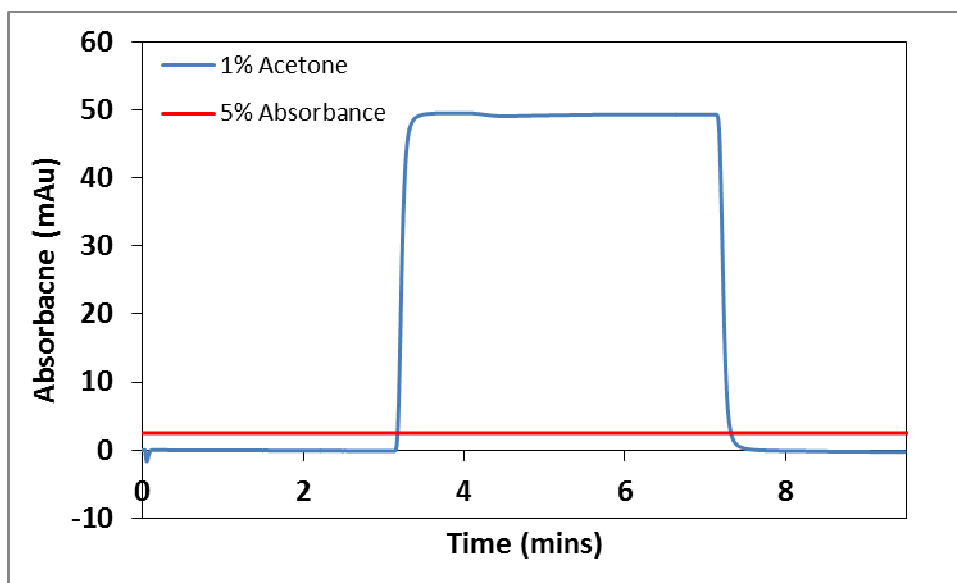


Fig. 2.3.24 Determination of void volume of Shimadzu Nexera UPLC utilising acetone. Conditions as outlined in Section 3.2.2.1.

5% of the maximum absorbance recorded for a 1% acetone solution was noted at 3.17 min. As the mobile phase composition did not change until 3.01 min, this was subtracted from the total time taken to give a value of 0.16 min. As the flow rate used was 1 mL/min, the dwell volume was calculated to be 0.160 mL.

2.3.2.3.2 Transfer of the 2.6 μm core-shell column RP HPLC method to a 1.7 μm core-shell column.

The gradient method which was previously developed and optimised for a 2.6 μm particle size stationary phase in Section 2.3.2.2.2 (Fig. 2.3.23, Table 2.3.14) was transferred to the 1.7 μm column with the necessary adjustments for differences in delay volume of the two instruments. Other parameters of the method included; 0.2 μL injection volume, column temperature; 50°C, flow rate; 0.6 mL/min and a detector wavelength of 256 nm.

The delay volume of the Agilent 1200 series liquid chromatograph and the Shimadzu Nexera UPLC chromatograph were experimentally determined to be 0.94 mL/0.94 min and 0.16 mL/0.16 min respectively in Section 2.3.2.2.1 and 2.3.2.3.1. To compensate for the decrease in delay volume, the isocratic hold at the start of the gradient was increased by 0.9 min. Below is the updated gradient profile (Table

2.3.15) with results of the separation given in Table 2.3.16 and the corresponding chromatogram in Fig. 2.3.25.

Table 2.3.15: Development of an optimum separation using a gradient method on a Phenomenex Kinetex 1.7 μm core-shell stationary phase (2.1 x 100 mm). Gradient 1a mobile phase conditions. All other parameters as per Fig. 3.18

Gradient 1a	
Time (mins)	% ACN
0.00	25%
1.00	25%
1.01	90%
1.40	90%
1.41	25%
4.30	25%

It was expected that increasing the isocratic hold time would maintain the resolution between peak pair compound X and compound C. From the results presented in Table 2.3.16 and Fig. 2.3.25 it was noted that resolution between the peak pair was indeed maintained above 2, however the dramatic gradient step at 1.01 min from 25% to 90% ACN caused resolution to be lost between peak pair impurity compound D and voriconazole with a resolution of just 0.9 between the two peaks.

Table 2.3.16: Results of separation of S3 where initial hold time is increase to 1.0 minute (gradient 1a)

Gradient opt_1A			
Peak	Retention Time	Retention Factor	Resolution
Void	0.380		
Compound X	0.990	1.605	
Compound C	1.087	1.861	2.070
compound D	1.613	3.245	4.950
Voriconazole	1.643	3.324	0.900

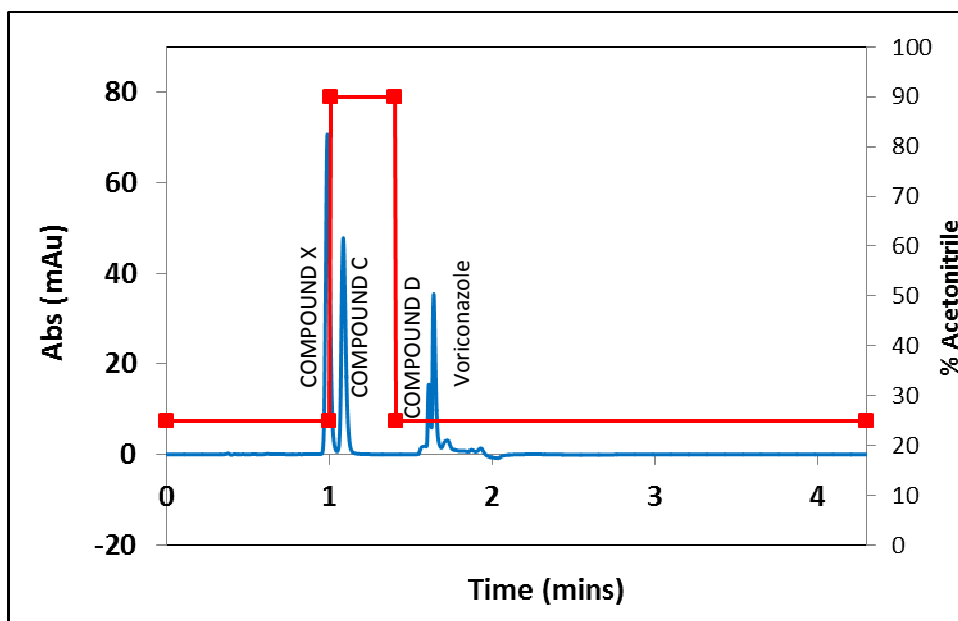


Fig 2.3.25: Chromatograms of a separation of Voriconazole and its related impurities compound X, compound C and compound D using gradient profiles 1a (shown in red). Conditions for the separation as per Fig 2.3.19.

In order to rectify this and restore resolution between compound D and voriconazole, a linear ramp was introduced from 1.01 min to 1.40 min and also a 90% isocratic hold from 1.40 to 2.00 min (Table 2.3.17).

Table 2.3.17: Development of an optimum separation using a gradient method on a Phenomenex Kinetex 1.7 μm core-shell stationary phase (2.1 x 100 mm). Gradient 2a mobile phase conditions. All other parameters as per Fig.2.3.19

Gradient 2a	
Time (mins)	% ACN
0.00	25%
1.00	25%
1.40	90%
2.00	90%
2.01	25%
4.30	25%

Table 2.3.18 and its representative chromatogram (Fig. 2.3.26) show that, similar to the previous gradient, a resolution of above 2 was maintained between impurity peaks compound X and compound C. While as anticipated, there was an increase in the resolution from 0.900 to 1.760 between compound D and Voriconazole, so that

this now passes the optimisation specification of 1.7, there was still scope for further optimising the gradient profile.

Table 2.3.18: Results of separation of S3 where initial hold time is reduced to 0.90 min, gradient 2a. Chromatographic conditions as per Fig 2.3.19.

Gradient 2A			
Peak	Retention Time	Retention Factor	Resolution
Void	0.380		
Compound X	0.990	1.605	
Compound C	1.088	1.863	2.090
compound D	1.797	3.729	17.950
Voriconazole	1.852	3.874	1.760

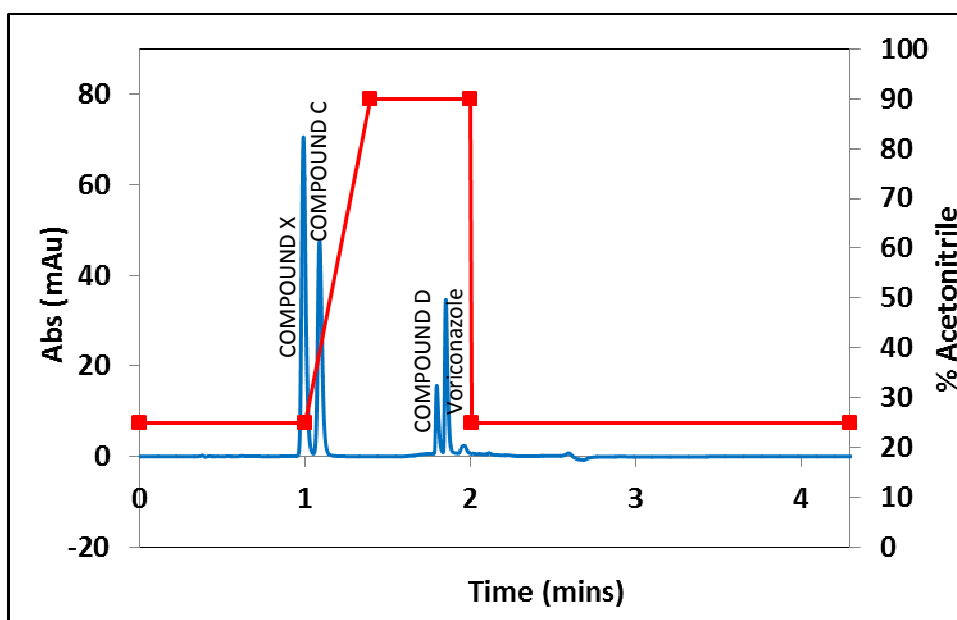


Fig. 2.3.26: Chromatograms of a separation of Voriconazole and its related impurities compound X, compound C and compound D using gradient profiles 2a (shown in red). Conditions for the separation as per Fig 2.3.19

It was hoped that a shallower gradient, despite resulting in a longer retention time would increase the resolution between impurity compound D and Voriconazole. By decreasing the initial gradient hold by 0.4 min to 0.6 min, the slope of the linear gradient was lessened. The new gradient profile is given below in Table 2.3.19 (gradient 3a).

Table 2.3.19: Development of an optimum separation using a gradient method on a Phenomenex Kinetex 1.7 μm core-shell stationary phase (2.1 x 100 mm). Gradient 3a mobile phase conditions. All other parameters as per Fig. 2.3.18

Gradient 3a	
Time (mins)	% ACN
0.00	25%
0.60	25%
1.40	90%
2.00	90%
2.01	25%
4.30	25%

Shortening the isocratic hold time at the beginning of the gradient, thus decreasing the slope of the gradient had the desired effect and the resolution between impurity compound D and Voriconazole peak increased from 1.76 to 2.66 with Voriconazole now eluting at 1.642 min as shown below in Table 2.3.20 and Fig. 2.3.27.

Table 2.3.20 Results of separation of S3 where initial hold time is reduced to 0.6 min, as gradient 3a (Table 2.3.19) All other parameters remain as per Fig. 2.3.19

Gradient 3A			
Peak	Retention Time	Retention Factor	Resolution
Void	0.380		
Compound X	0.994	1.616	
Compound C	1.095	1.882	2.160
compound D	1.554	3.089	11.290
Voriconazole	1.642	3.321	2.660

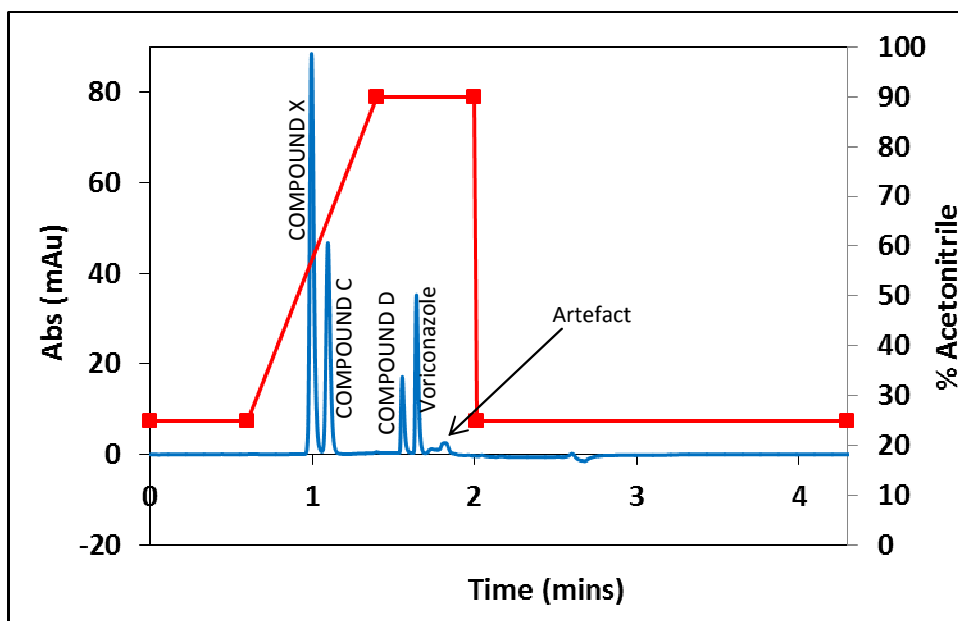


Fig. 2.3.27: Chromatograms of a separation of Voriconazole and its related impurities compound X, compound C and compound D using gradient profiles 3a (shown in red). Conditions for the separation as per Fig.2.3.19.

Due to the presence of an artefact eluting close to the Voriconazole peak it was decided to decrease the concentration of the ACN 80%. This gradient profile is shown in Fig 2.3.28. By decreasing %ACN, it was hoped to increase the resolution between the API and artefact on the column, while also maintaining the resolution between all peak pairs.

Table 2.3.27: Development of an optimum separation using a gradient method on a Phenomenex Kinetex 1.7 μm core-shell stationary phase (2.1 x 100 mm). Gradient 4a mobile phase conditions. All other parameters remain as per Fig. 2.3.19.

Gradient 4a	
Time (mins)	% ACN
0.00	25%
0.60	25%
1.40	80%
2.00	80%
2.01	25%
4.30	25%

Table 2.3.28 and its related chromatogram Fig. 2.3.27 show that resolution increased from 2.160 to 3.310. The resolution between impurity compound D and

Voriconazole decreased from 2.660 to 2.430, however this was within optimisation parameters that were set and was deemed acceptable. There was a resolution of 3.73 between the API peak and the artefact. A high resolution between these peak pairs was necessary to ensure that it did not impact on the separation. Compared to the original Pfizer impurity method there was a decrease in run time of 57 % - the same as the reduction seen for the newly developed impurity assay developed on a 2.6 μm core-shell column (Fig. 2.3.23, Table 2.3.14). While there was a decrease in retention of the latest eluting peak –Voriconazole of ~ 0.4 minutes from 2.031 min to 1.750 min, this decrease was negated by the time necessary to equilibrate the column after each run due to the gradient. Resolution between the critical peak pair of compound X and compound C was decreased slightly compared to the 2.6 μm column impurity assay from 3.800 to 3.310. Resolution between this peak pair was also compared to the original USP-36-NF-31 Voriconazole monograph (Section 2.3.1) whose resolution was 2.68 between the same peak pair.

Table 2.3.28: Results of separation of S3a where the final concentration of ACN lowered to 80% (gradient 4a)

Gradient 4A			
Peak	Retention Time	Retention Factor	Resolution
Void	0.380		
Compound X	1.293	2.403	
Compound C	1.433	2.771	3.310
compound D	1.669	3.392	6.820
Voriconazole	1.749	3.603	2.430
Artefact	1.936	4.095	3.730

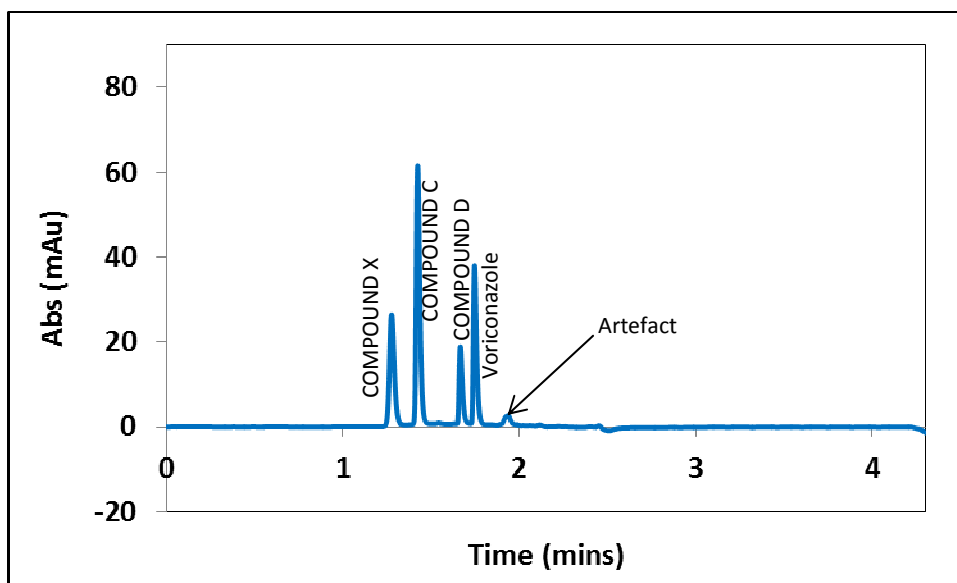


Fig. 2.3.27: Chromatograms of a separation of Voriconazole and its related impurities compound X, compound C and compound D using gradient profiles 4a. Conditions for the separation as per Fig 2.3.18.

2.4 Conclusions

Methods were successfully developed and optimised for use on Phenomenex Kinetex core-shell reversed phase C₁₈ columns (100 x 2.1 mm) of particle sizes 2.6 µm and 1.7 µm. Optimisation parameters were successfully met with resolution between peak pairs above 2.0 for all compounds. A 57% reduction in the total run time of the impurity assay was recorded when transferred to both 2.6 µm and 1.7 µm column.

Moving to smaller particles sizes has some distinct advantages such as; a decrease in retention time of analytes and an increase in efficiency. All three columns which were investigated were reversed phase C₁₈ columns and so as expected the elution order across the 3 columns remained the same, which is as follows compound X → compound C → compound D → Voriconazole. Changes in retention behaviour between columns of different manufacturer can be attributed to the differences in carbon loading between manufacturers.

The new optimised methods on both the core-shell 2.6 µm column and the 1.7 µm column were compared to the existing impurity assay in terms of retention factor and resolution. Table. 2.3.29 compares each of these parameters across all 3 columns.

Table. 2.3.29: Comparison of the 3 optimised methods in terms of their retention factor (left) resolution (right).

Retention Factor				Resolution			
Analyte	USP 36-NF-31	DCU 2.6 μm Method	DCU 1.7 μm Method	Analyte	USP 36-NF-31	DCU 2.6 μm Method	DCU 1.7 μm Method
Void	0.000	0.000	0.000	Void			
Compound X	1.005	1.682	2.403	Compound X			
Compound C	1.330	2.137	2.771	Compound C	2.680	3.800	3.310
Compound D	4.108	4.615	3.392	Compound D	14.530	25.540	6.820
Voriconazole	7.626	4.921	3.603	Voriconazole	10.830	4.500	2.430

As expected there was a decrease in overall retention time for newly optimised core-shell methods of 57%. This was due to smaller particle sizes having shorter flow pathlengths leading to faster separations. When moving from a 2.6 μm core-shell column to a 1.7 μm core-shell column there was a slight decrease in retention time from 2.031 min to 1.749 min, however this decrease in run was negated due to the time necessary to re-equilibrate the column before the next injection. While the 2.6 μm core-shell column could be operated on a standard HPLC with pressure capabilities of 400 bar, it was necessary to use a specialised instrument capable of withstanding pressures of up to 1000 bar when operating the 1.7 μm core-shell column. From the point of view of total run time, no time saving benefit was found in transferring to the 1.7 μm core-shell column; it was therefore concluded that the use of 1.7 μm core-shell columns and state of the art high pressure instruments for gradient analysis are unnecessary for this application as they provide no additional benefit.

3 Chapter 3: The evaluation of stationary phase/mobile phase combinations for the development of an pharmaceutical impurity assay using Supercritical Fluid Chromatography

3.1 Introduction

While faster and more efficient chromatography is a constant driver within chromatographic research, another driver is the desire for greener chromatography and reduced solvent consumption [110]. Supercritical Fluid Chromatography (SFC) has the potential to deliver greener chromatography, as it uses non-toxic carbon dioxide as its mobile phase. This technique sits between HPLC and GC and possesses qualities of both [48], for example, supercritical fluids have density and solvation power which is close to liquids whilst maintaining more gas like viscosity and diffusivity [48, 50]. As a result of its increased diffusion capabilities and the low viscosity of supercritical fluids compared to solvents used in HPLC, much higher linear velocities can be used, allowing faster separations and higher throughput [51].

An area where SFC has found great success and applicability has been preparative chromatography and chiral chromatography [63]. SFC is typically known as a technique which is analogous to normal phase HPLC due to the polarity of its primary mobile phase, which in most cases is supercritical carbon dioxide (sCO₂), however with the addition of polar additives, its scope can be extended to encompass more reverse phase HPLC applications. As SFC offers complementary selectivity to HPLC, its potential for enhancing resolution in problematic HPLC separations is being explored for multiple applications.

In Chapter 2, an existing reversed phase HPLC pharmaceutical impurity assay, previously carried out on a 5 µm C₁₈ column, was transferred to a core-shell reversed phase C₁₈ stationary phase. The aim of the study was to reduce the run time of the assay while maintaining adequate resolution between critical peak pairs. The run time of the assay was reduced by 57% from ~10 min to 4.3 min with the reduction in particle size from 5 µm fully porous to a 2.6 µm core-shell particle column. However, there was no subsequent decrease in run time when the 2.6 µm method was transferred to a 1.7 µm core-shell with the same particle morphology, due to re-method constraints.

The aim of this study was to develop a SFC pharmaceutical impurity assay to separate Voriconazole and related impurities, compound C, compound D and compound X which had orthogonal selectivity to the reversed phase HPLC assay optimised in Chapter 2. A range of stationary phase and mobile phase modifiers and additives were investigated to determine the most suitable stationary phase and mobile phase modifier for this assay. Across all 16 mobile phase/stationary phase combinations evaluated, orthogonal selectivity was demonstrated. Selectivity differences were also demonstrated on a cyano column depending on whether acidic or basic additives were used. In general the stationary phase and mobile phase combinations selected proved to be unsuitable for further method development as compound X, due to its very non-polar nature was not retained on the very polar stationary phase and mobile phase combinations. As regards retention of Voriconazole and its other impurities, compound C and D, the use of additives on a silica stationary phase lead to significant loss of retention and also resolution. This was mostly due to competition between the analytes and additives for hydrogen bonding with surface silanols necessary for retention. The use of TFA on a cyano stationary phase lead to an increase in retention for all compounds compared to MeOH alone. Both the diol and 2-ethylpyridine column performed poorly across all mobile phase combinations analysed.

3.2 Materials and Methods

3.2.1 Materials

3.2.1.1 Chemicals

API standard – Voriconazole, impurity standards - compound C, compound D and compound X and Voriconazole test material were obtained from Pfizer Process Development Centre (PDC) (Cork, Ireland). HPLC grade Methanol (MeOH) was purchased from Fisher Scientific (Cheshire, UK). Trifluoroacetic acid Reagent plus 99% (TFA), triethylamine $\geq 99\%$ (TEA) and ammonium acetate $\geq 99.99\%$ trace metals basis (AA) were purchased from Sigma Aldrich (Dublin, Ireland). All chemicals were used without further purification. Carbon dioxide (CO₂), food fresh grade was obtained from BOC Gases Ltd (Dublin, Ireland)

3.2.1.2 Mobile Phases

Mobile phases for SFC method development consisted of supercritical carbon dioxide (sCO₂) (mobile phase A) containing a MeOH modifier and, if indicated, a TFA, TEA or AA modifier (mobile phase B). Total modifier concentration ranged in concentration from 2% to 20% v/v. Mobile phases containing 0.1% TFA, 0.1% TEA and 20 mM AA were prepared in 100% MeOH. All mobile phases were vacuum filtered using Supelco 0.2 µm nylon 66 membrane filters. (Sigma Aldrich, Dublin, Ireland).

3.2.2 Apparatus

3.2.2.1 SFC Instrumentation.

The Agilent 1260 Infinity Analytical SFC system consisted of an Aurora SFC Fusion A5 module, Agilent 1260 Infinity SFC binary pump (G4303A), Agilent 1260 Infinity standard degasser (G1332A), Agilent 1260 Infinity standard autosampler (G4303A) and Agilent 1260 Infinity diode array detector with high pressure SFC flow cell (G1315C). The Aurora SFC Fusion A5 module provided the Agilent HPLC-SFC pump with predistilled and preconditioned CO₂, negating any compression requirements needed by the HPLC pump[111]. Mobile phase was redirected to the Aurora SFC Fusion A5 downstream of the detector to an integrated back pressure regulator which maintained back pressure across the system. A back pressure regulator kept the CO₂ mobile phase under subcritical conditions at all times. Columns used included the Agilent Zorbax silica column (150 x 4.6 mm, particle size 5 µm), (Agilent, Ireland) Waters Spherisorb Cyano column (250 x 4.6 mm, particle size 5 µm), (Waters, Ireland), Princeton SFC Diol column (150 x 4.6 mm, particle size 5 µm) and Princeton SFC 2-ethyl pyridine (150 x 4.6 mm, particle size 5 µm). Both the diol and 2-ethylpyridine columns were kindly donated by Pfizer Process Development Centre (PDC), Cork, Ireland

3.2.3 Methods

3.2.3.1 Preparation of Standards

Standards for SFC method development were prepared every 14 days in 100% MeOH diluent. A 250 µg/mL Voriconazole stock solution including its three known impurities, compound C, compound D and compound X was prepared. 12.5 mg of each standard was weighed out and dissolved in 50 mL diluent. This was further diluted 10 fold in 50 mL diluent. A 5 µL aliquot was injected for SFC analysis, known as S3b. The optimisation parameters selected for method development were the shortest run time possible, while maintaining a critical resolution of above 1.7 between peak pairs.

3.2.4 SFC Method Development

SFC method development was carried out on a variety of stationary phases and mobile phases as outlined in Section 3.2.1.2 and 3.2.2.1. Results were compared to a pre-existing reversed phase HPLC method. This method is detailed in Chapter 2, Section 3. Flow rate was 3 mL/min, detector wavelength selected was 256 nm while column temperature was set to 37.5°C on the inlet side and 40°C on the outlet side as recommended by Agilent engineers. An injection volume of 5 µL of sample S3b was used. It was necessary for the solvent path to be pressurized at all times during analysis to avoid expansion of supercritical fluid, therefore a fixed 5 µL sample loop injector was employed [111]. These conditions remained the same throughout method development.

3.2.4.1 Stationary Phase Selection

Stationary phase and mobile phase selection for a particular set of analytes can be challenging due to the wide range of both stationary phase and mobile phases which are available[112]. Any stationary phase which can be used in HPLC can also be used in SFC; this is also the case for mobile phases, as CO₂ is miscible with most

solvents used in HPLC. SFC is known to be typically analogous to normal phase liquid chromatography. CO₂ is generally considered very non-polar with a polarity similar to pentane[50]. Commonly used polar stationary phases utilised in normal phase HPLC were chosen, namely bare silica, cyano and diol stationary phases, and a 2-ethylpyridine stationary phase specially designed for SFC.

3.2.4.1.1 Stationary phase chemistry and mobile phase screening studies.

Stationary phase and mobile phases screening studies were carried out simultaneously. A total of 16 different experiments were carried out. Each experiment involved varying the % organic modifier in CO₂ over a range of 8% to 20%, unless otherwise stated. The four stationary phases bare silica, cyano, diol and ethyl pyridine were utilised with each of the modifier compositions MeOH only, MeOH with 0.1% TFA, MeOH with 0.1% TEA and MeOH with 20 mM AA. Other method parameters remained constant throughout the study; as detailed in Section 3.3. Results were analysed in terms of retention factor, and resolution achieved with varying modifier concentrations, modifier types and different stationary phase chemistries. Results were also compared to the existing USP 36-NF-31 reverse phase HPLC method and newly developed UPLC methods achieved on 2.6 µm and 1.7 µm C₁₈ reversed phased method discussed in Chapter 2.

3.3 Results and Discussion

3.3.1 Selection of the optimal stationary phase/mobile phase modifier combination for the separation of API Voriconazole and its related impurities, compound X, compound C and compound D.

As detailed in Section 3.2.4.1.1, the parameters which were varied in this study were stationary phase chemistry and modifier composition. The effect of both stationary phase and mobile phase on the retention of Voriconazole and related impurities, compound X, compound C and compound D were investigated simultaneously.

Injections of individual standards of Voriconazole and its related impurities compound X, compound C and compound D were carried out on each of the four stationary phases under all mobile phase conditions. It was found that impurity compound X was not retained under any of the stationary phases analysed. For example, retention times and retention factors for compound X analysed on a bare silica stationary phase using MeOH only as a modifier are shown in Table 3.3.1.

Table 3.3.1: The effect of modifier concentration on retention of impurity compound X. Modifier: MeOH only. Stationary phase: Agilent Zorbax Silica (150 x 4.6 mm, 5 µm)

Concentration of Modifier	Retention time of void (mins)	Retention time Compound X (mins)	Retention factor Compound X
20%	0.498	0.606	0.217
16%	0.51	0.615	0.206
12%	0.527	0.627	0.190
8%	0.567	0.632	0.115

As can be seen from Table 3.3.1, compound X is not retained on a silica stationary phase using MeOH as a modifier. Poor retention is likely due to the hydrophobic nature of the analyte, which has a greater affinity for the less polar CO₂ mobile phase over the polar silica stationary phase. Similar results were found for each of the other mobile phase/stationary phase combinations as all stationary phases which were chosen are polar in nature. An increase in void time was also noted with decreasing modifier concentration, a phenomenon that is not seen in reverse phase HPLC.

Since compound X was not found to be retained within any of the parameters of this investigation it was decided to omit this impurity from the mixed standard used in

the subsequent study. S3b used in this study contained, Voriconazole, compound C and compound D.

3.3.1.1 Optimisation of mobile phase for separation of Voriconazole and related impurities compound C and compound D.

The parameters for optimal separation of Voriconazole, compound C and compound D were a minimum resolution between all peak pairs of 1.7 with the shortest possible runtime. Addition of a mobile phase modifier such as MeOH in SFC is expected to have a number of different effects such as favouring compound solubility, inducing selectivity changes by specific interactions such as hydrogen bonding and dipole-dipole interactions[113]. Organic solvents are also known to change the density of the mobile phase as well as adsorbing onto the stationary phase surface, changing the polarity, volume and three dimensional structure of the stationary phase[114]. It was expected that with an increase in MeOH concentration there would be a decrease in retention of the analytes.

To enhance the improvements in separation observed with modifiers, modifier additives are also used in SFC for a number of reasons, including; coverage of stationary phase active sites and suppression of ionisation or ion pairing[62]. Another role is to promote elution of very polar analytes and also to improve peak shape[82].

A series of investigations were carried out to investigate the effect of mobile phase modifiers and additives on the separation in question. In the first series, the effect of the modifier MeOH in the sCO₂ mobile phase was examined. In the next three series, the effect of augmenting the MeOH modifier with additives with different properties were investigated. An acid – Trifluoroacetic acid (TFA), a base – Triethylamine (TEA) and a volatile salt – Ammonium Acetate (AA) were chosen for these studies.

3.3.1.1.1 Investigation of the effect of a MeOH mobile phase modifier on retention of Voriconazole and related impurities Compound C and Compound D on stationary phases of varying polarities.

The effect of MeOH modifiers of different concentrations in the sCO₂ mobile phase was investigated for the four stationary phases chemistries chosen for this study, namely; bare silica, cyano, diol and ethyl pyridine. A modifier concentration range of 6-20% was chosen. The upper limit of 20% was chosen to prevent a two phase (liquid vapour) system developing, as would happen if the solubility of the MeOH in the sCO₂ was exceeded[115]. Method conditions are given in Section 3.2.

The results were analysed in terms of retention factors and resolution between peak pairs. Retention factors for each of the four columns across the MeOH range analysed as shown in Fig. 3.3.1 – 3.3.4.

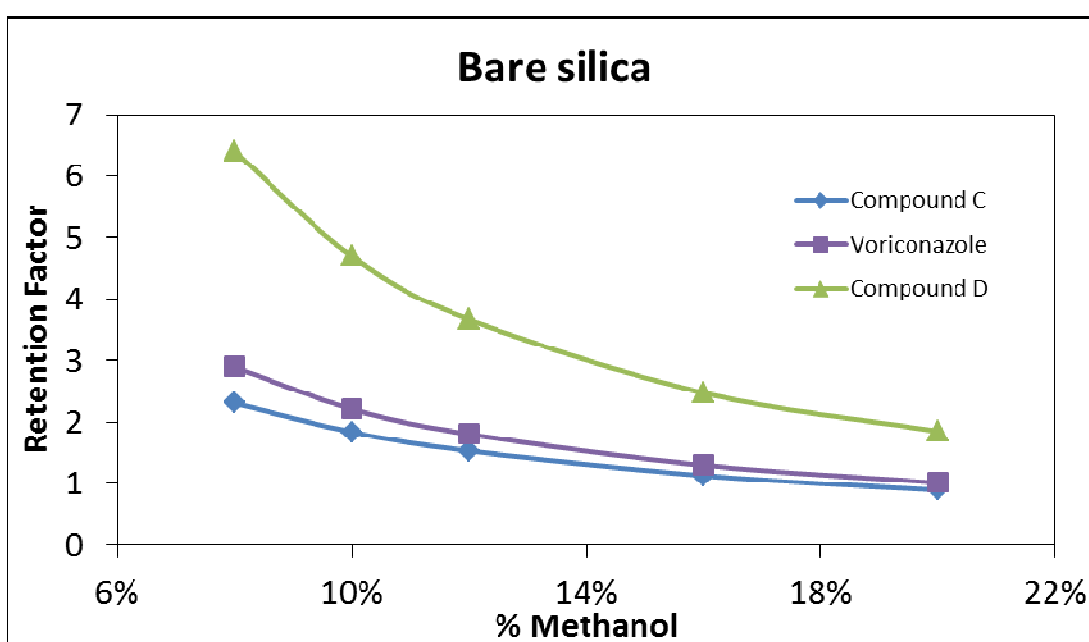


Fig. 3.3.1: Retention factor of Voriconazole(■) and related impurities compound C(◆) and compound D(▲) vs. concentration of MeOH in mobile phase on a bare silica stationary phase (Agilent Zorbax silica dimensions: 150 x 4.6 mm, 5 μm particle size) (Raw Data, Appendix 6.2, Table 6.2.1)

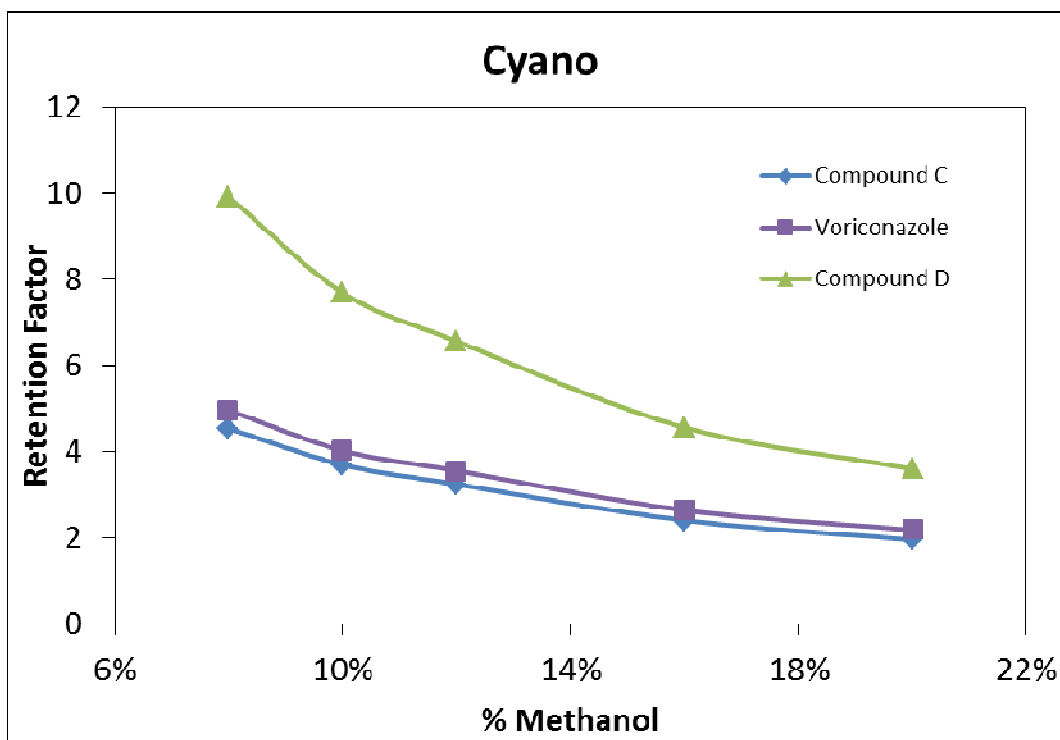


Fig. 3.3.2: Retention factor of Voriconazole (■) and related impurities compound C (◆) and Compound D (▲) vs. concentration of MeOH in mobile phase on a cyano stationary phase (Phenomenex Spherisorb CN dimensions: 250 x 4.6 mm, 5 μm particle size) (Raw Data, Appendix 6.2, Table 6.2.2)

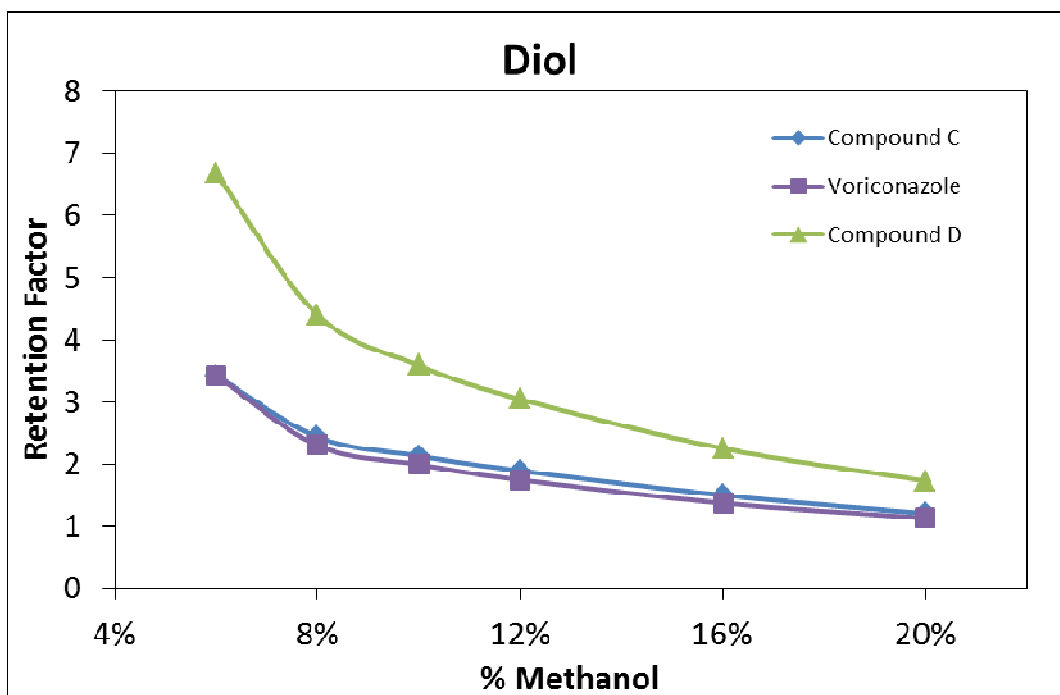


Fig. 3.3.3: Retention factor of Voriconazole(■) and related impurities compound C (◆) and compound D (▲) vs. concentration of MeOH in mobile phase on a diol stationary phase (Princeton Diol dimensions: 150 x 4.6 mm, 5 μm particle size) (Raw Data, Appendix 6.2, Table 6.2.3)

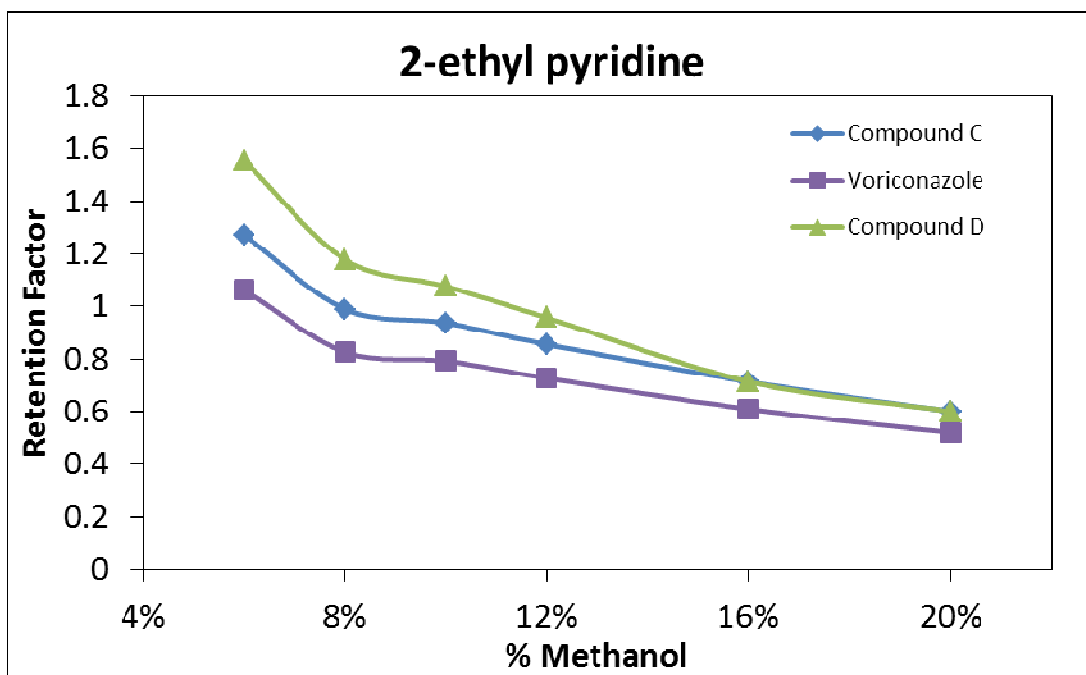


Fig. 3.3.4: Retention factor of Voriconazole (■) and related impurities UK-51-060 (◆) and compound D(▲) vs. concentration of MeOH in mobile phase on a ethyl pyridine stationary phase (Princeton 2-ethyl pyridine dimensions: 150 x 4.6 mm, 5 μm particle size) (Raw Data, Appendix 6.2, Table 6.2.4)

As expected, across all four stationary phases analysed there was a consistent trend of decreased retention with increased MeOH concentration. This was also seen by Patil *et al.*[116] for the separation of acetaminophen and other analgesics using a phenyl column where retention decreased across the MeOH concentration 4.8 to 16.7%. The decrease in retention shown in Fig. 3.3.1 – 3.3.4 appears to be more significant at lower concentrations of MeOH than at higher concentrations of MeOH. This trend is similar to that observed in normal phase HPLC where at higher concentrations of polar mobile phase, retention is not significantly affected[6]. For this reason, just as with normal phase HPLC, the dominant retention mechanism was hypothesised to be adsorption over partition on the stationary phases selected for this study. Again, this agrees with published literature, where polar stationary phases in SFC induce normal phase retention behaviour [113].

The cyano stationary phase was shown to result in longest retention, while the pyridine stationary phase retained least, with silica and diol stationary phases exhibiting intermediate retention. On a silica stationary phase Voriconazole had a retention factor of 2.894 at 8% MeOH while retention factor was reduced to 1.014 at 20% MeOH (raw data for this experiment is given in Fig. 6.2.1 and 6.2.2 in

Appendices). This was a reduction in retention factor of approximately 3. Retention factors for Voriconazole on the cyano stationary phase were almost twice that of a silica column with retention factors of 2.19 at 20% and 4.97 at 8% MeOH. Retention on the cyano column was hypothesised to be due both to hydrogen bonding between the cyano group and the analytes but also interaction between the hydrophobic carbon chain of the cyano column increasing retention, while retention on the silica stationary phase was hypothesised to be due to hydrogen bonding only. With increasing MeOH concentration, interactions between the mobile phase and analytes were increased through hydrogen bonding interactions.

There was significantly less retention on both an ethyl pyridine stationary phase with a maximum retention factor obtained of 1.06 with 6% MeOH. The poor retention of the analytes on a pyridine stationary phase was hypothesised to be due absence of significant hydrogen bonding capacity of the pyridine stationary phase. Zheng *et al.*[117] suggest that internal hydrogen bonding between surface silanols and the nitrogen moiety of the pyridine ring reduced active sites available for solute interaction. Similar retentions and retention factors were achieved on the diol stationary phase and the silica stationary phase across the range of MeOH concentrations analysed. Retention on both the silica and diol columns is thought to be due to hydrogen bonding with the surface silanols on the silica column and the hydroxyl groups of the diol stationary phase.

On all stationary phases, compound D was the latest eluting compound. Voriconazole and compound C switched elution order on the diol and pyridine column compared to the silica and cyano column. Compound D and Voriconazole are very similar in structure, however compound D was thought to be more retained due to the absence of the extra fluorine Voriconazole possesses. The presence of halogens reduces retention in normal phase HPLC; since it was anticipated that the columns would produce normal phase retention behaviour due to their polar nature, the decreased retention of Voriconazole was expected. The change in elution order between the silica and cyano and diol and pyridine column was also anticipated; due to increased steric hindrance between the analytes and the diol and pyridine stationary phase. While both analytes were thought to interact with the hydroxyl groups of the diol column and surface silanols, it thought that steric hindrance and

thus reduced capability for hydrogen bonding caused the larger Voriconazole analyte to be eluted first.

As in HPLC a good separation is defined as having a retention factor (k) of between 1 and 10[118]. A retention factor of less than 1 indicates compounds do not interact sufficiently with the stationary phase and therefore are not adequately retained, while retention factors of greater than 10 indicate excessive retention. It was noted that the pyridine column for concentrations of MeOH above 8% a retention factor of less than 1 achieved and therefore compounds were inadequately retained. It was therefore concluded that a pyridine column with a MeOH stationary phase was unsuitable for the separation of Voriconazole and its related impurities.

The silica, cyano and diol columns were analysed in terms of the resolution between critical peak pairs. A resolution of greater than 1.7 was selected as a critical performance parameter between all peak pairs. Resolutions values for peak pairs for each of the three columns are given below in Fig 3.3.5 – 3.3.7.

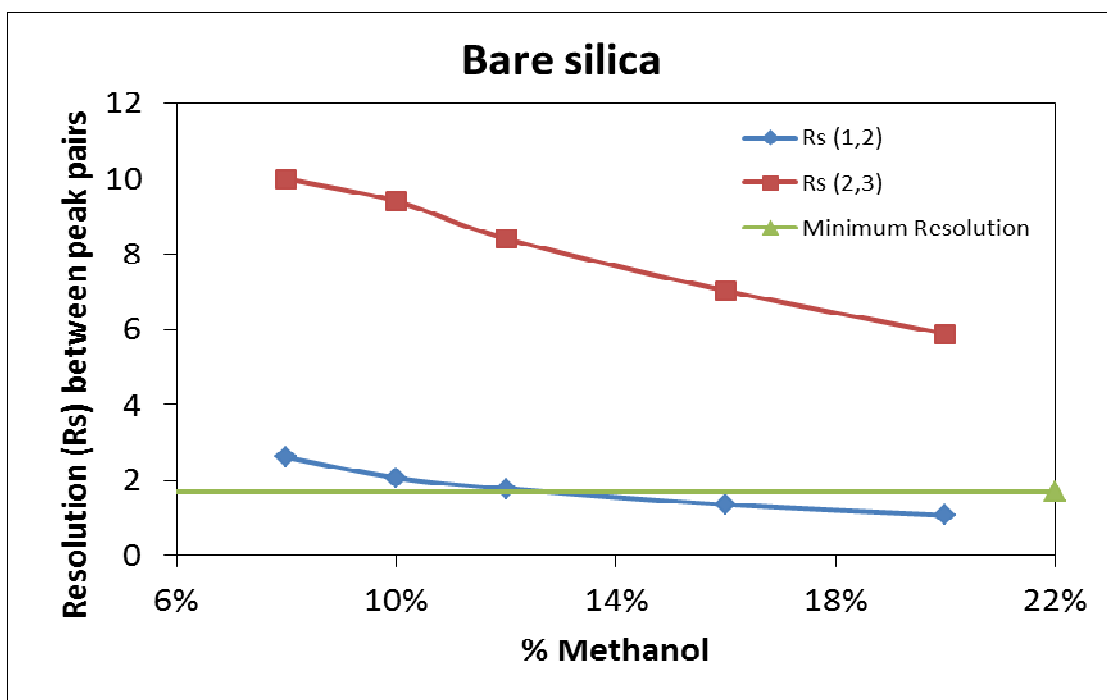


Fig. 3.3.5: Retention of peak pairs vs. concentration of MeOH in mobile phase. Peak pairs are as follows: (1,2)(\blacklozenge): compound C: Voriconazole, (2,3)(\blacksquare) Voriconazole: compound D on a bare silica stationary phase (Agilent Zorbax Silica dimensions: 150 x 4.6 mm , 5 μ m particle size) minimum resolution is shown by the green line (Raw Data, Appendix 6.2, Table 6.2.1)

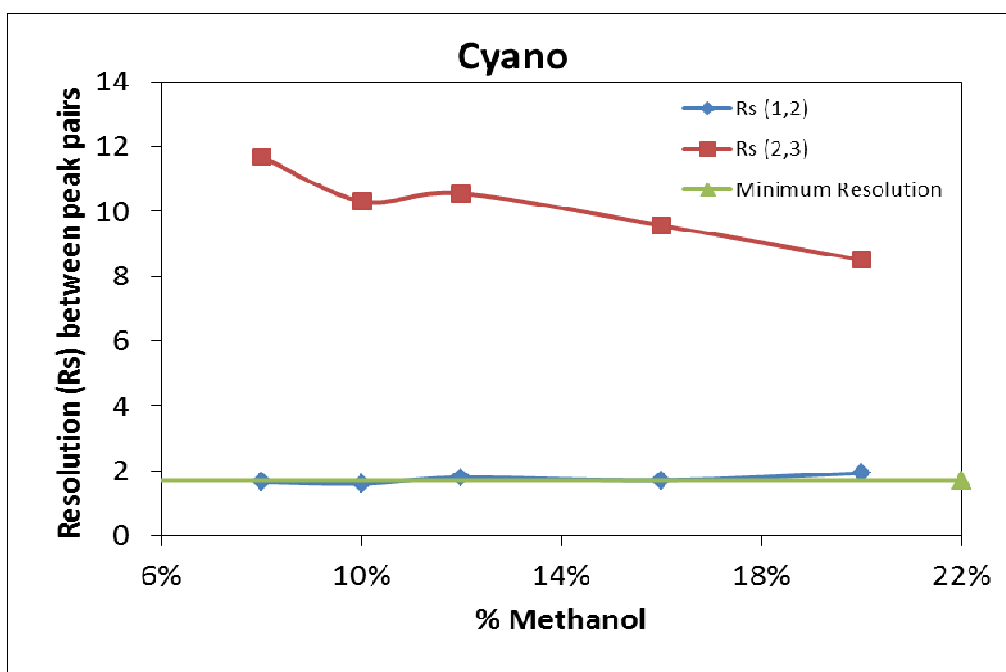


Fig. 3.3.6: Retention of peak pairs vs. concentration of MeOH in mobile phase. Peak pairs are as follows: (1,2)(\blacklozenge): compound C:Voriconazole, (2,3)(\blacksquare): Voriconazole:compound D on a cyano stationary phase (Phenomenex Spherisorb CN dimensions: 250 x 4.6 mm, 5 μ m particle size) minimum resolution is shown by the green line. (Raw Data, Appendix 6.2, Table 6.2.2)

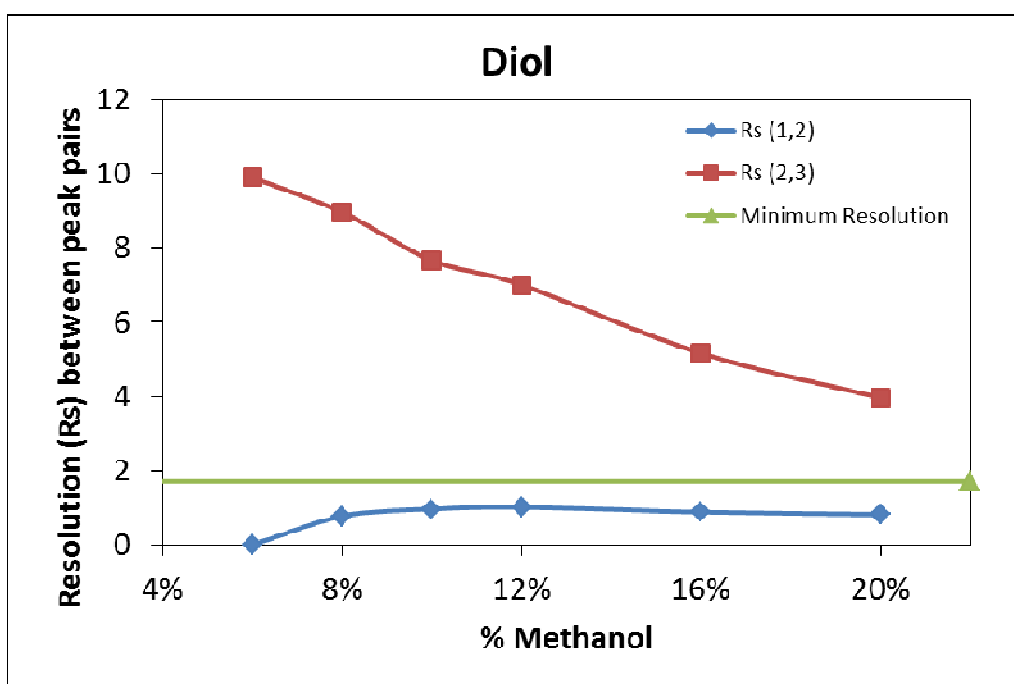


Fig. 3.3.7: Retention of peak pairs vs. concentration of MeOH in mobile phase. Peak pairs are as follows: (1,2)(\blacklozenge): compound C:Voriconazole, (2,3)(\blacksquare): Voriconazole:compound D on a diol stationary phase (Princeton Diol, dimensions: 150 x 4.6 mm, 5 μ m particle size) Minimum resolution is indicated by the green line. (Raw Data, Appendix 6.2, Table 6.2.3)

On a silica stationary phase, shown in Fig. 3.3.5, resolution between Voriconazole and compound D is above 1.7 at all MeOH concentrations selected for this study. At 8% MeOH resolution was 9.99 (see raw data, Appendix 6.2.1) with increasing MeOH concentration and resultant decreasing retention there was also a decrease in resolution between peaks with a final resolution of 5.89 at the highest concentration of MeOH of 20%. The critical peak pair on a silica stationary phase was compound C and Voriconazole. The green line in Fig 3.3.5 – resolution between peak pairs on a silica column, indicates the resolution threshold of 1.7. It can be seen that sufficient resolution was only achieved on a silica stationary phase with a modifier concentration of less than 12% with the greatest resolution achieved at 8% MeOH, of 2.61. It was found that resolution between the critical peak pair, Voriconazole:compound D on a cyano column (Fig. 3.3.6) increased with increasing MeOH concentration, the opposite effect than on a bare silica column. Critical resolution was achieved at a MeOH concentration above 12%, with the best resolution achieved at 20% of 1.92 (raw data; appendix 6.2, table 6.2.2). While on a diol column (Fig 3.3.7, raw data; appendix 6.2, table 6.2.3), using MeOH as a mobile phase modifier at no concentration investigated in this study was critical resolution achieved, rendering this stationary phase/mobile phase combination unsuitable.

3.3.1.1.2 Optimal MeOH modified mobile phases

It was concluded that stationary phase/MeOH combinations which provided the best resolution and suitable retention were a bare silica and cyano columns at 10% and 20% respectively. Chromatograms below in Fig. 3.3.8 and Fig. 3.3.9 show the optimal separations achieved on a bare silica column. In each case, all 3 components were shown to be resolved. The runtime for the bare silica stationary phase was slightly shorter than for the optimal cyano separation, at 3.5 minutes relative to 4.5 minutes.

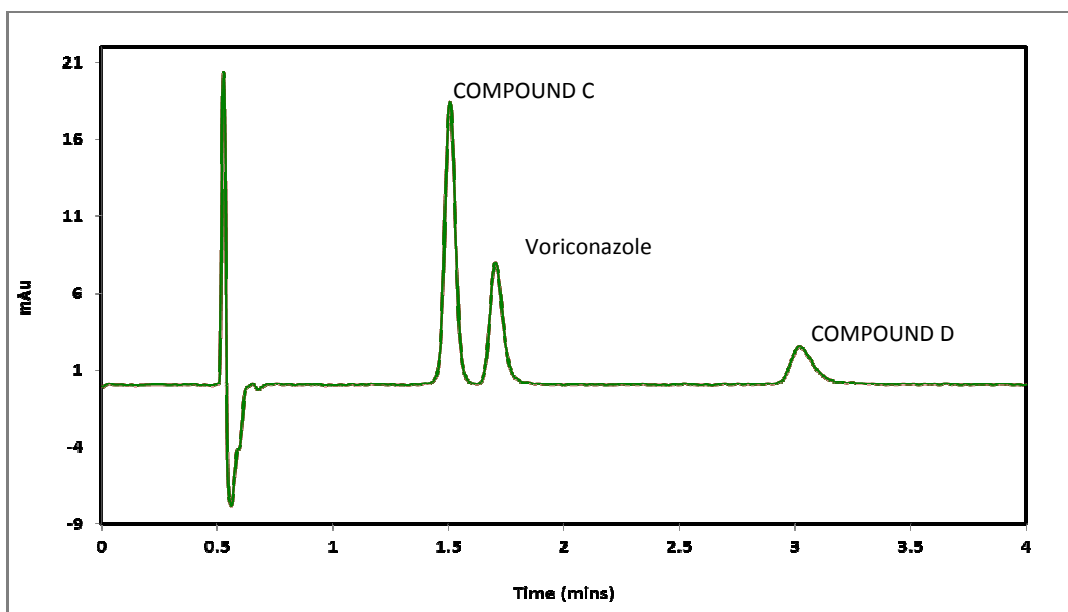


Fig 3.3.8: Chromatogram of the optimal separation of S3b achieved on a bare silica stationary phase using a 10% MeOH, 90% $s\text{CO}_2$ mobile phase. Conditions: Injection Volume: $5\mu\text{L}$, Column Temp: 37.5°C (in) 40.0°C (out), Detector wavelength: 256 nm, booster pressure: 130 bar.

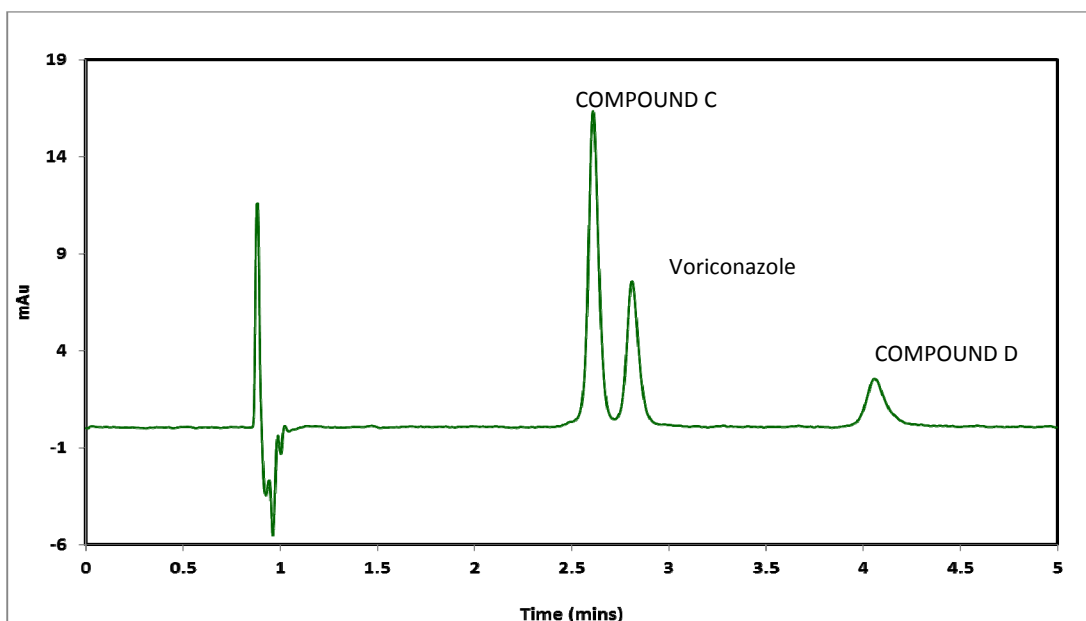


Fig 3.3.9: Chromatogram of the optimal separation of S3b achieved on a cyano stationary phase using a 20% MeOH, 80% $s\text{CO}_2$ mobile phase. Conditions: Injection Volume: $5\mu\text{L}$, Column Temp: 37.5°C (in) 40.0°C (out), Detector wavelength: 256 nm, booster pressure: 130 bar

3.3.1.1.3 Investigation of the effect of a MeOH mobile phase modifier with 0.1% TFA additive on retention of Voriconazole and related impurities compound C and compound D on stationary phases of varying polarities.

3.3.1.1.3.1 Bare silica stationary phase

The addition of TFA in SFC was reported to have a number of effects. De Klerck [97] reported a reduction in retention when TFA was added to a methanol modifier for the separation of a range of enantiomers. Reduced retention was thought to be due to de-activation of surface silanols and also the partial protonation of basic functional groups. Brunelli *et al.*[74] found that the addition of TFA to a methanol mobile phase reduced peak tailing for acidic pharmaceutical compounds on a cyanopropyl stationary phase, while Dispas *et al.*[119] found that TFA acted as an ion pairing reagent which interacted with the amine functionalities of pharmaceuticals and neurotransmitters analysed. It was expected that TFA would perform similarly on the stationary phases chosen. The first stationary phase chosen was a bare silica column. The results are given below in Fig. 3.3.10

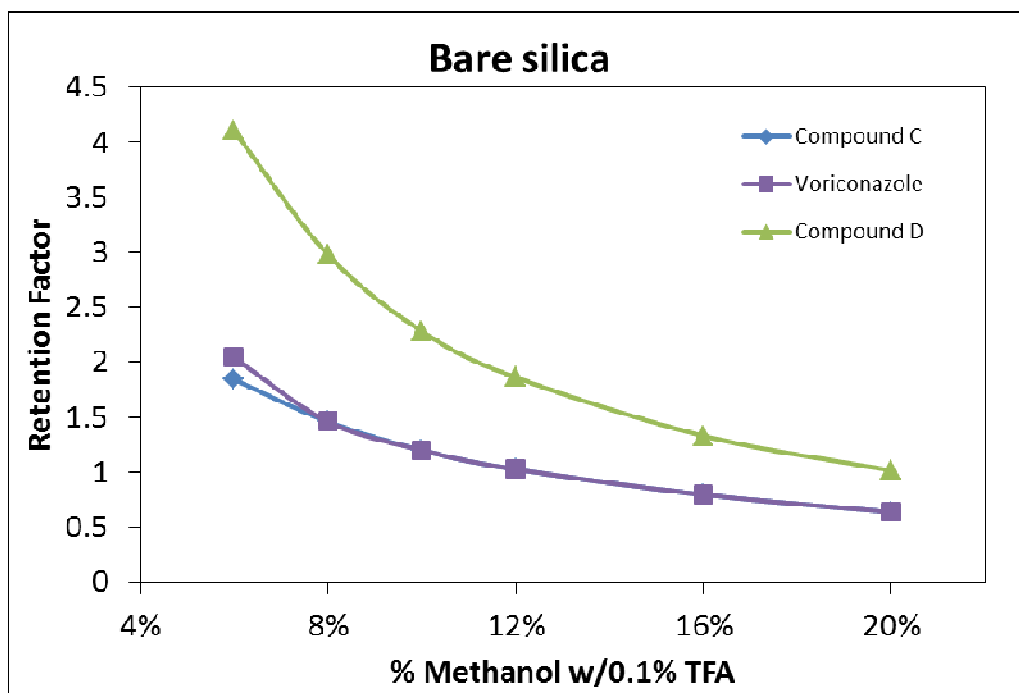


Fig. 3.3.10a: Retention factor of Voriconazole (■) and related impurities compound C (◆) and compound D(▲) vs. concentration of MeOH w/0.1% TFA in mobile phase on a bare silica stationary phase (Agilent Zorbax silica dimensions: 150 x 4.6 mm, 5 μm particle size.) (Raw Data, Appendix 6.2, Table 6.2.5)

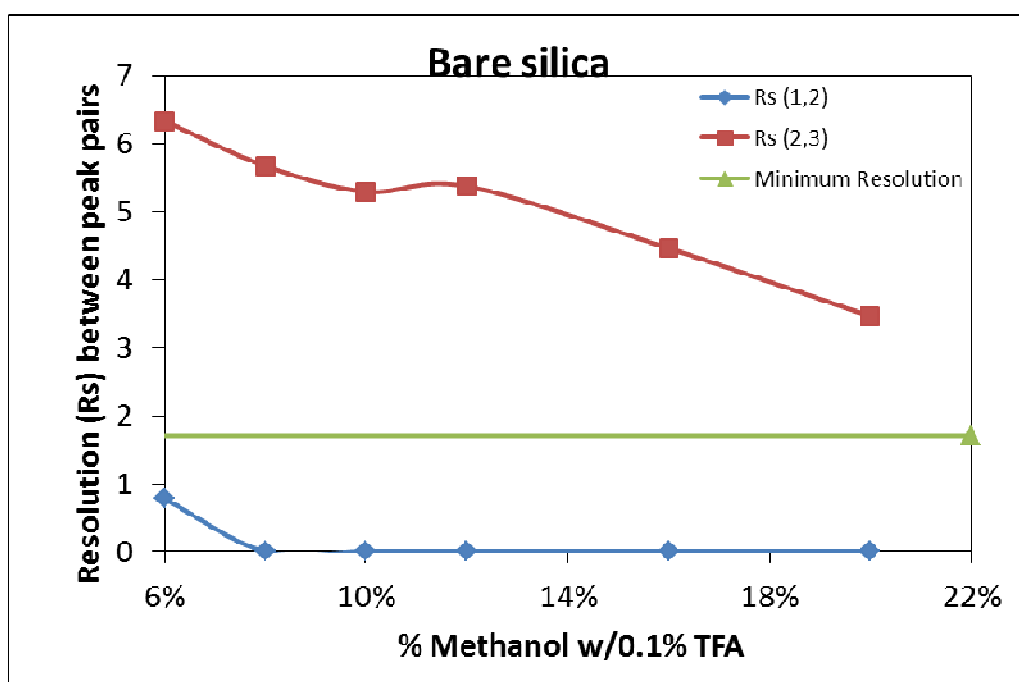


Fig. 3.3.10b: Resolution of peak pairs vs. concentration of MeOH w/0.1% TFA in the mobile phase. Peak pairs are as follows: (1,2) (◆): compound C:Voriconazole, (2,3) (■): Voriconazole:compound D on a bare silica stationary phase. (Agilent Zorbax Silica dimensions: 150 x 4.6 mm, 5 μm particle size) minimum resolution is shown by the green line. (Raw Data, Appendix 6.2, Table 6.2.5)

With the addition of TFA to the mobile phase, at a concentration of modifier above 8% Voriconazole and compound C co-elute (Fig. 3.3.10a). An overall decrease in retention of Voriconazole and its impurities was noted using TFA compared to a MeOH only mobile phase as seen in Fig. 3.3.1. It was hypothesised that coverage of surface silanols on the surface of the silica by TFA, causing less active sites being available for bonding by the analytes, led to the reduced retention noted on this stationary phase. This behaviour is similar to trends reported by DeKlerck where the addition of TFA to the mobile phase led to a reduction in retention for enantiomers[84] As can be seen due to co-elution of compound C and Voriconazole resolution between this peak pair is 0 above 8% modifier. At 6% resolution is below the critical resolution value of 1.7 as denoted by the green line in Fig 3.3.10b (raw data; appendix 6.2, Table 6.2.5) It was therefore concluded that the addition of TFA to the MeOH modified mobile phase was unsuitable at any concentration used in this study.

3.3.1.1.3.2 Cyano stationary phase

This study was repeated on a cyano stationary phase using identical parameters. Results of this study are given in Fig 3.3.11.

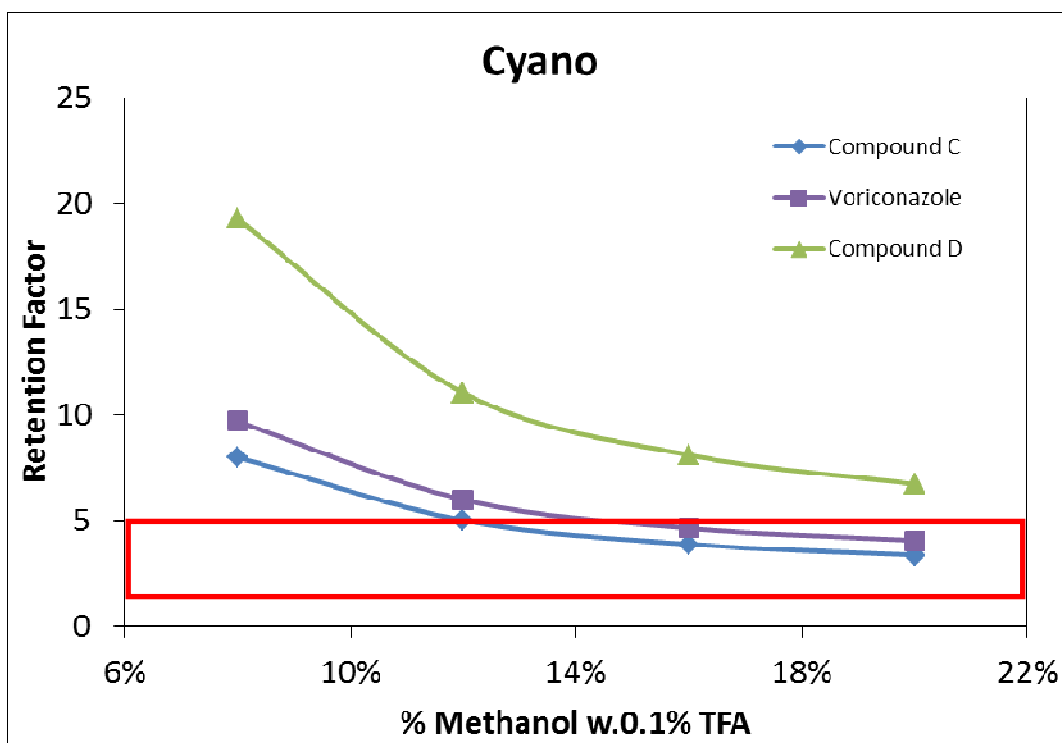


Fig. 3.3.11a: Retention factor of Voriconazole (■) and related impurities compound C (◆) and compound D (▲), with ideal retention window illustrated by the area within the red box vs. concentration of MeOH w/0.1% TFA in mobile phase on a cyano stationary phase (Phenomenex Spherisorb CN dimensions: 250 x 4.6 mm , 5 μm particle size). (Raw Data, Appendix 6.2, Table 6.2.6)

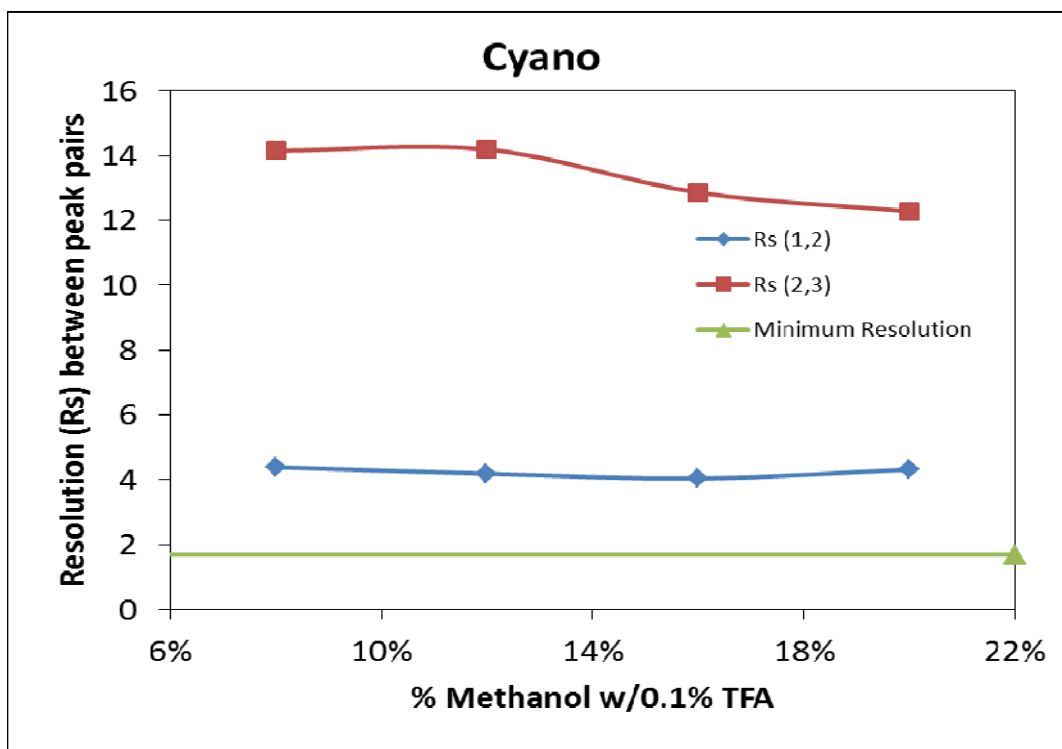


Fig. 3.3.11b: Resolution of peak pairs vs. concentration of MeOH w/0.1% TFA in mobile phase on a cyano stationary phase (Phenomenex Spherisorb CN dimensions: 250 x 4.6 mm , 5 μ m particle size. Peak pairs are as follows: (1,2)(\blacklozenge): compound C:Voriconazole, (2,3)(\blacksquare) Voriconazole:compound D. Minimum resolution illustrated by the green line(Raw Data, Appendix 6.2, Table 6.2.6)

When compared to a MeOH only mobile phase (Fig 3.3.2), the addition of TFA has increased retention of all 3 components of S3b. This increase in retention was hypothesised to be due to protonation of the cyano group on the stationary phase by TFA and deprotonation of the hydroxyl groups on both Voriconazole and compound D resulting in ion pairing increasing retention. Ideally a retention factor window of between 1 and 5 (as indicated by the red box in Fig. 3.3.11a) is optimum and as can be seen in Fig. 3.11a, 16% and 20% MeOH w/0.1% TFA provided retention factors for Voriconazole and compound C within this window. Resolution across the entire modifier concentration (Fig. 3.3.11b) is above 1.7 for both peak pairs. 20% MeOH w/0.1% TFA was deemed to be the most suitable with a complete run time of 6.542 min (appendix 6.2, table 6.2.6)

3.3.1.1.3.3 Diol stationary phase

This study was continued on a diol stationary phase using identical parameters. Results of this study are given in Fig 3.3.12.

(a)

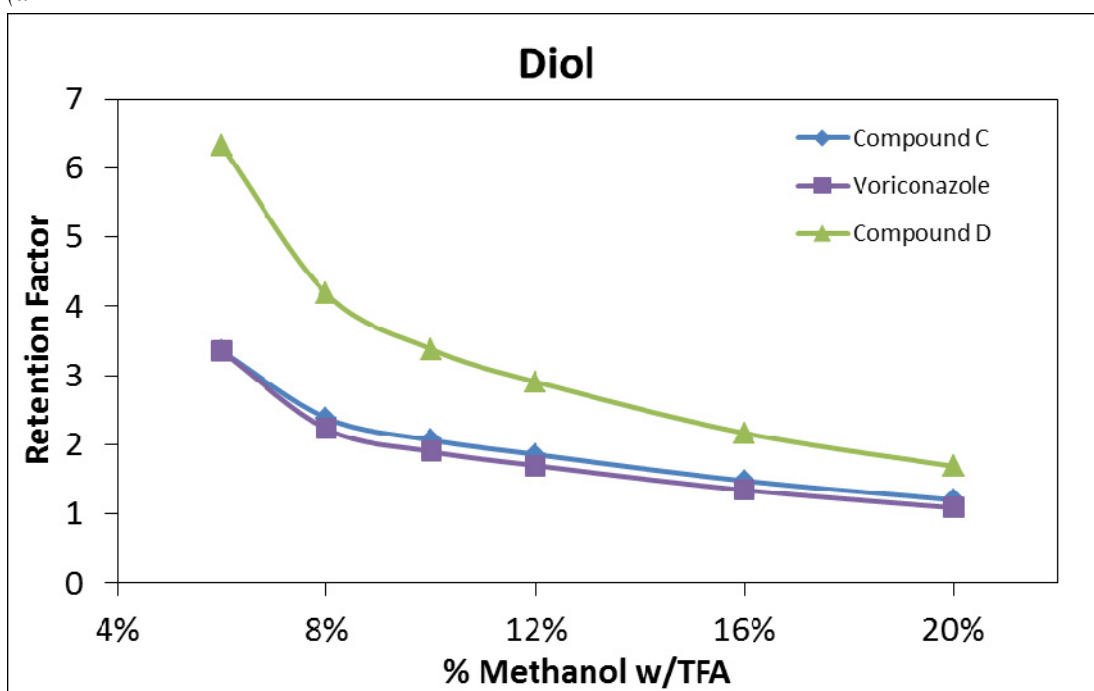


Fig. 3.3.12a: Retention factor of Voriconazole (■) and related impurities compound C (◆) and compound D (▲) vs. concentration of MeOH w/0.1% TFA in mobile phase on a diol stationary phase (Princeton Diol dimensions: 150 x 4.6 mm, 5 μm particle size) (Raw Data, Appendix 6.2, Table 6.2.7)

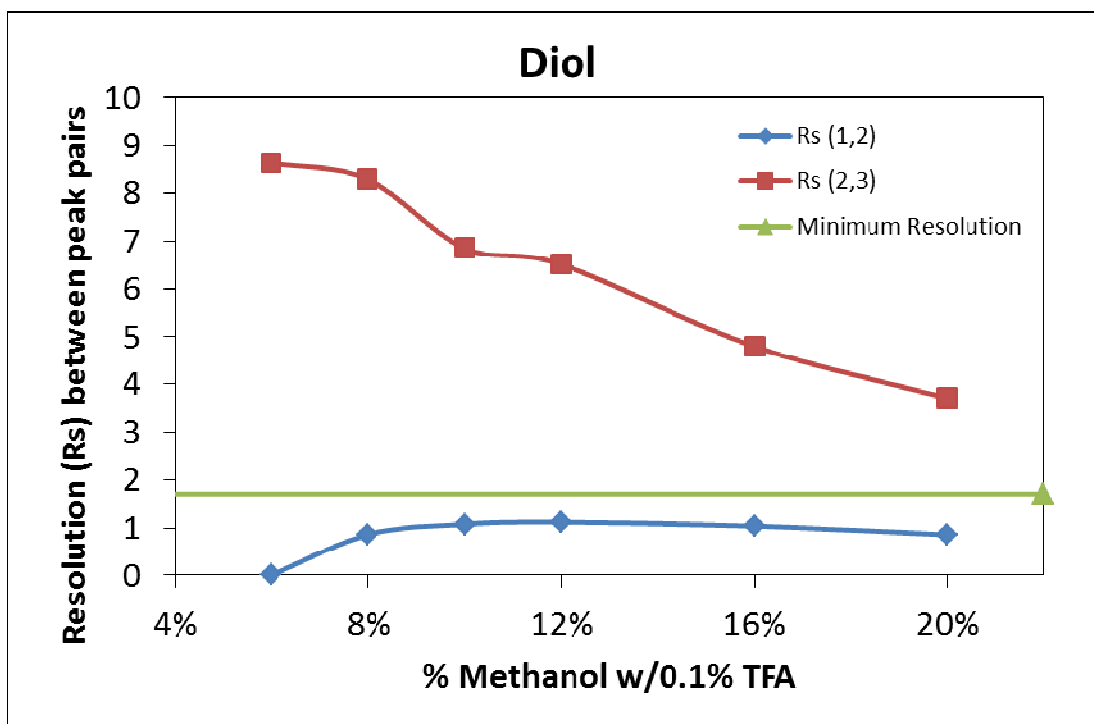


Fig 3.3.12b: Retention of peak pairs vs. concentration of MeOH w/0.1% TFA in mobile phase on a diol stationary phase (Princeton Diol dimensions: 150 x 4.6 mm , 5 μ m particle size) Peak pairs are as follows: (1,2) (◆): compound C:Voriconazole, (2,3) (■): Voriconazole:compound D. (Raw Data, Appendix 6.2, Table 6.2.7)

Retention behaviour on a diol stationary phase when TFA was added to the MeOH was similar to that observed when a MeOH only mobile phase was used. While the addition of TFA has a major effect on retention on a silica column (Fig 3.3.10a), it was not expected to have as major as effect as the TFA does not have as strong of an interaction with the diol functionality as with surface silanols. Retention factors across the range of modifier and additive concentrations as expected decreased with modifier concentration (appendix 6.2, Table 6.2.7). As with a MeOH only mobile phase (Fig. 3.3.7), there was inadequate resolution between analytes compound C and Voriconazole over the entire range of MeOH w/0.1% TFA concentrations as shown in Fig 3.3.12b. Elution order also remained the same as with a MeOH only mobile phase.

3.3.1.1.3.4 ethyl-pyridine stationary phase

An identical experiment was then carried out on an ethyl-pyridine stationary phase using identical parameters. Results of this study are given in Fig 3.3.13.

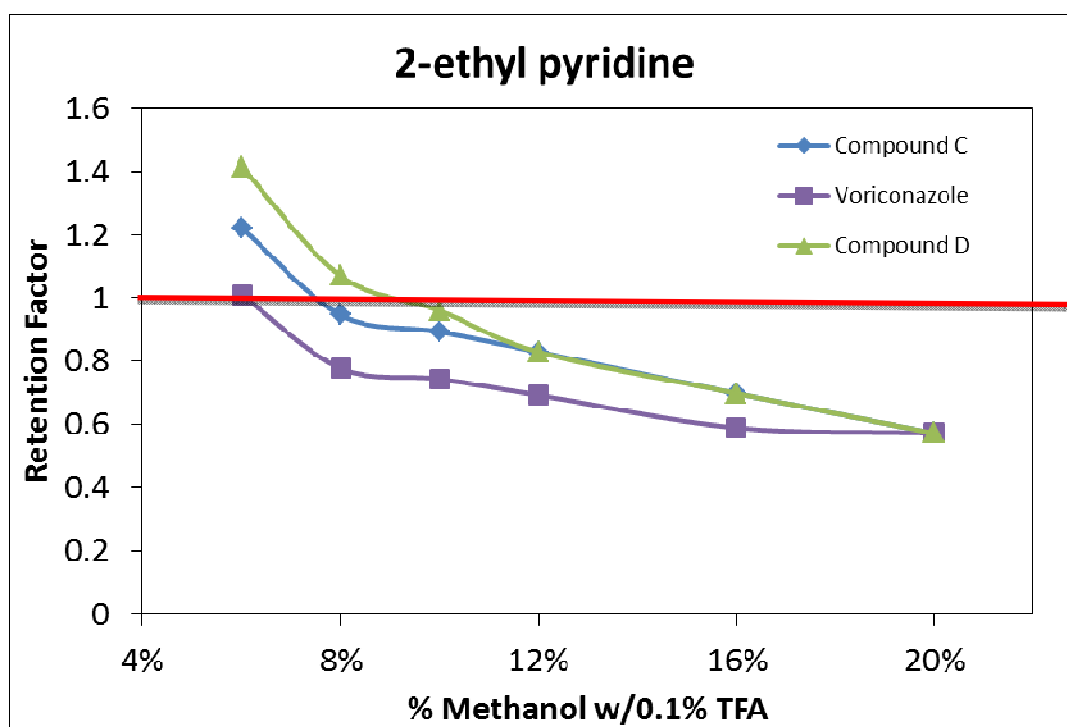


Fig. 3.3.13a: Retention factor of Voriconazole (■) and related impurities compound C (◆) and compound D(▲) with retention factor threshold (≥ 1) indicated by the red line vs. concentration of MeOH w/0.1% TFA in mobile phase on an ethyl pyridine stationary phase (Princeton Ethylpyridine dimensions: 150 x 4.6 mm , 5 μ m particle size) (Raw Data, Appendix 6.2, Table 6.2.8)

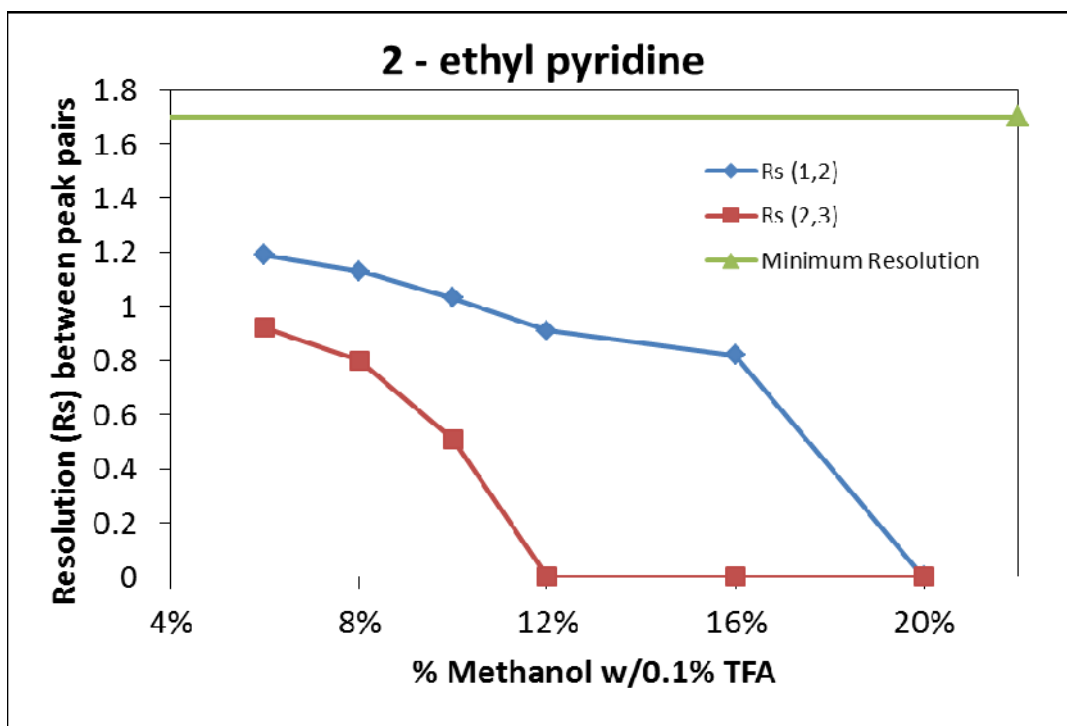


Fig. 3.3.13b: Retention of peak pairs vs. concentration of MeOH w/0.1% TFA in mobile phase on a ethyl pyridine stationary phase (Princeton Ethylpyridine dimensions: 150 x 4.6 mm , 5 μ m particle size) Peak pairs are as follows: (1,2)(\blacklozenge): compound C:Voriconazole, (2,3)(\blacksquare): Voriconazole:compound D. Minimum resolution threshold is indicated by the green line. (Raw Data, Appendix 6.2, Table 6.2.8)

To allow sufficient interaction with the stationary phase, retention factors of analytes should be greater than one. The red line in Fig 3.3.13a indicates that Retention factors of greater than 1 are only achieved on an ethyl pyridine column using a MeOH w/ 0.1% TFA modifier at a concentration of 6%. However resolution at this concentration of modifier is inadequate for both peak pairs. This stationary phase mobile phase combination is entirely unsuitable.

3.3.1.1.3.5 Optimal MeOH modified mobile phases with TFA additive

The addition of TFA to a MeOH modifier was only suitable on a cyano stationary phase. On all other stationary phases, i.e. bare silica, diol and pyridine columns, analytes were either not sufficiently retained, such as in the case of a pyridine column, or the threshold set out for resolution for critical peak pairs was not met as

occurred for both the bare silica and diol stationary phases. Fig.3.3.14 below illustrates the separation of S3b using 20% MeOH, 0.1 % TFA on a cyano stationary phase. All the optimisation parameters are met, as the resolution exceeds 1.7 for all pairs. However, the runtime, at almost 7 minutes is significantly greater than the 4.5 minutes recorded when MeOH was added as a mobile phase modifier without any additive.

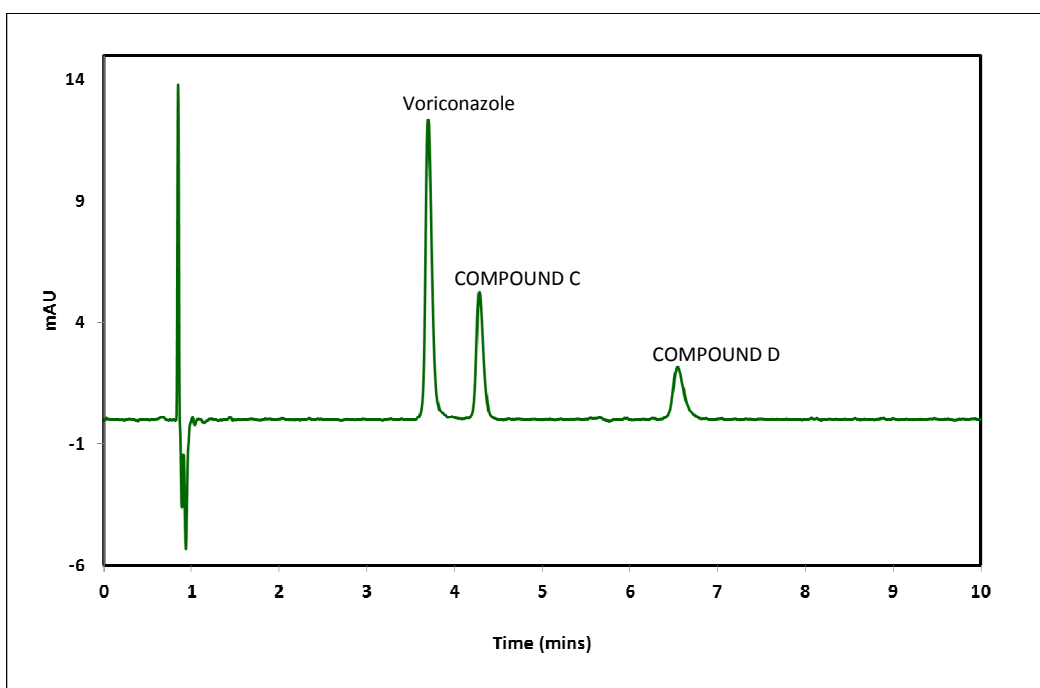


Fig 3.3.14: Chromatogram of the best separation of S3b achieved on a cyano stationary phase using a 20% MeOH, 0.1% TFA, 80% *s*CO₂ mobile phase. Conditions: Injection Volume: 5 μ L, Column Temp: 37.5°C (in) 40.0°C(out), Detector wavelength: 256 nm, booster pressure: 130 bar

3.3.1.1.4 Investigation of the effect of MeOH mobile phase modifier with 0.1% TEA on retention of Voriconazole and related impurities compound C and compound D

Triethylamine (TEA) is a base which is commonly used as an additive in both HPLC and SFC. Phinney *et al.*[120] hypothesised that TEA had a number of different effects on retention including ion suppression of analytes and/or stationary phase leading to a change in retention as well as reducing solute interactions with surface silanols which gave rise to unwanted retention.

3.3.1.1.4.1 Bare silica stationary phase

Results of the separation of S3b on the bare silica stationary phases is given below in Fig. 3.3.15.

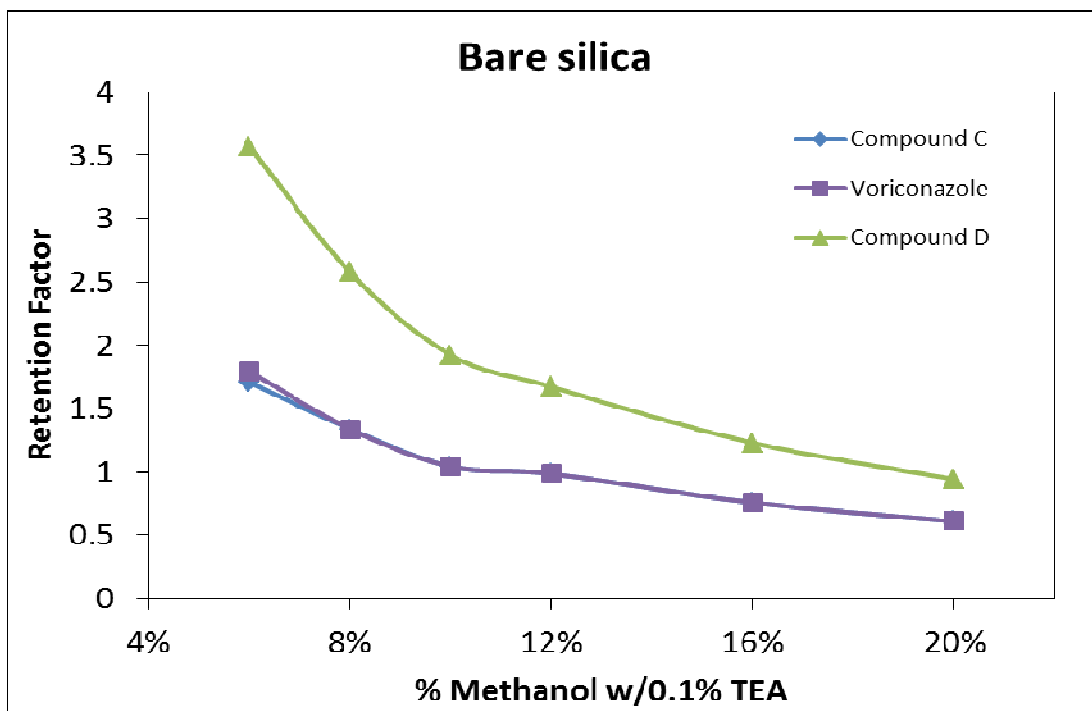


Fig. 3.3.15a: Retention factor of Voriconazole (■) and related impurities compound C (◆) and compound D (▲) vs. concentration of MeOH in mobile phase w/0.1% TEA in mobile phase on a bare silica stationary phase (Agilent Zorbax silica dimensions: 150 x 4.6 mm, 5 μm particle size) (Raw Data, Appendix 6.2, Table 6.2.9)

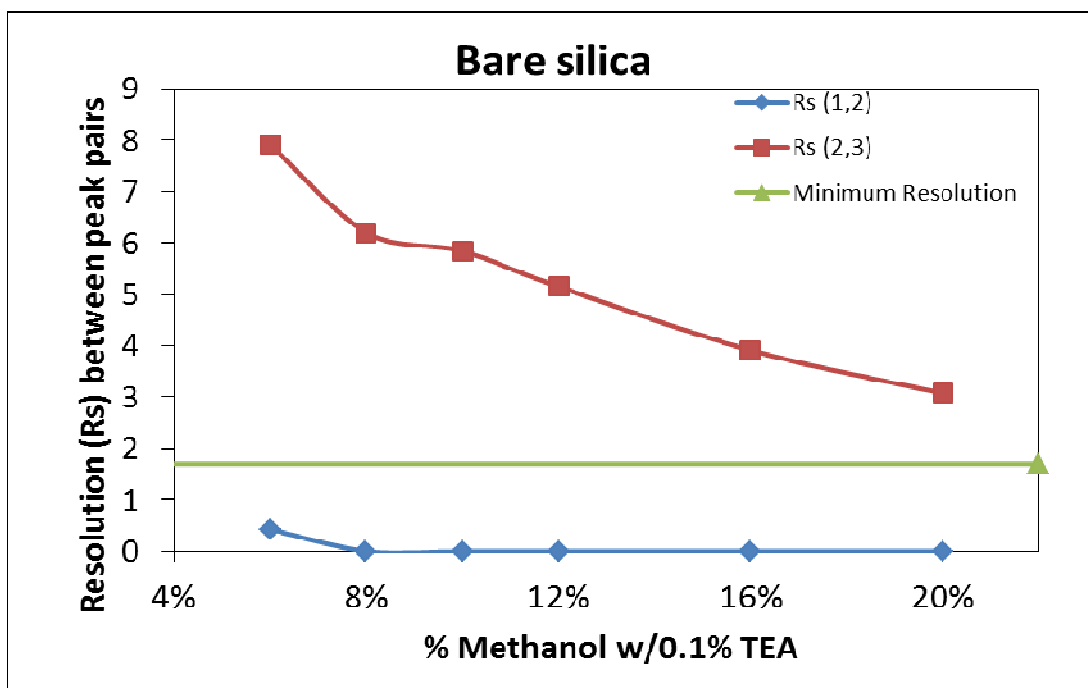


Fig. 3.3.15b: Retention of peak pairs vs. concentration of MeOH in mobile phase w/0.1% TEA in mobile phase on a bare silica stationary phase (Agilent Zorbax silica dimensions: 150 x 4.6 mm , 5 μ m particle size). Peak pairs are as follows: (1,2)(\blacklozenge): compound C:Voriconazole, (2,3)(\blacksquare): Voriconazole:compound D. Minimum resolution threshold is indicated by the green line.(Raw data; Appendix 6.2, Table 6.2.9)

As was the case when TFA was added to the MeOH modifier peaks 2 and 3, Voriconazole and compound D, co-elute with a concentration of greater than 8% modifier. As was the case with TFA, it was hypothesised that TEA played the same role in retention in covering surface silanols on the silica stationary phase rendering them unavailable for interaction with the solute, decreasing retention. Retention factors and retention times were similar for both TEA and TFA. It is hypothesised that decreasing the modifier concentration below 6% would not provide a significant increase in resolution between critical peaks to satisfy the experimental critical parameters set out at the start of the experiment.

3.3.1.1.4.2 cyano stationary phase

Results of the separation of S3b on the cyano stationary phases is given below in Fig. 3.3.16.

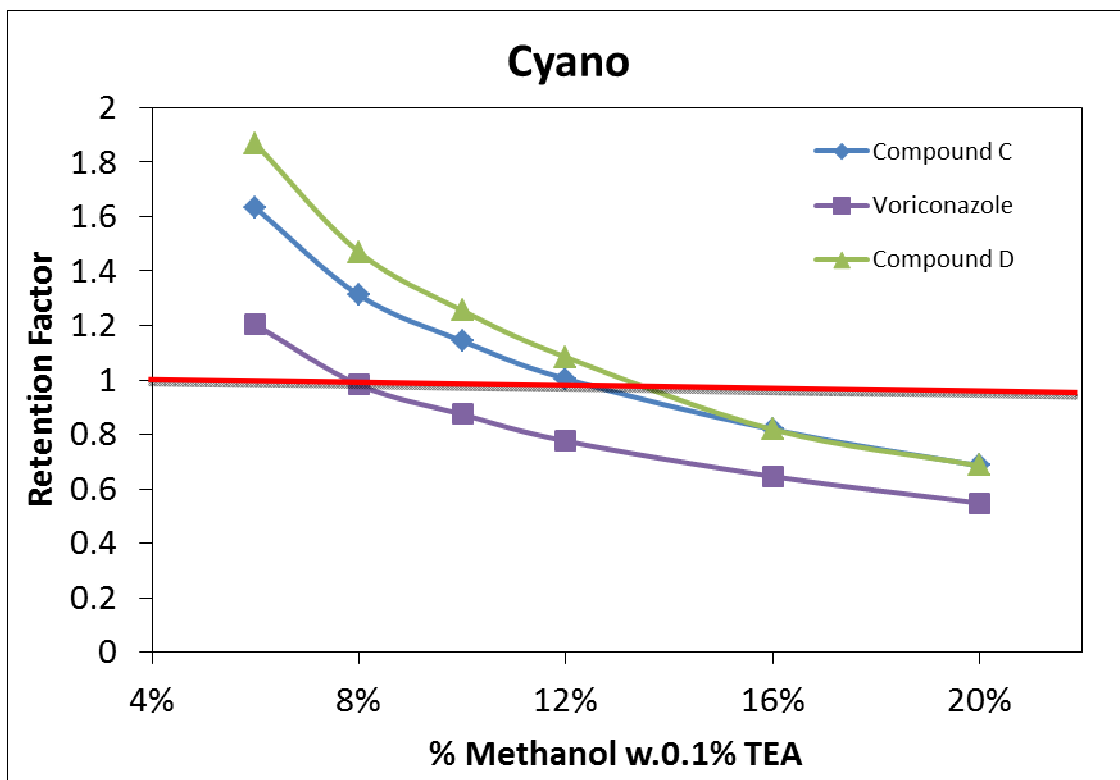


Fig. 3.3.16a: Retention factor of Voriconazole (■) and related impurities compound C (◆) and compound D (▲), with retention factor threshold (≥ 1) indicated by the red line vs. concentration of MeOH w/0.1% TEA in mobile phase on a cyano stationary phase (Phenomenex Spherisorb CN dimensions: 250 x 4.6 mm , 5 μ m particle size). (Raw Data, Appendix 6.2, Table 6.2.10)

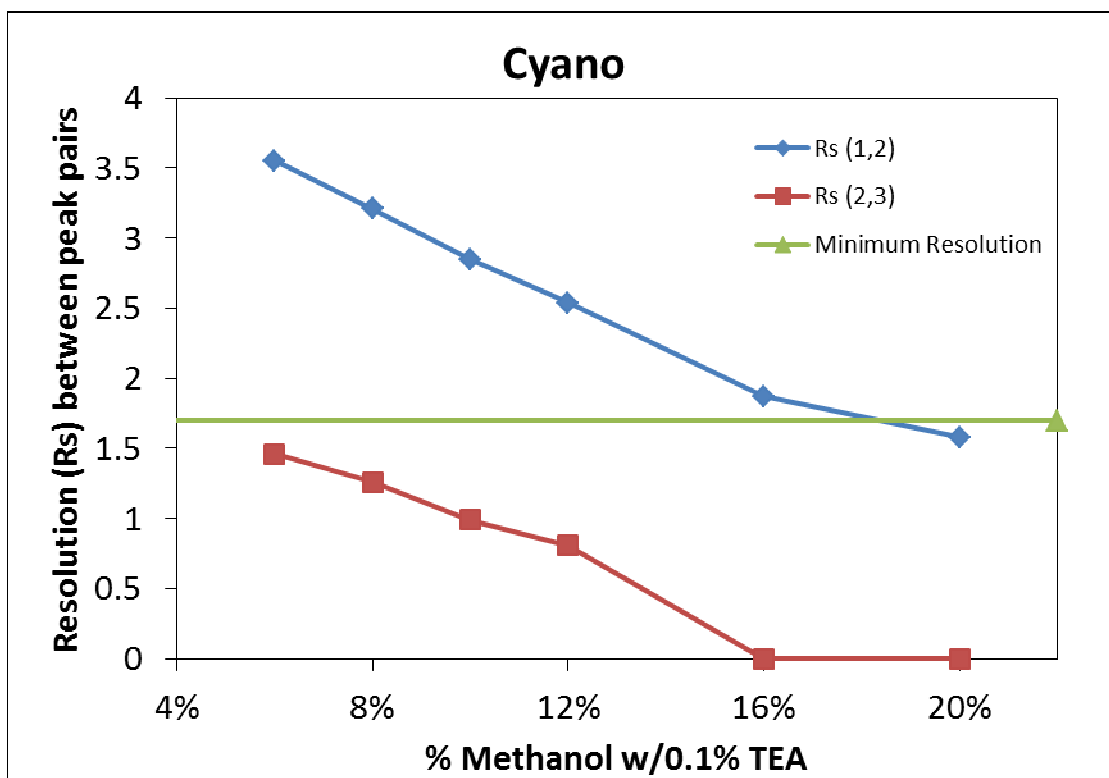


Fig. 3.3.16b: Resolution of peak pairs vs. concentration of MeOH w/0.1% TEA in mobile phase on a cyano stationary phase (Phenomenex Spherisorb CN dimensions: 250 x 4.6 mm , 5 μ m particle size). Peak pairs are as follows: (1,2) (◆): Voriconazole:compound C (2,3) (■) compound C:compound D. Minimum resolution threshold is illustrated by the green line. (Raw Data, Appendix 6.2, Table 6.2.10)

Firstly, when compared to a MeOH only modifier (Fig. 3.3.2) and a MeOH with 0.1% TFA additive (Fig. 3.3.11), the elution order of compound C and Voriconazole has switched with Voriconazole now eluting first (Fig. 3.3.15). TEA was hypothesised to cause the analytes to become ionised, while the stationary remained neutral leading to a reduction in retention. The switch in elution order was hypothesised to be due to the combination of the repulsion of the now ionised Voriconazole molecule with the neutral stationary phase as well as fact that Voriconazole is a bulkier molecule and so will be less retained, compared to the smaller molecule compound C.

3.3.1.1.4.3 Diol stationary phase

The results of the study carried out on diol stationary phase are given below in Fig. 3.3.17.

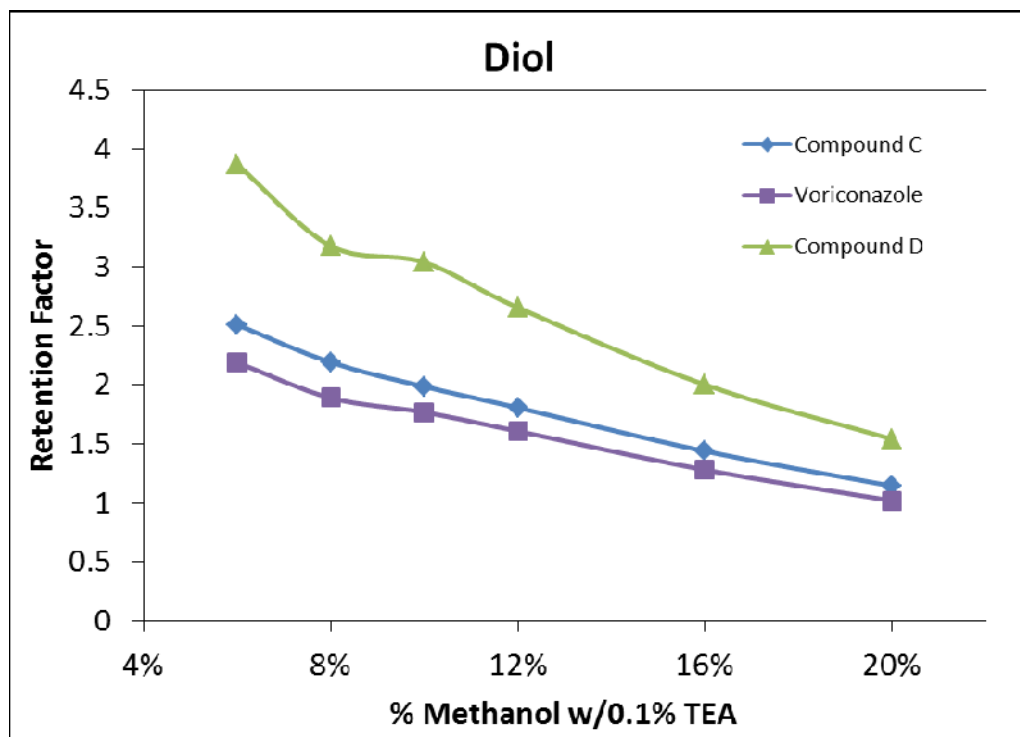


Fig. 3.3.17a: Retention factor of Voriconazole (◆) and related impurities compound C (■) and compound D(▲) vs. concentration of MeOH w/0.1% TEA in mobile phase on a diol stationary phase (Princeton Diol dimensions: 150 x 4.6 mm, 5 μm particle size)(Raw Data, Appendix 6.2, Table 6.2.11)

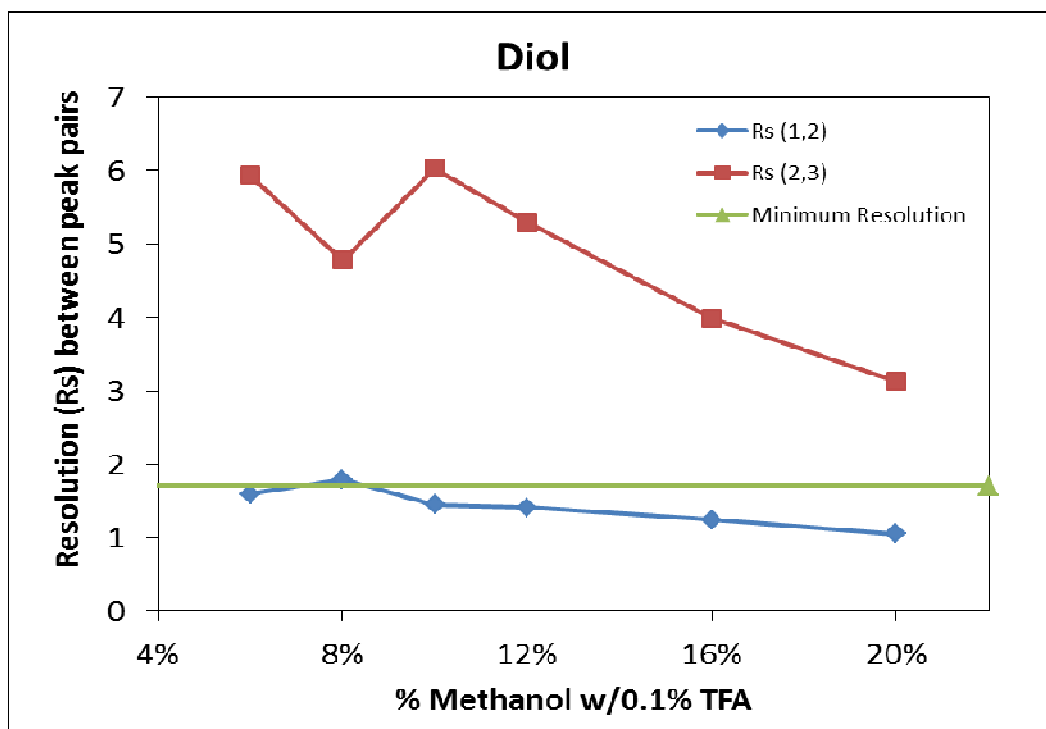


Fig. 3.3.17b: Resolution of peak pairs vs. concentration of MeOH w/0.1% TEA in mobile phase on a diol stationary phase (Princeton Diol dimensions: 150 x 4.6 mm, 5 μ m particle size) Peak pairs are as follows: (1,2)(\blacklozenge): compound C:Voriconazole, (2,3)(\blacksquare): Voriconazole:compound D. Minimum resolution threshold is illustrated by the green line.

The increase in retention noted with the addition of TEA to the MeOH modified mobile phase compared to a MeOH only modified mobile phase (Fig. 3.3.3) and a MeOH modifier with 0.1% TFA additive (Fig. 3.3.12) may be attributed deprotonation of the diol stationary phase and the ionisation of the solute in a now basic mobile phase causing ion pairing to occur between the stationary and solutes increasing retention. Resolution of the critical peak pair Voriconazole and compound C remained below the threshold set for resolution for all concentrations of modifier, apart from 8%.

3.3.1.1.4.4 Ethyl pyridine stationary phase

It was noted throughout this experiment on each of the four stationary phases that with the use of TEA an extra peak appeared in each chromatogram. After ruling out contamination of the TEA, it was concluded that peak was due to the TEA additive itself. On a diol, bare silica and cyano stationary phase, the system peak eluted after the analytes of interest with reasonable resolution between the last eluting peak and

the system peak, however when an ethyl pyridine column was used, this peak co-eluted with analytes of interest and thus this experiment was discontinued.

3.3.1.1.4.5 Optimal TEA additive mobile phases

While 8% MeOH modified mobile phase with 0.1% TEA additive provided a good separation of S3b on a diol stationary phase (Fig. 3.3.17) it was decided to reject this mobile phase, stationary phase combination as a viable option due to the presence of the system peak. TEA has a detrimental effect on retention on both the cyano and silica stationary phases, due to interaction with surface silanols on the silica stationary phase and ionisation of analytes on the cyano stationary phase, therefore were not suitable. The final additive which was investigated in this study was Ammonium Acetate (AA).

3.3.1.1.5 Investigation of the effect of MeOH modified mobile phase with 20 mM AA additive on retention of Voriconazole and related impurities compound C and compound D

Aside from the use of acids and bases as mobile additives in SFC, volatile organic salts are also used. The advantage of the use of such salts over acids and bases is due to their compatibility with mass spectrometric detection as they do not cause ion suppression[82]. As was the case for all previous studies of modifiers and additives, a MeOH modified mobile phase was used with 20 mM AA additive over the range 6% to 20% was analysed on all four stationary phases. The first stationary phase investigated was a bare silica column.

3.3.1.1.5.1 Silica stationary phase

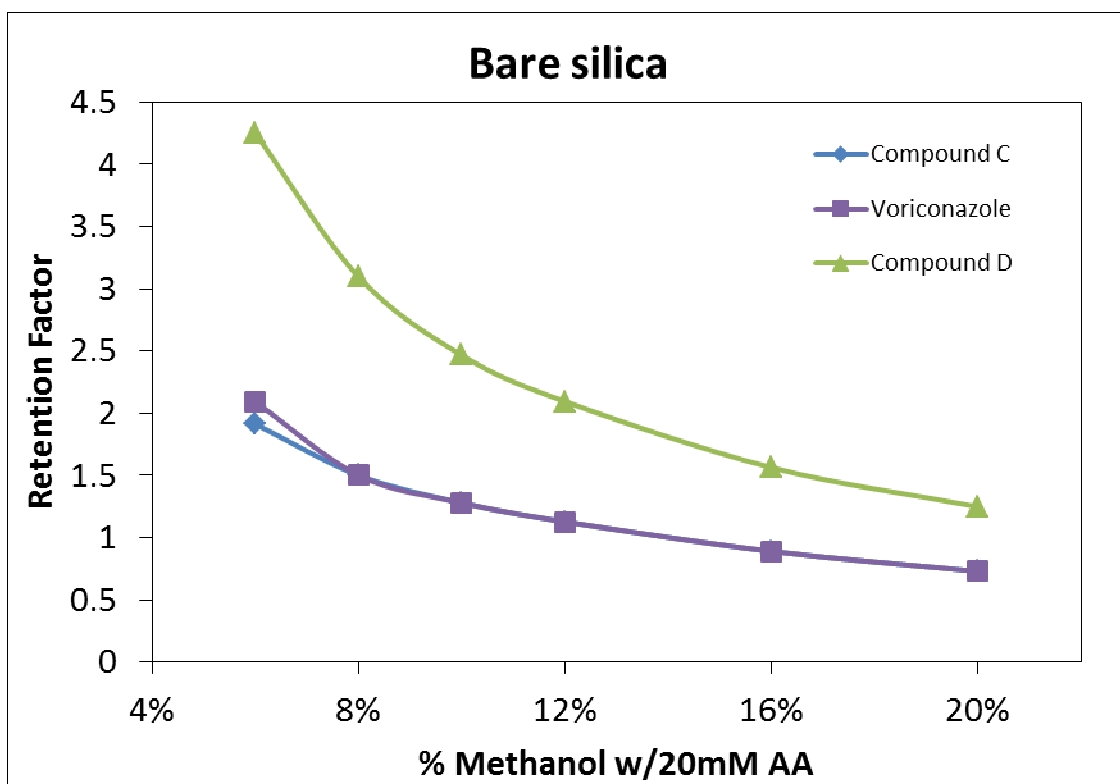


Fig. 3.3.18: Retention factor of Voriconazole(■) and related impurities compound C (◆) and compound D (▲) vs. concentration of MeOH w/20 mM AA in mobile phase on a bare silica stationary phase (Agilent Zorbax Silica, dimensions: 150 x 4.6 mm , 5 μm particle size. (Raw Data, Appendix 6.2, Table 6.2.12)

The reduced retention which was seen with a MeOH plus additives TFA and TEA stationary phase was also seen with the addition of an AA additive to the MeOH modified mobile phase (Fig. 3.3.18). This reduced retention was hypothesised to be due to coverage of surface silanols which were then unavailable for hydrogen bonding interaction with solute molecules, the same retention mechanism as was the dominant throughout this study. The next stationary phase investigated was cyano stationary phase.

3.3.1.1.5.2 Cyano and Diol stationary phases.

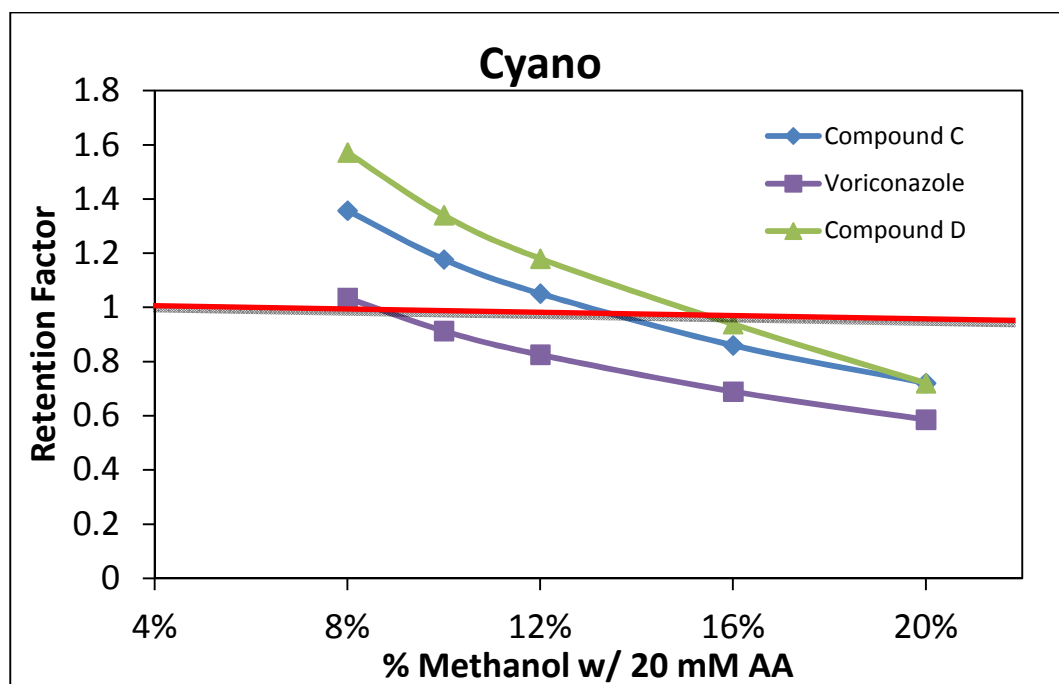


Fig. 3.3.19a: Retention factor of Voriconazole (■) and related impurities compound C (◆) and compound D (▲) with retention factor threshold (≥ 1) indicated by the red line vs. concentration of MeOH w/ 20 mM AA in mobile phase on a cyano stationary phase (Phenomenex Spherisorb CN dimensions: 250 x 4.6 mm , 5 μ m particle size. (Raw Data, Appendix 6.2, Table 6.2.13)

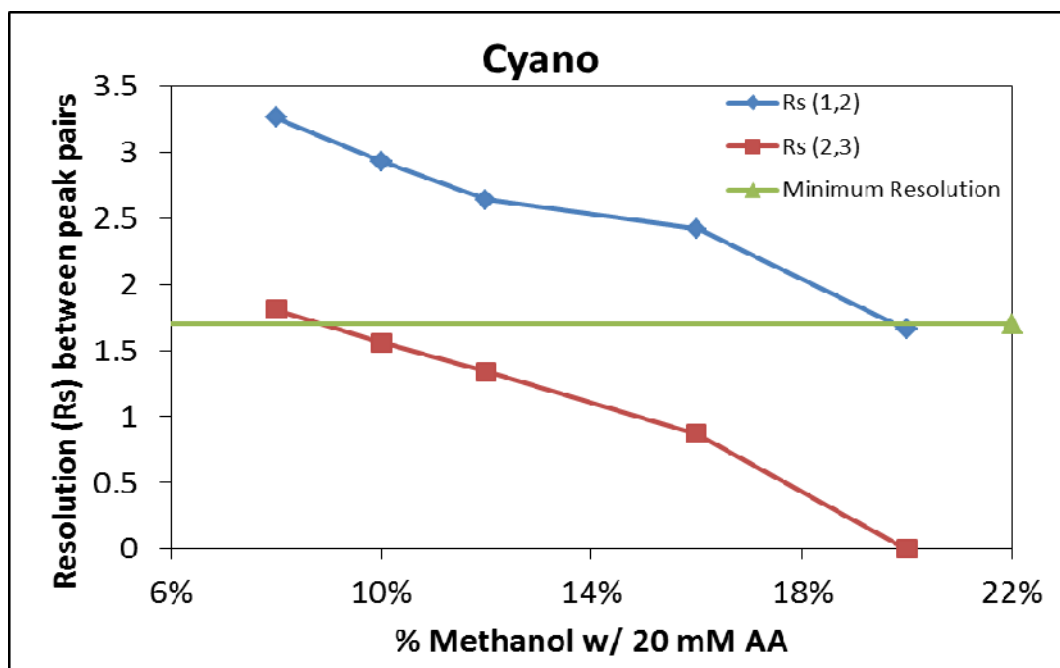


Fig. 3.3.19b: Resolution of peak pairs vs. concentration of MeOH w/ 20 mM AA in mobile phase on a cyano stationary phase (Phenomenex Spherisorb CN dimensions: 250 x 4.6 mm , 5 μ m particle size. Peak pairs are as follows: (1,2)(\blacklozenge)Voriconazole:compound C (2,3)(\blacksquare) compound C:compound D. Minimum resolution threshold indicated by the green line. (Raw Data, Appendix 6.2, Table 6.2.11)

As can be seen in Fig 3.3.19, with the addition of AA to the MeOH modified mobile phase there is a significant reduction in retention and thus resolution compared to the when no additive was used (Fig 3.3.2) and when TFA was added (Fig. 3.3.11). It is hypothesised that AA has the same effect on retention as TEA (Fig 3.3.17), that is; ionisation of the analytes in the basic mobile phase causing retention to decrease due to decreased interaction with the stationary phase. Finally, a concentration study of MeOH modified mobile phase with 20 mM AA additive was carried out on a diol stationary phase (Fig 3.3.20). As retention was poor for all other mobile phases on an ethyl pyridine column, this column was disregarded from this study.

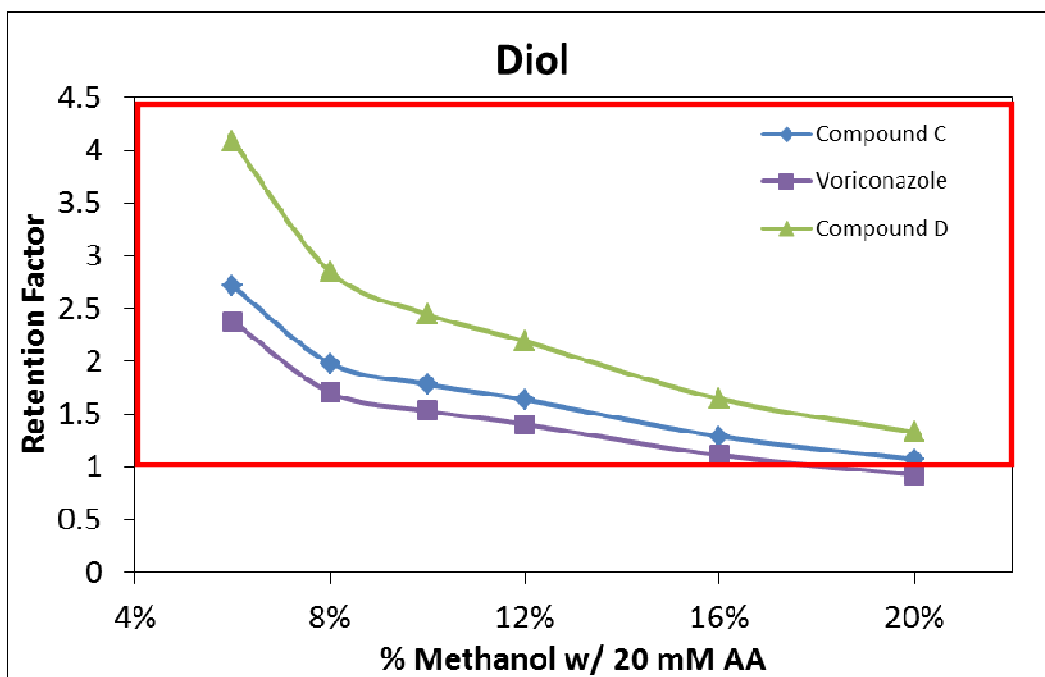


Fig. 3.3.20a: Retention factor of Voriconazole (■) and related impurities compound C (◆) and compound D (▲) with ideal retention window illustrated by the area within the red box vs. concentration of MeOH w/ 20 mM AA in mobile phase on a diol stationary phase (Princeton Diol dimensions: 150 x 4.6 mm , 5 μm particle size) (Raw Data, Appendix 6.2, Table 6.2.14)

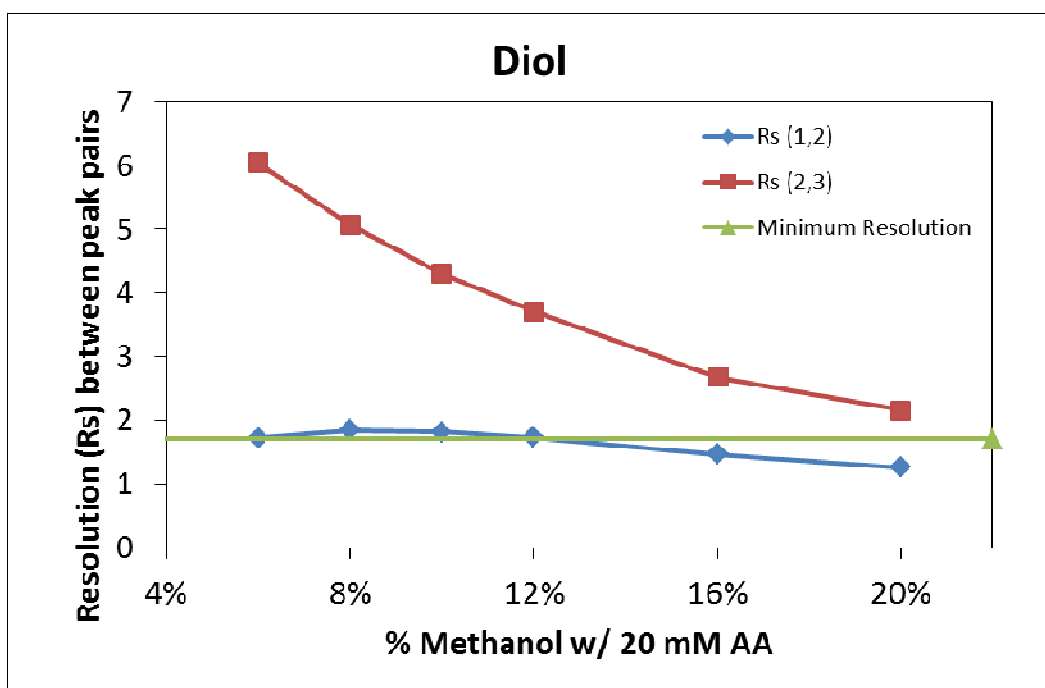


Fig. 3.3.20b: Resolution of peak pairs vs. concentration of MeOH w/ 20 mM AA in mobile phase on a diol stationary phase (Princeton Diol dimensions: 150 x 4.6 mm , 5 μm particle size) Peak pairs are as follows: (1,2)(◆): compound C:Voriconazole, (2,3)(■): Voriconazole:compound D. Minimum resolution threshold is illustrated by the green line. (Raw Data, Appendix 6.2, Table 6.2.14)

As was also the case for a cyano column, TEA and AA were hypothesised to have a similar effect on retention on diol column. With the addition of AA to the MeOH overall retention of all analytes were increased. It was hypothesised that the increase in retention compared to a methanol only modifier on this stationary phase was due to ion pairing of the ionised solutes and the deprotonated diolic stationary phase.

3.3.1.1.5.3 Optimal AA additive mobile phases

The addition of AA to a MeOH modifier was found to be advantageous on a diol and a cyano stationary phase but not a silica stationary phase as was previously discussed. Fig.3.3.21 below illustrates the separation of S3b using 8% MeOH modified mobile phase with 20 mM AA additive on a cyano stationary phase. Run time for this separation was 2.263 minutes with a critical resolution of 1.81 between compound C and D. Fig.3.3.22 illustrates the separation of S3b using 10% MeOH modified mobile phase with 20 mM AA additive on a diol column, the run time of this assay was 2.272 minutes with a critical resolution between compound Voriconazole and compound C of 1.82.

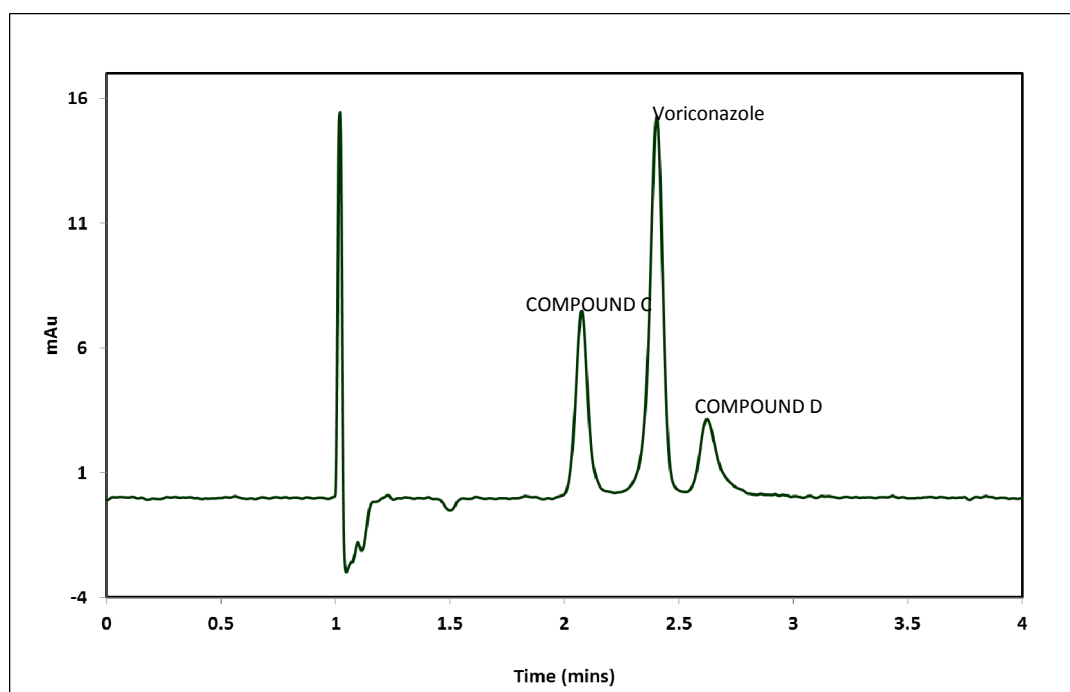


Fig 3.3.21: Chromatogram of the best separation of S3b achieved on a cyano stationary phase using a 8% MeOH, 20 mM AA, 92% sCO₂ mobile phase. Conditions: Injection Volume: 5 μ L, Column Temp: 37.5°C (in) 40.0°C(out), Detector wavelength: 256 nm, booster pressure: 130 bar

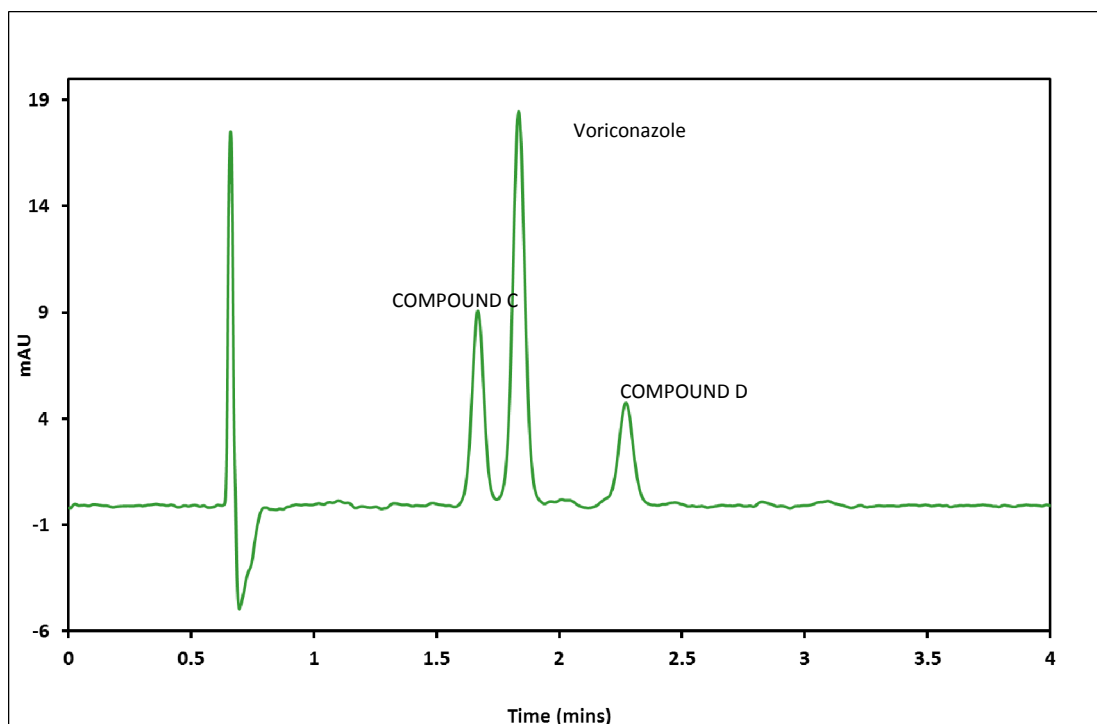


Fig 3.3.22: Chromatogram of the best separation of S3b achieved on a diol stationary phase using a 10% MeOH, 20mM AA, 90% sCO₂ mobile phase. Conditions: Injection Volume: 5 μ L, Column Temp: 37.5°C (in) 40.0°C(out), Detector wavelength: 256 nm, booster pressure: 130 bar

3.4 Conclusions

The first conclusion which can be drawn from this study was that polar stationary phases such as the ones selected for this study, with MeOH based modifiers are unsuitable for the retention of some impurities associated with Voriconazole such as compound X. It was hypothesised that this compound was not retained due to the higher polar nature of each of the stationary phases shown. Compound X is a non polar molecule and thus none of the stationary phases chosen were suitable. It is hypothesised that on a more non-polar stationary phase such as a C₈ or C₁₈ column, retention of this compound may be achieved.

An advantage of SFC to chromatographers is its orthogonality compared to reversed phase HPLC. For this reason, SFC is a very attractive alternative or complementary technique to HPLC. Orthogonality compared to the existing reversed phase USP-36-NF-31 method as shown in Fig 2.3.1 was demonstrated. The original elution order of the HPLC method was compound X, compound C, compound D and Voriconazole. Two other elution orders were demonstrated in this study. The first elution order was; compound C, Voriconazole, and compound D which was demonstrated in Figs. 3.3.1, 3.3.2, 3.3.8, 3.3.9, 3.3.10, 3.3.11, 3.3.15 and 3.3.18. The second retention order was Voriconazole compound C, and compound D which was demonstrated in Figs. 3.3.3, 3.3.4, 3.3.12, 3.3.13, 3.3.14, 3.3.16, 3.3.17, 3.3.19, and 3.3.20

A general trend of decreasing retention with increasing modifier concentration was seen across the entire mobile phase/stationary phase study including when various additives were added to the mobile phase. It is therefore concluded that the concentration of modifier in the mobile phase played a significant role in the overall retention of S3b, while the addition of additives had a more specific effect on retention of particular analytes. This can be seen on a cyano stationary phase where a methanol only modifier showed intermediate retention between that seen when an acidic or basic additive was included in the mobile phase. On a cyano stationary phase, the addition of TFA to the mobile phase was hypothesised to cause ion pairing between the solute and the stationary phase increasing retention while the addition of a basic additive such as TEA or a salt such as AA were found to decrease retention which was hypothesised to be due to ionisation of analytes causing

retention to decrease. Voriconazole and compound D were most affected by basic analytes due to the easy protonation of their alcohol functionality.

On a silica stationary phase the addition of additives were found to have a detrimental effect on retention of S3b and a loss of resolution and co-elution was noted across all 3 modifiers across all modifier concentrations. It was hypothesised that the reduction of retention was due to coverage of surface silanols on the silica stationary phase by the additive molecules which provided valuable retention when a methanol only mobile phase was used.

It was found that a pyridine column was entirely unsuitable for the separation of this API and related impurities. Pyridine columns were designed especially for use with highly polar analytes, however as the analytes in question are more hydrophobic in nature they were not well retained at all. MeOH with a TEA or AA additive included in the MeOH modifier provided reasonable retention and resolution of Voriconazole and two of the related impurities, however the presence of a system peak due to TEA lead to this mobile phase being disregarded.

Following the study it was concluded that a cyano stationary phase with a 20% MeOH modified mobile phase with 0.1% TFA additive or diol stationary phase with a 8% MeOH modified mobile phase with 0.1% AA additive were the most suitable for the separation of Voriconazole and related impurities compound C and compound D. These stationary phase combinations had a complete run time of 6.54 minutes and 2.272 minutes respectively. Runtime on a cyano stationary phase was almost three times that of the diol stationary stationary phase using AA as a modifier, however, resolution is significantly higher at 4.32 for peak pair compound C:Voriconazole and 12.28 for peak pair Voriconazole:Compound D, compared to 1.82 for peak pair Voriconazole:compound C and 4.3 for compound C:compound D. It is also worth mentioning here the switch in elution order of Voriconazole and compound C between the two columns. Both columns used in conjunction with each other, could provide valuable complementary information in confirming the identity and quantity of an unknown impurity should it elute in this region as both columns would provide a different elution order and could be used to confirm whether the impurity existed in a test sample or was caused by some other source. When compared to the original USP 36-NF-31 method (section 2.3.1) run times have been

reduced by more than 30% in the case of the cyano column from ~ 10 min to 6.5 min and more than 75% in the case of the diol column from ~10 min to 2.3 minutes. When compared to the newly developed DCU 2.6 μm (section 2.3.2.2) and 1.7 μm (section 2.3.2.4.2) methods, run time on the diol stationary phase with a AA additive is 50% less. Compound X, however was not retained on any of the stationary phases chosen. As a result further stationary phase investigation would be necessary in order to develop a comprehensive impurity assay for analysis of Voriconazole which is capable of separating all related impurities.

4 Final conclusions and future work

The aim of this thesis was to investigate if improvements could be made to the method USP 36-NF-31, given recent advances both in chromatographic column stationary phases such as core-shell phases, and in emerging chromatographic technologies such as supercritical fluid chromatography. Separations developed were compared primarily using runtime, once a minimum resolution between critical eluting analyte pairs of at least 1.7 was maintained.

In Chapter 2, the USP 36-NF 31 method was successfully replicated and subsequently transferred to a stationary phase consisting of new 3rd generation, core-shell technology of 2.6 μm particle size. The method was further optimised in line with the project objectives, namely the development of a fast pharmaceutical impurity assay while maintaining a resolution between critical peak pair of above 1.7. There was a reduction of the run time of the assay by 56% while resolution between peak pairs was maintained above 2.0. This method was further optimised on a smaller 1.7 μm core-shell column, albeit with no decrease in runtime demonstrated, resolution of above 2 however was still maintained. It was therefore noted that for the method developed, the reduction in particle size did not provide any additional benefit in terms of reducing run times. The absence of a runtime reduction was attributed to the equilibration time necessary for the gradient elution. Additionally, the use of a 1.7 μm column necessitated the use of specialised UPLC instrumentation capable of withstanding pressures of up to 1000 bar as the very small particle size produced back pressures of in excess of 550 bar, therefore it was also concluded that from a cost saving perspective – an increasingly important driver of research and innovation across all industries, the use of 1.7 μm core-shell stationary phase lead to unnecessary extra expenditure, as the method developed on a 2.6 μm core-shell particle stationary phase on a standard HPLC demonstrated equal performance based on the optimisation parameters set out, without the need for specialised high pressure instrumentation.

It is however anticipated that should an isocratic method have been developed instead, there would have been a reduction in run time, due to shorter diffusion pathways[5]. The 1.7 μm core-shell stationary phase used in this study was capable

of withstanding pressures of up to 1000 bar, typical back pressures observed throughout the study were in the region of 550 bar. In order to take advantage of the pressure capabilities of both the instruments used in this study and the columns, gradient and isocratic Poppe plots[43] could be used to determine optimum conditions to achieve the best possible run time and efficiency on both particle sizes using maximum pressure. This study could then be used as a measure of the value – if any, of using 1.7 μm particles as opposed to 2.6 μm for the development of chromatographic methods in the long term.

In *Chapter 3*, a total of 16 stationary phase and mobile phase combinations were evaluated for the development of a new SFC pharmaceutical impurity assay. The general trend which was observed was that SFC did indeed provide orthogonal separation when compared to reversed phase HPLC, as a change in elution order of the compounds was observed. However, all 16 combinations were unsuitable to fully develop an SFC method for the assay and impurity determination of Voriconazole as compound X was very weakly retained, if at all, for all combinations chosen, due to its very non polar nature. Further work should include the evaluation of non polar stationary phase chemistries such as C_8 , C_{18} or a phenyl based column. Since SFC tends to give normal phase behaviour with polar stationary phases and reversed phase behaviour with non-polar stationary phases it is anticipated that the use of non polar stationary phases will provide better retention for the compound X and will improve resolution between peak pairs while providing the added advantages of higher resolution, efficiency and speed compared to reversed phase chromatography[113]. A major area of interest in SFC in terms of its application is in the area of chiral separations [77, 78]. Since Voriconazole is a chiral compound, future work could also focus on the development of a chiral SFC method.

In summary, USP 36-NF 31 has been significantly improved in terms of runtime by transfer to 2.6 μm core-shell stationary phase technology. There is scope to further enhance this improvement by exploration of isocratic elutions, as outlined above. SFC has also been demonstrated to provide orthogonal separation capabilities, which can be further investigated by broadening the types of stationary phase utilised, as described earlier in this section. Future work should also include a complete validation of the core-shell method, investigating for example the ruggedness and repeatability.

The work carried out in this thesis improving USP 36-NF 31 demonstrates the potential advantages in terms of runtime, and therefore analysis cost, in applying new separation technologies to existing methods in use by the pharmaceutical industry. There is therefore huge scope for expanding this research to a broad range of methods which use traditional packed chromatographic stationary phases.

5 References

- [1] L.R. Snyder, J.J. Kirkland, J.W. Dolan, *Introduction to Modern Liquid Chromatography*, John Wiley & Sons, Inc., 2010, p. 1.
- [2] S.A.C. Wren, P. Tchelitcheff, *Journal of Chromatography A*, 1119 (2006) 140.
- [3] S. El Deeb, *Chromatographia*, 74 (2011) 681.
- [4] D. Guillarme, J. Ruta, S. Rudaz, J.-L. Veuthey, *Analytical and Bioanalytical Chemistry*, 397 (2010) 1069.
- [5] J.J. van Deemter, F.J. Zuiderweg, A. Klinkenberg, *Chemical Engineering Science*, 5 (1956) 271.
- [6] LCGC's Chromacademy, powered by Crawford Scientific (2014) Available at www.chromacademy.com/training.html [Accessed 12 September 2013].
- [7] L. Nováková, L. Matysová, P. Solich, *Talanta*, 68 (2006) 908.
- [8] R.E. Majors, *LC-GC Europe*, 25 (2012) 31.
- [9] F. Gritti, M. Martin, G. Guiochon, *Analytical Chemistry*, 81 (2009) 3365.
- [10] L. Nováková, J.L. Veuthey, D. Guillarme, *Journal of Chromatography A*, 1218 (2011) 7971.
- [11] A. de Villiers, H. Lauer, R. Szucs, S. Goodall, P. Sandra, *Journal of Chromatography A*, 1113 (2006) 84.
- [12] J.O. Omamogho, E. Nesterenko, D Connolly, *LC-GC Europe* (2012).
- [13] J.J. Kirkland, *Analytical Chemistry*, 37 (1965) 1458.
- [14] J.J. Kirkland, *Analytical Chemistry*, 41 (1969) 218.
- [15] C.G. Horvath, B.A. Preiss, S.R. Lipsky, *Analytical Chemistry*, 39 (1967) 1422.
- [16] J.M. Cunliffe, T.D. Maloney, *Journal of Separation Science*, 30 (2007) 3104.
- [17] G. Guiochon, F. Gritti, *Journal of Chromatography A*, 1218 (2011) 1915.
- [18] J.J. Kirkland, *Analytical Chemistry*, 64 (1992) 1239.
- [19] J.J. Kirkland, F.A. Truszkowski, C.H. Dilks Jr, G.S. Engel, *Journal of Chromatography A*, 890 (2000) 3.
- [20] X. Wang, D.R. Stoll, A.P. Schellinger, P.W. Carr, *Analytical Chemistry*, 78 (2006) 3406.
- [21] X. Wang, W.E. Barber, P.W. Carr, *Journal of Chromatography A*, 1107 (2006) 139.
- [22] F. Gritti, I. Leonardis, D. Shock, P. Stevenson, A. Shalliker, G. Guiochon, *Journal of Chromatography A*, 1217 (2010) 1589.
- [23] J.J. DeStefano, T.J. Langlois, J.J. Kirkland, *Journal of Chromatographic Science*, 46 (2008) 254.
- [24] J.O. Omamogho, J.D. Glennon, *Analytical Chemistry*, 83 (2011) 1547.
- [25] F. Gritti, G. Guiochon, *Journal of Chromatography A*, 1217 (2010) 8167.
- [26] F. Gritti, J. Omamogho, G. Guiochon, *Journal of Chromatography A*, 1218 (2011) 7078.
- [27] J.J. Kirkland, S.A. Schuster, W.L. Johnson, B.E. Boyes, *Journal of Pharmaceutical Analysis* (2013).
- [28] J.J. DeStefano, S.A. Schuster, J.M. Lawhorn, J.J. Kirkland, *Journal of Chromatography A*, 1258 (2012) 76.
- [29] J.O. Omamogho, J.P. Hanrahan, J. Tobin, J.D. Glennon, *Journal of Chromatography A*, 1218 (2011) 1942.
- [30] F. Gritti, I. Leonardis, J. Abia, G. Guiochon, *Journal of Chromatography A*, 1217 (2010) 3819.
- [31] W. Stöber, A. Fink, E. Bohn, *Journal of Colloid And Interface Science*, 26 (1968) 62.
- [32] F. Gritti, A. Cavazzini, N. Marchetti, G. Guiochon, *Journal of Chromatography A*, 1157 (2007) 289.
- [33] <http://www.chromtech.com.au/pdf/winter02-silica-1.pdf>, (Vol. 02 September 2013).

- [34] E. Oláh, S. Fekete, J. Fekete, K. Ganzler, *Journal of Chromatography A*, 1217 (2010) 3642.
- [35] J.H. Knox, *Journal of Chromatography A*, 831 (1999) 3.
- [36] P. Bristow, J. Knox, *Chromatographia*, 10 (1977) 279.
- [37] L.R. Snyder, J.J. Kirkland, J.W. Dolan, *Introduction to Modern Liquid Chromatography*, John Wiley & Sons, Inc., 2010, p. 19.
- [38] V.R. Meyer, *Practical High-Performance Liquid Chromatography*, John Wiley & Sons, Ltd, 2010, p. 141.
- [39] J.H. Knox, *Analytical Chemistry*, 38 (1966) 253.
- [40] U.D. Neue, *LC-GC North America* (2009).
- [41] K. Horváth, F. Griitti, J.N. Fairchild, G. Guiochon, *Journal of Chromatography A*, 1217 (2010) 6373.
- [42] Y. Zhang, X. Wang, P. Mukherjee, P. Petersson, *Journal of Chromatography A*, 1216 (2009) 4597.
- [43] H. Poppe, *Journal of Chromatography A*, 778 (1997) 3.
- [44] X. Wang, D.R. Stoll, P.W. Carr, P.J. Schoenmakers, *Journal of Chromatography A*, 1125 (2006) 177.
- [45] X. Wang, W.E. Barber, W.J. Long, *Journal of Chromatography A*, 1228 (2012) 72.
- [46] S. Fekete, R. Berky, J. Fekete, J.-L. Veuthey, D. Guillarme, *Journal of Chromatography A*, 1236 (2012) 177.
- [47] S.A. Schuster, B.E. Boyes, B.M. Wagner, J.J. Kirkland, *Journal of Chromatography A*, 1228 (2012) 232.
- [48] in: T.A. Berger, R.M. Smith (Eds.), *Packed Column SFC*, The Royal Society of Chemistry, 1995, p. 1.
- [49] L.T. Taylor, *The Journal of Supercritical Fluids*, 47 (2009) 566.
- [50] T.A. Berger, *Journal of Chromatography A*, 785 (1997) 3.
- [51] W. Majewski, E. Valery, O. Ludemann-Hombourger, *Journal of Liquid Chromatography & Related Technologies*, 28 (2005) 1233.
- [52] A.H.C. Klesper, D.A. Turner, *The Journal of Organic Chemistry*, 27 (1962) 700.
- [53] M.N.M. J.C. Giddings, J.W. King, *Journal of Chromatographic Science*, 7 (1969) 276.
- [54] M. Saito, *Journal of Bioscience and Bioengineering*, 115 (2013) 590.
- [55] A.T. Inc., 2010, p. 1.
- [56] R.M. Smith, *Pure and Applied Chemistry*, 65 (1993) 2397.
- [57] R.M. Smith, *Journal of Chromatography A*, 856 (1999) 83.
- [58] B.W. Wright, H.T. Kalinoski, R.D. Smith, *Analytical Chemistry*, 57 (1985) 2823.
- [59] D.E. Raynie, *Analytical Chemistry*, 65 (1993) 3127.
- [60] in: T.A. Berger, R.M. Smith (Eds.), *Packed Column SFC*, The Royal Society of Chemistry, 1995, p. 43.
- [61] B. Terry A, *Journal of Chromatography A*, 785 (1997) 3.
- [62] in: T.A. Berger, R.M. Smith (Eds.), *Packed Column SFC*, The Royal Society of Chemistry, 1995, p. 72.
- [63] H.N. Weller, K. Ebinger, W. Bullock, K.J. Edinger, M.A. Hermsmeier, S.L. Hoffman, D.S. Nirschl, T. Swann, J.A. Zhao, J. Kiplinger, P. Lefebvre, *Journal of Combinatorial Chemistry*, 12 (2010) 877.
- [64] J. Cole, C. Rui, *LC-GC Europe*, 21 (2008) 29.
- [65] C. West, E. Lesellier, *Journal of Chromatography A*, 1087 (2005) 64.
- [66] D. Pyo, K. Lee, H. Kim, *Journal of Liquid Chromatography and Related Technologies*, 21 (1998) 989.
- [67] O. Gyllenhaal, A. Karlsson, *Journal of Biochemical and Biophysical Methods*, 43 (2000) 135.
- [68] C. Wenda, A. Rajendran, *Journal of Chromatography A*, 1216 (2009) 8750.
- [69] B.J. Hoffman, L.T. Taylor, S. Rumbelow, L. Goff, J.D. Pinkston, *Journal of Chromatography A*, 1043 (2004) 285.

- [70] L. Toribio, M.J. del Nozal, J.L. Bernal, C. Alonso, J.J. Jiménez, *Journal of Separation Science*, 29 (2006) 1373.
- [71] M.Z. Wang, M.S. Klee, S.K. Yang, *Journal of Chromatography B: Biomedical Applications*, 665 (1995) 139.
- [72] T. Bamba, E. Fukusaki, S. Kajiyama, K. Ute, T. Kitayama, A. Kobayashi, *Journal of Chromatography A*, 911 (2001) 113.
- [73] A. Villermet, D. Thiebaut, M. Caude, R. Rosset, *Journal of Chromatography*, 557 (1991) 85.
- [74] C. Brunelli, Y. Zhao, M.H. Brown, P. Sandra, *Journal of Chromatography A*, 1185 (2008) 263.
- [75] M. Ashraf-Khorassani, J.M. Levy, *Chromatographia*, 40 (1995) 78.
- [76] C. West, A. Bouet, I. Gillaizeau, G. Coudert, M. Lafosse, E. Lesellier, *Chirality*, 22 (2010) 242.
- [77] M. Maftouh, C. Granier-Loyaux, E. Chavana, J. Marini, A. Pradines, Y.V. Heyden, C. Picard, *Journal of Chromatography A*, 1088 (2005) 67.
- [78] M. Li, Z. Bao, B. Su, H. Xing, Y. Yang, Q. Ren, *Journal of Separation Science*, 36 (2013) 3093.
- [79] C. Wang, Y. Zhang, *Journal of Chromatography A*, 1281 (2013) 127.
- [80] M. Ashraf-Khorassani, L.T. Taylor, *Journal of Separation Science*, 33 (2010) 1682.
- [81] J. Liu, E.L. Regalado, I. Mergelsberg, C.J. Welch, *Organic & Biomolecular Chemistry*, 11 (2013) 4925.
- [82] A. Cazenave-Gassiot, R. Boughtflower, J. Caldwell, L. Hitzel, C. Holyoak, S. Lane, P. Oakley, F. Pullen, S. Richardson, G.J. Langley, *Journal of Chromatography A*, 1216 (2009) 6441.
- [83] M. Ventura, B. Murphy, W. Goetzinger, *Journal of Chromatography A*, 1220 (2012) 147.
- [84] K. De Klerck, G. Parewyck, D. Mangelings, Y. Vander Heyden, *Journal of Chromatography A*, 1269 (2012) 336.
- [85] M.A. Patel, F. Riley, J. Wang, M. Lovdahl, L.T. Taylor, *Journal of Chromatography A*, 1218 (2011) 2593.
- [86] J. Zheng, T. Glass, L.T. Taylor, J.D. Pinkston, *Journal of Chromatography A*, 1090 (2005) 155.
- [87] J. Zheng, L.T. Taylor, J.D. Pinkston, M.L. Mangels, *Journal of Chromatography A*, 1082 (2005) 220.
- [88] L.T. Taylor, *Journal of Chromatography A*, 1250 (2012) 196.
- [89] X. Lou, H.-G. Janssen, C.A. Cramers, *Journal of Chromatography A*, 785 (1997) 57.
- [90] L. Toribio, J.L. Bernal, M.T. Martín, J. Bernal, M.J. del Nozal, *Biomedical Chromatography* (2013).
- [91] in: T.A. Berger, R.M. Smith (Eds.), *Packed Column SFC*, The Royal Society of Chemistry, 1995, p. 97.
- [92] K. Anton, J. Eppinger, L. Frederiksen, E. Francotte, T.A. Berger, W.H. Wilson, *Journal of Chromatography A*, 666 (1994) 395.
- [93] G. Gubitz, M.G. Schmid, *Biopharmaceutics & Drug Disposition*, 22 (2001) 291.
- [94] G. Terfloth, *Journal of Chromatography A*, 906 (2001) 301.
- [95] K.L. Williams, L.C. Sander, *Journal of Chromatography A*, 785 (1997) 149.
- [96] R.-Q. Wang, T.-T. Ong, S.-C. Ng, *Journal of Chromatography A*, 1224 (2012) 97.
- [97] K. De Klerck, D. Mangelings, D. Clicq, F. De Boever, Y. Vander Heyden, *Journal of Chromatography A*, 1234 (2012) 72.
- [98] L. Miller, *Journal of Chromatography A*, 1250 (2012) 250.
- [99] C.J. Welch, W.R. Leonard Jr, J.O. DaSilva, M. Biba, J. Albaneze-Walker, D.W. Henderson, B. Laing, D.J. Mathre, *LC-GC Europe*, 18 (2005) 264.
- [100] Y. Xiang, J.R. Dunetz, M. Lovdahl, *Journal of Chromatography A*, 1293 (2013) 150.
- [101] L. Toribio, M.J. del Nozal, J.L. Bernal, J. Bernal, M.T. Martín, *Journal of Chromatography A*, 1218 (2011) 4886.

- [102] F. Gritti, G. Guiochon, *Journal of Chromatography A*, 1228 (2012) 2.
- [103] F. Gritti, G. Guiochon, *Journal of Chromatography A*, 1217 (2010) 1604.
- [104] I. Ali, Z.A. Al-Othman, N. Nagae, V.D. Gaitonde, K.K. Dutta, *Journal of Separation Science*, 35 (2012) 3235.
- [105] R.D. Ricker, C.B. Woodward, K. Forrer, B.J. Permar, W. Chen, *Journal of Chromatographic Science*, 46 (2008) 261.
- [106] National Institutes of Health (2014) Voriconazole: MedlinePlus Drug Information. Available at: <http://www.nlm.nih.gov/medlineplus/druginfo/meds/a605022.html>. [Accessed 16 September 2013]
- [107] RxList Inc (2014) Vfend (Voriconazole) Drug Information: Description, User Reviews, Drug Side Effects, Interactions. Available at <http://www.rxlist.com/vfend-drug.htm>. [Accessed 16 September 2013]
- [108] L.R. Snyder, J.J. Kirkland, J.W. Dolan, *Introduction to Modern Liquid Chromatography*, John Wiley & Sons, Inc., 2010, p. 303.
- [109] L.R. Snyder, J.J. Kirkland, J.W. Dolan, *Introduction to Modern Liquid Chromatography*, John Wiley & Sons, Inc., 2010, p. 403.
- [110] C.J. Welch, N.J. Wu, M. Biba, R. Hartman, T. Brkovic, X.Y. Gong, R. Helmy, W. Schafer, J. Cuff, Z. Pirzada, L.L. Zhou, *Trac-Trends in Analytical Chemistry*, 29 (2010) 667.
- [111] A.T. Inc., Agilent Technologies Inc, Germany, 2012, p. 12.
- [112] C. West, E. Lesellier, *Journal of Chromatography A*, 1110 (2006) 200.
- [113] E. Lesellier, *Journal of Chromatography A*, 1216 (2009) 1881.
- [114] C. West, E. Lesellier, *Journal of Chromatography A*, 1302 (2013) 152.
- [115] L.T. Taylor, *Journal of Chromatographic Science*, 35 (1997) 374.
- [116] S.T. Patil, M. Sundaresan, I.C. Bhoir, A.M. Bhagwat, *Talanta*, 47 (1998) 3.
- [117] J. Zheng, J.D. Pinkston, P.H. Zoutendam, L.T. Taylor, *Analytical Chemistry*, 78 (2006) 1535.
- [118] V.R. Meyer, *Practical High-Performance Liquid Chromatography*, John Wiley & Sons, Ltd, 2010, p. 17.
- [119] A. Dispas, P. Lebrun, P. Sassi, E. Ziemons, D. Thiébaud, J. Vial, P. Hubert, *Journal of Chromatography A*, 1256 (2012) 253.
- [120] K.W. Phinney, L.C. Sander, *Chirality*, 15 (2003) 287.

6 Appendices

6.1 Chapter 2:

Table 6.1.1: Results of varying the ratio of MeOH:ACN in mobile phase B whilst keeping Mobile A (FB) constant at 55% on the separation of S3a (Section 2.3.2.1.1)

Eluent 1: 0% Acetonitrile : 45% Methanol						
	Retention time (mins)	Retention Factor	Symmetry	Peak Width @ half height (mins)	Efficiency (plates per metre)	Resolution
Void	0.680					
Compound X	1.548	1.276	0.740	0.046	76460	
Compound C	1.677	1.466	0.770	0.491	86380	1.810
Compound D	5.938	7.732	0.920	0.121	141030	31.260
Voriconazole	10.121	13.884	1.140	0.123	156400	15.950
Eluent 2: 5% Acetonitrile : 40% Methanol						
	Retention time (mins)	Retention Factor	Symmetry	Peak Width @ half height (mins)	Efficiency (plates per metre)	Resolution
Void	0.682					
Compound X	1.537	1.254	0.820	0.043	78470	
Compound C	1.612	1.364	0.730	0.046	84620	1.050
Compound D	5.310	6.786	1.100	0.108	143450	29.830
Voriconazole	8.984	12.173	1.130	0.174	154960	15.740
Eluent 3: 10% Acetonitrile : 35% Methanol						
	Retention time (mins)	Retention Factor	Symmetry	Peak Width @ half height (mins)	Efficiency (plates per metre)	Resolution
Void	0.686					
Compound X	1.497	1.182	1.430	0.032	104650	
Compound C	1.534	1.236	0.640	0.461	72270	1.020
Compound D	4.585	5.684	0.940	0.091	144490	26.520
Voriconazole	7.683	10.200	1.140	0.144	162280	15.710
Eluent 4: 15% Acetonitrile : 30% Methanol						
	Retention time (mins)	Retention Factor	Symmetry	Peak Width @ half height (mins)	Efficiency (plates per metre)	Resolution
Void	0.683					
Compound X	1.448	1.120	0.830	0.056	40720	
Compound C	1.448	1.120	0.830	0.056	40720	0.000
Compound D	3.876	4.675	1.000	0.855	122290	21.000
Voriconazole	6.431	8.416	1.130	0.128	151580	14.610
Eluent 5: 20% Acetonitrile : 25% Methanol						
Peak	Retention time (mins)	Retention Factor	Symmetry	Peak Width @ half height (mins)	Efficiency (plates per metre)	Resolution
Void	0.763					
Compound X	1.368	0.793	0.750	0.046	68810	
Compound C	1.368	0.793	0.750	0.046	68810	0.000
Compound D	3.157	3.138	0.950	0.058	136080	20.500
Voriconazole	5.132	5.726	1.080	0.083	158810	14.540
Eluent 6: 25% Acetonitrile : 20% Methanol						
Peak	Retention time (mins)	Retention Factor	Symmetry	Peak Width @ half height (mins)	Efficiency (plates per metre)	Resolution
Void	0.756					
Compound X	1.301	0.721	0.760	0.043	55080	
Compound C	1.301	0.721	0.760	0.433	55080	0.000
Compound D	2.610	2.452	0.870	0.673	129440	16.150
Voriconazole	4.148	4.487	1.030	0.099	155640	13.870
Eluent 7: 30% Acetonitrile : 15% Methanol						
Peak	Retention time (mins)	Retention Factor	Symmetry	Peak Width @ half height (mins)	Efficiency (plates per metre)	Resolution
Void	0.694					
Compound X	1.214	0.749	0.720	0.059	29710	
Compound C	1.214	0.749	0.720	0.059	29710	0.000
Compound D	2.132	2.072	0.860	0.061	72460	9.720
Voriconazole	3.272	3.715	0.990	0.075	118110	10.470

Table 6.1.2: Results of optimising the concentration of the organic mobile phase (MeOH) on the retention of S3a (Section 2.3.2.1.2.)

Eluent 8: 70% Formate Buffer : 30% Methanol						
	Retention time (mins)	Retention Factor	Symmetry	Peak Width @ half height (mins)	Efficiency (plates per metre)	Resolution
Void	0.672					
Compound C	3.135	3.665	0.800		131690	
Compound X	3.551	4.284	0.740		136350	3.600
Compound D	35.784	52.250	1.040		139370	48.250
Voriconazole	67.029	98.746	0.910		136240	17.780
Eluent 9: 60% Formate Buffer : 40% Methanol						
	Retention time (mins)	Retention Factor	Symmetry	Peak Width @ half height (mins)	Efficiency (plates per metre)	Resolution
Void	0.675					
Compound C	1.963	1.908	1.030		83100	
Compound X	2.005	1.970	0.360		118540	0.540
Compound D	10.466	14.505	0.950		151400	40.820
Voriconazole	18.625	26.593	0.980		157380	17.440
Eluent 10: 50% Formate Buffer : 50% Methanol						
	Retention time (mins)	Retention Factor	Symmetry	Peak Width @ half height (mins)	Efficiency (plates per metre)	Resolution
Void	0.728					
Compound C	1.302	0.788	0.670	0.043	62260	
Compound X	1.459	1.004	0.670	0.045	83390	2.420
Compound D	3.803	4.224	0.950	0.083	124970	23.400
Voriconazole	6.140	7.434	1.030	0.122	150780	13.880
Eluent 11: 40% Formate Buffer : 60% Methanol						
	Retention time (mins)	Retention Factor	Symmetry	Peak Width @ half height (mins)	Efficiency (plates per metre)	Resolution
Void	0.622					
Compound C	0.922	0.482	0.680	0.040	38950	
Compound X	1.065	0.712	0.630	0.040	54450	2.440
Compound D	1.445	1.323	0.720	0.048	65020	5.990
Voriconazole	1.923	2.092	0.820	0.054	91460	6.120
Eluent 12: 30% Formate Buffer : 70% Methanol						
	Retention time (mins)	Retention Factor	Symmetry	Peak Width @ half height (mins)	Efficiency (plates per metre)	Resolution
Void	0.671					
Compound C	0.827	0.232	0.640	0.036	34700	
Compound X	0.944	0.407	0.590	0.035	48700	2.110
Compound D	1.045	0.557	0.720	0.045	44160	1.710
Voriconazole	1.224	0.824	0.680	0.043	60640	2.840

Table 6.1.3: Results of optimising the concentration of the organic mobile phase (ACN) on the retention of S3a. (Section 2.3.2.1.2)

Eluent 13: 75% Formate Buffer : 25% Acetonitrile						
Peak	Retention time (mins)	Retention Factor	Symmetry	Peak Width @ half height (mins)	Efficiency (plates per metre)	Resolution
Void	0.685					
Compound X	1.864	1.402	0.750	0.045	0	
Compound C	2.287	1.947	0.870	0.053	143830	5.940
Compound D	6.616	7.526	0.950	0.139	164730	30.600
Voriconazole	12.882	15.601	0.970	0.267	159290	20.360
Eluent 14: 70% Formate Buffer : 30% Acetonitrile						
Peak	Retention time (mins)	Retention Factor	Symmetry	Peak Width @ half height (mins)	Efficiency (plates per metre)	Resolution
Void	0.683					
Compound X	1.560	1.284	0.770	0.043	99480	
Compound C	1.700	1.489	0.720	0.046	113220	2.220
Compound D	3.552	4.201	0.870	0.074	141140	20.150
Voriconazole	6.315	8.246	0.960	0.121	156270	17.150
Eluent 15: 60% Formate Buffer : 40% Acetonitrile						
Peak	Retention time (mins)	Retention Factor	Symmetry	Peak Width @ half height (mins)	Efficiency (plates per metre)	Resolution
Void	0.660					
Compound X	1.159	0.756	0.820	0.034	70730	
Compound C	1.211	0.835	0.710	0.040	70390	0.920
Compound D	1.643	1.489	0.750	0.047	96180	6.920
Voriconazole	2.403	2.641	0.890	0.058	132510	10.090
Eluent 16: 50% Formate Buffer : 50% Acetonitrile						
Peak	Retention time (mins)	Retention Factor	Symmetry	Peak Width @ half height (mins)	Efficiency (plates per metre)	Resolution
Void	0.629					
Compound X	0.944	0.501	0.670	0.034	56990	
Compound C	1.041	0.655	0.650	0.035	68480	1.940
Compound D	1.134	0.803	0.680	0.040	58930	1.710
Voriconazole	1.432	1.277	0.760	0.041	91760	5.000
Eluent 17: 40% Formate Buffer : 60% Acetonitrile						
Peak	Retention time (mins)	Retention Factor	Symmetry	Peak Width @ half height (mins)	Efficiency (plates per metre)	Resolution
Void	0.620					
Compound X	0.828	0.335	0.610	0.030	48790	
Compound C	0.828	0.335	0.610	0.030	48790	0.000
Compound D	0.931	0.502	0.700	0.032	55430	2.100
Voriconazole	1.052	0.697	0.640	0.035	64070	2.370
Eluent 18: 30% Formate Buffer : 70% Acetonitrile						
Peak	Retention time (mins)	Retention Factor	Symmetry	Peak Width @ half height (mins)	Efficiency (plates per metre)	Resolution
Void	0.776					
Compound X	0.776	0.000	0.690	0.030	0	
Compound C	0.835	0.076	1.710	0.023	77930	1.410
Compound D	0.873	0.125	0.760	0.030	33530	0.770
Voriconazole	0.909	0.171	0.450	0.033	46050	0.630

Table 6.1.4: Results of optimising the concentration of Mobile Phase A Buffer (FB) (on retention characteristics of S3a. Buffer pH: 4.00 (Section 2.3.2.1.3.1))

Eluent 19: 10 mM FB						
Peak	Retention time (mins)	Retention Factor	Symmetry	Peak Width @ half height (mins)	Efficiency (plates per metre)	Resolution
Void	0.642					
Compound X	1.501	1.338	0.790	0.419	96360	
Compound C	1.654	1.576	0.760	0.046	107130	2.440
Compound D	3.509	4.466	0.840	0.074	142640	20.420
Voriconazole	6.301	8.815	1.070	0.122	158810	17.560
Eluent 20: 20 mM FB						
Peak	Retention time (mins)	Retention Factor	Symmetry	Peak Width @ half height (mins)	Efficiency (plates per metre)	Resolution
Void	0.679					
Compound X	1.551	1.284	0.750	0.041	105180	
Compound C	1.697	1.499	0.730	0.042	112730	2.340
Compound D	3.535	4.206	0.800	0.073	149990	20.470
Voriconazole	6.289	8.262	0.970	0.120	161510	17.550
Eluent 21: 30 mM FB						
Peak	Retention time (mins)	Retention Factor	Symmetry	Peak Width @ half height (mins)	Efficiency (plates per metre)	Resolution
Void	0.683					
Compound X	1.560	1.284	0.770	0.043	99480	
Compound C	1.700	1.489	0.720	0.046	113220	2.220
Compound D	3.552	4.201	0.870	0.074	141140	20.150
Voriconazole	6.315	8.246	0.960	0.121	156270	17.150
Eluent 22: 40 mM FB						
Peak	Retention time (mins)	Retention Factor	Symmetry	Peak Width @ half height (mins)	Efficiency (plates per metre)	Resolution
Void	0.678					
Compound X	1.553	1.291	0.740	0.042	103190	
Compound C	1.698	1.504	0.730	0.046	112940	2.310
Compound D	3.535	4.214	0.880	0.074	144730	20.210
Voriconazole	6.294	8.283	1.020	0.122	161760	17.460
Eluent 23: 50 mM FB						
Peak	Retention time (mins)	Retention Factor	Symmetry	Peak Width @ half height (mins)	Efficiency (plates per metre)	Resolution
Void	0.679					
Compound X	1.551	1.284	0.770	0.042	102280	
Compound C	1.695	1.496	0.730	0.459	105620	2.260
Compound D	3.506	4.163	0.810	0.074	142410	19.710
Voriconazole	6.267	8.230	0.970	0.120	157060	17.360

Table 6.1.5:: Results of optimising pH of Mobile Phase A Buffer (FB) on the retention characteristics of S3a. Buffer concentration: 30 mM (Section 2.3.2.1.3.2)

Eluent 24: pH 3.00						
Peak	Retention time (mins)	Retention Factor	Symmetry	Peak Width @ half height (mins)	Efficiency (plates per metre)	Resolution
Void	0.681					
Compound X	1.582	1.323	0.720	0.425	107030	
Compound C	1.750	1.570	0.800	0.464	109090	2.610
Compound D	3.860	4.668	0.920	0.785	150670	21.850
Voriconazole	6.949	9.204	1.030	0.137	155780	17.700
Eluent 25: pH 3.50						
Peak	Retention time (mins)	Retention Factor	Symmetry	Peak Width @ half height (mins)	Efficiency (plates per metre)	Resolution
Void	0.676					
Compound X	1.546	1.287	0.760	0.038	106960	
Compound C	1.694	1.506	0.740	0.042	119940	2.420
Compound D	3.539	4.235	0.870	0.731	145060	20.540
Voriconazole	6.307	8.330	1.070	0.121	155850	17.290
Eluent 21: pH 4.00						
Peak	Retention time (mins)	Retention Factor	Symmetry	Peak Width @ half height (mins)	Efficiency (plates per metre)	Resolution
Void	0.683					
Compound X	1.560	1.291	0.770	0.043	99480	
Compound C	1.700	1.496	0.720	0.046	113220	2.220
Compound D	3.552	4.216	0.870	0.074	141140	20.150
Voriconazole	6.315	8.273	0.960	0.121	156270	17.150
Eluent 26: pH 4.50						
Peak	Retention time (mins)	Retention Factor	Symmetry	Peak Width @ half height (mins)	Efficiency (plates per metre)	Resolution
Void	0.678					
Compound X	1.554	1.292	0.720	0.042	0	
Compound C	1.804	1.661	0.730	0.453	113680	2.400
Compound D	3.571	4.267	0.800	0.743	147730	20.550
Voriconazole	6.371	8.397	1.030	0.123	155830	17.380
Eluent 27: pH 5.00						
Peak	Retention time (mins)	Retention Factor	Symmetry	Peak Width @ half height (mins)	Efficiency (plates per metre)	Resolution
Void	0.678					
Compound X	1.552	1.289	0.740	0.041	105410	
Compound C	1.703	1.512	0.720	0.045	113510	2.410
Compound D	3.556	4.245	0.830	0.074	151750	20.630
Voriconazole	6.341	8.353	1.040	0.123	160830	17.630

Table 6.1.6: Results of temperature study using 30% ACN:70% FB as mobile phase on the retention characteristics of S3a. (Section 2.3.2.1.4)

30% ACN - 35°C						
	Retention time (mins)	Retention Factor	Symmetry	Efficiency (plates per column)	Efficiency (plates per metre)	Resolution
Void	0.683					
Compound X	1.560		0.770	9948	99480	
Compound C	1.700	1.489	0.720	11322	113220	2.220
Compound D	3.552	4.201	0.870	14114	141140	20.150
Voriconazole	6.315	8.246	0.960	15627	156270	17.150
30% ACN - 40°C						
	Retention time (mins)	Retention Factor	Symmetry	Efficiency (plates per column)	Efficiency (plates per metre)	Resolution
Void	0.683					
Compound X	1.548	1.266	0.750	10249	102490	
Compound C	1.656	1.425	0.730	10744	107440	1.730
Compound D	3.457	4.061	0.880	14864	148640	20.270
Voriconazole	6.068	7.884	1.040	15454	154540	16.980
30% ACN - 45°C						
	Retention time (mins)	Retention Factor	Symmetry	Efficiency (plates per column)	Efficiency (plates per metre)	Resolution
Void	0.679					
Compound X	1.545	1.275	0.820	9980	99800	
Compound C	1.619	1.384	0.950	9628	96280	1.160
Compound D	3.397	4.003	0.920	14353	143530	19.780
Voriconazole	5.912	7.707	1.080	15208	152080	16.460
30% ACN - 50°C						
	Retention time (mins)	Retention Factor	Symmetry	Efficiency (plates per column)	Efficiency (plates per metre)	Resolution
Void	0.683					
Compound X	1.537	1.250	1.100	10499	104990	
Compound C	1.576	1.307	0.600	7819	78190	0.590
Compound D	3.300	3.832	0.890	14589	145890	19.070
Voriconazole	5.676	7.310	1.060	14968	149680	16.090
30% ACN - 55°C						
	Retention time (mins)	Retention Factor	Symmetry	Efficiency (plates per column)	Efficiency (plates per metre)	Resolution
Void	0.682					
Compound X	1.531	1.245	0.710	8616	86160	
Compound C	1.531	1.245	0.710	8616	86160	0.000
Compound D	3.201	3.694	0.920	14287	142870	19.290
Voriconazole	5.438	6.974	1.090	15048	150480	15.680

Table 6.1.7: Exp 4b: Results of temperature study using 25% ACN:75% FB as mobile phase on the retention characteristics of S3a. (Section 2.3.2.1.4)

25% ACN - 35°C						
	Retention time (mins)	Retention Factor	Symmetry	Peak Width @ half height (mins)	Efficiency (plates per metre)	Resolution
Void	0.685					
Compound X	1.864	1.721	0.750	0.045	127750	
Compound C	2.287	2.339	0.870	0.053	143850	5.940
Compound D	6.616	8.658	0.950	0.139	164730	30.600
Voriconazole	12.882	17.806	0.970	0.027	159290	20.360
25% ACN - 40°C						
	Retention time (mins)	Retention Factor	Symmetry	Peak Width @ half height (mins)	Efficiency (plates per metre)	Resolution
Void	0.686					
Compound X	1.856	1.706	0.850	0.043	129230	
Compound C	2.209	2.220	0.820	0.051	141720	5.060
Compound D	6.340	8.242	0.920	0.119	167630	30.540
Voriconazole	12.214	16.805	1.030	0.220	160530	20.170
25% ACN - 45°C						
	Retention time (mins)	Retention Factor	Symmetry	Peak Width @ half height (mins)	Efficiency (plates per metre)	Resolution
Void	0.688					
Compound X	1.845	1.682	0.840	0.044	127700	
Compound C	2.132	2.099	0.770	0.050	139580	4.170
Compound D	6.051	7.795	0.870	0.012	166400	30.130
Voriconazole	11.604	15.866	0.970	0.021	155420	19.560
25% ACN - 50°C						
	Retention time (mins)	Retention Factor	Symmetry	Peak Width @ half height (mins)	Efficiency (plates per metre)	Resolution
Void	0.687					
Compound X	1.832	1.667	0.940	0.044	131460	
Compound C	2.062	2.001	0.800	0.049	134440	3.400
Compound D	5.822	7.475	0.920	0.109	164730	29.730
Voriconazole	10.916	14.889	1.020	0.205	155150	19.120
25% ACN - 55°C						
	Retention time (mins)	Retention Factor	Symmetry	Peak Width @ half height (mins)	Efficiency (plates per metre)	Resolution
Void	0.687					
Compound X	1.819	1.648	0.750	0.043	121550	
Compound C	1.992	1.900	0.750	0.048	137150	2.590
Compound D	5.560	7.093	0.990	0.105	160990	29.280
Voriconazole	10.277	13.959	1.060	0.194	151140	18.490

6.2 Chapter 3

Table 6.2.1: The effect of modifier concentration on retention of API, Voriconazole and related impurities; compound C and compound D. Modifier: MeOH only. Stationary phase: Agilent Zorbax bare silica. (150 mm X 4.6 mm, 5 μ m)

Agilent Zorbax Silica (5 μ m, 150mm*4.6mm)					
@20% Methanol					
	Retention time (mins)	Retention Factor	Symmetry	Resolution	Selectivity
Void	0.500				
Compound C	0.946	0.892	0.960		
Voriconazole	1.007	1.014	0.820	1.080	1.137
Compound D	1.424	1.848	0.730	5.890	1.822
@16% Methanol					
	Retention time (mins)	Retention Factor	Symmetry	Resolution	Selectivity
Void	0.510				
Compound C	1.086	1.129	0.960		
Voriconazole	1.172	1.298	0.840	1.360	1.149
Compound D	1.772	2.475	0.730	7.030	1.906
@12% Methanol					
	Retention time (mins)	Retention Factor	Symmetry	Resolution	Selectivity
Void	0.527				
Compound C	1.334	1.531	0.850		
Voriconazole	1.479	1.806	0.790	1.780	1.180
Compound D	2.460	3.668	0.700	8.410	2.030
@10% Methanol					
	Retention time (mins)	Retention Factor	Symmetry	Resolution	Selectivity
Void	0.530				
Compound C	1.505	1.840	0.900		
Voriconazole	1.703	2.213	0.760	2.070	1.203
Compound D	3.019	4.696	0.760	9.400	2.122
@8% Methanol					
	Retention time (mins)	Retention Factor	Symmetry	Resolution	Selectivity
Void	0.567				
Compound C	1.875	2.307	0.830		
Voriconazole	2.208	2.894	0.710	2.610	1.255
Compound D	4.196	6.400	0.550	9.990	2.211

Table 6.2.2: The effect of modifier concentration on retention of API, Voriconazole and related impurities; compound C and compound D. Modifier: MeOH only. Stationary phase: Waters Spherisorb CN (250 mm X 4.6 mm, 5 μ m)

Waters Spherisorb CN (5μm, 250mm*4.6mm)					
@20% Methanol					
	Retention time (mins)	Retention Factor	Symmetry	Resolution	Selectivity
Void	0.882				
Compound C	2.610	1.959	0.860		
Voriconazole	2.810	2.186	0.810	1.920	1.116
Compound D	4.058	3.601	0.740	8.500	1.647
@16% Methanol					
	Retention time (mins)	Retention Factor	Symmetry	Resolution	Selectivity
Void	0.897				
Compound C	3.056	2.407	0.810		
Voriconazole	3.268	2.643	0.750	1.700	1.098
Compound D	4.990	4.563	0.690	9.560	1.726
@12% Methanol					
	Retention time (mins)	Retention Factor	Symmetry	Resolution	Selectivity
Void	0.943				
Compound C	4.004	3.246	0.740		
Voriconazole	4.301	3.561	0.680	1.780	1.097
Compound D	7.135	6.566	0.620	10.540	1.844
@10% Methanol					
	Retention time (mins)	Retention Factor	Symmetry	Resolution	Selectivity
Void	0.978				
Compound C	4.598	3.701	0.710		
Voriconazole	4.916	4.027	0.660	1.600	1.088
Compound D	8.505	7.696	0.710	10.310	1.911
@8% Methanol					
	Retention time (mins)	Retention Factor	Symmetry	Resolution	Selectivity
Void	1.028				
Compound C	5.696	4.541	0.690		
Voriconazole	6.133	4.966	0.680	1.650	1.094
Compound D	11.226	9.920	0.670	11.660	1.998

Table 6.2.3: The effect of modifier concentration on retention of API, Voriconazole and related impurities; compound C and compound D. Modifier: MeOH only. Stationary phase: Princeton Diol (150 mm X 4.6 mm, 5 μ m)

Princeton Diol SFC (5μm, 150mm*4.6mm)					
@20% methanol					
	Retention time (mins)	Retention Factor	Symmetry	Resolution	Selectivity
Void	0.534	0.000	0.930		
Voriconazole	1.140	1.135	1.030		
Compound C	1.179	1.208	0.940	0.810	1.064
Compound D	1.460	1.734	0.950	3.960	1.436
@16% methanol					
	Retention time (mins)	Retention Factor	Symmetry	Resolution	Selectivity
Void	0.550	0.000	0.860		
Voriconazole	1.306	1.375	0.980		
Compound C	1.376	1.502	0.950	0.880	1.093
Compound D	1.790	2.255	0.960	5.160	1.501
@12% methanol					
	Retention time (mins)	Retention Factor	Symmetry	Resolution	Selectivity
Void	0.590	0.000	0.94		
Voriconazole	1.622	1.749	0.980		
Compound C	1.709	1.897	0.950	1.010	1.084
Compound D	2.389	3.049	0.980	7.000	1.608
@10% methanol					
	Retention time (mins)	Retention Factor	Symmetry	Resolution	Selectivity
Void	0.630	0.000	0.800		
Voriconazole	1.887	1.995	1.000		
Compound C	1.974	2.133	0.970	0.960	1.069
Compound D	2.893	3.592	0.910	7.660	1.684
@8% methanol					
	Retention time (mins)	Retention Factor	Symmetry	Resolution	Selectivity
Void	0.693		0.890		
Voriconazole	2.288	2.302	1.160		
Compound C	2.383	2.439	0.970	0.770	1.060
Compound D	3.746	4.405	0.970	8.960	1.807
@6% methanol					
	Retention time (mins)	Retention Factor	Symmetry	Resolution	Selectivity
Void	0.796		0.920		
Voriconazole	3.072	3.433	1.330		
Compound C	3.072	3.433	1.330		1.000
Compound D	5.325	6.684	0.890	9.890	1.947

Table 6.2.4: The effect of modifier concentration on retention of API, Voriconazole and related impurities; compound C and compound D. Modifier: MeOH only. Stationary phase: Princeton ethyl-pyridine (150 mm X 4.6 mm, 5 μ m)

Princeton Pyridine SFC (5μm, 150mm*4.6mm)					
@20% Methanol					
	Retention time (mins)	Retention Factor	Symmetry	Resolution	Selectivity
Void	0.510	0.000	0.840		
Voriconazole	0.775	0.520	1.720		
Compound C	0.816	0.600	0.816	0.670	1.155
Compound D	0.816	0.600	0.816	0.670	1.000
@16% Methanol					
	Retention time (mins)	Retention Factor	Symmetry	Resolution	Selectivity
Void	0.527	0.000	0.860		
Voriconazole	0.848	0.609	1.130		
Compound C	0.903	0.713	0.690	0.720	1.171
Compound D	0.903	0.713	0.690	0.720	1.000
@12% Methanol					
	Retention time (mins)	Retention Factor	Symmetry	Resolution	Selectivity
Void	0.553	0.000			
Voriconazole	0.955	0.727	1.100		
Compound C	1.026	0.855	0.940	0.920	1.177
Compound D	1.082	0.957	0.500	0.750	1.118
@10% Methanol					
	Retention time (mins)	Retention Factor	Symmetry	Resolution	Selectivity
Void	0.581	0.000			
Voriconazole	1.041	0.792	1.113		
Compound C	1.125	0.936	0.990	1.020	1.183
Compound D	1.206	1.076	0.990	0.890	1.149
@8% Methanol					
	Retention time (mins)	Retention Factor	Symmetry	Resolution	Selectivity
Void	0.631				
Voriconazole	1.152	0.826	1.220		
Compound C	1.255	0.989	1.030	1.110	1.198
Compound D	1.374	1.177	1.150	1.180	1.191
@6% Methanol					
	Retention time (mins)	Retention Factor	Symmetry	Resolution	Selectivity
Void	0.687				
Voriconazole	1.302	1.063	1.320		
Compound C	1.434	1.273	1.020	1.150	1.197
Compound D	1.613	1.556	1.170	1.450	1.223

Table 6.2.5: The effect of modifier concentration on retention of API, Voriconazole and related impurities; compound C and compound D. Modifier: MeOH w/0.1% TFA. Stationary phase: Agilent Zorbax bare silica. (150 mm X 4.6 mm, 5µm)

Agilent Zorbax Silica (5µm, 150mm*4.6mm)					
@20% Methanol w/0.1% TFA					
	Retention time (mins)	Retention Factor	Symmetry	Resolution	Selectivity
Void	0.510		0.850		
Compound C	0.835	0.637	0.970		
Voriconazole	0.835	0.637	0.970	0.000	1.000
Compound D	1.028	1.016	0.830	3.460	1.594
@16% Methanol w/0.1% TFA					
	Retention time (mins)	Retention Factor	Symmetry	Resolution	Selectivity
Void	0.520		0.940		
Compound C	0.934	0.796	0.910		
Voriconazole	0.934	0.796	0.910	0.000	1.000
Compound D	1.212	1.331	0.830	4.460	1.671
@12% Methanol w/0.1% TFA					
	Retention time (mins)	Retention Factor	Symmetry	Resolution	Selectivity
Void	0.537		0.890		
Compound C	1.088	1.026	0.650		
Voriconazole	1.088	1.026	0.650	0.000	1.000
Compound D	1.537	1.862	0.750	5.370	1.815
@10% Methanol w/0.1% TFA					
	Retention time (mins)	Retention Factor	Symmetry	Resolution	Selectivity
Void	0.553		0.900		
Compound C	1.217	1.201	0.710		
Voriconazole	1.217	1.201	0.710	0.000	1.000
Compound D	1.815	2.282	0.780	5.290	1.901
@8% Methanol w/0.1% TFA					
	Retention time (mins)	Retention Factor	Symmetry	Resolution	Selectivity
Void	0.577		0.910		
Compound C	1.419	1.459	0.640		
Voriconazole	1.419	1.459	0.640	0.000	1.000
Compound D	2.296	2.979	0.820	5.670	2.042
@6% Methanol w/0.1% TFA					
	Retention time (mins)	Retention Factor	Symmetry	Resolution	Selectivity
Void	0.611	0.000	0.880		
Compound C	1.737	1.843	0.880	0.000	
Voriconazole	1.859	2.043	0.740	0.780	1.108
Compound D	3.120	4.106	0.790	6.330	2.010

Table 6.2.6: The effect of modifier concentration on retention of API, Voriconazole and related impurities; compound C and compound D. Modifier: MeOH w/0.1% TFA. Stationary phase: Waters Spherisorb CN (250 mm X 4.6 mm, 5 μ m)

Waters Spherisorb CN (5μm, 250mm*4.6mm)					
@20% Methanol w/0.1% TFA					
	Retention time (mins)	Retention Factor	Symmetry	Resolution	Selectivity
Void	0.847		0.740		
Compound C	3.698	3.366	0.680		
Voriconazole	4.283	4.057	0.760	4.320	1.205
Compound D	6.542	6.724	0.690	12.280	1.657
@16% Methanol w/0.1% TFA					
	Retention time (mins)	Retention Factor	Symmetry	Resolution	Selectivity
Void	0.865		0.760		
Compound C	4.223	3.882	0.810		
Voriconazole	4.872	4.632	0.750	4.040	1.193
Compound D	7.872	8.101	0.690	12.860	1.749
@12% Methanol w/0.1% TFA					
	Retention time (mins)	Retention Factor	Symmetry	Resolution	Selectivity
Void	0.908		0.850		
Compound C	5.452	5.004	0.660		
Voriconazole	6.345	5.988	0.810	4.190	1.197
Compound D	10.932	11.040	0.610	14.190	1.844
@8% Methanol w/0.1% TFA					
	Retention time (mins)	Retention Factor	Symmetry	Resolution	Selectivity
Void	0.917				
Compound C	8.251	7.998	0.630		
Voriconazole	9.801	9.688	0.650	4.390	1.211
Compound D	18.591	19.274	0.480	14.150	1.989

Table 6.2.7: The effect of modifier concentration on retention of API, Voriconazole and related impurities; compound C and compound D. Modifier: MeOH w/0.1% TFA. Stationary phase: Princeton Diol CN (150 mm X 4.6 mm, 5µm)

Princeton Diol SFC (5µm, 150mm*4.6mm)					
@20% Methanol w/0.1% TFA					
	Retention time (mins)	Retention Factor	Symmetry	Resolution	Selectivity
Void	0.528	0.000	0.940		
Voriconazole	1.102	1.087	0.970		
Compound C	1.162	1.201	0.940	0.860	1.105
Compound D	1.419	1.688	0.880	3.700	1.405
@16% Methanol w/0.1% TFA					
	Retention time (mins)	Retention Factor	Symmetry	Resolution	Selectivity
Void	0.550	0.000	0.950		
Voriconazole	1.289	1.344	0.950		
Compound C	1.363	1.478	0.930	1.040	1.100
Compound D	1.742	2.167	0.930	4.800	1.466
@12% Methanol w/0.1% TFA					
	Retention time (mins)	Retention Factor	Symmetry	Resolution	Selectivity
Void	0.593	0.000	0.910		
Voriconazole	1.600	1.698	0.980		
Compound C	1.695	1.858	0.940	1.120	1.094
Compound D	2.318	2.909	0.960	6.510	1.565
@10% Methanol w/0.1% TFA					
	Retention time (mins)	Retention Factor	Symmetry	Resolution	Selectivity
Void	0.637	0.000	1.080		
Voriconazole	1.847	1.900	0.960		
Compound C	1.953	2.066	0.970	1.080	1.088
Compound D	2.791	3.381	0.840	6.850	1.637
@8% Methanol w/0.1% TFA					
	Retention time (mins)	Retention Factor	Symmetry	Resolution	Selectivity
Void	0.694		1.080		
Voriconazole	2.238	2.225	0.960		
Compound C	2.348	2.383	0.970	0.860	1.071
Compound D	3.595	4.180	0.840	8.280	1.754
@6% Methanol w/0.1% TFA					
	Retention time (mins)	Retention Factor	Symmetry	Resolution	Selectivity
Void	0.796				
Voriconazole	3.018	3.349	1.320		
Compound C	3.018	3.349	1.320	0.000	1.000
Compound D	5.077	6.316	1.020	8.630	1.886

Table 6.2.8: The effect of modifier concentration on retention of API, Voriconazole and related impurities; compound C and compound D. Modifier: MeOH w/0.1% TFA. Stationary phase: Princeton ethyl-pyridine (150 mm X 4.6 mm, 5µm)

Princeton Pyridine SFC (5µm, 150mm*4.6mm)					
@20% Methanol w/0.1% TFA					
	Retention time (mins)	Retention Factor	Symmetry	Resolution	Selectivity
Void	0.507	0.000	0.780		
Voriconazole	0.797	0.572	1.500		
Compound C	0.797	0.572	1.500	0.000	1.000
Compound D	0.797	0.572	1.500	0.000	1.000
@16% Methanol w/0.1% TFA					
	Retention time (mins)	Retention Factor	Symmetry	Resolution	Selectivity
Void	0.524	0.000	0.900		
Voriconazole	0.833	0.590	1.130		
Compound C	0.890	0.698	0.860	0.820	1.184
Compound D	0.890	0.698	0.860	0.000	1.000
@12% Methanol w/0.1% TFA					
	Retention time (mins)	Retention Factor	Symmetry	Resolution	Selectivity
Void	0.557	0.000	0.870		
Voriconazole	0.943	0.693	1.100		
Compound C	1.019	0.829	0.680	0.910	1.197
Compound D	1.019	0.829	0.680	0.000	1.000
@10% Methanol w/0.1% TFA					
	Retention time (mins)	Retention Factor	Symmetry	Resolution	Selectivity
Void	0.581	0.000	0.950		
Voriconazole	1.013	0.744	1.130		
Compound C	1.100	0.893	0.980	1.030	1.201
Compound D	1.139	0.960	0.680	0.510	1.075
@8% Methanol w/0.1% TFA					
	Retention time (mins)	Retention Factor	Symmetry	Resolution	Selectivity
Void	0.630		0.880		
Voriconazole	1.120	0.778	1.200		
Compound C	1.226	0.946	1.000	1.130	1.216
Compound D	1.304	1.070	0.650	0.800	1.131
@6% Methanol w/0.1% TFA					
	Retention time (mins)	Retention Factor	Symmetry	Resolution	Selectivity
Void	0.698		0.970		
Voriconazole	1.266	1.010	1.280		
Compound C	1.400	1.222	1.050	1.190	1.211
Compound D	1.521	1.414	1.040	0.920	1.157

Table 6.2.9: The effect of modifier concentration on retention of API, Voriconazole and related impurities; compound C and compound D. Modifier: MeOH w/0.1% TEA. Stationary phase: Agilent Zorbax bare silica. (150 mm X 4.6 mm, 5µm)

@20% Methanol w/0.1% TEA					
	Retention time (mins)	Retention Factor	Symmetry	Resolution	Selectivity
Void	0.510	0.000	0.740		
Compound C	0.821	0.610	1.040		
Voriconazole	0.821	0.610	1.040	0.000	1.000
Compound D	0.991	0.943	0.910	3.070	1.207
System Peak	2.116	3.149		7.060	2.135
@16% Methanol w/0.1% TEA					
	Retention time (mins)	Retention Factor	Symmetry	Resolution	Selectivity
Void	0.517	0.000	0.940		
Compound C	0.909	0.758	0.910		
Voriconazole	0.909	0.758	0.910	0.000	1.000
Compound D	1.153	1.230	0.830	3.910	1.268
System Peak	2.694	4.211		8.290	2.337
@12% Methanol w/0.1% TEA					
	Retention time (mins)	Retention Factor	Symmetry	Resolution	Selectivity
Void	0.540	0.000	0.960		
Compound C	1.073	0.987	1.050		
Voriconazole	1.073	0.987	1.050	0.000	1.000
Compound D	1.443	1.672	0.900	5.150	1.345
System Peak	3.736	5.919	0.000	8.360	2.589
@10% Methanol w/0.1% TEA					
	Retention time (mins)	Retention Factor	Symmetry	Resolution	Selectivity
Void	0.577	0.000	0.920		
Compound C	1.179	1.043	1.000		
Voriconazole	1.179	1.043	1.000	0.000	1.000
Compound D	1.687	1.924	0.920	5.840	1.431
System Peak	4.599	6.971	0.000	8.440	2.726
@8% Methanol w/0.1% TEA					
	Retention time (mins)	Retention Factor	Symmetry	Resolution	Selectivity
Void	0.580	0.000	0.850		
Compound C	1.357	1.340	0.870		
Voriconazole	1.357	1.340	0.870	0.000	1.000
Compound D	2.074	2.576	0.830	6.200	1.528
System Peak	5.890	9.155	0.000	7.990	2.840
@6% Methanol w/0.1% TEA					
	Retention time (mins)	Retention Factor	Symmetry	Resolution	Selectivity
Void	0.610	0.000	0.790		
Compound C	1.653	1.710	1.000		
Voriconazole	1.705	1.795	0.000	0.430	1.031
Compound D	2.789	3.572	0.940	7.920	1.636
System Peak	7.988	12.095	0.000	7.940	2.864

Table 6.2.10: The effect of modifier concentration on retention of API, Voriconazole and related impurities; compound C and compound D. Modifier: MeOH w/0.1% TEA. Stationary phase: Waters Spherisorb CN (250 mm X 4.6 mm, 5µm)

Waters Spherisorb Cyano (5µm, 150mm*4.6mm)					
@20% Methanol w/0.1% TEA					
	Retention time (mins)	Retention Factor	Symmetry	Resolution	Selectivity
Void	0.851	0.000	1.030		
Voriconazole	1.317	0.548	0.890		
Compound C	1.434	0.685	0.820	1.580	1.251
Compound D	1.434	0.685	0.820	1.580	1.000
System Peak	2.689	2.160	0.000	6.380	3.153
@16% Methanol w/0.1% TEA					
	Retention time (mins)	Retention Factor	Symmetry	Resolution	Selectivity
Void	0.875	0.000	0.870		
Voriconazole	1.440	0.646	0.840		
Compound C	1.591	0.818	0.650	1.870	1.267
Compound D	1.591	0.818	0.650	1.870	1.000
System Peak	3.303	2.775	0.000	6.410	3.391
@12% Methanol w/0.1% TEA					
	Retention time (mins)	Retention Factor	Symmetry	Resolution	Selectivity
Void	0.927	0.000	0.880		
Voriconazole	1.646	0.776	0.810		
Compound C	1.858	1.004	0.960	2.540	1.295
Compound D	1.932	1.084	0.420	0.810	1.079
System Peak	4.402	3.749	0.000	7.810	3.458
@10% Methanol w/0.1% TEA					
	Retention time (mins)	Retention Factor	Symmetry	Resolution	Selectivity
Void	0.963	0.000	0.900		
Voriconazole	1.804	0.873	0.770		
Compound C	2.064	1.143	1.060	2.850	1.309
Compound D	2.172	1.255	0.590	0.990	1.098
System Peak	5.270	4.472	0.000	7.930	3.562
@8% Methanol w/0.1% TEA					
	Retention time (mins)	Retention Factor	Symmetry	Resolution	Selectivity
Void	1.020	0.000	0.730		
Voriconazole	2.022	0.982	0.850		
Compound C	2.358	1.312	1.020	3.210	1.335
Compound D	2.519	1.470	0.560	1.260	1.120
System Peak	6.634	5.504	0.000	8.220	3.745
@6% Methanol w/0.1% TEA					
	Retention time (mins)	Retention Factor	Symmetry	Resolution	Selectivity
Void	1.080	0.000	0.860		
Voriconazole	2.379	1.203	0.740		
Compound C	2.843	1.632	1.090	3.550	1.357
Compound D	3.097	1.868	0.530	1.460	1.144
System Peak	8.863	7.206	4.490	7.680	3.859

Table 6.2.11: The effect of modifier concentration on retention of API, Voriconazole and related impurities; compound C and compound D. Modifier: MeOH w/0.1% TEA. Stationary phase: Princeton Diol (150 mm X 4.6 mm, 5 μ m)

Princeton Diol SFC (5μm, 150mm*4.6mm)					
@20% Methanol w/0.1% TEA					
	Retention time (mins)	Retention Factor	Symmetry	Resolution	Selectivity
Void	0.547	0.000	0.950		
Voriconazole	1.105	1.020	0.940		
UK-51,060	1.173	1.144	0.910	1.050	1.122
UK-83,610	1.390	1.541	0.830	3.130	1.347
System Peak	4.028	1.898	0.000	10.390	1.231
@16% Methanol w/0.1% TEA					
	Retention time (mins)	Retention Factor	Symmetry	Resolution	Selectivity
Void	0.561	0.000	0.810		
Voriconazole	1.279	1.280	0.950		
UK-51,060	1.368	1.439	0.930	1.240	1.124
UK-83,610	1.684	2.002	0.960	3.990	1.392
System Peak	5.222	8.308	0.000	11.110	4.150
@12% Methanol w/0.1% TEA					
	Retention time (mins)	Retention Factor	Symmetry	Resolution	Selectivity
Void	0.600	0.000	0.900		
Voriconazole	1.565	1.608	0.970		
UK-51,060	1.684	1.807	0.940	1.410	1.123
UK-83,610	2.193	2.655	0.940	5.290	1.470
System Peak	7.353	11.255	0.000	12.050	4.239
@10% Methanol w/0.1% TEA					
	Retention time (mins)	Retention Factor	Symmetry	Resolution	Selectivity
Void	0.647	0.000	0.770		
Voriconazole	1.791	1.768	1.000		
UK-51,060	1.932	1.986	0.970	1.450	1.123
UK-83,610	2.613	3.039	1.010	6.030	1.530
System Peak	9.074	13.025	0.000	11.890	4.286
@8% Methanol w/0.1% TEA					
	Retention time (mins)	Retention Factor	Symmetry	Resolution	Selectivity
Void	0.701	0.000	0.910		
Voriconazole	2.026	1.890	0.970		
UK-51,060	2.237	2.191	0.910	1.790	1.159
UK-83,610	2.929	3.178	0.890	4.780	1.451
System Peak	7.200	9.271	0.000	7.860	2.917
@6% Methanol w/0.1% TEA					
	Retention time (mins)	Retention Factor	Symmetry	Resolution	Selectivity
Void	0.804	0.000	0.890		
Voriconazole	2.565	2.190	0.960		
UK-51,060	2.822	2.510	0.870	1.590	1.146
UK-83,610	3.915	3.869	0.850	5.940	1.542
System Peak	9.565	10.897	0.000	8.150	2.816

Table 6.2.12: The effect of modifier concentration on retention of API, Voriconazole and related impurities; compound C and compound D. Modifier: MeOH w/ 20 mM AA. Stationary phase: Agilent Zorbax bare silica. (150 mm X 4.6 mm, 5µm)

Agilent Zorbax Silica (5µm, 150mm*4.6mm)					
@20% Methanol, 20 mM AA					
	Retention time (mins)	Retention Factor	Symmetry	Resolution	Selectivity
Void	0.500		0.790		
Compound C	0.865	0.730	0.970		
Voriconazole	0.865	0.730	0.970	0.000	1.000
Compound D	1.124	1.248	0.950	4.450	1.710
@16% Methanol, 20 mM AA					
	Retention time (mins)	Retention Factor	Symmetry	Resolution	Selectivity
Void	0.511		0.860		
Compound C	0.966	0.890	0.980		
Voriconazole	0.966	0.890	0.980	0.000	1.000
Compound D	1.310	1.564	0.890	5.250	1.756
@12% Methanol, 20 mM AA					
	Retention time (mins)	Retention Factor	Symmetry	Resolution	Selectivity
Void	0.537		0.920		
Compound C	1.143	1.128	0.970		
Voriconazole	1.143	1.128	0.970	0.000	1.000
Compound D	1.662	2.095	0.930	6.200	1.856
@10% Methanol, 20 mM AA					
	Retention time (mins)	Retention Factor	Symmetry	Resolution	Selectivity
Void	0.557		0.800		
Compound C	1.270	1.280	0.970		
Voriconazole	1.270	1.280	0.970	0.000	1.000
Compound D	1.931	2.467	0.950	6.800	1.927
@8% Methanol, 20 mM AA					
	Retention time (mins)	Retention Factor	Symmetry	Resolution	Selectivity
Void	0.580		0.800		
Compound C	1.451	1.502	0.970		
Voriconazole	1.451	1.502	0.970	0.000	1.000
Compound D	2.376	3.097	0.930	7.070	2.062
@6% Methanol, 20 mM AA					
	Retention time (mins)	Retention Factor	Symmetry	Resolution	Selectivity
Void	0.613	0.000	0.860		
Compound C	1.786	1.914	0.930		
Voriconazole	1.896	2.093	0.760	0.740	1.094
Compound D	3.219	4.251	0.880	7.210	2.031

Table 6.2.13: The effect of modifier concentration on retention of API, Voriconazole and related impurities; compound C and compound D. Modifier: MeOH w/20 mM AA. Stationary phase: Phenomenex Spherisorb CN (250 mm X 4.6 mm, 5µm)

Waters Spherisorb CN (5µm, 250mm*4.6mm)					
@20% Methanol, 20 mM AA					
	Retention time (mins)	Retention Factor	Symmetry	Resolution	Selectivity
Void	0.844	0.000	0.950		
Voriconazole	1.338	0.585	0.900		
Compound C	1.452	0.720	0.000	1.660	1.085
Compound D	1.452	0.720	0.000	0.000	1.000
@16% Methanol, 20 mM AA					
	Retention time (mins)	Retention Factor	Symmetry	Resolution	Selectivity
Void	0.875		0.960		
Voriconazole	1.478	0.689	0.880		
Compound C	1.627	0.859	1.080	2.420	1.101
Compound D	1.696	0.938	0.590	0.870	1.042
@12% Methanol, 20 mM AA					
	Retention time (mins)	Retention Factor	Symmetry	Resolution	Selectivity
Void	0.927		0.960		
Voriconazole	1.692	0.825	0.880		
Compound C	1.901	1.051	1.080	2.640	1.124
Compound D	2.021	1.180	0.590	1.340	1.063
@10% Methanol, 20 mM AA					
	Retention time (mins)	Retention Factor	Symmetry	Resolution	Selectivity
Void	0.967		0.540		
Voriconazole	1.850	0.913	0.890		
Compound C	2.105	1.177	1.190	2.930	1.138
Compound D	2.263	1.340	0.670	1.560	1.075
@8% Methanol, 20 mM AA					
	Retention time (mins)	Retention Factor	Symmetry	Resolution	Selectivity
Void	1.020		0.940		
Voriconazole	2.076	1.035	0.900		
Compound C	2.404	1.357	1.210	3.260	1.158
Compound D	2.623	1.572	0.670	1.810	1.091
@6% Methanol, 20 mM AA					
	Retention time (mins)	Retention Factor	Symmetry	Resolution	Selectivity
Void	1.081		0.930		
Voriconazole	2.450	1.402	0.850		
Compound C	2.903	1.846	1.210	3.590	1.185
Compound D	3.238	2.175	0.670	1.180	1.115

Table 6.2.14: The effect of modifier concentration on retention of API, Voriconazole and related impurities; compound C and compound D. Modifier: MeOH w/ 20 mM AA. Stationary phase: Princeton Diol (150 mm X 4.6 mm, 5 μ m)

Princeton Diol SFC (5μm, 150mm*4.6mm)					
@20% Methanol, 20 mM AA					
	Retention time (mins)	Retention Factor	Symmetry	Resolution	Selectivity
Void	0.550	0.000	0.940		
Voriconazole	1.058	0.924	1.000		
Compound C	1.137	1.067	0.910	1.260	1.156
Compound D	1.280	1.327	0.950	2.160	1.244
@16% Methanol, 20 mM AA					
	Retention time (mins)	Retention Factor	Symmetry	Resolution	Selectivity
Void	0.577	0.000	0.880		
Voriconazole	1.216	1.107	0.960		
Compound C	1.319	1.286	0.940	1.470	1.161
Compound D	1.524	1.641	0.780	2.680	1.276
@12% Methanol, 20 mM AA					
	Retention time (mins)	Retention Factor	Symmetry	Resolution	Selectivity
Void	0.610	0.000	0.920		
Voriconazole	1.465	1.402	0.970		
Compound C	1.607	1.634	1.000	1.730	1.166
Compound D	1.944	2.187	1.010	3.710	1.338
@10% Methanol, 20 mM AA					
	Retention time (mins)	Retention Factor	Symmetry	Resolution	Selectivity
Void	0.660	0.000	1.080		
Voriconazole	1.668	1.527	0.960		
Compound C	1.835	1.780	0.970	1.820	1.166
Compound D	2.272	2.442	0.840	4.300	1.372
@8% Methanol, 20 mM AA					
	Retention time (mins)	Retention Factor	Symmetry	Resolution	Selectivity
Void	0.725		0.950		
Voriconazole	1.959	1.702	1.050		
Compound C	2.161	1.981	0.930	1.840	1.164
Compound D	2.791	2.850	0.990	5.070	1.439
@6% Methanol, 20 mM AA					
	Retention time (mins)	Retention Factor	Symmetry	Resolution	Selectivity
Void	0.831		0.950		
Voriconazole	2.448	2.377	1.070		
Compound C	2.689	2.709	1.030	1.720	1.140
Compound D	3.685	4.083	1.060	6.040	1.507